

RESEDIMENTED CARBONATES FROM THE JURASSIC OF MALLORCA

BY

SIMON KETTLE

A thesis submitted to the
University of Birmingham
For the degree of
MASTER OF PHILOSOPHY

Geography, Earth and Environmental Sciences

College of Life and Environmental Sciences

University of Birmingham

October 2011

UNIVERSITY OF
BIRMINGHAM

University of Birmingham Research Archive

e-theses repository

This unpublished thesis/dissertation is copyright of the author and/or third parties. The intellectual property rights of the author or third parties in respect of this work are as defined by The Copyright Designs and Patents Act 1988 or as modified by any successor legislation.

Any use made of information contained in this thesis/dissertation must be in accordance with that legislation and must be properly acknowledged. Further distribution or reproduction in any format is prohibited without the permission of the copyright holder.

ABSTRACT

The Cutri Formation of Mallorca consists of sediments which formed during the rifting of the Neotethys Ocean. It comprises thick carbonate turbidite sequences (interbedded with bioturbated marls, calcisilts and *Posidonia* bivalve coquinas) interpreted to have formed along a line source. The most abundant deposits are oolitic-peloidal grainstones and packstones, with sedimentary structures indicating primary deposition by high-density turbidity flows and debris flows which fed slope and base of slope sediments into a current-swept basin. With continued filling and diminishing sediment supply, a basin-plain association developed, comprising fine-grained and thin-bedded turbidites intercalated with bioturbated marls. A diagenetic history is developed that determined porosity was destroyed very quickly, mainly through compaction. The sedimentological and diagenetic history is compared to examples of resedimented carbonates that do provide good reservoir quality to try and understand the reason for porosity preservation compared to the Cutri Formation.

ACKNOWLEDGEMENT

This thesis was funded by Cambridge Carbonates Ltd and would not have been possible without the companies support and time. I am indebted to many of my colleagues who supported me during this period, including Dr. Andrew Horbury, Dr Pete Gutteridge and Dr. Joanna Garland. Their experience and willingness to help, guided me through this project.

I am heartily thankful to my supervisors Dr Ian Fairchild and Dr James Wheeley whose encouragement, guidance and support from the initiation to completion enabled me to develop a thorough understanding of the subject.

Lastly, I offer my regards and blessings to all of those who supported me in any respect during the project, including Dr. Luis Pomar, Dr. Jennifer Waters, Mr. Francis Witkowski and Ms Veronica Szlapak.

CONTENTS

CONTENTS	1
LIST OF FIGURES.....	3
1. INTRODUCTION.....	7
1.1 BACKGROUND AND AIMS	7
1.2 FIELD AREA	8
1.3 THE GEOLOGY OF MALLORCA	11
1.4 STRATIGRAPHY AND SEDIMENTOLOGY OF THE JURASSIC	12
1.4.1 <i>Dating of the Cutri Formation</i>	16
1.5 PRESENT TECTONIC SETTING: TECTONICS OF THE BETIC CORDILLERA AND THE BALEARIC ISLANDS.....	17
1.5.1 <i>The Betic Cordillera</i>	20
2. GEOLOGICAL SETTING	22
2.1 GLOBAL PALAEOGEOGRAPHY DURING THE TRIASSIC TO CRETACEOUS	22
2.2 TECTONIC SETTING OF THE WESTERN MEDITERRANEAN DURING THE LATE TRIASSIC TO EARLY CRETACEOUS	24
2.3 PALAEO-TETHYS LATE TRIASSIC-EARLY JURASSIC: A PALAEOGEOGRAPHIC PERSPECTIVE	25
2.4 MID-JURASSIC: OPENING OF THE NEOTETHYS OCEAN AND END OF THE PALAEO-TETHYS: A PALAEOGEOGRAPHIC PERSPECTIVE	26
2.5 NEOTETHYS MID TO LATE JURASSIC RIFTING AND DRIFT	27
2.6 IBERIA AND THE BALEARIC ISLANDS	31
2.6.1 <i>Local Tectonic Structures</i>	34
2.7 PALAEOCLIMATE AND PALAEOCEANOGRAPHY.....	35
2.7.1 <i>Palaeoclimate</i>	35
2.7.2 <i>Ocean surface circulation</i>	36
2.7.3 <i>Oceanographic and climatic effects on carbonate margins</i>	39
3. REVIEW OF DEEP WATER DEPOSITS AND PROCESSES.....	42
3.1 DEFINITIONS OF DEPOSITS.....	42
3.2 RESEDIMENTATION: AN INTRODUCTION.....	44
3.3 TURBIDITES	46
3.3.1 <i>Classic Turbidites</i>	47
3.3.2 <i>Coarse Grained Turbidites</i>	48
3.3.3 <i>Fine-Grained Turbidites</i>	49
3.3.4 <i>Carbonate Turbidites</i>	51
3.3.5 <i>Distance from source</i>	52
3.4 DEBRITES	54
3.5 HYBRID BEDS.....	55
3.6 CONTOURITES.....	57
3.6.1 <i>Contourite depositional settings</i>	59
3.6.2 <i>Idealised contourite deposits</i>	60
3.6.3 <i>Geometry of contourites</i>	62
3.6.4 <i>Distinction of turbidites from contourites</i>	66
3.7 FORESLOPE CHARACTERISTICS	68
3.7.1 <i>Carbonate Fans and Aprons</i>	68
4. FACIES ANALYSIS.....	70
4.1 INTRODUCTION	70
4.1.1 <i>Facies 1 (Boulder pebble conglomerate):</i>	72

4.1.2 Facies 2 (<i>Graded pebble conglomerate</i>):	79
4.1.3 Facies 3 (<i>Graded peloidal ooid packstone</i>):	84
4.1.4 Facies 4 (<i>Graded oolites</i>):	88
4.1.5 Facies 5 (<i>Calcilutites</i>):	90
4.1.6 Facies 6 (<i>Coquina</i>):	93
4.1.7 Facies 7 (<i>Mudstones</i>):	98
4.2 FIELD LOCATIONS	100
4.2.1 Puig Cutri Area (C001)	102
4.2.2 Puig Cutri southern section (C002)	106
4.2.3 Puig Poloni-Puig de Ses Fites (C003)	110
4.2.4 Puig Poloni East (C003s)	115
4.3 DISCUSSION	118
4.3.1 <i>Deposition Model</i>	122
4.3.2 <i>Eustasy and the Cutri Formation: A Sequence stratigraphic framework</i>	125
5. DIAGENESIS AND RESERVOIR PROPERTIES	130
5.1 INTRODUCTION	130
5.2 DIAGENETIC HISTORY	130
5.2.1 <i>Micritisation, micrite coats and seafloor micrite</i>	130
5.2.2 <i>Early isopachous fringe cements</i>	133
5.2.3 <i>Silicification</i>	134
5.2.4 <i>Compaction</i>	138
5.2.5 <i>Burial Cement 1 and continued chemical compaction</i>	141
5.2.6 <i>Microfractures</i>	142
5.2.7 <i>Dolomitisation</i>	143
5.2.8 <i>Fracturing- Calcite Veins</i>	145
5.2.9 <i>Calcification (Dedolomitisation)</i>	146
5.3 DIAGENETIC CONCLUSIONS	147
6. PETROLEUM RESERVOIR PROPERTIES AND CONCLUSIONS	151
6.1 INTRODUCTION	151
6.2 DISCUSSION OF KEY PRODUCING FIELDS	151
6.2.1 RESERVOIR PROPERTIES	152
6.2.2 CONCLUSIONS	153
7. FINAL CONCLUSIONS	155
7.1 SYNOPSIS	155
7.1 FURTHER STUDY	156
REFERENCES	157
APPENDIX A	180
A.1 PREPARATION TECHNIQUES AND OBSERVATION TECHNIQUES	180
A.1.1 <i>Production of acetate peels and thin sections</i>	180
A.1.2 <i>Cathodoluminescence</i>	180

LIST OF FIGURES

Figure 1.1 Line map of study location. Study area outlined in green.	8
Figure 1.2 Location map of study area. Based on CNIG (División 672-IV Artá).	9
Figure 1.3 Geological map of area (with data from IGME, 2010)	10
Figure 1.4 Chronostratigraphy of the Sierra de Levante during the Jurassic Period.	13
Figure 1.5 Summary sedimentary log of the Jurassic Period in the Sierra de Levante. Adapted from Jenkyns et al., (1990); and authors own observations.	15
Figure 1.6 Present day tectonostratigraphic terrains in the western Mediterranean. The Maghrebien-Rif and Betics comprise sediments of Mesozoic and Cenozoic age, which overlie Variscan basement (Azañón et al., 2002; Ábalos et al., 2002; Aurell et al., 2002). These palaeomargins were deformed during the Alpine orogeny and now form the external zones of the two Cordilleras (Ábalos et al., 2002; Aurell et al., 2002), of which Mallorca (within red box) is part.	19
Figure 1.7a An idealised scheme showing the evolution of the Tethys during the Triassic-Jurassic periods, the onset of extension occurring during the Triassic to early Jurassic.	21
Figure 1.7b. An idealised scheme showing the tectonic evolution of the Tethys during the Jurassic Period (adapted from Lagabriele et al. (1984) and Laubscher and Bernoulli, 1977). Oceanic spreading of the Tethys Ocean occurred during the Jurassic-Cretaceous Periods.	21
Figure 2.1. Global palaeogeography of the Earth during the Jurassic Period (adapted from Scotese, 2002). Area of study is indicated by red box.	23
Figure 2.2. A regional palaeogeographical interpretation of the Neotethys during the closure of the Palaeotethys and opening of the proto-Atlantic in the Middle Jurassic; note the position of Mallorca by the green star. During this time a large part of the central and western Iberian plate formed an emergent massif, whilst the surrounding areas were occupied by intracratonic basins that were filled by shallow epicontinental seas (Dercourt et al., 1986; Azañón et al., 2002). The Iberian Massif became isolated due to the opening Pyrenean-Cantabrian basins to the north and the Betic basin to the south. The rifting basins were linked to the separation of Africa from North America. AR- Ammorican Massif, C-S- Corsica-Sardinia High, E- Ebro Massif, IM- Irish Massif, MB- Mesomediterranean block, MC- Massif Central, RHB- Rockall-Hatton block.	28
Figure 2.3 Evolution of sedimentary environments during the opening of the Tethys. The Middle Jurassic sedimentary sequence demonstrates the opening and rifting of the Neotethys Ocean characterised by swells and troughs (Aurell et al., 2002). Open marine conditions prevailed in this area during the Late Jurassic. Radiolarian accumulation characterises this period (adapted from Bernoulli and Jenkyns, 1974)	30
Figure 2.4. Palaeogeography of the Iberian Massif during the Early Jurassic and Middle Jurassic. In the Early Jurassic it is dominated by a vast carbonate platform. The opening Atlantic and Neotethys during Middle Jurassic led to a new NW-SE seaway, and carbonate platforms lined the newly created oceans with isolated carbonate platforms forming with the Tethys. Adapted from Colom and Escandell, 1962; Dercourt et al., 1986 ; Ziegler, 1990; Puga et al., 1993; Aurell, 2002; Vera, 1998; Olóriz, 2000; Golonka, 2007; Martin-Rojas et al., 2009.	33
Figure 2.5. Representation of oceanic surface circulation in the Tethys Ocean during the winter monsoon (A) and the summer monsoon (B). Red box indicates the area immediately around the Iberian massif. Adapted from Arias (2008).	38
Figure 2.6 Schematic illustration of windward and leeward margin characteristics. Note that sand waves migrate off-bank at the windward margin and on-bank at the leeward margin.	40
Figure 3.1 The range of processes that operate in deep sea environments (adapted from Stow, 1994; Reading 1998)	43
Figure 3.2. The Bouma Sequence. Bouma (1962) presented the first classic model for medium-grained sand mud turbidites. This is the result of deceleration of relatively low concentration turbidity currents followed by a progression of bed forms representing fallout during high to low flow regime, and finally deposition from the	

turbidity current tail and then completed by the deposition of pelagic/hemipelagic sediments (adapted from Bouma, 1962 and Reading, 1998).....	48
Figure 3.3 The Lowe (1982) sequence that represents the deceleration of relatively high concentration and coarse grained turbidity currents followed by bed forms representing fallout during a reduction in flow energy, completed by the deposition of pelagic/hemipelagic sediments (adapted from Lowe, 1982 and Reading, 1998).	49
Figure 3.4 The Stow and Shanmugam (1980) sequence representing the deceleration of low concentration and fine grained turbidity currents followed by bed forms representing the reduction in flow energy (adapted from Stow and Shanmugam, 1980).....	50
Figure 3.5 Idealised sedimentary logs of distal and proximal carbonate turbidites (adapted from Einsele, 1998)	53
Figure 3.6 The Haughton et al., (2009) sequence that represents an ideal hybrid event bed, which includes the amalgamation of a turbidite and a debris flow (adapted from Haughton et al., 2009).	56
Figure 3.7 Sedimentary characteristics of individual beds deposited by different processes found in contourites (taken from Reading, 1998)	58
Figure 3.8 Sedimentological log for muddy, silty and sandy contourites (adapted from Stow, 2002; Reading, 1996).....	61
Figure 3.9 Different contourite drift models (adapted from Stow et al., 2002)	63
Figure 3.10 Carbonate apron models adapted from Mullins and Cook (1986).	69
Figure 4.1 Facies types of the Cutri Formation.....	71
Figure 4.2 Examples of Facies 1 contained in channels. Image A photograph with corresponding field sketch of Puig Cutri looking towards the SW. Image B looking at Puig Poloni and a small channel looking towards NE. C photograph and field sketch of oblique view of a channel, looking towards the SW.	73
Figure 4.3 An abundance of clasts types and sizes found in facies 1, and appear 'frozen' in flow (A). In image A note the calcite filled fractures in the clasts (outlined in black) that indicate that they were lithified before resedimentation (Hammer head is 15 cm across; Location C003, 2110 cm). (B) Thin section scan of a debris flow note that this is majority matrix (Location C001, 2150 cm). (C) Thin section scan of a channel fill, note the abundance of tabular extraclasts (arrowed) and chert (white clasts) (Location C003, Channel deposit).....	75
Figure 4.4 Clast type1. Mudstone that consists of tiny abraded fragments of thin shelled bivalves. Note the grainstone matrix (from location C003s). FoV 5.78 x 4.31 mm.	76
Figure 4.5 Clast type 2. Dense assemblage dominated by disarticulated and abraded Posidonia bivalve fragments that are commonly concentrated in regions (from channel deposit at location C003). Note the tabular nature of this clast. FoV 5.78 x 4.31 mm.....	76
Figure 4.6. Outcrop image of Facies 2 in comparison to background sedimentation at location C002. B- graded pebble conglomerate; note the hammer is 30cm in length (C002 approx 475-510 cm). Detail of erosive basal contact between Facies 2 and finer background sediments (C001 approx. 600cm).	80
Figure 4.7 Thin section scan of typical Facies 2 microfacies (C001 515cm). Note the abundance of micritic clasts throughout the sample and finer oolitic-peloid matrix.	82
Figure 4.8. Comparison of microfacies 2 and 3. (A) S1 division of Lowe (1989) found in facies 2, (B) S2 and (C) S3 division of Lower (1989) within facies 3. Note the change in grain size from A-C.	85
Figure 4.9 Outcrop of facies 4.....	88
Figure 4.10 Sedimentary structures of facies 5. All Figures consist of part of a succession of subtle ripples (1-2m wavelength) that dampen up section where planar laminations prevail (note D). Ripple features (10-40 cm wavelength). Top left arrow in image B indicates a large burrow that truncates underlying laminations.	91
Figure 4.11 A and C Outcrop image of facies 5 note the very clear graded sequences in A and bioturbation, wispy laminations and cross bedding in C. B is a photomicrograph of facies 5 note the change in orientation of allochems in off centre position; this is due to bioturbation (FoV 5.78 x 4.31 mm).	91
Figure 4.12 Photomicrograph (FoV 2.89 x 2.15 mm) and outcrop photograph of facies 6	94

Figure 4.13 Photomicrograph and cathodoluminescence view of a Bositra bivalve amongst fine bivalve debris. A and 1 indicate the internal structure of a shell, consisting of calcite crystals oblique to the outer and inner shell surfaces. B and 2 indicate matrix composition (FoV 1.16 x 0.86mm)	95
Figure 4.14 Sedimentary log of accumulation of facies 6 and annotated facies at Location C003.	97
Figure 4.15 Outcrop of facies 7. Note the abundance of chert nodules that follow bedding planes. Hammer 30cm in length.	99
Figure 4.16 Location names found in this report with logging locations. Triangles indicate individual start log locations (sedimentary logs are presented as composite). Based on CNIG (División 672-IV Artá).	101
Figure 4.17 Photograph and field sketch of Abbots, (1989) Puig Cutri Area. Facing ESE.	103
Figure 4.18a Sedimentary log of Puig Cutri Area. Multiple locations combined into a composite log.	104
Figure 4.18b Sedimentary log of Puig Cutri Area continued	105
Figure 4.19 Photograph of major turbidite units found in Puig Cutri Southern Section. Facing NE.....	107
Figure 4.20 Photograph and field sketch of Puig Cutri Southern Section. Facing ESE.....	108
Figure 4.21 Sedimentary log of Puig Cutri Southern Section.....	109
Figure 4.22 Photograph and field sketch of the Puig Poloni-Puig de Ses Fites outcrop. Note the dark coquina facies overlain by much lighter coloured turbidite packages. Facing NE.	111
Figure 4.23 Photograph and field sketch of the Puig Poloni-Puig de Ses Fites. Facing NE.	112
Figure 4.24a Sedimentary log of Puig Poloni-Puig de Ses Fites.	113
Figure 4.24b Sedimentary log of Puig Poloni-Puig de Ses Fites continued.....	114
Figure 4.25 Polished slab of facies 1 in Puig Poloni east outcrop (Appendix B Hand Specimen 350). Note the variety of clast colours indicating a shallow water origin.....	115
Figure 4.26a Sedimentary log of Puig Poloni east	116
Figure 4.26b Sedimentary log of Puig Poloni east continued	117
Figure 4.27. Fence diagram summarizing the 2D associations between facies.....	121
Figure 4.28 Depositional model for final deposition of the Cutri Formation. Note the location of logs which have been incorporated to indicate the spatial distribution of sedimentary geometries illustrated in 2D from Figure 2.27.	124
Figure 4.29 Depositional models for periods during deposition with arrow indicators for flow directions. See key in Figure 4.28.....	124
Figure 4.30 Global relative sea level chart from Haq et al. (1987).	126
Figure 5.1. Photomicrograph (x10 obj.) and CL image illustrating host micrite matrix and micrite coats. A- Microcrystalline matrix hosting calcisiltite sediment displaying a dull luminescence. B- A micritised abraded bivalve fragment. C- Rip-up clast containing a different matrix to host deposit. D- Aggregate grains. E- Micritic ooid with a poor concentric structure. 2-Darker micrite of ooids and other allochems 3-A much brighter luminescence found in other allochems 4- intraclasts derived from the shelf edge. FoV 1.16 x 0.86mm. Appendix B C003 590cm.	132
Figure 5.2 Chert accumulations in the Cutri Formation. A (1175 cm C001), chert forms large isolated nodules (>30 cm in length) and B (1600, C001) forming nodular beds which are rarely over 2 cm thick. Chalcedony is relatively common as replacement and detrital grains in thin section. XPL, FoV 2.89 x 2.15 mm, Appendix B C002 530cm	135
Figure 5.3 Ooids (A), dissolved ooid (B) and silica (C) amongst a micrite matrix and pore filling cement (D). Note the cements associated with stylolite display a different luminescence compared to the host calcisiltite matrix. A silica grain is found at (4) and (5) is the migrating replacing front between silica and calcite. FoV 1.16 x 0.86mm. Appendix B C003 590cm.....	136
Figure 5.4 Note the common calcite fringe that is the replacing front for calcite to silica and ghosts within some silica grains. Dolomite postdates microfractures. A=Chalcedony B=Ghost of replaced allochem C=Microfracture D=Dolomite E=Calcite rim. FoV 2.89 x 2.15 mm. Appendix B C001 1250cm.	137
Figure 5.5. Mechanical compaction. A-Point contacts, B-Longitudinal contacts, C- concavo-convex contacts D- Deformed grains. FoV 5.78 x 4.31 mm. Appendix B C001 560cm.	140

Figure 5.6 Burial cement filling intergranular pore space in close proximity to stylolites cutting across the matrix. FoV 2.89 x 2.15 mm. Appendix B C001 1450cm	141
Figure 5.7 Microfractures that cut the dolomites and any remaining porosity are often filled with dull to non-luminescent calcite that rarely contains bright yellow micropatches. Note the predominance of dolomite crystals along grain edges, microfractures and dissolution seams. FoV 1.16 x 0.86mm. Appendix B C001 2450 cm	144
Figure 5.8 Top image is a cross polar reflective photomicrograph indicating the dominance of iron oxide deposits in the matrix. The middle image, PPL, and bottom image, CL, illustrate selective replacement of dolomite rims has occurred giving the orange luminescence in CL. The cloudy luminescence of the outer bright orange rims is due to the presence of small red spots that are dolomite remnants. FoV 5.78 x 4.31 mm. Appendix B C002 520 cm.	147
Figure 5.9 Diagenetic history of the Cutri Formation.. Red line indicates burial curve.	150

1. INTRODUCTION

1.1 BACKGROUND AND AIMS

This study of the Cutri Formation of Mallorca has been carried out because resedimented carbonates are a relatively unexplored hydrocarbon play with very few fields producing from these types of rocks. The principal aim of this study is to determine the sedimentological and diagenetic processes that control the reservoir properties.

Aims

1. To characterise and understand the processes involved in resedimentation of carbonates of the Cutri Formation.
2. To understand and evaluate the diagenetic history of the Cutri Formation and to understand the reservoir rock properties of these resedimented carbonates. Resedimented carbonate reservoirs are relatively rare, why?

Objectives

1. Literature review of the context and character of the Cutri Formation and of resedimented carbonates in general.
2. Undertake field work so as to create a facies framework.
3. Undertake laboratory work to describe and interpret the rocks through petrographic methods (cathodoluminescence, petrography)

A total of 127 m was logged and 52 thin sections described and interpreted.

1.2 FIELD AREA

This study investigates the Mesozoic sedimentary rocks found in the east of Mallorca, the largest of the Balearic Islands which are located approximately 175 km SE of Barcelona, in the Ligurian Sea.

The investigated strata are well-exposed forming part of the Sierra de Levante that spans the island from the ENE to the SSW. The area of interest where the resedimented carbonates are exposed is between the large towns of Artá and Capdepera (Figure 1.1). The Sierra de Levante forms a range of mountains that reaches nearly 400 m above sea level and forms a series of rolling hills with steep sides and rocky outcrops that reach to the Mediterranean coast.

The outcrops in this study form a distinctive N-S 2 km long ridge reaching heights of 30 m (Figure 1.2). The peaks (“puig” in Catalan) along these ridges give their names to the areas noted within this thesis (Figure 1.3). The outcrop length associated with the Puig Cutri is constrained to just less than 1 km length by a WNW-ESE strike-slip fault to the north and a NE-SW normal fault to the south (Figure 1.4). The ridge is additionally dissected by E-W normal faults, which progressively downthrow the section to the south (Figure 1.4).

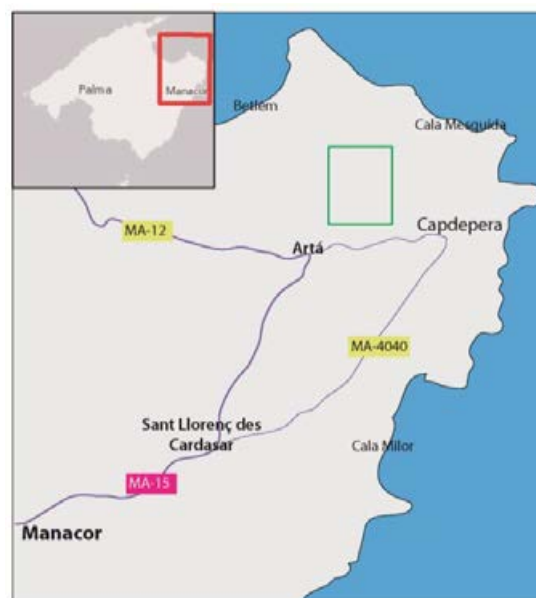


Figure 1.1 Line map of study location. Study area outlined in green.

Geography of the Study Area

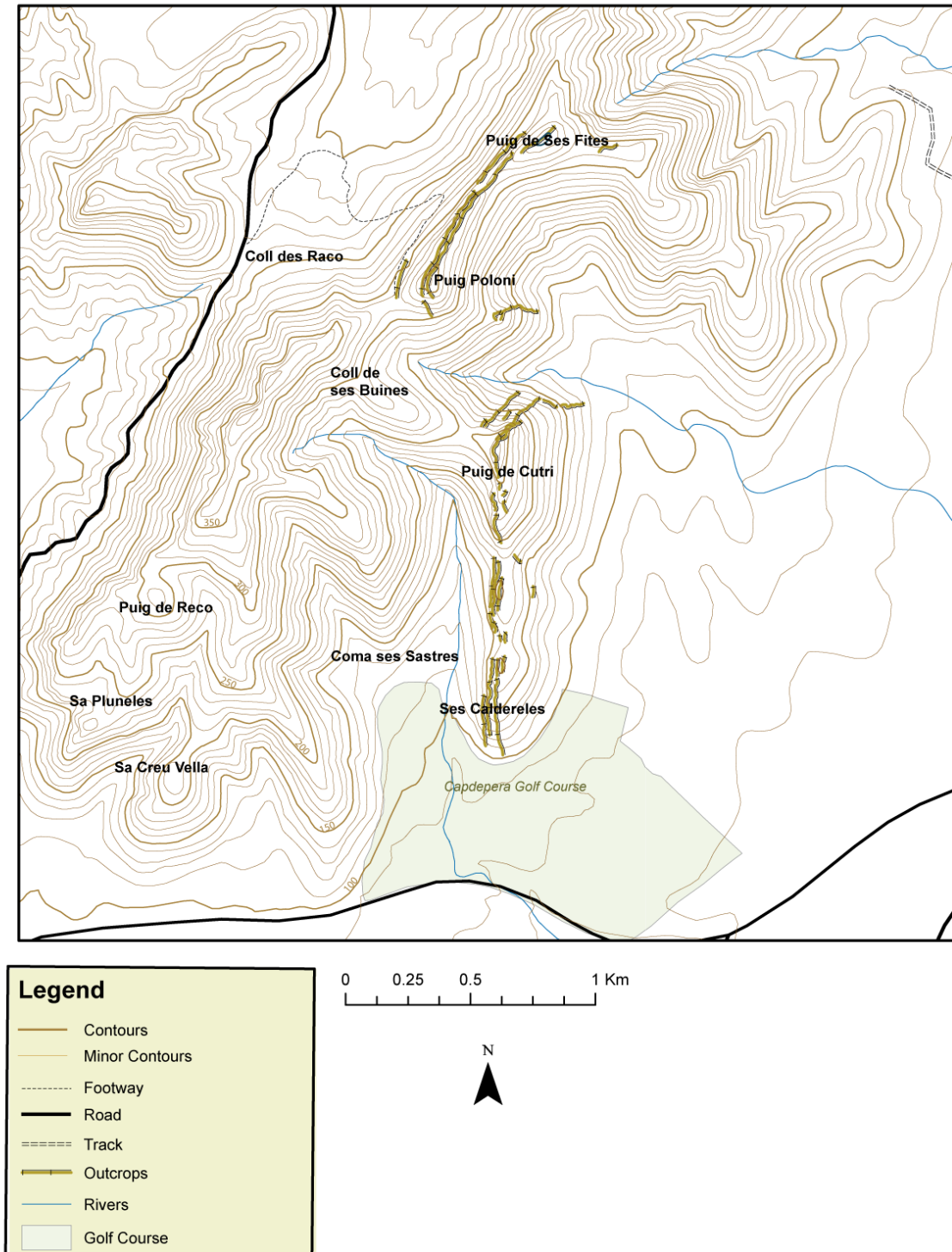


Figure 1.2 Location map of study area. Based on CNIG (División 672-IV Artá).

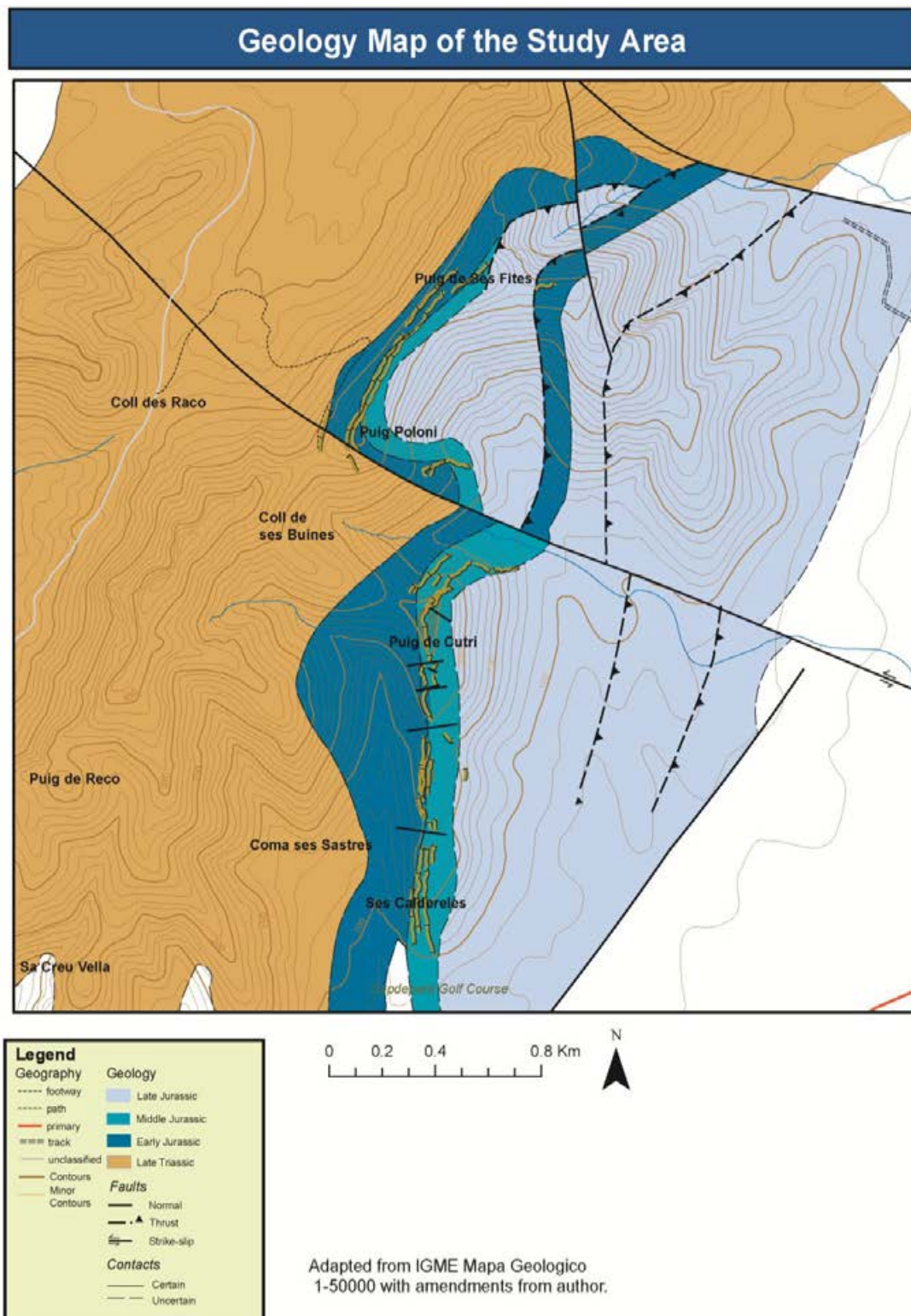


Figure 1.3 Geological map of area (with data from IGME, 2010)

1.3 THE GEOLOGY OF MALLORCA

The geology of Mallorca spans the Late Palaeozoic to the Holocene. Mesozoic rocks are widespread and are mainly found in the mountainous regions of the Sierra de Levante and Sierra Norte (late Palaeozoic rocks crop out in one small area of the Sierra Norte). The Sierra de Levante, the easterly mountainous region, and the higher Sierra de Norte, in the north, illustrate a sedimentological history that records an overall deepening sequence from the complex shallow marine carbonate platforms of the Triassic and Early Jurassic (see section 1.3.1), to the development of rift basins during the Middle Jurassic where sediments were shed from the surrounding platformal source areas (Bernoulli and Jenkyns, 1974; Alvaro *et al.*, 1984a), to the oceanic basinal radiolarian facies of the Late Jurassic and Cretaceous (Bernoulli and Jenkyns, 1974; Aurell *et al.*, 2002) associated with the opening of the Atlantic Ocean. The Middle Jurassic Cutri Formation is found within this sequence as a thin division along a 10 km NNW-SSE ridge. During the Middle Jurassic, a complex block and basin palaeotopography existed which was controlled by strike-slip tectonics that created the two major structural units, represented by the Sierra Norte and Sierra de Levante today (Aurell *et al.*, 2002).

Palaeogene to Neogene rocks are widespread over Mallorca, these rocks recording convergence of the Iberian plate with the African and European plates which resulted in two Alpine mountain ranges, the Pyrenean-Basque-Cantabrian and the Betic-Balearic (Alonso-Zarza *et al.*, 2002). The distribution of Palaeogene-Neogene rocks is mainly between the areas of elevated Mesozoic strata. These intervening graben areas are filled by Upper Miocene and younger sediments that can be >1000 m thick (Benedicto *et al.*, 1993). Mallorca's Palaeogene-Pliocene geology has been divided into nine sequences that comprise the pre-orogenic, syn-orogenic and post-orogenic sequences (Alonso-Zarza *et al.*, 2002). Quaternary strata on Mallorca are primarily found as marine terraces (Goy *et al.*, 1997), alluvial fans (Gutiérrez-Elorza *et al.*, 2002), aeolian and fluvial deposits.

1.4 STRATIGRAPHY AND SEDIMENTOLOGY OF THE JURASSIC

The Jurassic stratigraphy in the Sierra de Levante illustrates the shifting sedimentary environments associated with the rifting of the Neotethys Ocean, which resulted in the emergence of the Proto-Atlantic during the Late Jurassic (Bernoulli and Jenkyns, 1974; Alvaro *et al.*, 1984a, 1989; Ziegler, 1990; Vera, 1998). The sedimentology of the study area is summarised by Figure 1.5 and the chronostratigraphic relationships between sediments are indicated in Figure 1.6.

The oldest sediments in the area are in the Mal Pas Formation, which consists of a 100 m thick dolomitic (partly brecciated) (Figure 1.5 and 1.6) sequence that has been dated to the Hettangian (Aurell *et al.*, 2002; Figure 1.6). Overlying this is the Sóller Formation, which represents a shallowing-up sequence in its oldest part (Es Barraca Limestone) and dated as Sinemurian-Pliensbachian by biostratigraphic analysis. The study area focuses on the lower carbonate slope environment during the Callovian to Oxfordian by which time carbonate ramps that lined the Neotethys Ocean were broken up and isolated due to the rifting of the Neotethys. The following stratigraphy tells the story of this break-up. This stratigraphic evolution is illustrated by Figure 1.6 which indicates the beginning of tectonic activity and opening of basins associated with the increasing influence of the rifting Neotethys (Bernoulli and Jenkyns, 1974).

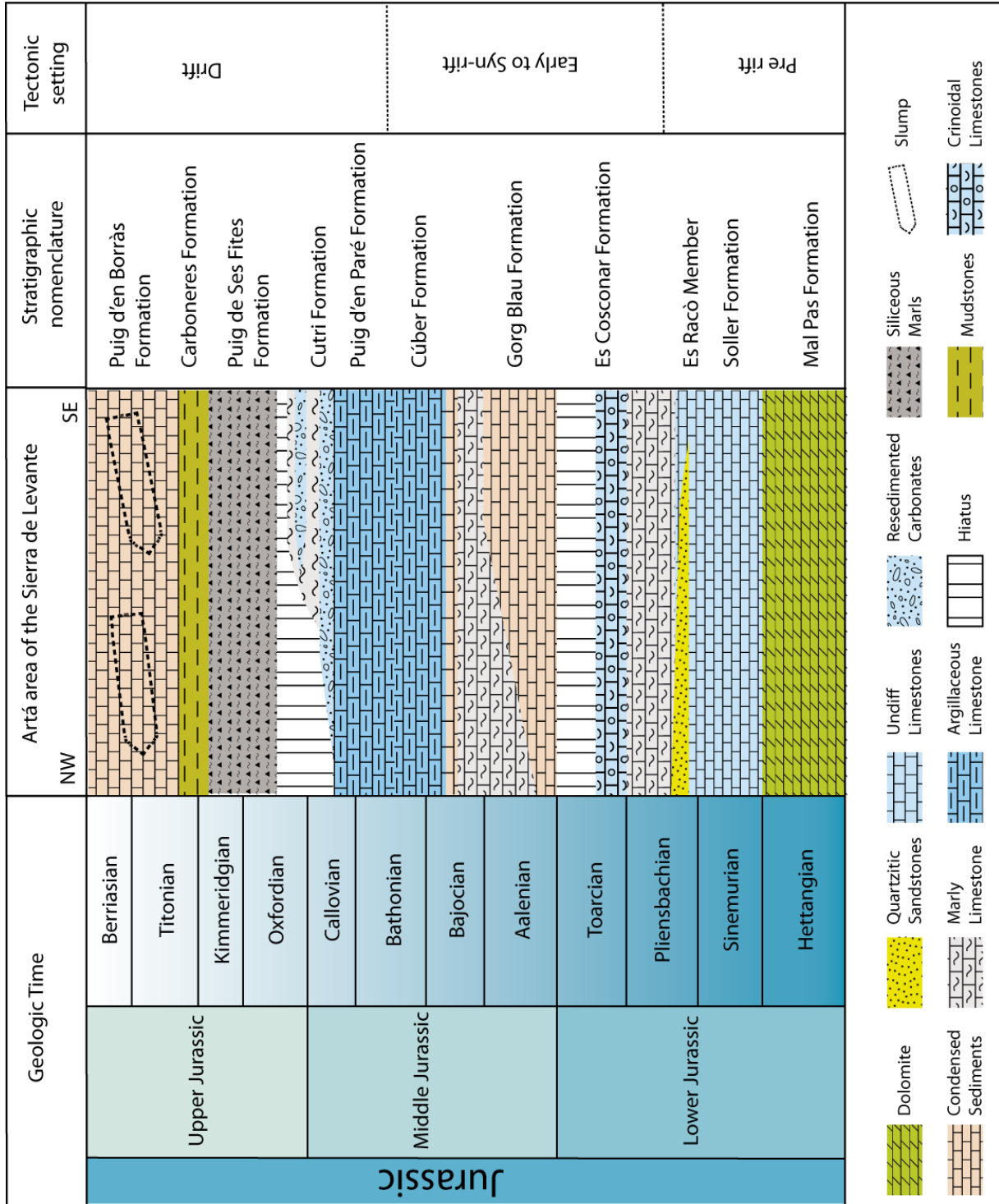


Figure 1.4 Chronostratigraphy of the Sierra de Levante during the Jurassic Period.

The Es Racó Quartzitic Sandstone Member is early Pliensbachian in age and associated with instability of the slope environment. Lying above is the Es Cosconar Formation which contains marls and crinoidal limestones and is capped by a ferruginous hardground, which suggests a period of reduced sedimentation (Figure 1.5; 1.6). Lying directly on top of the Cosconar Formation is a ferruginous horizon which separates the Es Corconar and Gorg Blau Formations in the study area, containing a mix of Upper Toarcian to Lower Aalenian ammonite assemblages (Alvaro *et al.*, 1989; Goy *et al.*, 1995; Figure 1.6). This ferruginous layer is a condensed sequence known from around the Tethys as *Ammonitico Rosso*. These contain winnowed iron-rich ammonite debris (Goy *et al.*, 1995), marly limestones containing ammonites from the Late Toarcian and Aalenian, and nodular and in some areas well bedded limestones containing Early Bajocian ammonites. This is overlain by a thin (5 m) Mid-Late Aalenian succession of partially nodular red-limestones, coquinas and a succession of stratified grey marly limestone and marls of the Gorg Blau Formation (Alvaro *et al.*, 1989; Sandoval, 1994; Figure 1.6). Capping the Gorg Blau Formation is a bioturbated, winnowed ferruginous hardground.

Bajocian and earliest Bathonian sediments include an approximately 50 m thick succession of sediments representing the Gorg Blau, Cuber and the lower part of the Puig d'en Paré Formations (Figure 1.6). These sediments consist of bioturbated (*Zoophycos* and *Chondrites*) well bedded grey marly limestones, cherty limestones, thin interbedded grey marls and locally occurring coquina microfacies. The Early Bathonian interval is represented by the uppermost Puig d'en Pare Formation (Figure 1.6), which consists of a few centimetres of nodular limestone with abundant *Posidonia* bivalves and rare radiolarians. A hiatus is interpreted to occur in the Middle-Late Callovian (recorded as a maximum time gap of Bathonian-middle Oxfordian by Caracuel *et al.*, 1995), where the carbonate slope stopped prograding and became unstable, possibly due to sea-level change and/or palaeogeographical influences. The only exception to this stratigraphic gap, in the whole of Mallorca, is the accumulation of Middle Bathonian-Callovian sediments in the study area represented by the accumulation of strongly laminated carbonate muds and silts (Alvaro *et al.*, 1984a; Pomar, pers. com 2010; Abbots, 1989) that are punctuated by oolitic pack-grainstone calciturbidites of the Cutri Formation (Figure 1.6). The muddy

interbedded units of the Cutri Formation are of similar nature to the Cuber Formation where the resedimented oolites of the Cutri Formation, represent temporary disruption to background hemipelagic sedimentation. The Middle Jurassic represents the rifting stage of the opening of the Neotethys (Figure 1.6).

The Late Jurassic in the studied area is represented by the lower slopes of a carbonate shelf in open marine conditions. Siliceous marls and marly limestones of the Puig de Ses Fites Formation (Middle-Late Oxfordian), are interpreted to have been deposited during the opening of the Proto-Atlantic and the initiation of pelagic deposition associated with oceanic conditions.

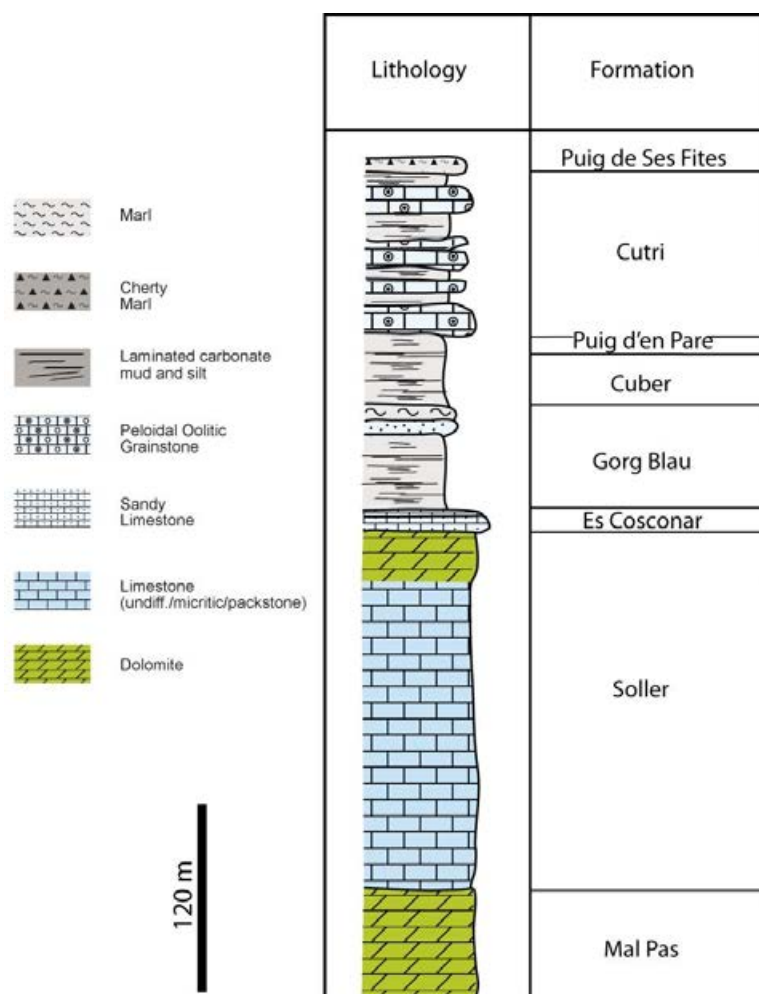


Figure 1.5 Summary sedimentary log of the Jurassic Period in the Sierra de Levante. Adapted from Jenkyns et al., (1990); and authors own observations.

1.4.1 DATING OF THE CUTRI FORMATION

Underlying the Cutri Formation is the Cuber Formation, which consist of marls and limestones, and contain radiolaria and ammonites that have been correlated with the upper part of the Puig d'en Paré Formation (Caracuel *et al.*, 1995; Figure 1.6). This has led to better evaluation of the stratigraphic gap in the Middle-Late Callovian and Early-Mid Oxfordian suggesting a Mid-Late Callovian onset date for the carbonate turbidites of the Cutri Formation.

The lack of any age-diagnostic microfauna within the Cutri Formation prevents accurate biostratigraphic determination. However, it is overlain by the Puig de Ses Fites Formation, which is rich in radiolarians (Abbots, 1989) that are indicative of deep environments (Racki and Cordey, 2000). Radiolarian cherts are abundant throughout the western Tethys during the Callovian-Oxfordian (e.g. Baudin *et al.*, 1988; Baudin and Lachkar, 1990; Danelian and Baudin, 1990; Weissert, 1994; Aurell *et al.*, 2002) suggesting a probable Late Callovian-Early Oxfordian date for the end of deposition of the Cutri Formation. The radiolarites and radiolarian cherts found elsewhere in rocks of the western Tethys Ocean correlate with the onset of drift tectonics, where sedimentation styles changed in the latest Bathonian producing condensed facies, like the *Ammonitico Rosso*, throughout the Callovian-Oxfordian. This change was brought about as the region developed a connected seaway between the Tethys Ocean and the Proto-Atlantic Ocean. Therefore, it is probable that the termination of Cutri Formation deposition took place during this major palaeogeographical and oceanographic change in the Callovian. Hence the overlying Puig de Ses Fites Formation possibly represents the Middle-Oxfordian to Middle Kimmeridgian (Figure 1.6).

1.5 PRESENT TECTONIC SETTING: TECTONICS OF THE BETIC CORDILLERA AND THE BALEARIC ISLANDS

The largest of the Balearic Islands is Mallorca followed in rank size by Menorca, Ibiza, Formentera and Cabrera. These islands are the surface expression of the mostly submerged Balearic Promontory that has been interpreted as the NE extensional zone of the Betic Cordillera, (Gelabert-Ferrer, 1998; Bourrouilh, 1973; Azéma *et al.*, 1971; Banda *et al.*, 1981; Vera, 1988; Figure 1.7). The Betic Cordillera is a mountain system in the south and southeast of Spain, which forms along the south coast of Spain from Cadiz through Andalusia to Murcia and all the way through Valencia and extending as a submerged promontory into the Mediterranean where it is exposed as the Balearic Islands (Figure 1.7). The Betic Cordillera is related directly to the Rif Cordillera in Morocco (Moratti and Chalouan, 2006). The Rif Cordillera is found to the south of the Betic Cordillera and follows the Moroccan coast from Tangier to the Moulouya River in eastern Morocco (Figure 1.7).

Together, the Betic and Rif Cordilleras lie to the north and south of the Alborán Sea and presently form an arc-shaped mountain belt joining across the Straits of Gibraltar. The arc developed throughout the Mesozoic-Cenozoic convergence of the African and Eurasian plates (Dewey *et al.*, 1989; Comas *et al.*, 1992, 1999; Ábalos *et al.*, 2002) and now show their configuration as an arc due to the westward movement of the Alborán Microplate (García-Dueñas and Balanyá, 1986).

The Betic and Rif Cordilleras expose a succession of rocks from the Mesozoic (Azañón *et al.*, 2002; Ábalos *et al.*, 2002; Aurell *et al.*, 2002), which have been deformed by the Alpine orogeny. The cordilleras represent the palaeomargins of the Iberian and African plates respectively and record the evolution and interaction of the Eurasian-African plate boundary during the Mesozoic (Azañón *et al.*, 2002; Ábalos *et al.*, 2002; Aurell *et al.*, 2002). The intensity of deformation within the Betic Cordillera is characterised by packaging the cordillera into internal and external zones (Figure 1.7). The internal zone was affected by Alpine events before the Early Miocene, and has a complex and varied metamorphic history, whilst the external zone is unmetamorphosed and characterised as a thin-skinned fold and thrust belt formed

by shortening of the Mesozoic and Tertiary cover of the original south Iberian margin (Figure 1.7).

The Balearic Islands form part of the southern Iberian palaeomargin and are most closely associated with the external Sub-Betic of southern Spain, where Jurassic to Cretaceous sediments are characteristically of deep-water affinity (Garcia-Hernandez *et al.*, 1980; Ruiz-Ortiz, 1983; Vera, 1988). The Balearic Promontory consists of continental crust of crystalline Hercynian basement (Banda *et al.*, 1981; Abbotts, 1989) and serves to separate the thinned continental crust of the North Balearic Basin (or Valencia Trough).

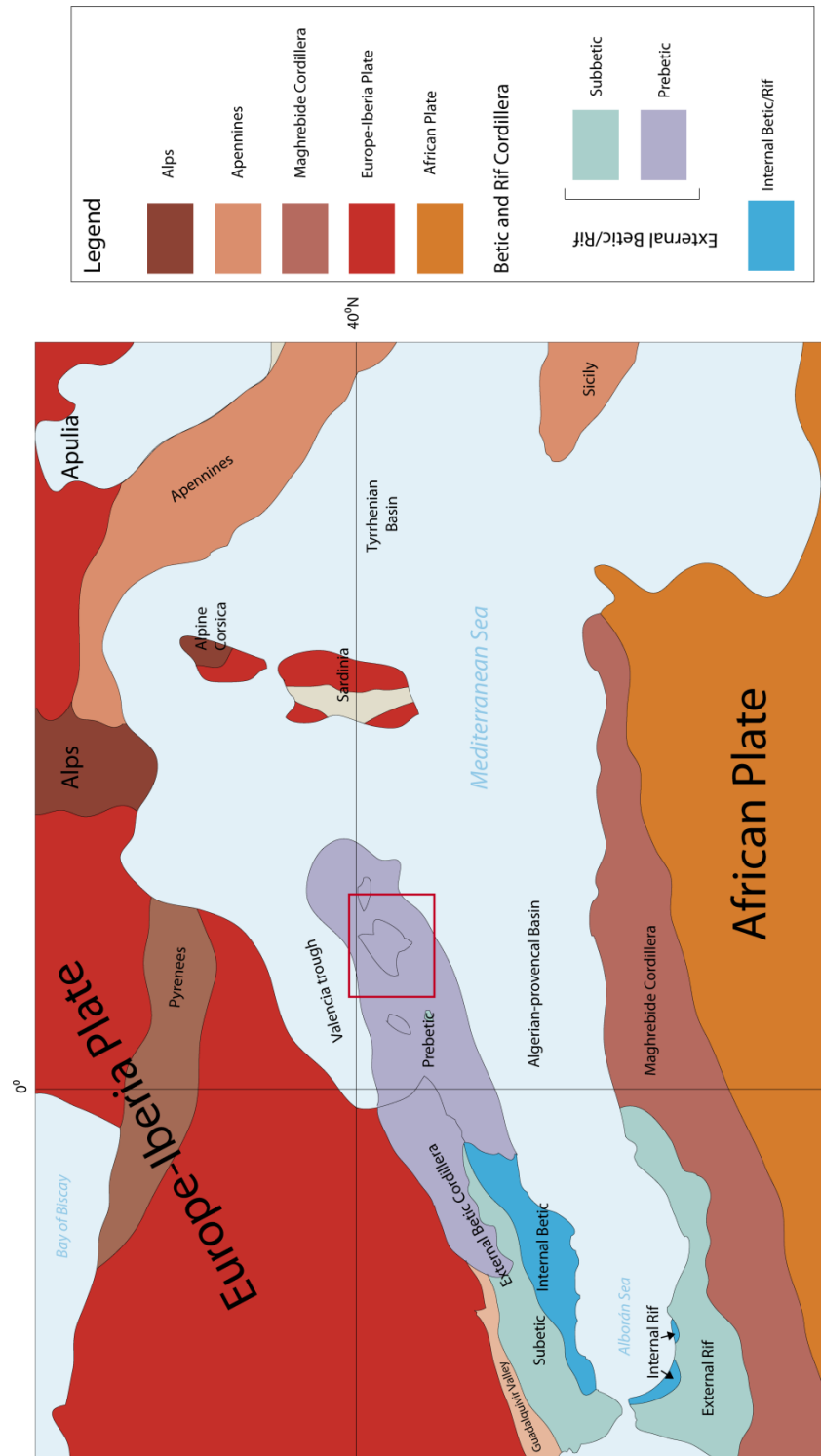


Figure 1.6 Present day tectonostratigraphic terrains in the western Mediterranean. The Maghrebian-Rif and Betics comprise sediments of Mesozoic and Cenozoic age, which overlie Variscan basement (Azañón et al., 2002; Ábalos et al., 2002; Aurell et al., 2002). These palaeomargins were deformed during the Alpine orogeny and now form the external zones of the two Cordilleras (Ábalos et al., 2002; Aurell et al., 2002), of which Mallorca (within red box) is part.

1.5.1 THE BETIC CORDILLERA

Post-Hercynian evolution of the Betic Cordillera began in the Mesozoic, when southern Spain constituted the margin of the Iberian Massif and underwent primarily extensional tectonics associated with opening deformation of the Tethyan Ocean (Lagabriele *et al.*, 1984; Lemoine *et al.*, 1987; Laubscher and Bernoulli, 1977; Ábalos *et al.*, 2002; Figure 1.8a). Palaeogeographical reconstructions indicate that the maximum distance between Iberia and Africa was less than 200 km during the Early to Middle Jurassic (Dercourt *et al.*, 1986; Ziegler, 1990) and that a large transform fault relating to the opening of the Tethys and the Atlantic Ocean separated the two (Martin-Rojas, 2009). Continental thinning in this tectonic regime may have progressed to the beginnings of oceanic spreading (Lagabriele *et al.*, 1984; Ábalos *et al.*, 2002).

The rocks of the Betic Cordillera can be divided broadly into the Prebetic and Subbetic zones according to the proximity of deposition to the Iberian margin (Figure 1.7). The Prebetic zone crops out mainly in the eastern sector of the Cordillera and mainly consists of Triassic to Miocene (Tortonian) platform carbonates, although there are local siliciclastic deposits. The Subbetic zone crops out further south as an ENE-WSW orientated belt comprising rocks of Triassic to Miocene age, that are mostly carbonates with some basalts. Whilst the Triassic-Lower Jurassic rocks show continental or shallow marine facies, those of the Middle to Upper Jurassic constitute shallow-platform to pelagic facies (Lagabriele *et al.*, 1984; Azañón *et al.*, 2002).

The Prebetic was located proximally to the Iberian margin and the Subbetic located basinwards. During the Jurassic, the region was broken up by normal faults in a basin-and-swell structure that determined the differences seen in the sedimentary record (Chapter 1; Bernoulli and Jenkyns, 1974; Azañón *et al.*, 2002). The internal zone was probably located eastward of its current location in the Algiers-Balearic Basin.

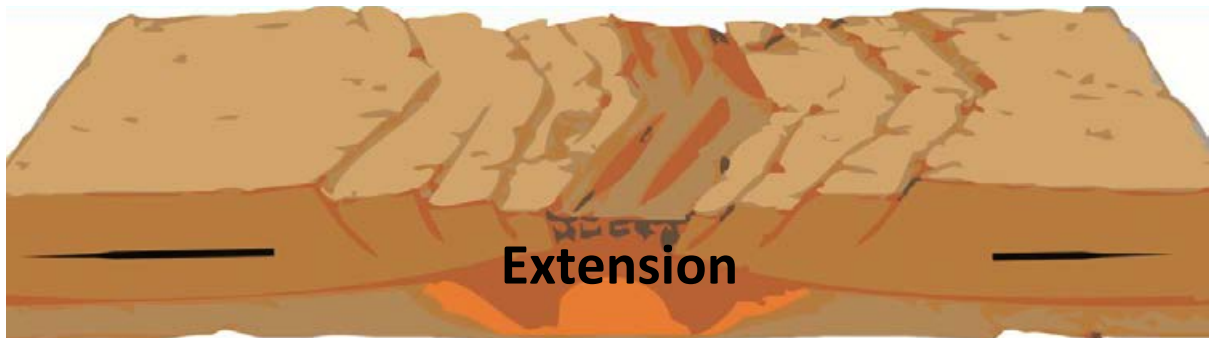


Figure 1.7a An idealised scheme showing the evolution of the Tethys during the Triassic-Jurassic periods, the onset of extension occurring during the Triassic to early Jurassic.



Figure 1.7b. An idealised scheme showing the tectonic evolution of the Tethys during the Jurassic Period (adapted from Lagabrielle et al. (1984) and Laubscher and Bernoulli, 1977). Oceanic spreading of the Tethys Ocean occurred during the Jurassic-Cretaceous Periods.

2. GEOLOGICAL SETTING

2.1 GLOBAL PALAEOGEOGRAPHY DURING THE TRIASSIC TO CRETACEOUS

During the Triassic-Jurassic all major continents formed the supercontinent Pangaea (Golonka, 2007; Dercourt *et al.*, 1993; Stampfli and Borel, 2004; Figure 2.1).

Pangaea was centred over the equator and spanned latitudes 80°N to 80°S with a characteristic wedge-shaped sea incising into its eastern margin, the Tethys Ocean (Dewey *et al.*, 1989; Smith *et al.*, 1973; Bju-Duval *et al.*, 1977; Dercourt *et al.*, 1985; Ziegler, 1988; Van der Voo, 1993; Scotese, 2002; Golonka and Kiessling, 2002; Golonka, 2007; Arias, 2008; Figure 2.1). Pangaea constituted two large landmasses: Laurasia (N America and the majority of the Eurasian plate) to the north and Gondwana (S America, India, Australia and Antarctica), to the south of the Tethys Ocean (Scotese, 2002; Golonka, 2007; Figure 2.1).

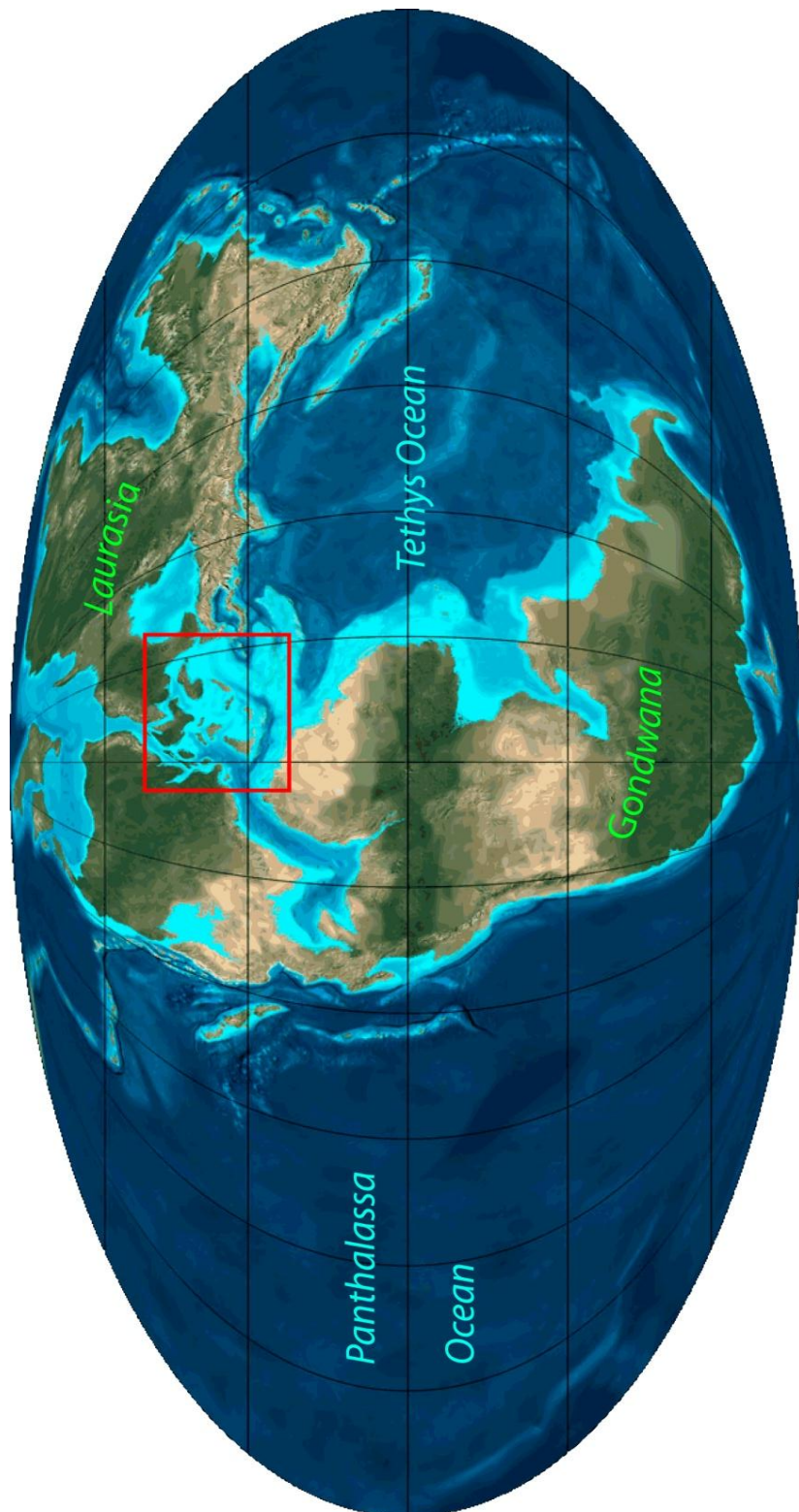


Figure 2.1. Global palaeogeography of the Earth during the Jurassic Period (adapted from Scotese, 2002). Area of study is indicated by red box.

2.2 TECTONIC SETTING OF THE WESTERN MEDITERRANEAN DURING THE LATE TRIASSIC TO EARLY CRETACEOUS

The post Triassic palaeogeography of the western Mediterranean, and more specifically the area around the Ligurian Ocean, has been presented via an overarching model, the Liguria Mode (Piccardo, 2006). This model divides the Triassic-Cretaceous period into three phases associated with the opening and subsequent closure of the Ligurian Ocean (Piccardo and Vissers, 2007; Piccardo, 2008). These three stages are described below:

- **Late Triassic-Early Jurassic:** The extensional pre-drift evolution of the lithosphere led to the opening of the Ligurian Tethys. This has been estimated to date to 220 Ma to 180 Ma, with the minimum time being given by dated igneous intrusions (e.g. Tribuzio *et al.*, 2004)
- **Mid-Jurassic:** this is the drifting-to-rifting phase where progressive thinning of the continental lithosphere induced adiabatic upwelling, which culminated with the onset of shear zones, block-faulting (Vissers *et al.*, 1991), and the start of sea-floor spreading in the latest Bathonian to Callovian.
- **Upper Jurassic to Cretaceous:** Oceanic spreading where complete failure of the continental crust and direct exposure of peridotites (cropping out in the Western Alps and Northern Apennines in NW Italy) on the sea floor began (Piccardo, 2008). This sea-floor spreading continued until the Neotethys closure in the Cretaceous, and culminated in the Subbetic Orogeny during the Neogene.

2.3 PALAEOTETHYS LATE TRIASSIC-EARLY JURASSIC: A PALAEOGEOGRAPHIC PERSPECTIVE

The Mediterranean region was a united landmass at the end of the Palaeozoic, formed by the Hercynian Orogeny. By the Late Triassic to Early Jurassic, the area was of low relief, having reached an advanced stage of peneplanation by the end of the Permian. By the beginning of the Mesozoic the Tethys Ocean was already thousands of kilometres wide (Dercourt *et al.*, 1993; Ziegler, 1982; Golonka, 2007), and extending further by northern subduction and southern distention and rifting. During the Middle Triassic, the Tethys Ocean started to transgress westwards in response to downwarping of the present Atlantic margins as pre-drift extension commenced. This transgression gave rise to the development of marine conditions, typically recorded by initial deposition of thick evaporites followed by shallow water carbonates as seen in the Betic Cordillera and the Rif Cordillera. Basic volcanism in the Middle to Upper Triassic facies of the Betic Cordillera suggests that drifting/rifting may have started as early as the Early Triassic in the Betic Cordillera of southern Spain (Morata, 1993).

By the Middle Triassic, a shallow epeiric sea existed over the most part of the European platforms, and carbonate platform facies were widespread and persisted well into the Lower Jurassic (e.g. Southern Alps, Bosellini *et al.*, 1981b; Northern Pyrenees, Sander, 1970). Growth of these platforms was enhanced by strong subsidence that was balanced by increased production rates forming widespread, extensive carbonate platform sequences, hundreds to thousands of metres thick. The Upper Triassic marks the commencement of the pre-drift extension and rifting that was to shape the western Tethys and the Atlantic margin for the next 35 million years.

In the Late Triassic to Early Jurassic, a widespread belt of doming and rifting divided the former Pangaea into Gondwanaland and Laurasia along the Gulf of Mexico-Central Atlantic-Western Tethys line. Tensional features were widespread on both sides of the Atlantic and throughout the Tethys during this time (Vissers *et al.*, 1991). In western Tethys early continental distention, often accompanied by basaltic volcanism, was widespread.

The increasing tectonic activity during this time is evidenced by faulting and fissure-related mafic volcanism (e.g. Ragusa Zone (Patacca et al, 1979) as well as common tuff intercalations and neptunian dykes and sills in carbonate platform sediments of Mallorca and the northern Pyrenees.

Continued extension throughout the western Tethys led to widespread faulting that broke the extensive carbonate platforms into a complex series of fault-bounded tilt blocks and basins, which underwent differential subsidence as extension proceeded. This facies trend is seen on both the northern and southern continental margins of the western Tethys and is characterised by the development of carbonate facies, varying with depth and current strength.

Throughout the Jurassic, Africa moved west laterally with respect to Europe, causing the narrowing of the eastern Tethys by subduction along its northern margins and extension in the western Tethys and the central Atlantic. Jurassic oceanic crust and consequently true oceanic environments have been interpreted to exist between Iberia and Africa southwards from the Betic External Zones during this time (Argyriadis *et al.*, 1980; Puga, 1980; Puga *et al.*, 1993, 1995). The age postulated for the appearance of this oceanic crust varies from earliest Jurassic to mid-Early Jurassic (Bourgois, 1980), whilst Laubscher and Bernoulli (1977) suggested the area was connected to the Atlantic by the Early to Mid Jurassic.

2.4 MID-JURASSIC: OPENING OF THE NEOTETHYS OCEAN AND END OF THE PALAEOTETHYS: A PALAEOGEOGRAPHIC PERSPECTIVE

Palaeotethys closure was in its last stage during the Early Jurassic. South China, North China, Indo-china, and Southeast Asia had already amalgamated during the Norian stage. The Qiantang microplate was in the final stage of collision (Sengör, 1984; Dercourt *et al.*, 1993; Sengör and Natalin, 1996; Jolivet *et al.*, 2001) that led to the Palaeotethys closure. During closure of the Palaeotethys, the Africa-Arabia plate rotated to the NE facilitating closure (Vera, 1998; Golonka, 2007). In addition, during the Mid-Jurassic, a basin formed shortly before the Palaeotethys Ocean was completely closed at the eastern end: this is the Neotethys Ocean (Golonka, 2007; Arias, 2008). After the collision of the Chinese plates, a new northward-dipping

subduction zone developed along the northern margin of Neotethys (Ziegler, 1990; Golonka, 2007), south of the accreted continent. Extensive volcanism would likely have occurred along this zone.

The closure of Palaeotethys created a vast system of mountains, extending from what is now Spain to Eastern Europe (Moores and Fairbridge, 1998). Neotethys increased in width diachronously (Stampfli, 2001) during this orogeny opening at the same time as the central and south Atlantic during the Middle Jurassic (Golonka, 2004; Golonka, 2007). Bill *et al.*, (2001) date the onset of oceanic spreading in Neotethys as Bajocian, but there is some evidence of rifting between Africa and the Iberian Massif as early as the Triassic (Morata, 1993).

2.5 NEOTETHYS MID TO LATE JURASSIC RIFTING AND DRIFT

Westward extension created the Ligurian Ocean, the sea north of Mallorca and south of Barcelona, where sea-floor spreading commenced simultaneously with the central Atlantic (Figure 2.2), in the Late Bathonian to Callovian. This oceanic crust related to oceanic basins of Middle Jurassic age, which separated the Betic External Zone from the Internal Zones in the Alborán Domain. In these basins a swell-trough physiography has been interpreted in an area which was later to become the Nevado-Filábride Complex (Guerrera *et al.*, 1993; Puga *et al.*, 1993; Figure 2.3). The narrow and deepening seaway between Africa and Europe created by this extension was the Ligurian Ocean. The appearance of the first oceanic crust in the Ligurian Ocean, and therefore the commencement of drift between Europe and Africa, did not occur until the Late Bathonian or Early Callovian, this event corresponds to the onset of drift in the central Atlantic. During the preceding syn-rift phase, Africa had moved about 250 km west with respect to Europe, creating the extension observed over western Tethys.

The evolution of the Ligurian Ocean was governed by extensional tectonics and long-term strike-slip and transform lateral motions. In this tectonic regime the general downward movement of some fault blocks was interrupted by episodic still-stand and uplift. During the Mid to Late Jurassic the Sierra de Levante in the east of Mallorca

served to separate a platform source area to the ESE from a submerged pelagic plateau to the WNW, represented by the present day Sierra Norte.

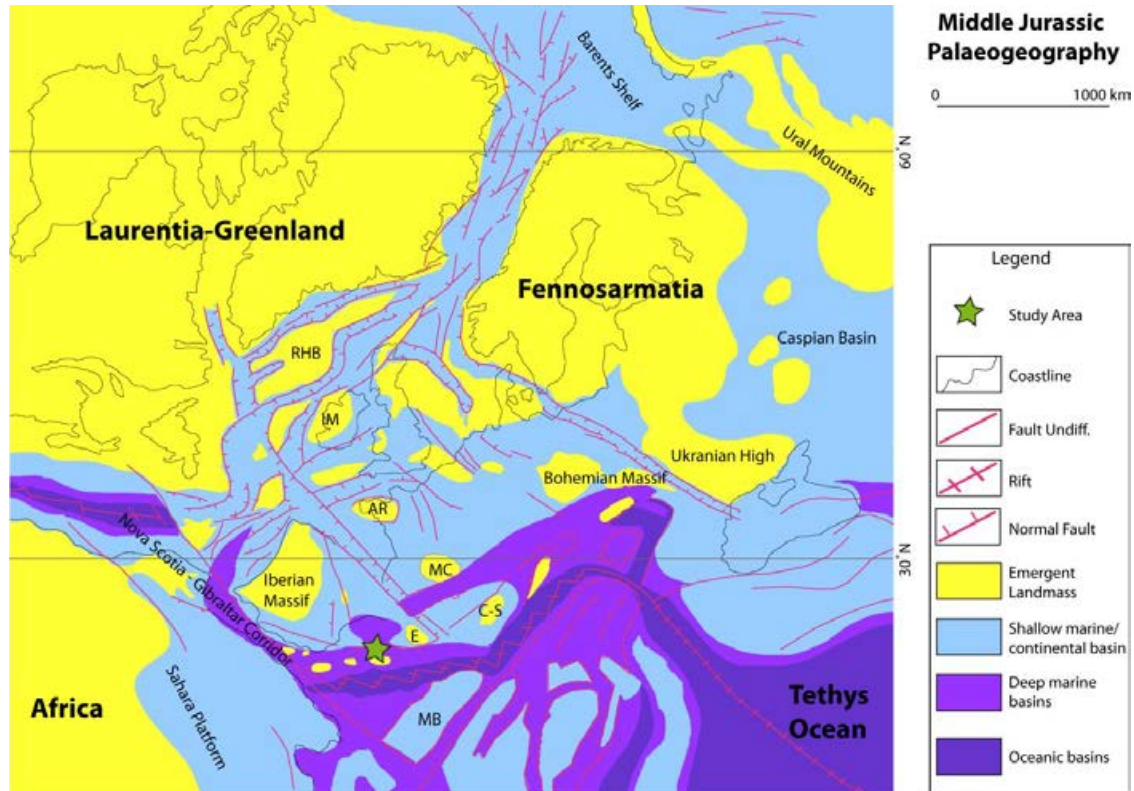


Figure 2.2. A regional palaeogeographical interpretation of the Neotethys during the closure of the Palaeotethys and opening of the proto-Atlantic in the Middle Jurassic; note the position of Mallorca by the green star. During this time a large part of the central and western Iberian plate formed an emergent massif, whilst the surrounding areas were occupied by intracratonic basins that were filled by shallow epicontinental seas (Dercourt et al., 1986; Azañón et al., 2002). The Iberian Massif became isolated due to the opening Pyrenean-Cantabrian basins to the north and the Betic basin to the south. The rifting basins were linked to the separation of Africa from North America. AR- Ammorican Massif, C-S- Corsica-Sardinia High, E- Ebro Massif, IM- Irish Massif, MB- Mesomediterranean block, MC- Massif Central, RHB- Rockall-Hatton block.

During the opening of the Neotethys the majority of western Europe was divided into several small fault-bounded massifs (emergent areas). These were surrounded by an expansive, tectonically active carbonate platform with a single larger continental craton open to the east, running parallel to the Asian landmass (Figure, 2.2).

Carbonate sedimentation predominated along Neotethyan margins, between 35°N and 35°S latitudes (Ziegler, 1990; Dercourt *et al.*, 1993; Kiessling *et al.*, 1999; Golonka and Ford, 2000; Leinfelder *et al.*, 2002; Kiessling *et al.*, 2003; Figure, 2.2). The north-western Neotethys region consisted of numerous tectonic blocks capped by carbonate platforms with adjacent graben filled with deeper-water pelagic carbonate sediments and organic-rich shale facies (Bernoulli and Jenkyns, 1974; Aurell *et al.*, 2002; Figure 2.2). This tectonic situation created the palaeotopography described by Bernoulli and Jenkyns, (1980). As a consequence a range of shallow platform grainstones to argillaceous deeper-water carbonates accumulated on the passive margin shelves of the western Neotethys. In contrast, mixed carbonate–evaporite facies were deposited on the platform areas on the Arabian Peninsula and also on the northern Africa margins (Jassim and Goff, 2006) and siliciclastic deposition prevailed in the northern Africa interior (Golonka and Ford, 2000).

The separation of North America from Gondwana was initiated in the Mid-to-Late Triassic by a rifting phase (Favre & Stampfli 1992; Steiner *et al.*, 1998; Morata, 1993; Golonka, 2007) that continued during Early–Middle Jurassic time and into the Cretaceous period (Golonka and Ford, 2000; Ford and Golonka, 2003). This rifting is evidenced by the continental siliciclastics and volcanics that formed in the area located between Africa and North America (Golonka, 2007). Evidence of seafloor-spreading is dated as Toarcian in the Canary Islands (Carracedo *et al.*, 2002). These volcanics belong to the Central Atlantic Magmatic Province (CAMP; Golonka, 2007), one of the largest known Phanerozoic flood basalt provinces (e.g. Olsen, 1997; Withjack *et al.*, 1998; Marzoli *et al.*, 1999, 2004; Hallam, 2002). This spreading coincides with the Triassic-Jurassic mass extinction event impacting carbonate deposition at this time (Marzoli *et al.*, 1999, 2004; Pálffy *et al.*, 2000).

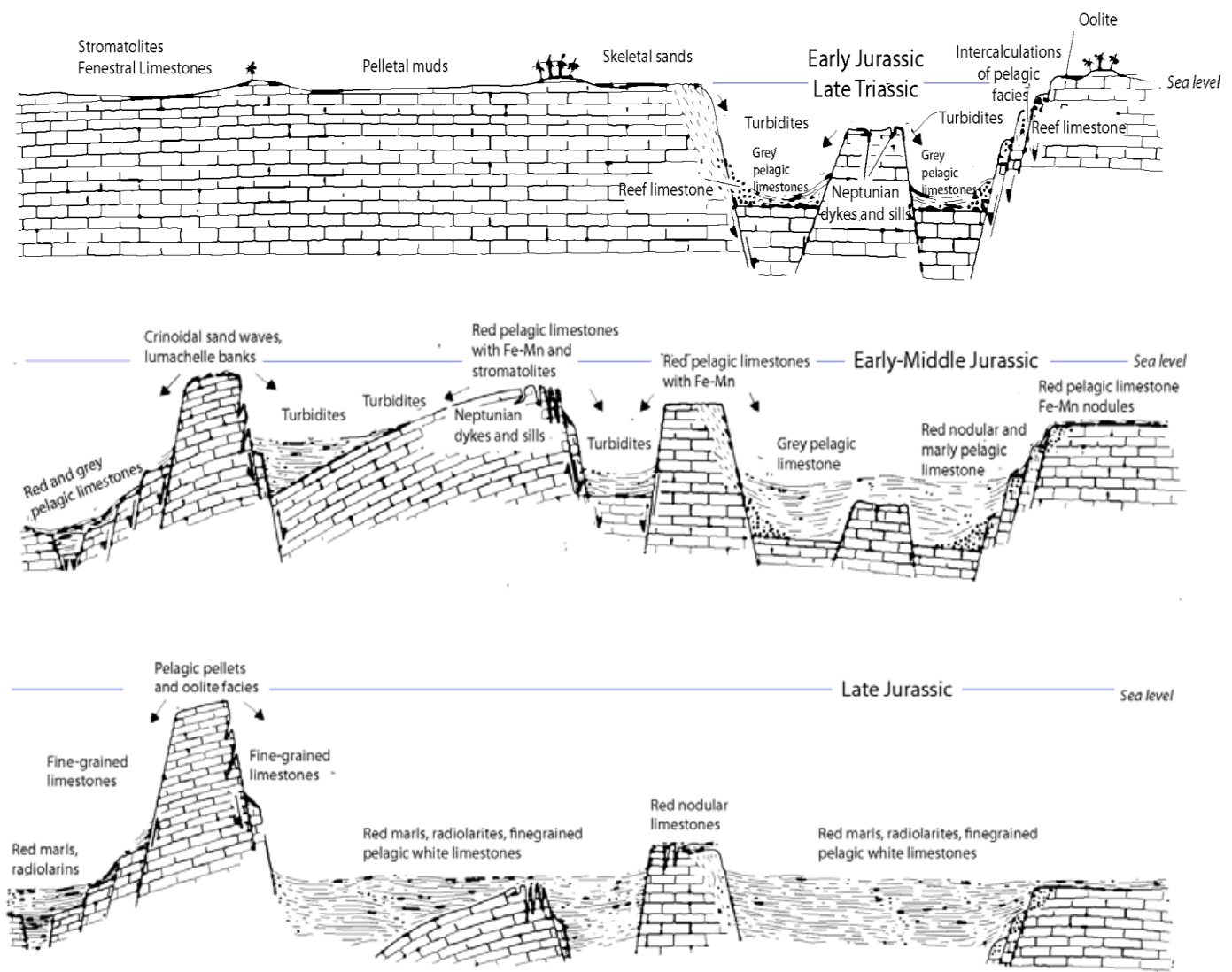


Figure 2.3 Evolution of sedimentary environments during the opening of the Tethys. The Middle Jurassic sedimentary sequence demonstrates the opening and rifting of the Neotethys Ocean characterised by swells and troughs (Aurell *et al.*, 2002). Open marine conditions prevailed in this area during the Late Jurassic. Radiolarian accumulation characterises this period (adapted from Bernoulli and Jenkyns, 1974)

2.6 IBERIA AND THE BALEARIC ISLANDS

During the Early Jurassic, the Iberian micro-plate was located between latitude 25°N and 35°N (Vera, 1998; Aurell *et al.*, 2002; Golonka, 2007; Figure 2.4). It was separated from the larger European plate to the NE by a fault-bounded trough corresponding to the early rifting of the Bay of Biscay. To the NW it was separated from the Laurentia-Greenland Plate by an epicontinental sea with a typical graben and horst structure, which would eventually become the palaeogeographical connection between the northern and central Atlantic (Figure 2.4). The opening of the Bay of Biscay gave rise to the south-easterly movement and anti-clockwise rotation of the Iberian Plate (e.g. Ziegler, 1988b; Osete *et al.*, 2000; Gómez and Fernández-López, 2006). To the south was the Maghrebian Trough adding to subsidence-related distention (Dercourt *et al.*, 1986). Two emerged parts of the Iberian plate can be seen in Figure 2.4: the Iberian Massif and the Ebro-Catalonian Massif. The Iberian Massif was limited to the north by an additional zone of distention (Brunet, 1986), known as the Aquitaine Basin. Both this basin and the present Cantabrian margin were occupied by a submerged carbonate platform until the end of the Mid-Jurassic (Curnelle *et al.*, 1982). The Balearic Islands lay to the east of the Iberian massif as part of an extensive carbonate platform; overall, the area formed a basin-and-platform topography. Basinal facies appear in the west in what is now Portugal and to the south in the Sub-Betic trough (Garcia-Hernandez *et al.*, 1980; Martin-Rojas *et al.*, 2009).

The Ebro-Catalonian massif in the east was created from the assembly of the Calabrian, Alborán, Corsican, Sardinian and Briançonnais massifs (Michard *et al.*, 2002). On its southern border basinal sedimentation is indicated, succeeding that of the lowest Lower Jurassic platform (Dercourt, 1989) where fault breccias indicate that deepening was probably caused by limiting tilted blocks (Lagabrielle *et al.*, 1987).

Subsidence of the Iberian massif is signified by the thick limestones deposited south of the Ebro-Catalonian Massif during the Lower Jurassic (Colom and Escandell, 1962; Ríos, 1978). There are no indications on either Mallorca or Menorca of deep water environments during the Lower Jurassic, although they do occur on the island

of Cabrera just to the south (Abbots, 1989), suggesting that Mallorca and Menorca probably were on the edge of a subsiding basin.

The Balearic Islands appear to have become more tectonically active during the late Early Jurassic, as is suggested by the initiation of deep water deposition and the expansion of the shallow waters at the expense of the Ebro-Catalonian Massif (Colom and Escandell, 1962; Aurell *et al.*, 2002; Martin-Rojas *et al.*, 2009).

During the Middle-Upper Jurassic this region consisted of numerous horst blocks capped by carbonate platforms with adjacent grabens filled with pelagic sediments. Shallow-platform grainstones to argillaceous deeper carbonates accumulated on the passive margin shelves of the western Neotethys where isolated carbonate platforms were associated with the microplates that made up the north-western Neotethys. Central and western Iberia continued to form an emergent area through these times, but reduced in size by further encroachment of shallow epicontinental seas from the north, east and south. The Betic shelf formed a wide Early Jurassic carbonate platform bordering a narrow oceanic trough that connected the Neotethys to the newly opening Atlantic Ocean, and separated Africa from Iberia. Extensional breakup of the Betic shelf created offshore pelagic and hemipelagic troughs and swells where the marl-limestone successions and condensed sequences such as *Ammonitico Rosso* were deposited on the classic representation of the Tethyan bathymetric topography.

During the Middle and Late Jurassic the Catalonian Massif northwest of the Balearic Islands subsided, with the islands of Ibiza and Mallorca being covered by deeper water. Menorca, on the other hand became a new emergent massif extending to the east.

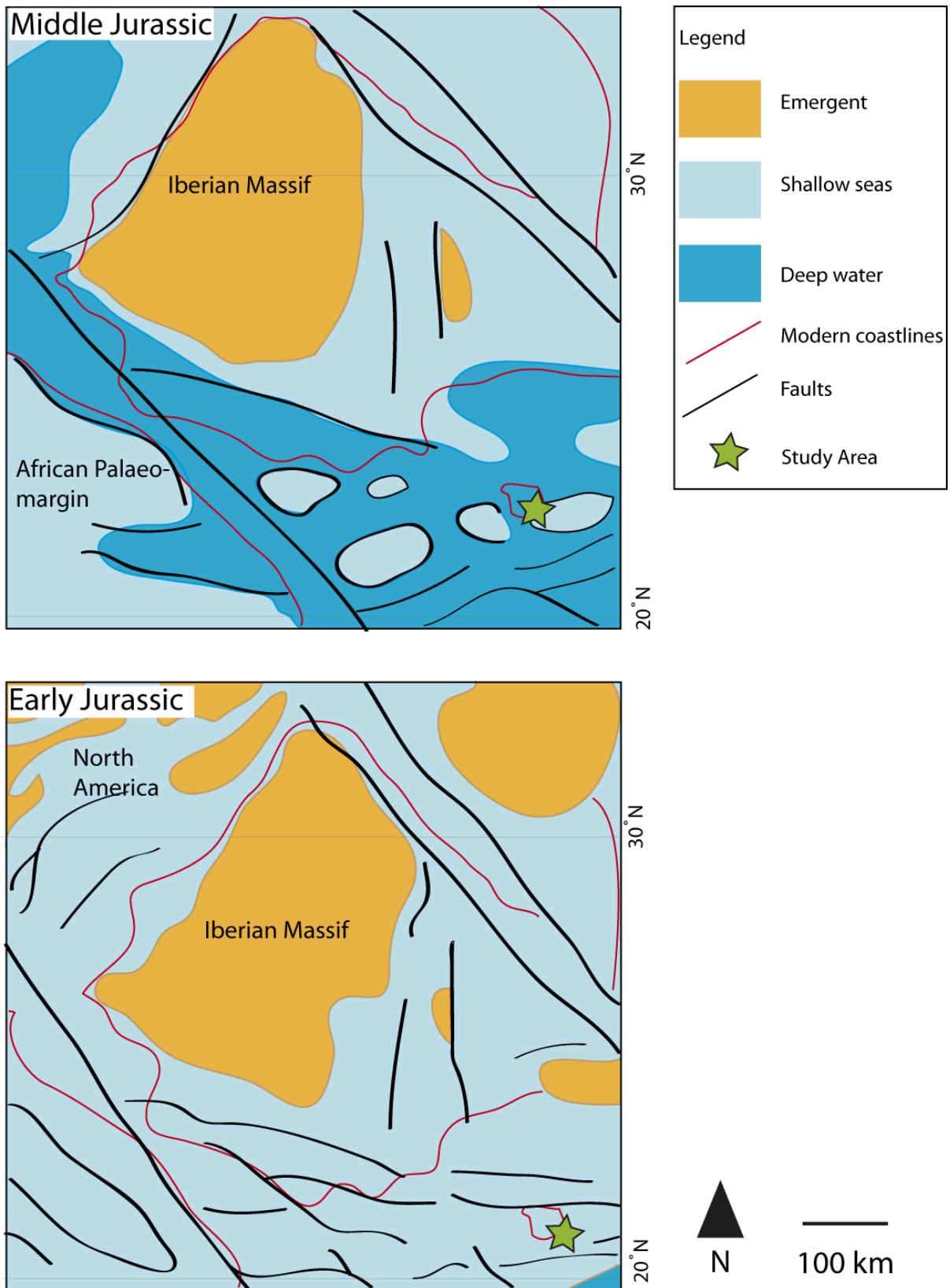


Figure 2.4. Palaeogeography of the Iberian Massif during the Early Jurassic and Middle Jurassic. In the Early Jurassic it is dominated by a vast carbonate platform. The opening Atlantic and Neotethys during Middle Jurassic led to a new NW-SE seaway, and carbonate platforms lined the newly created oceans with isolated carbonate platforms forming with the Tethys. Adapted from Colom and Escandell, 1962; Dercourt *et al.*, 1986 ; Ziegler, 1990; Puga *et al.*, 1993; Aurell, 2002; Vera, 1998; Olóriz, 2000; Golonka, 2007; Martin-Rojas *et al.*, 2009.

2.6.1 LOCAL TECTONIC STRUCTURES

The island of Mallorca is made up of various tectonic units, which correspond to a set of horsts and graben. The tectonic study by Gelabert-Ferrer (1998) suggests Mallorca was formed by the superposition of several thrust-bound tectonostratigraphic units of Mesozoic to Paleogene age; the thrusts have a NW- vergence (Sabat, 1986). This is reflected in the orientation of out cropping Mesozoic strata. There are five tectonic zones as identified by Sabat (1986), Pares *et al.* (1986) and Sabat *et al.* (1988). The major thrust units in Mallorca were most likely emplaced during the Oligocene, and faults were probably active into the Langhian (Colom, 1975; Sabat, 1986). Basin areas are among the main relief of the island: the Tertiary Campos Basin and the small basins of Palma-Inca-Sa Wall (Alonzo-Zara *et al.*, 2002). The thrust and basin topography of modern day Mallorca is the result of subsidence due to listric normal faults, with lateral displacement in terms of kilometers; with a general NE-SW orientation (Gelabert-Ferrer, 1998; Azañón *et al.*, 2002).

2.7 PALAEOCLIMATE AND PALAEOCEANOGRAPHY

2.7.1 PALAEOCLIMATE

It is important to understand the relationships between palaeoclimate, oceanography and tectonics of the area because of their influence on the sedimentary environment. For example, climate affects surface currents of the oceans, and tectonics can modify the submarine topography, enhancing or altering bottom currents.

The morphology of the continents and oceans during the Mesozoic made climate different from the present time. However, the dynamics of the Earth's rotation was the same and hence it is acceptable to suggest that the three major atmospheric circulatory cells existed as they do today: the Hadley, mid-latitude and Polar cells. These assumptions have led to the development of atmospheric models that simulate climates during the Middle Jurassic. The majority of Early and Mid-Jurassic palaeoclimate reconstructions show the dominance of monsoonal circulation (that is, the seasonal alteration in pressures and wind direction producing a strongly seasonal climate) along the eastern part of Pangaea and the northern shores of the Tethys Ocean (e.g. Scotese and Summerhayes, 1986; Crowley *et al.*, 1989; Parrish and Curtis, 1982; Chandler *et al.*, 1992; Kutzbach *et al.*, 1990; Fawcett *et al.*, 1994; Barron and Fawcett, 1995).

The simulated global distribution of Early to Mid-Jurassic sea-level pressures show that winter high-pressure cells alternated with summer low-pressure cells over Pangaea (Arias, 2008). Sub-polar low-pressure cells developed over the Panthalassa Ocean contrasting with subtropical high-pressure zones (Arias, 2008), which created a seasonal climate.

It is postulated that during the summer in the northern hemisphere, weak insolation and strong heat loss over the very southern part of Pangaea (Gondwana) caused a decrease in the temperature over the more northerly interior of Pangaea (which was predominantly located in the southern hemisphere). Subsequently, the descending cool air possibly created a high-pressure belt over the Gondwana continent. The warmer temperatures in the centre of Pangaea probably generated an extensive low-pressure zone over central Laurasia, in north-eastern Pangaea (between 10 and 30°N latitude) that deepened above the higher elevations in the eastern part of the continent.

During the northern hemisphere winter, strong solar heating over Gondwana caused heated air to rise and likely developed a strong low-pressure zone positioned over the southern part of Gondwana and eastern part of the Neotethys Ocean. In the northern hemisphere, the

reduced seasonal insolation, high elevations, and extensive nature of the landmass could have generated extremely cold temperatures (colder than -30°C) north of 35° latitude in both continents (Arias, 2008). This would have stabilised continental air masses and could possibly have generated a high-pressure belt across the northern hemisphere over the Laurasia continental masses.

Understanding the palaeoclimate of the study area helps to understand the depositional setting and therefore how sediments and water bodies interacted with climate and how these affected the resedimentation process. The position of the study area during the Middle Jurassic ($25\text{-}30^{\circ}\text{N}$) suggests that it had a subtropical, seasonal climate where a high pressure zone is postulated to have sat over the area and most of western Tethys during the northern hemisphere winter. This probably would have created a dry, possibly hot climate where evaporation rates would have increased significantly (Arias, 2008). During the northern hemisphere summer low pressure is considered to have migrated south from Laurasia creating a more humid and wet climate and possibly more unstable weather, with storms becoming common during the season (Arias, 2008). The study area had a distinctively seasonal climate and a sensible modern comparison is the subtropical Caribbean Sea, where winters are dry and warm whilst summers are hot, humid and stormy (hurricanes).

2.7.2 OCEAN SURFACE CIRCULATION

Kutzbach and Gallimore (1989) and Kutzbach *et al.* (1990) provided the first oceanic general circulation model for an idealised Tethys Ocean. This model showed an important surface westward current in the equatorial regions, with both ocean boundary currents along the northern and southern margins of the Tethys Ocean heading westward and an eastward flow at higher latitudes. Alternatively, Barron and Petersen (1990), proposed a clockwise circulation within the Tethys Ocean, with an eastward-flowing current along the northern margin of the Tethys Ocean.

In the study area, during the Early-Middle Jurassic, the continental landmasses of Laurasia bordered the north and Gondwana bordered the Neotethys in the south. Numerous continental blocks, derived from the northern margin of Gondwana, were drifting northward across the Neotethys (Engelbreton *et al.*, 1985; Debiche *et al.*, 1987; Sengör and Natalin, 1996; Keppie and Dostal, 2001; Metcalfe, 1994; Golonka, 2007) and growing carbonate platforms. These drifting continental blocks may have created relatively narrow passages connecting Neotethys to the Panthalassa Ocean in the east (Arias, 2008). Therefore the western Tethys may have been subjected to laterally constricted and/or enhanced

circulation, which may have affected deeper circulation disturbing the deeper sedimentary environments on the carbonate slope.

Surface circulation is mainly wind-driven and during the Middle Jurassic an equatorial ocean current circulation mainly characterised the Tethys Ocean (Kutzbach *et al.*, 1990). The surface circulation in the northern Tethyan Ocean is not a simple continuance of the West Panthalassa Ocean circulation pattern (Figure 2.5). Currents from Panthalassa Ocean interact with Tethys Ocean waters that, during the northern hemisphere's summer, along the northern margin of the Tethys, south-west monsoon winds and the Ekman effect create a clockwise gyre, with an eastward flowing Monsoon Tethys Current and from the equator to 20°S there is the westward-flowing South Tethys Current (Arias, 2008; Golonka and Kiessling, 2002). The majority of surface currents were influenced by the clockwise gyre and probably weakened upon entry into the shallower waters associated with carbonate platforms of the study area. During the winter, the northeast monsoon wind produces a westward-flowing surface current, the South Panthalassa Equatorial Current, which is a continuation of the Panthalassa circulation (Arias, 2008); this probably had a minimal effect on the study area due to flow away from the area.

During the Middle Jurassic the dominant feature of the southern hemisphere ocean circulation is the subtropical anticyclonic gyre (Kutzbach *et al.*, 1990; Arias, 2008), which comprises the westward-flowing South Equatorial Panthalassa Current and the east-flowing South Tethys Current along the southern margin of the Tethys Ocean (Arias, 2008). This gyre is the response of the ocean to the mean basin-wide wind stress curl distribution and exhibits most of the features of a classical mid-latitude gyre, modified by the large seasonal variability in wind directions (e.g. Woodberry *et al.*, 1989). As a result of the great size of Pangaea, it is probable that the monsoon winds were proportionately greater than those of today (Arias, 2008), producing storms and stronger currents during the monsoon. Therefore as discussed previously, monsoonal winds possibly increased the amount of energy transported via surface currents (which were restricted between continental blocks of the study area) and hence at deeper depths energy levels probably increased, which encouraged erosion and mass failure events along carbonate slope.

The surface currents of the Tethys Ocean are extensively modelled, but the deep water currents are less well understood due to the lack of preserved evidence such as deep-sea features such as those been created today by contour currents. In the present day, deep-water circulation is inter-polar in nature and is hence dominated by cold, dense waters that form at high latitudes and travel through the oceans, which mostly have access to both Polar Regions (i.e. the Atlantic and Pacific Oceans). However, the Tethys Ocean formed an

equatorial wedge-shaped sea which was marginal to the Panthalassa Ocean creating a non-polar circulation current. The Tethys probably hosted a large circular current that was influenced by inter-polar currents in Panthalassa, with relatively weaker bottom currents passing through the newly rifting zone into the Proto-Atlantic Ocean.

In relation to the globally warmer climate, shorelines would have suffered stronger evaporation possibly leading to denser water in coastal waters. These warmer waters would have sunk creating convection currents where denser waters sank and less dense waters rose. A similar process occurs in restricted seas, such as the Mediterranean and Red Sea (Reading, 1998), this process may have played a part in deeper ocean circulation within the area of study. However, it is more likely that deeper currents were modified by the submarine topography enhancing their flows creating strong bottom currents within basins.

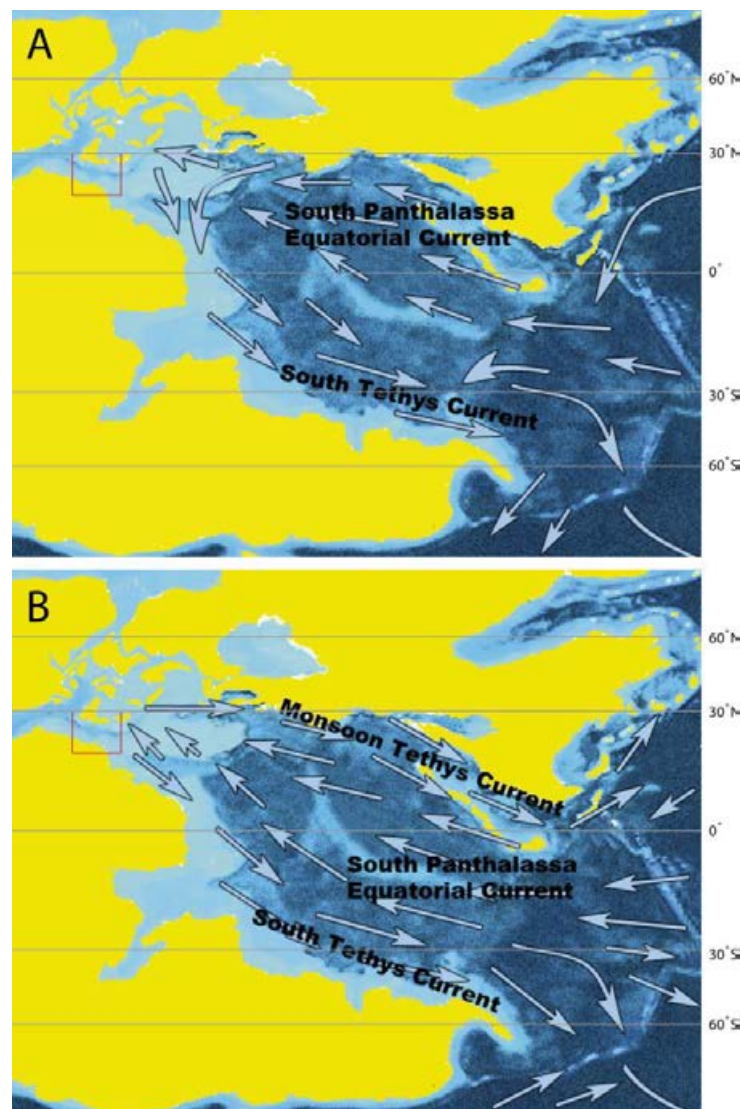


Figure 2.5. Representation of oceanic surface circulation in the Tethys Ocean during the winter monsoon (A) and the summer monsoon (B). Red box indicates the area immediately around the Iberian massif. Adapted from Arias (2008).

2.7.3 OCEANOGRAPHIC AND CLIMATIC EFFECTS ON CARBONATE MARGINS

The primary controlling factors that result in platform margin deposition are its orientation to prevailing winds (windward/leeward) and therefore waves, storms and tidal currents and whether these margins are protected or not (Playton, 2008). The windward-leeward orientation affects the characteristics of a carbonate margin and is an important consideration for evaluating factors that affect sediment transport and their distribution patterns on the margin and on slope to base-of-slope environments (e.g. Great Bahama Bank; Eberli and Ginsburg, 1989, Valles-San Luis Potosi Platform, NE Mexico; Minero, 1991, Western Continental Margin of Australia; Collins, 2010).

Leeward margins face away from the prevailing wind and wave energy and are defined as having a net off-bank energy flux rather than offshore-directed winds (Figure 2.6). Leeward margins have a net transport of detritus over the bank margin into the basin where sand banks are actively transported towards the bank edge. Wave and tidal energy winnows the sediments creating an abundance of grainstones and packstones on the leeward side of a margin (e.g Lily Bank on the Little Bahama Bank; Hine, 1977, Middle Jurassic Fruli Platform margin; Abbots, 1989). However, it is noted that storms and high energy events are needed to transport sediments over the bank edge into the basin (Hine et al., 1981).

Along windward margins (e.g. Western margin of the Tongue of the Ocean, Eberli and Ginsburg, 1989; mid-Cretaceous Valles-San Potosí carbonate platform, Minero, 1991) there is a dominance of on-bank transport of coarse sediment, due to wind and wave energy impacting this side of the carbonate platform (Figure 2.6). This continuous wind and wave direction means that carbonate sands are transported into the carbonate platform centre and are mixed with fine sediments associated with that environment.

Depositional environments vary markedly with margin type (see Blendinger and Blendinger, 1989; Playton, 2008). Margins are divisible by their windward/leeward orientation and whether they are open, closed or tide-dominated.

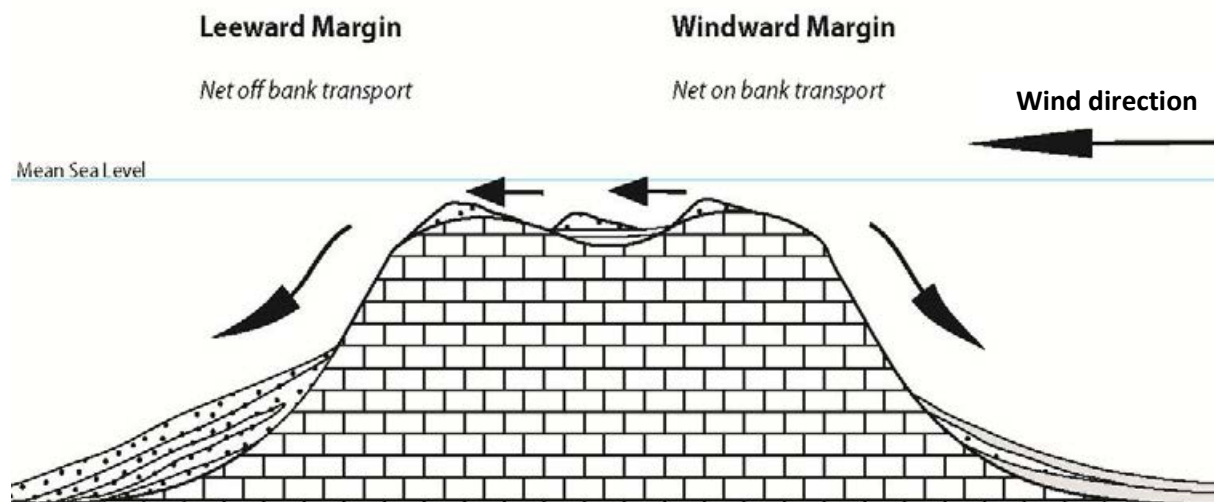


Figure 2.6 Schematic illustration of windward and leeward margin characteristics. Note that sand waves migrate off-bank at the windward margin and on-bank at the leeward margin.

Windward open margins have few or no barriers to restrict water flow on and off the margin. These margins are typified by barren surfaces where little sediment is deposited. However, those examples that host oolitic shoals illustrate migration onto the bank top moving away from the wind direction (e.g. Lily Bank; Hine, 1977).

Windward closed/restricted margins are characterised by islands, ridges and/or reefs (e.g. Lighthouse Reef and Glovers Reef, Belize) that are situated on the bank edge. These barriers restrict the flow of water on and off bank. This leads to the deposition of fines in the platform centre and accumulation of sand bodies on the bank margin (e.g. El Abra Formation, Mexico; Minero, 1991). These accumulations of sands on the bank margin are often resedimented downslope due to storms (e.g. Upper Jurassic of the Iberian Basin; Aurell et al. 1998). Due to the prevailing winds in the Bahaman examples these storm events are concentrated against the windward bank margin. Sediments derived from this margin type have been known to travel kilometers (e.g. Mullins and Neumann, 1979) and in the case of the Tuxpan Platform, in Mexico have a 1:3 ratio of distance travelled when comparing the East and West side of this platform (Andrew Horbury pers. comm. 2012).

Leeward open margins have few or no barriers to water flow on and off the margin. However, these margins are typified by off-bank sedimentation of sandy shoals that migrate towards the leeward margin and are deposited over the edge onto the slope

and base-of-slope. The sediments are characteristically coarse grainstones and packstones. This type of margin is strongly controlled by storm events as is noted by Hine (1983).

Leeward closed/restricted margins are characterised by a barrier to off-bank deposition (e.g. western shore of Cozumel, Mexico; Fenner, 1988). This creates a build-up of sand banks or reefal sediments leading to a slope that is starved of sediments. Closed windward and open leeward margins are noted to produce the most off-platform sediments (Playton, 2008).

The facies produced from each margin are distinguishable and can be applied to those sediments studied. On leeward margins, grain-dominated sediments are deposited due to off-bank deposition (e.g. Schlager et al. 1994; Minero, 1991) whilst windward microfacies reflect the extensive off-bank transport of redeposited grains and finer muds and silts (e.g. eastern side of the Valles-San Luis Potosi and Tuxpan Platforms; Enos and Stephen, 1991).

3. REVIEW OF DEEP WATER DEPOSITS AND PROCESSES

3.1 DEFINITIONS OF DEPOSITS

Much of the sediments that are removed from continental shelves and redeposited in the deep sea are transported by sediment gravity flows rather than ocean currents, waves or tides (Reading, 1998). A list of some of the most common processes and deposits that transport sediments into basins are demonstrated in Figure 3.1.













Resedimentation Process	Character	Deposit Name
Rockfall		Mélange/ Avalanche deposit
Slide		
Slump		Slide
Debris flow		Slump
Grain flow		Debrite
Turbidity flow		Grain flow
Creep		Turbidite
		Creep deposit
Internal tides and waves		Normal current deposit
Contour currents		Contourite
Surface currents/ pelagic production		Pelagite
Pelletisation		Pelagite
FeMn Nodules hardgrounds/ umbers		Chemogenic deposit

Figure 3.1 The range of processes that operate in deep sea environments (adapted from Stow, 1994; Reading 1998)

Below are the definitions of sedimentary processes and deposits used in this thesis.

A *turbidity current (turbidite)* deposit is transported by a flow in which the sediment is supported by the upward-moving component of fluid turbulence. This is characterised in the rock record by a variety of grading sequences that are dependent on the density, sediment type and distance from source of the turbidite.

A *turbidite system* is a body of genetically related turbidite facies and other facies associations. These were deposited in stratigraphic continuity forming structures like aprons and fan complexes that are dominated by turbidite deposition.

A *debris flow (debrite)* deposit is defined here as a high density, plastic-viscous flow in which the larger particles are supported and moved by matrix strength, where the fluid component increases shear strength until a fine-grained matrix via grain: grain contact moves the coarser elements into a flow. Debrites are coarse-grained breccias or conglomerates and are characterised by poor sorting, lack of stratification and often chaotic clast fabrics. The final deposit is characterised by large-scale slope collapse structures of semi-lithified carbonate material which, often form sheet-like megabreccia beds that contain little fine-grained matrix material and therefore are primarily clast-supported.

Finally, a *geostrophic current deposit (contourite)* is distinguished from downslope events and process and is defined here as a continuous/semi-continuous oceanic current which is continuously reworking and depositing sediments that are caught in the current (Hollister, 1993). Heezen *et al.*, (1966) demonstrated the importance of contour-following currents and their semi-permanent status. The deposits are characterised by grading sequences of normally fine-grade sediment and heavy bioturbation.

All the deposits defined here can grade into each other (*hybrid flows*) via changing energy levels and sediment densities whilst travelling downslope: for example the dilution of a debris flow into a turbidity current. This complicates interpretation and understanding of any flow deposit.

3.2 RESEDIMENTATION: AN INTRODUCTION

Submarine resedimentation flows move down slope because the mixtures have a density greater than the surrounding water body. Gravity acts on the solid particles in the sedimentary mixture, inducing downwards flow thus creating dispersive pressures between grains resulting in the turbulence of water/sediments mixtures. The gravity flow will continue if the following conditions are satisfied (Lowe, 1982; Ahr, 2008):

- 1) Shear stress generated by the downslope gravity component acting on the excess density of the mixture exceeds frictional resistance;

- 2) Grains are inhibited from settling by a support mechanism (such as water turbulence).

Bagnold (1962) observed that below a certain grain size, the sediment in a turbidity current flowing down an incline appeared to be supported by the turbulence created through the disturbance of the water column. This lead him to suggest that under certain circumstances *'the power provided by the tangential gravity component on the excess weight of entrained sediment is sufficient not only to maintain the suspension, but also to contribute towards the power needed to maintain the flow of the fluid drag exerted at the bed boundary'* suggesting that once a flow has started it can, in theory, continue to flow under the influence of water turbulence alone until turbulence is reduced to that just able to entrain the sediment.

When there is a very high concentration of sediment in water (where the volume and mass of sediment exceeds those of water), the mixture forms a debris flow (Leeder, 1982). These dense mixtures move by gravity over land or under water, behaving in a different way than sediment dispersed in a water body through water turbulence. These gravity-driven flow mechanisms are important as means of transporting coarse material into the deep oceans. True grain-flows are described by Bagnold (1954) in theory where *'dispersion of cohesionless grains is maintained against gravity by grain dispersive pressure and in which ...fluid interstitial to the grains is the same as the ambient flow above the flow'* (Lowe, 1976), however no naturally occurring resedimentation is *'gravity-free... [or]...fully confined'* (Lowe, 1976) and therefore the processes described hereafter are based on observation rather than theory.

Sanders (1965) interpreted sedimentary sequences of flows to consist essentially of two flow types: the most important component process is the basal grain flow and an overlying turbulent flow, which provide turbulent water flow keeping sediments in suspension. Coarse grains are moved under bedload and finer grains travel via grain to grain contacts and the sediment gathers energy by shear stress that is imparted from the overlying turbulent flow where finer grains are individually kept in suspension by turbulence. Turbidites and debrites are the end member sediment gravity flows seen in the outcrops of the Cutri Formation, and thus are reviewed below.

3.3 TURBIDITES

Turbidity currents tend to move downslope, accelerate, and form a turbulent undercurrent, which transports its load into deeper water (Stow, 1994; Reading, 1998) with finer material travelling further than coarser material due to the finer material being held in suspension for longer. Many other types of similar density currents exist in nature, travelling in all directions (Edwards *et al.*, 1994), including pyroclastic base-surges and vertical density flows caused by plumes of volcanic ash falling through the atmosphere and oceans (Allen, 1985; Stow, 1994).

The concept of a turbidity current has been studied intensively and is possibly the most theoretically understood sediment gravity flow, although a significant event has yet to be closely documented in nature. The evidence, through natural observation, for their existence comes from underflows in lakes, delta fronts and possibly the most prominent example in 1929 by the sequential breaking of telegraph cables (Heezen and Ewing, 1952; Heezen *et al.*, 1954).

The driving force of turbidity currents is primarily a function of the difference in the densities of the suspension (water between grains in the sediment) and the overlying water body, the submarine topography, i.e. the angle and length of slope (Kenter, 1990), and the thickness and grain size of the suspension current, which supplies turbulence to underlying sediments. Turbidite successions vary greatly in sedimentary structures, bed thickness, and textural features. These variations are controlled by the distance between the source and of the depositional setting, point or line sources, and composition of the available sediment and topography of the depositional area as well as density of the turbidity current.

The deceleration of turbidity currents causes the deposition of their contents in a predictable order which produces internal structures and trends that have been recognized and catalogued by various authors (Figure 3.2). The sedimentary structures can be divided first in terms of the density of the flow regime. Low-density turbidity currents and high density currents can be distinguished creating categories

of recognition for fine and medium grained turbidity currents and coarse grained turbidity currents.

Generally sediments that are finer than medium sand can be maintained for longer in suspension giving rise to low density currents: this is presented via the Bouma sequence and fine-grained turbidite model of Bouma, (1962) and Stow and Shanmugam, (1980) respectively. Coarser-grained turbidites, which cannot support suspension for as long, are presented via the Lowe (1982) model.

3.3.1 CLASSIC TURBIDITES

Turbidites were first recognised and catalogued via a succession of sedimentary characteristics by Bouma (1962). This is known as the *Bouma Sequence*, an idealised turbidite sequence interpreted from clastic sediments that consists of a well defined vertical succession of sedimentary structures (Figure 3.2).

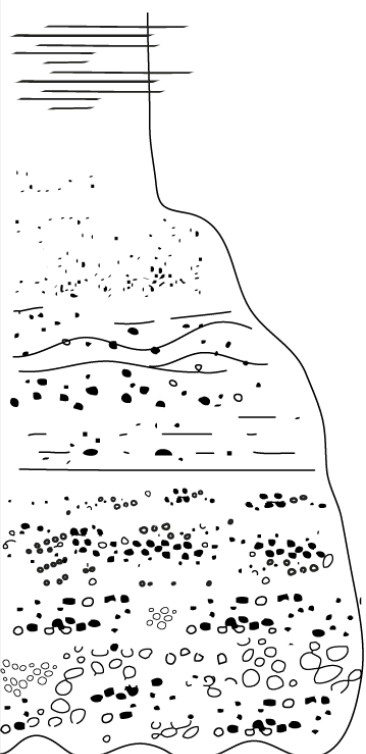
	Grain Size		Bouma (1962) Divisions	Interpretation
	Mud	Te	Pelagic and hemipelagic mud Fine grained grading	Pelagic sedimentation Fine grained, low density turbidity current deposition
		Td	Upper parallel silty laminae	
	Sand	Tc	Ripples, wavy or convoluted laminae	Lower part of lower flow regime
		Tb	Plane parallel sandy laminae	Upper flow regime plane bed
	Sand to gravel	Ta	Graded sands and gravels Scoured base	Upper flow regime rapid deposition Flow cutting into underlying sediment

Figure 3.2. The Bouma Sequence. Bouma (1962) presented the first classic model for medium-grained sand mud turbidites. This is the result of deceleration of relatively low concentration turbidity currents followed by a progression of bed forms representing fallout during high to low flow regime, and finally deposition from the turbidity current tail and then completed by the deposition of pelagic/hemipelagic sediments (adapted from Bouma, 1962 and Reading, 1998).

However, the Bouma Sequence does not include features, as discussed earlier, of the variety of other turbidite deposits. The variety in models for distinguishing between turbidites comes from grain size and the relative density of currents, so the key models for turbidites are derived from density of sediment and the grain sizes within flow. These include medium-grained turbidites, represented by the Bouma sequence, and fine-grained turbidites (Stow and Shanmugam, 1980), which are low density and coarse-grained turbidites (Lowe, 1982), which are held in the high-density category. Complete sequences of any turbidite are rarely encountered in nature with partial sequences being relatively common.

3.3.2 COARSE GRAINED TURBIDITES

Coarse-grained turbidites are commonly found in proximal regions in relation to the sediment source compared to low density turbidites. They are generated by high-density turbidity currents carrying pebble- to boulder-sized clasts as bedload and

finer material in suspension. The model by Lowe (1982) indicates that the deposits show initial traction sedimentation where the coarsest fragments of the flow are transported via traction and clast to clast contacts, the finer fraction of sediment, via dispersive water pressures, becomes suspended creating a turbulent flow, which leads to a graded and stratified sequence represented in Figure 3.3.

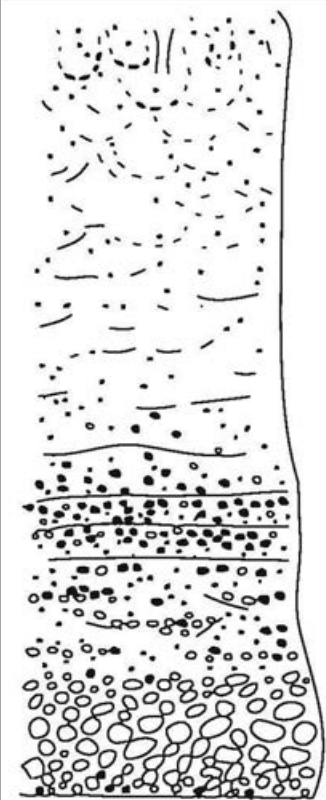
	Grain Size	Lowe(1982) Divisions		Interpretation
	Sand and fine gravel		Pelagic and hemipelagic mud	Pelagic Sedimentation
		S ₃	Extensive water-escape structures	
		S ₂	Gravelly bed load	Traction Carpet
		S ₁	Gravelly bed load	Traction
	Gravel	R ₃	Suspension	Suspension
		R ₂	Inverse graded gravelly bedload	Traction Carpet

Figure 3.3 The Lowe (1982) sequence that represents the deceleration of relatively high concentration and coarse grained turbidity currents followed by bed forms representing fallout during a reduction in flow energy, completed by the deposition of pelagic/hemipelagic sediments (adapted from Lowe, 1982 and Reading, 1998).

3.3.3 FINE-GRAINED TURBIDITES

A standard sedimentary sequence for fine grained turbidites was developed by Stow and Shanmugam, (1980). It has nine sub-divisions termed T₀ to T₈. These divisions are show graphically in Figure 3.4.

It must be noted that this model follows the characteristically very thin sequences that are attributed to fine grained turbidites, which are commonly 5-10 cm in thickness. The coarsest division is T₀ that comprises silt laminations which can have a scoured or planar base chiefly depending on the underlying sediment. The

overlying sequences show textural and sedimentary changes that consist of grading through alternating silt and mud layers that generally become more subtle up section until mud finishes the sequence grades into background hemipelagic sediments.

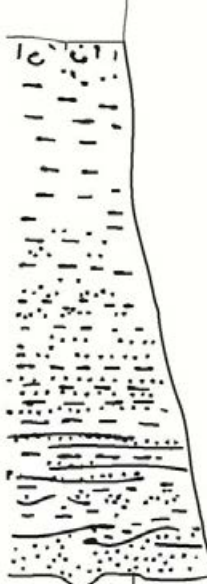
	Grain Size	Stow and Shanmugam (1980) Divisions		Interpretation
	Mud	T8	Typically bioturbated surface	Return to calm basin conditions
		T7	Ungraded, bioturbated muds with rare patches of silty laminations	Remains of fine suspended material being deposited
		T6		
	Silt	T5	Wispy/convolute laminations	Influence of dispersive pressures fading until sediment fallout
		T4	Faded planar laminations	
		T3	Regular planar laminations	
		T2	Planar to wavy laminations	Rapid deposition of silty material
		T1		
		T0	Silt laminations with sharp to scoured base	Flow cutting into underlying finer material or flows over coarser material
	Mud			

Figure 3.4 The Stow and Shanmugam (1980) sequence representing the deceleration of low concentration and fine grained turbidity currents followed by bed forms representing the reduction in flow energy (adapted from Stow and Shanmugam, 1980).

3.3.4 CARBONATE TURBIDITES

Carbonate turbidites (also called allodapic limestones and calciturbidites) often consist of skeletal or carbonate mud material produced on carbonate shelves and platforms (Flügel, 2004; Meischner, 1964). Abundant shell material, reefal detritus and early lithification of different types of carbonates provide various medium- and coarse-grained materials that are incorporated into carbonate turbidites.

Complete Bouma sequences are rare in carbonate sediments. It is important to note that this may be due to the different hydraulic behaviour of all carbonate sediments compared to siliciclastic sediments (Einsele, 2000). Flügel (2004) suggests that this may be caused by the relatively weak thixotropy of calcareous muds as compared to siliciclastic muds; as a result other internal sedimentary sequences develop in carbonate turbidites.

Other differences between clastic turbidites and carbonate turbidites should be considered:

1. The size of the bioclastic and chemical particles that are controlled by the ecological constraints at the source area as well as taphonomic factors.
2. The abundance of lithified particles compared to clastic turbidites. Carbonate platforms are rapidly cemented (compared to clastic slopes) and therefore lithified to semi-lithified intraclasts are much more abundant than in clastic turbidites.
3. The high variability of grain types in carbonate turbidites contrast with the rather homogenous grain types of clastic turbidites due to the heterogeneous nature of carbonate platforms. It is also common that hydraulic sorting is more powerful as bioclasts and other carbonate grains are influenced by differences in size, geometry, porosity, density, microstructure etc.
4. Provenance of source, which determines the type of components within carbonate turbidites which are crudely divided mainly into bioclastic and non-skeletal material.
5. The age of sediment deposition and resedimentation since carbonate rocks are heavily influenced by evolution of flora and fauna.

6. Highstand, transgressive, and lowstand shedding of carbonate where the compositions of the deposit are characteristically different (see Hanford and Loucks, 1993). Lowstand deposits tend to consist of a higher amount of lithoclasts whilst highstand deposits typically are dominated by bioclasts and other allochems (e.g. highstand deposits of Vecsei, (1997) and lowstand deposits of Borgomano, (2000)).

The source areas of carbonate turbidites are generally shallow-water environments and slope environments (Reading 1998; Flügel, 2004). Carbonate turbidites can be traced laterally over hundreds of metres to several kilometres (Belderson and Laughton, 1966; Bennetts and Pilkey, 1976; Kenter, 1990; Aas *et al.*, 2010), with bed thicknesses ranging from <1 cm to several metres and, as suggested by the Puig Cutri area, amalgamation can be a common feature.

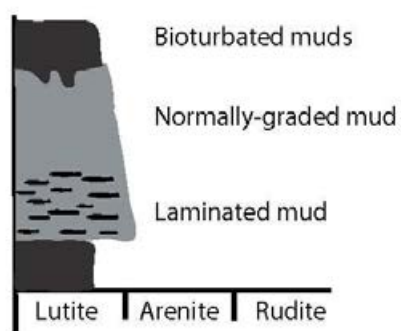
3.3.5 DISTANCE FROM SOURCE

Turbidites contain different sedimentary successions associated with their proximity to the sediment source since. A distal turbidite will commonly contain finer grained and higher quantities of suspended material since these sediments travel further requiring less energy to move them. A proximal turbidity current consisting of much coarser material will be undergo more grain to grain interactions. Turbidites can be differentiated into distal and proximal categories (Figure 3.5):

Proximal Turbidites: These are deposited relatively close to the source area, which tend to be massive, weakly graded and exhibit poorly defined tractional structures and little interbedded pelagic sediment.

Distal Turbidites: These are formed far away from the source region, and are characterised by thin, fine-grained bedded layers, of well developed cross-laminations and an absence of massive intervals and parallel laminations.

A. Distal



B. Proximal

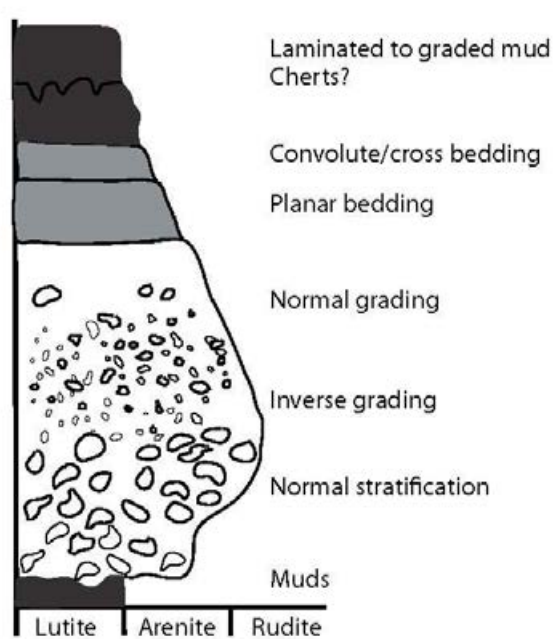


Figure 3.5 Idealised sedimentary logs of distal and proximal carbonate turbidites (adapted from Einsele, 1998)

3.4 DEBRITES

Carbonate debris flows are predominantly deposited on deep marine slopes or at the base of slopes (Reading, 1998). Unlike turbidites, that are deposited in proximal (slope regions) and distal (deep marine) regions, debris flows are generally only found closer to source. This is primarily due to their behaviour of internal movement, which only begins when critical yield strength is exceeded and then deformation begins in a basal zone of highest shear stress, destabilising the overlying sediments. During this time there is a complex region of the flow where grain: grain and clast: clast interaction such as: sliding, rolling, and laminar flow increase in abundance. Higher in the flow, where shear stresses are less, the material may be seen as surfing along as a semi-rigid plug (Reading, 1998; Einsele, 1998). Final deposition occurs by downward thickening of this plug until the entire mass freezes (Stow, 1994), leaving many components frozen in place.

The chief components of debrites are commonly boulder- to pebble-sized clasts, which are supported by a highly viscous fine grained muddy-water mixture leading to the deposition of sediments that have variously been called debrites, debris sheets and mass breccia flows. Many debris flows have been described with a granular matrix that is non-cohesive (e.g. Johnson, 1970; Stow, 1994; Hsu *et al.*, 2008) whilst it is understood that debris flows tend to be mud-rich. Debris flows are capable of travelling over very gentle slopes (<0.5 degree) (Flügel, 2004; Felix *et al.*, 2009).

Debrites range in thickness from a few tens of centimetres to tens of metres. Most debrites form lenticular bodies with conformable, sometimes erosional contacts with underlying fine-grained sediment. Upper contacts are sharp or the debrite bed passes upward into turbidite deposits (Krause and Oldershaw, 1979; Felix *et al.*, 2009), acting as a hybrid bed.

Many models have been constructed to characterise the motion of debris flows and these models have suggested many forces are present in these flows, ranging from cohesive stress (Lowe, 1982), to dispersive pressure (Takahashi, 1981). However, it is much more likely that in nature debris flows display a wide mixture of rheological

properties, being more or less cohesive plastic, viscous fluid and containing only small amounts of grain to grain collisions that are more often associated with turbidite behaviour (Pickering *et al.*, 1989).

3.5 HYBRID BEDS

Many sediment gravity flow deposits do not conform to simple individual models that show simple successions derived from diminishing dispersive energy (e.g. Stow, 1979; Lowe and Guy, 2000; Gee *et al.*, 2001; McCaffrey and Kneller, 2001; Mulder and Alexander, 2001; Hodgson and Haughton, 2004; Jackson *et al.*, 2009). Beds that show evidence for more than one flow type (e.g. cohesive and laminar flow) are referred to as hybrid beds (Haughton *et al.*, 2009). One type of hybrid bed is essentially turbidites with a linked debrite, and have been discussed in various papers (e.g. Haughton *et al.*, 2003; Barker *et al.*, 2008; Haughton *et al.*, 2009). Typically, this turbidite-linked debrite bed comprises basal graded sediment that is interpreted as a turbidite, followed by chaotic to poorly sorted muddy divisions with sedimentary characteristics that are interpreted as cohesive debris-flow deposits.


	Modal Grain Size	Haughton et al. (2009) Divisions		Interpretation
	Silt	H5	Massive Muds	Suspension fallout
		H4	Parallel and cross lamination	Traction by dilute turbidity
	Fine Sand	H3	Muddy sand (including mud clasts), sandy regions and shear fabrics. Lamination is common at the top of this section	Cohesive debris flow, locally modified by sand injection from underlying sediment
	Medium Sand	H2	Alternating muddy and not-muddy sandstones. Shearing features and dewatering features are common	Transitional flow with intermittent turbulence suppression due to near bed displacement and internal shearing
	Coarse Sand	H1	Isolated mudclasts Graded to structureless relatively clean sands with isolated mudclasts at the top of bed	Progressive aggradation beneath non-cohesive high-density turbidity current

Figure 3.6 The Haughton et al., (2009) sequence that represents an ideal hybrid event bed, which includes the amalgamation of a turbidite and a debris flow (adapted from Haughton et al., 2009).

A range of mechanisms and sedimentary characteristics for the commencement, development and emplacement of hybrid flows has been raised including (Haughton *et al.*, 2009; Figure 3.6):

1. Partial flow transformation of an initial mass flow;
2. Flow transformation from non-cohesive to cohesive rheology through entrainment of (commonly mud-rich) substrate;
3. Flow transformation from non-cohesive to cohesive forces;
4. Debris-flow generation from interaction with intra-basinal topography (e.g. Haughton *et al.*, 2003 and Talling *et al.*, 2004).

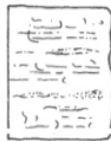
Correlation of beds over tens of kilometres between isolated exposures (Talling *et al.*, 2004; Amy and Talling, 2006; Hodgson, 2004) suggests that this style of sediment gravity flow deposit is found most commonly in the proximal to distal settings of submarine fan/apron systems such as the proximal regions of the Mississippi delta (e.g. Nelson *et al.*, 1992; Schwab *et al.*, 1996; Talling *et al.*, 2010).

This suggests that hybrid beds can be used as an indicator of distal or fringe settings in submarine fan systems.

3.6 CONTOURITES

The definition of contourites was proposed by Stow *et al.* (2002) as '*the sediments deposited by or significantly affected by the action of bottom currents*'. Bottom currents are commonly semi-permanent and often have relationships with other processes in the deep-sea environment, frequently turbidites. These relationships can be seen in many examples, including the Cenozoic of the southern Brazil Basin (Johnson and Rasmussen, 1984). Sorting of these bottom current sediments is created by the incorporation of fine-grained material from other processes (e.g. currents, turbidity flows etc), furthermore these currents can both winnow, erode and deposit onto the sea floor creating hiatuses, sand waves and other such features in the sedimentary record (sedimentary characteristics of contourites are summarised in Figure 3.7).

Clastic contourites



Muddy bioturbated
trace lamination



Silt-muddy mottled
irregular layers
bioturbated



Sandy bioturbated
trace lamination

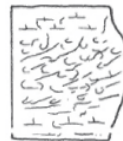


Micro-brecciated
shale-chip layer
in muddy
contourite



Gravel-lag
irregular, poorly-
sorted
reverse graded

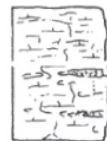
Biogenic contourites



Carbonate sand,
clean, laminated,
bioturbated



Silica sand,
clean, laminated,
bioturbated



Biogenic mud/silt,
bioturbated,
trace lamination

Chemogenic contourites



Fe Mn-muddy
contourites

Shallow water contourites



Clastic +/- or biogenic
laminated and bio-
turbated. Gradational
grainsize variation

Figure 3.7 Sedimentary characteristics of individual beds deposited by different processes found in contourites (taken from Reading, 1998)

3.6.1 CONTOURITE DEPOSITIONAL SETTINGS

There are several settings that accommodate contourite deposits and their processes (Stow and Faugères, 1993; Viana *et al.*, 1998). These are generally categorised by the water depth and relation to slope processes.

The first category occurs in deep water settings in waters deeper than 2000 m in areas of permanent to semi-permanent bottom currents. These most commonly occur along the foot of the continental slope (e.g. Viana, 2001) and are typically associated with deep-sea passages that act as gateways between the deeper portions of ocean basins, and also cover parts of the abyssal plains (Stow *et al.*, 2002). The sediments found in these settings are frequently mainly fine grained (silt and mud grade deposits with rare sands) and rich in both planktonic and benthic life. These types of contourites have been well researched in the literature and are represented in examples such as Stow and Lovell (1979) and Gonthier *et al.* (1984).

Intermediate-water drifts, the second category, occur in water depths of between 300 and 2000 m on the continental slopes (e.g. Huvenne *et al.*, 2009) of the oceans as well as in intermediate depth passageways and sills (such as the Mediterranean gateway). Although some significant elongate drifts form at this depth, many are smaller elongate bodies or much flattened contourite sheets. They form in association with geostrophic bottom waters flowing along slope at intermediate levels in the water column and with water masses flowing downslope from their surface origin or following the breaching of shallow intra-ocean basin gateways. Contourites at these depths interact with other gravity flows such as turbidites (e.g. Michels, 2001; Kuvaas, 2005), due to their proximity to steeper topography, such as the Cenozoic of the South Brazil Basin (Viana *et al.*, 2003), the Argentine Continental Margin (Hernandez-Molina *et al.*, 2009) and the Gela and South Adriatic basins (Verdicchio and Trincardi, 2007). The sedimentary characteristics of this type of deposit are similar to those of deeper deposition including being fine grained, bioturbated and mainly homogeneous. Ancient examples of these include the Talme Yafe Formation in Israel (Bein and Weiler, 1976), the Jiuxi Drift in south-central China (Duan *et al.*, 1993), and the Misaki Formation in Japan (Stow and Faugères, 1993).

Other contourite deposits have formed in shallower non-coastal conditions between 50 and 300 metres depth (e.g. Gaudin *et al.*, 2006). These commonly form on the outer shelf and inner shelf under the influence of shallow depth bottom currents such as underflows or other surface currents like the Gulf Stream. Deposits here are characterised by showing strong sorting, sand waves and dunes as well as accumulations of fine grained sediments, strong bioturbation and traction current structures (Stow *et al.*, 1998).

3.6.2 IDEALISED CONTOURITE DEPOSITS

An idealised contourite deposit incorporates both muddy (<15% sand) and sandy (>15% sand) contourites suggests that current deposits occurring as sandy and/or muddy sediments do have a common sequence that is often between 0.2 to 3 m in thickness (Stow *et al.*, 2002). In this model, muddy and sandy contourites commonly blend together in characteristic vertical sequences (Figure 3.8).

The mud, silts and sands of the contourite model have distinguishing parts that include poor sorting of silt-sized biogenic/clastic sediment in muddy parts as well as a general homogeneous and well bioturbated mass that shows little sedimentary structure. Silty sections of the model commonly show mottling from bioturbation with indistinct discontinuous lamination. Sharp to irregular tops and bases of silty layers characterise this part of the contourite model, together with thin lenses of coarser and finer material as it blends into either finer or coarser material. The sandy, coarsest part of the model commonly occurs as thin irregular beds that are commonly structureless with strong bioturbation and frequently contain primary horizontal and cross laminations (Stow *et al.*, 2002; Figure 3.8). They both show negative or positive grading and have sharp gradational bed contacts. The grain size is most commonly fine sand.

Proposed by Stow *et al.* (1998, 2002) the complete sequence for contourites not only shows a change in grain size but also indicates the importance of positive grading from sandy to muddy contourites and inverse grading consisting of silty-muddy contourites, as the contour currents flow and wane. Bioturbation is characteristically

found everywhere throughout the theoretical model (Figure 3.8), which destroys the majority of sedimentary structures.

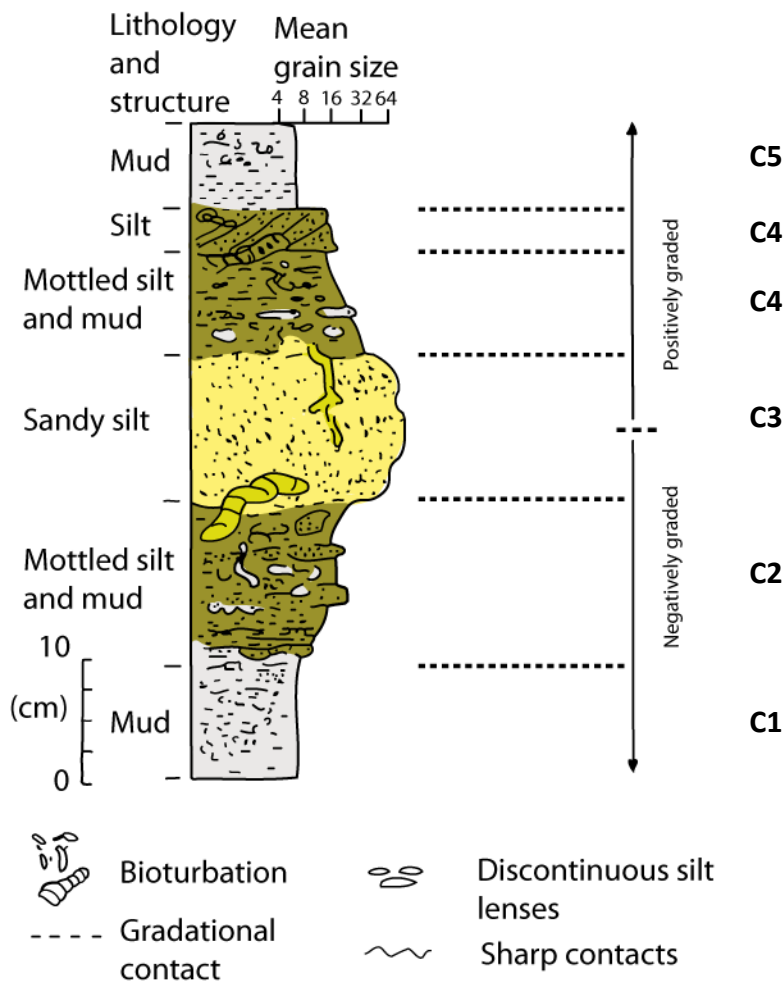


Figure 3.8 Sedimentological log for muddy, silty and sandy contourites (adapted from Stow, 2002; Reading, 1996)

The contourite facies sequence scheme in Figure 3.8 includes from the top:

C5= upper muddy contourite division

C4= upper mottled silty contourite division

C3= middle sandy contourite division

C2= lower mottled silty contourite division

C1= lower muddy contourite division

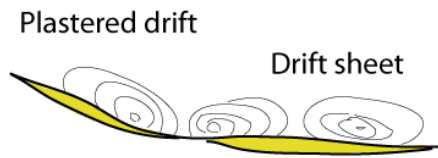
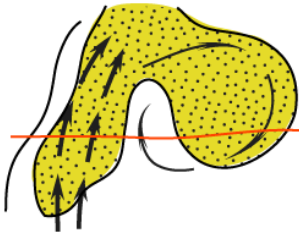
Therefore a complete sequence from muddy through sandy and back to muddy contourite must include C1-C5 sequences. An example of such a sequence is shown in Duan *et al.* (1998), where an Early Ordovician carbonate contourite is exposed in Jiuxi, Northern Hunan, China.

3.6.3 GEOMETRY OF CONTOURITES

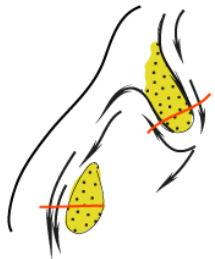
Contourite drifts are grouped into 6 main categories, as defined by Stow *et al.*, (2002). These are strongly controlled by the topography of the basin hosting the drifts as well as water depth. These include (Figure 3.9): contourite sheets drifts, elongated mounded drifts, channel related drifts, confined drifts, infill drifts (drifts that fill areas where mass movement has left an opening), and modified drifts (which are often part of turbidite systems). However, these groups grade into each other and due to their extensive nature creating large contourite systems such as the Giant mounded drifts in the Argentine Continental margin (Hernández-Molina *et al.*, 2009), the Gulf of Cadiz (Hernández-Molina *et al.*, 2006), the Le Danois Contourite Depositional System (Rooij *et al.*, 2010) and the NW European Atlantic margin (e.g. McDonnell and Shannon, 2001; Laberg *et al.*, 2005) that contain several classifications of contourite.

The principal controls on the groups indicated in Figure 3.9 are topography, current velocity, quantities of sediment available and modification by interaction with other slope processes such as turbidity currents, debris flow and creep (Stow *et al.*, 2002).

Type 1 Contourite Sheets



Type 2 Elongate drifts



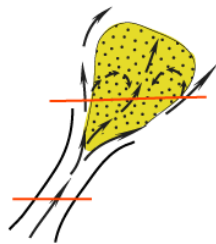
Detached drift



Separated drift



Type 3 Channel-related drifts



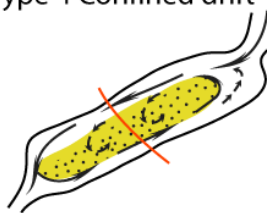
Contourite 'fan'



Lateral and axial patch drifts



Type 4 Confined drift



Type 5 Modified fan-drift

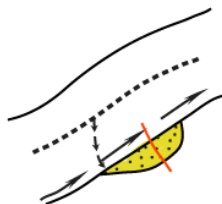


Figure 3.9 Different contourite drift models (adapted from Stow et al., 2002)

Contourite sheets

These form extensive accumulations as part of the fill of basin plains that may extend up to continental margins and basin edges. These contourite drifts generally comprise layers of homogenous sands (e.g. Smith *et al.*, 2010; Stow *et al.*, 2002) that cover a large area, but demonstrate a very slight decrease in thickness towards their margins (e.g. Akhurst, 1993; Amante and Eakins, 2009).

Continental sheet drifts

Sheet drifts that occur on the continental slopes (slope sheets) occur near the foot of slopes where overwelling or down-welling bottom currents exist such as the Gulf of Cadiz because of Mediterranean Sea Water out-welling at an intermediate water level into the Atlantic Ocean (Hernández-Molina *et al.*, 2006; Gonthier *et al.*, 1984; Llave *et al.*, 2001). Another example is found in the Weddell Sea (Antarctica), where these drifts consist of fine-grained muds to sandy contourites that were created due to the down-welling of cold waters coming from the ice sheets (Pudsey, 2002). These sheets also contain sediment deposited by other processes such as turbidity currents (e.g. Michels *et al.*, 2002).

Abyssal sheet drifts

Abyssal sheet drifts typically comprise fine-grained contourite facies, including silts and muds, biogenic-rich pelagic material, interbedded with other basin plain facies. Accumulation rates are generally low, around 2-4 cm per hundred years. Slope sheets are more varied in grain size, composition and rates of accumulation. Thick sandy contourites have been recovered from base-of-slope sheets in the Gulf of Cadiz, and rates of over 20 cm per 100 years are found in sandy-muddy contourite sheets on the Hebridean slope.

Elongated mounded and confined drifts

A mounded and elongate shape characterises these contourite drift deposits which have dimensions in the order of tens of km to over 1000 km long, length and

thicknesses up to 2 km (e.g. Jones and Okada, 2006). They occur from the upper slope to abyssal plains. The margins are commonly flanked by moats along which flows travel and erode into the drift. Elongate drifts associated with channels or confined basins are classified separately as confined drifts.

The elongate geometry of these drifts is governed by the interaction topography, current intensity, and the Coriolis Force (e.g. Michels *et al.*, 2002). Stow *et al.* (2002) suggest that elongation is commonly adjacent to the margin, running parallel to it, with progradation leading to deformation of the drifts. Characteristic sedimentary structures include lenticular, convex-upward depositional units with migrating sediment waves. These drifts can occur as any sediment type; this varies with inputs, that include biogenic, volcanoclastic and terrigenous grains. Grain size varies from mud to sand as a result of long-term fluctuations in bottom current strength (Stow *et al.*, 2002).

Confined drifts are documented to occur in small basins and typically occur in tectonically active areas, such as the Sunda fore arc basin of the Indonesian arc system. These drifts have a similar sedimentary characteristic to elongated mounded drifts with distinct moats along margin edges and sediment type and grain size depending on the nature of input to the bottom current system.

Channel-related drifts

Deep ocean channels, such as oceanic trenches, where bottom circulation is constrained, characterise the location and geometry for this type of sediment drift deposit. These restricted parts of the ocean produce high current velocities and in some cases act as the link between ocean basins such as the Mediterranean and Atlantic thereby allowing the exchange of different oceanic currents. The high velocity of these currents promotes high erosion rates, creating irregular discontinuous sediment bodies, axial and lateral patch drifts, at the down current exit of the channel.

Sedimentary characteristics of these deposits include patches of coarse-grained lag contourites, clast-rich contourites and associated hiatuses that result from substrate

erosion. Sand waves, ripples and dunes are likely to be deposited due to the high current rates in these drifts.

Infill drifts and modified drift-turbidite systems

These deposits infill the scars and irregular topography left by slumps and other gravity flows such as slide deposits (e.g. the “Storegga Slide” (Bryn *et al.* 2005) and “Alexander sedimentary mound” (Viana and Rebesco, 2007). They have been described from the Faro-Albufeira complex in the Gulf of Cadiz (Hernández-Molina *et al.*, 2006) and the Algarve Margin (Salles *et al.*, 2010) and are likely to be common where large scale mass wasting takes place (e.g. Marchès *et al.*, 2010; Lima *et al.*, 2009 ; Bryn *et al.*, 2005).

The interaction of resedimentation events and slope processes appear to be quite common as instability of the continental margin interacts with oceanic currents (e.g. Marchès *et al.*, 2010; Solli *et al.*, 2008). Interactions between downslope or along slope processes are suggested to interact (Huppertz and Piper, 2010) with the dominance of one or the other, because of variations such as sea level change and tectonics (Stow *et al.*, 2002). The interaction between various processes has been described in Pliocene deposits of North East Java (Wilson, 2002).

3.6.4 DISTINCTION OF TURBIDITES FROM CONTOURITES

Several different seismic and sedimentary characteristics for distinguishing turbidite and contourite deposits exist. Levees with wedge-shaped geometries parallel with channels characterise turbidite channels along slopes where commonly the turbidity currents overspill (Rasmussen *et al.*, 2003).

Seismic characteristics of contourite drifts include internal lack of structure with few moderate- to high-amplitude sub-parallel reflectors internal reflections and top surface with waves. Marked erosional surfaces are common features in a contour current deposit, whereas turbidites are commonly even-layered, continuous with on-

lapping reflectors and generally show high reflectivity and strong stratification (Rasmussen *et al.*, 2003).

Alterations between structureless and more structured facies may manifest (Stow *et al.*, 2002) in sedimentary bodies suggesting a mix of sedimentary processes (i.e. turbidites and contourite deposits). In addition, the direction of sediment wave crests on seismic data may also indicate the depositional mode due to direction of sources (i.e. continental slope).

The sedimentological characteristics are further important indicators for distinguishing between turbidite and contourite deposits. Contourites show quite variable sorting and few primary sedimentary structures although cross lamination may be preserved in the sands and in some cases a concentrated gravel lag may form (Stow *et al.*, 2002). The overall sequence may have a negatively (inverse) and positively (normal) graded sequence with no regular sequence of sedimentary structures. Petrographic studies may further help to distinguish between contourites and turbidites, since detrital minerals and lithic clasts can be used to infer the source areas of the sand (Lovell and Stow, 1981).

Turbidites are characterised by a variable grain size distribution, commonly showing grading, but in some cases display basal inverse graded beds. Sandy beds are characterised by a regular sequence of sedimentary structures (Bouma, 1962) that are commonly poorly preserved. Turbidite successions commonly show downslope fining with large-scale sand sheets or turbidite lobes in the basin.

3.7 FORESLOPE CHARACTERISTICS

In both clastic and carbonate marine systems, morphology of the depositional system is limited by interaction of topography, sediment type and rate of sediment accumulation. One of the most important factors creating separate morphological types of resedimented carbonate geometries is how the sediment is supplied, be this via a line source or point source. However, as noted by Playton (2008) the two most important limiting factors in carbonate resedimentation are the effects of early lithification and gravitational instability. This includes reef accretion beyond angle-of-repose, mechanical and chemical erosion due to exposure, changes in pore pressure, displacive early marine cementation and external triggers such as seismicity, storms or tsunamis.

3.7.1 CARBONATE FANS AND APRONS

Submarine fans and aprons are distinctive constructional features found on the sea floor that develop seawards of a carbonate source. They are typified by a constrained nature, which typically concentrates resedimented debris into channels (Playton, 2008) or debris sheets. Fans originate from single sediment source (Payros and Pujalte, 2010) and aprons from a line source (Mullins and Cook, 1986), typically along carbonate platform margins. Both features contain canyons and gullies that transport sediments downslope.

Carbonate fans and aprons are commonly constructed by grain-dominated elements (e.g. gravity flow deposits such as carbonate turbidites and debrites: Wright and Wilson, 1984; Mullins and Cook 1986; Payros et al, 2007; Playton, 2008). However, they range from examples of completely devoid of mud (e.g. Isili Basin, Sardinia, Vigorito et al. 2005) to those dominated by mud (e.g. Savary, 2005).

Ancient carbonate fans show similarities in lithofacies and architecture to siliciclastic fans, although they have less variable grain size: Payros and Pujalte (2010) imply that the most common grain types are loose carbonate allochems derived from shallow-water areas (skeletal, ooids, peloids etc) with most textures being described as packstones and grainstones. Submarine fans can be subdivided into three main

categories as described by Payros and Pujalte (2010): channelled inner/upper fan, mid-fan consisting of branching channels and unchannelled outer/lower fan that grades into the basinal plain. The overriding theme for these models is that fans are derived from a point source.

Two models for carbonate aprons are recognized and were devised by Mullins and Cook (1986): the slope apron and base-of-slope apron. Slope aprons characteristically develop on gentle slopes and base-of-slope aprons steeper slopes. The main difference between the two models is that the slope model is continuous with shallow-water platform sediments whilst the base-of-slope model includes a bypass margin where sediments are transferred to the base-of-slope through gullies and channels.

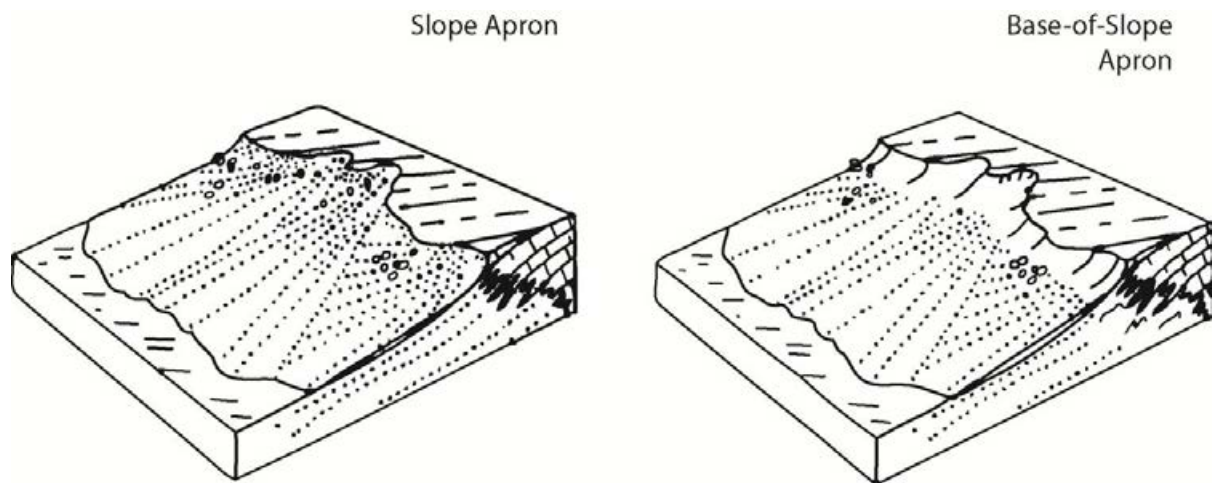


Figure 3.10 Carbonate apron models adapted from Mullins and Cook (1986).

The typical sedimentary deposits seen in both types of apron are megabreccias, proximal turbidites and periplatform oozes. In base-of-slope aprons these deposits are interrupted by numerous gullies and intervals of periplatform ooze. Furthermore previously lithified rip-up clasts from the upper slope are commonly found amongst the resedimented facies.

4. FACIES ANALYSIS

4.1 INTRODUCTION

There are seven principal lithofacies displayed in the outcrops of the Cutri Formation expanded from Barnolas and Simo (1987). These facies are displayed in Figure 4.1.

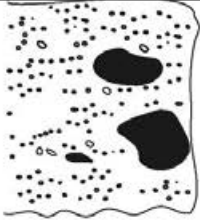
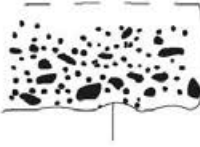
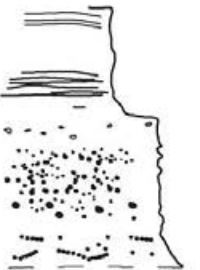
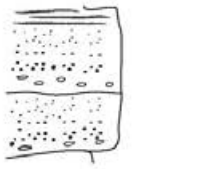
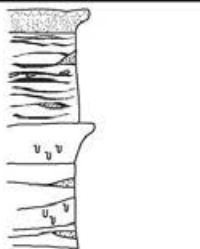


Facies	Schematic Drawing	Key Features
1 Boulder Pebble Conglomerate		<p>Average thickness: 1-5m</p> <p>Clasts: Wackestone and mudstone; 10 to 175 cm in diameter</p> <p>Matrix: Fine to medium sand grade ooids and peloids</p> <p>Structures: Massive, crude orientation of clasts</p> <p>Form/Geometry: Forms individual beds and as channel fills</p> <p>Interpretation: Debrite and channel fill</p>
2 Graded Pebble Conglomerate		<p>Average thickness: 30-40cm</p> <p>Clasts: Clasts make up >20% of the bed and are <15cm in diameter</p> <p>Matrix: Very coarse sand grade (oversized) peloids in a medium sand grade ooid-peloidal matrix</p> <p>Structures: Inverse grading of oversized peloids and erosive bed base</p> <p>Form/Geometry: Always forms the basal part to facies 3</p> <p>Interpretation: Erosive base and coarsest part of proximal turbidites showing R1+R2 divisions (Lowe, 1989)</p>
3 Graded Peloidal Ooid Packstone		<p>Average thickness: 1-4m</p> <p>Clasts: Very coarse wackestone clasts</p> <p>Matrix: Coarse to medium ooid-peloid packstone grading to micrite matrix</p> <p>Structures: A general fining-up character; stratified concentrations of peloids; inverse grading of oversized peloids; stratification of wackestone clasts and planar to wavy lamination</p> <p>Form/Geometry: Beds that always sit on top of facies 2 and are both bounded by facies 5</p> <p>Interpretation: Proximal turbidite showing S1, S2 and S3 divisions (Lowe, 1989)</p>
4 Graded Oolites		<p>Average thickness: 50cm-1m</p> <p>Clasts: Fine sand grade wackestone clasts</p> <p>Matrix: Very fine ooid-peloidal to silt/mud matrix</p> <p>Structures: Normal grading and subtle laminations</p> <p>Form/Geometry: Beds encased in facies 5</p> <p>Interpretation: Distal turbidites</p>
5 Calclutites		<p>Average thickness: 2-5 cm individual beds that commonly aggregate to form a body of sediment average 2-5m thick</p> <p>Clasts: None</p> <p>Matrix: Silt and mud grade</p> <p>Structures: Bioturbation; normal grading; silt lenses; planar laminations</p> <p>Form/Geometry: Thick bodies of sediment bounded by facies 1, 2, 3 and 4</p> <p>Interpretation: Winnowed current deposit</p>
6 Coqunia		<p>Average thickness: 4m</p> <p>Matrix: None; the rock is made up almost completely of <i>Posidonia</i> bivalves</p> <p>Structures: Pseudo-laminations created by accumulations of <i>Posidonia</i> bivalves</p> <p>Form/Geometry: Isolated lenses up to 70m wide that thin and grade into facies 5</p> <p>Interpretation: <i>Coqunia</i> banks</p>
7 Cherty Mudstones		<p>Average thickness: 2m</p> <p>Matrix: None; the rock is made up almost completely of micrite</p> <p>Structures: Chert nodules that occur parallel to bedding</p> <p>Form/Geometry: Thin continuous body that caps the Cutri Formation</p> <p>Interpretation: Deep water (pelagic) mud deposition</p>

Figure 4.1 Facies types of the Cutri Formation.

4.1.1 FACIES 1 (BOULDER PEBBLE CONGLOMERATE):

Field Description: Calcirudites occur in the Cutri Formation as parts of thicker graded bed sequences, and individually as distinctive channel fills. The calcirudites contain a variable size distribution of matrix supported tabular to subrounded clasts ranging from 10 cm to 1.75 m in diameter within in a medium-to-coarse-sand grade ooids and peloids matrix. Locally occurring mudstone-silt matrix is noted. This facies is the coarsest facies type in the Cutri Formation and predominantly occurs within the major oolitic channel at Puig Cutri (Figure 4.2 A; 30m thick by 240 m wide) and smaller channels at Puig de Poloni and Puig de Ses Fites (see Figure 4.2 B and C; 5m thick by 50m wide). Pebble to boulder conglomerate calcirudites occur as individual beds that form on top of the Puig Cutri and amongst other facies at Puig de Ses Fites. This facies never exceeds 6 m in thickness.

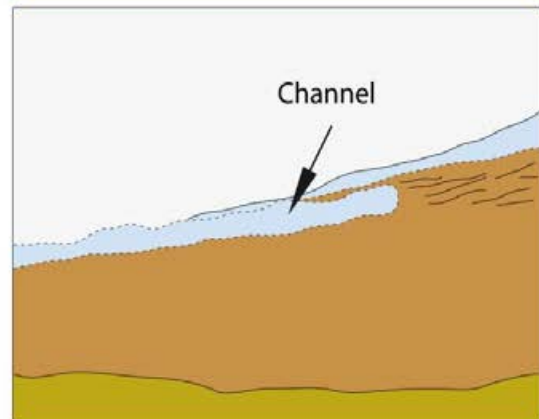
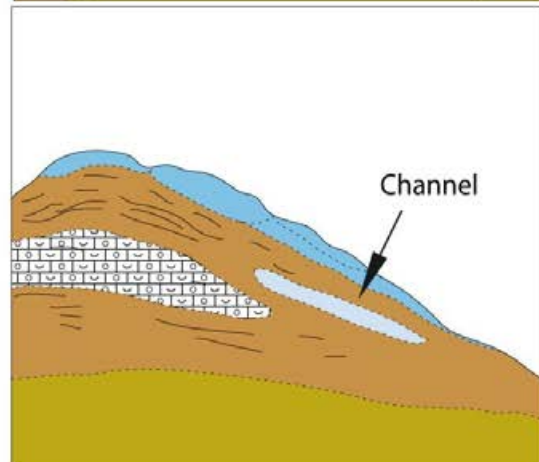
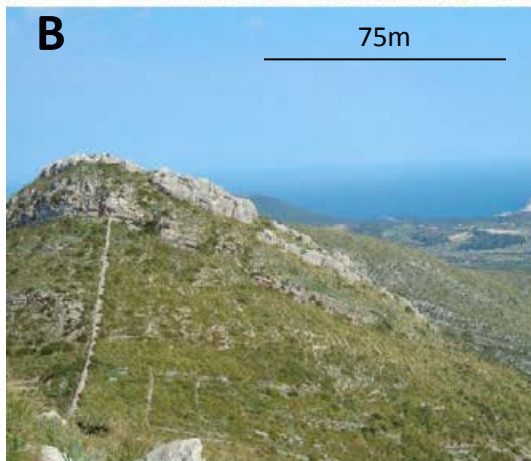
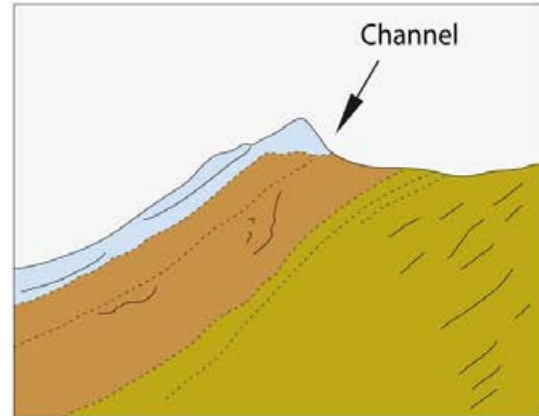


Figure 4.2 Examples of Facies 1 contained in channels. Image A photograph with corresponding field sketch of Puig Cutri looking towards the SW. Image B looking at Puig Poloni and a small channel looking towards NE. C photograph and field sketch of oblique view of a channel, looking towards the SW.

Sedimentary Structures: The pebble boulder conglomerate facies is a poorly sorted, relatively structureless, fine to medium sand grade ooid-peloidal matrix-supported rock. Clasts range from rounded granules to sub-rounded chips, rounded and tabular pebbles and boulder sized clasts. Only clasts found within channels show alignment which trends to the east, these have a tabular nature. The boulders appear broken up and frozen in place, and they show no preferential settling or gradation (Figure 4.2A).

Microfacies: The matrix is mainly packstone with some local grainstone; this microfacies shows weak alignment when in proximity to a clast. The majority of allochems in the matrix are made up of micritised ooids and peloids forming a poorly sorted assemblage of medium to coarse sand grade matrix (Figure 4.3B; Appendix B C001, 2300, 2350; C003, Oolitic Channel). Other minor allochems consist of superficial ooids, coated, disarticulated and abraded shell fragments.

Boulder to coarse sand sized extraclasts (Figure 4.3C) characterise this facies and are composed of two microfacies types. Clast type 1 ranges from mudstone to wackestone where a relatively diverse assemblage of micro-ooids, fine echinoderm fragments, sponge spicules and fine abraded shell material where the muddy matrix is dark grey-green in plane-polarise light (PPL) (Figure 4.4; Appendix B C003s, 1150). Clast type 2 has an allochem suite that is almost completely dominated by strongly aligned disarticulated and abraded thin shelled bivalves (?*Posidonia*) and small quantities of fine micropeloids that appear light grey in PPL (Figure 4.5; Appendix B C003 Oolitic Channel). In CL the clast types display different cements. Clast type 1 has a dull orange luminescence whilst clast type 2 is brightly luminescent. The matrix of the conglomerate is dull orange with patches of bright orange.

The clasts contain cements that are not present in the host matrix, which suggests that these clasts were incorporated as semi-lithified slope sediments and hence probably originated from the shelf edge where marine cements and/or platform top meteoric cements lithified the sediment.

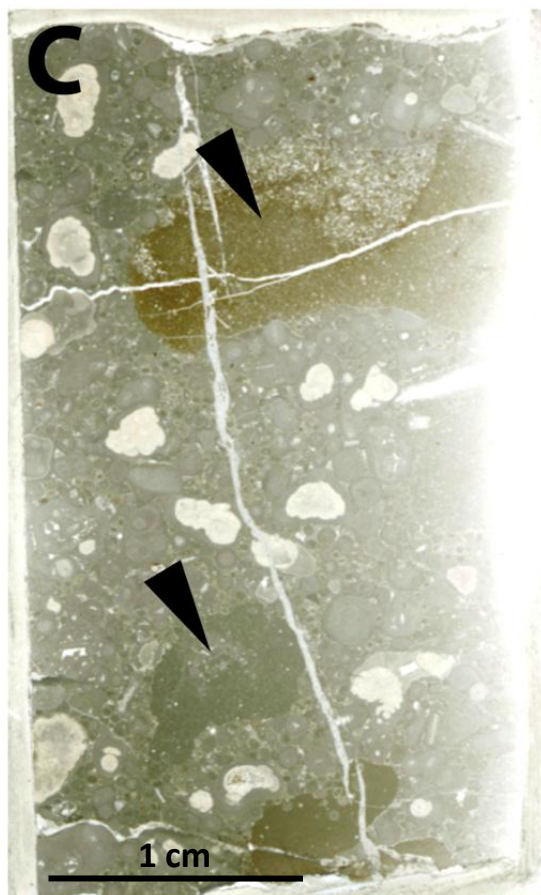
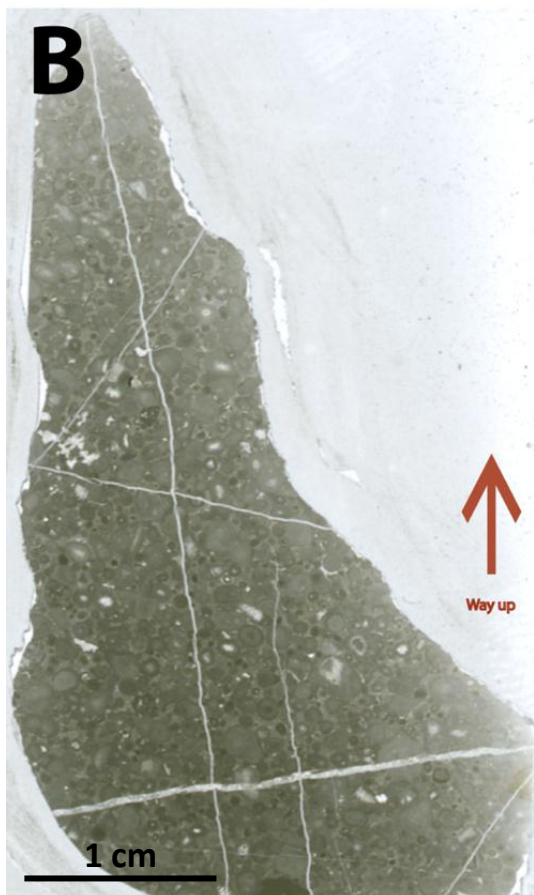


Figure 4.3 An abundance of clasts types and sizes found in facies 1, and appear 'frozen' in flow (A). In image A note the calcite filled fractures in the clasts (outlined in black) that indicate that they were lithified before resedimentation (Hammer head is 15 cm across; Location C003, 2110 cm). (B) Thin section scan of a debris flow note that this is majority matrix (Location C001, 2150 cm). (C) Thin section scan of a channel fill, note the abundance of tabular extraclasts (arrowed) and chert (white clasts) (Location C003, Channel deposit).

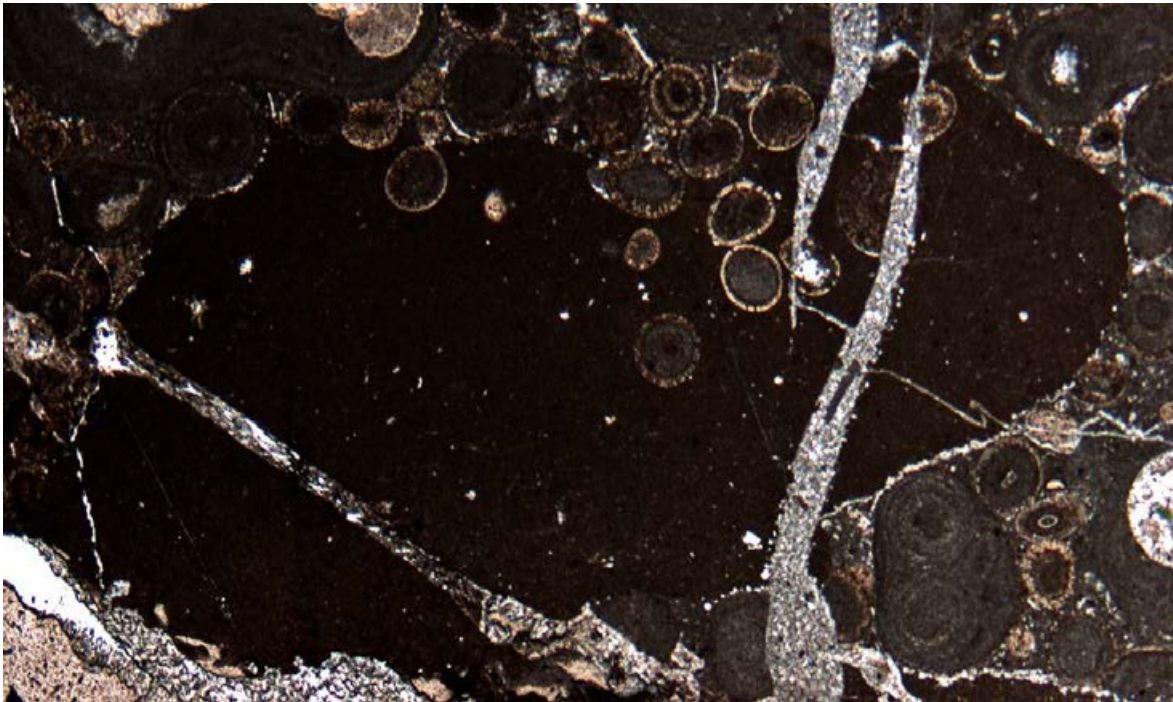


Figure 4.4 Clast type1. Mudstone that consists of tiny abraded fragments of thin shelled bivalves. Note the grainstone matrix (from location C003s). FoV 5.78 x 4.31 mm.

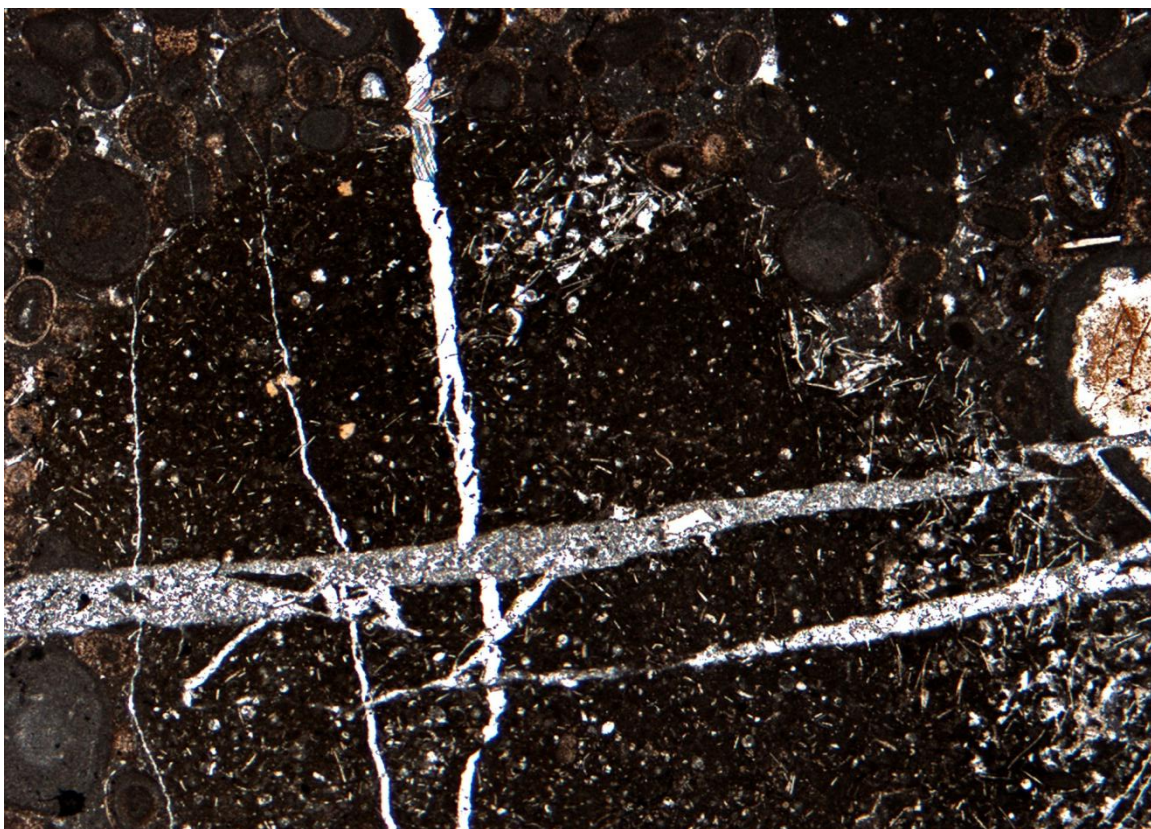


Figure 4.5 Clast type 2. Dense assemblage dominated by disarticulated and abraded *Posidonia* bivalve fragments that are commonly concentrated in regions (from channel deposit at location C003). Note the tabular nature of this clast. FoV 5.78 x 4.31 mm.

Interpretation: The variable clast size, poor sorting and matrix-supported nature of this facies all point to a mixture of processes shared by gravity flow deposits (Mulder and Alexander, 2001; Flügel, 2004; Amy *et al.*, 2005; Felix *et al.*, 2009). However, based on field geometries, clasts size and morphology (whether rounded, tabular etc), the coarsest calcirudites that contain boulder sized clasts are interpreted to be debris flows as they form consistently thick beds and contain boulders that show no orientation, whilst the calcirudites that fill channels contain tabular clasts (orientated E-W) and are interpreted to be channel fills that carried coarse sand grade material from the slope edge into the basin.

The matrix-supported nature of a debris flow is considered by Amy *et al.* (2005) to be indicative of a proximal debris flow (e.g. Haughton *et al.*, 2003; Amy and Talling, 2006). The interpretation herein is the rip-up clasts have a shelf edge to upper slope provenance and this is further verified by evidence seen in CL where the clasts host different cement to that found in the matrix. Structureless debris flows with a similar sand grade matrix have been described by studies such as Pierson and Costa (1987) and Amy *et al.* (2005) and are interpreted as resulting from hyperconcentrated debris flow as modeled by Mulder and Alexander (2001). This is characterised by the rapid en-masse freezing of a highly concentrated flow, which explains the presentation of boulders appearing to be splitting up in transport.

In both channel fill and debris flows the clasts are all observed, through CL, to have different cement to the matrix and therefore probably were cemented before they were incorporated into either debris flows or channel fills. Early cements suggest that the clasts were derived from upper slope to lower shelf edge environments.

Additionally, during transport within debris flows the clasts appear to have started to break up, this is indicative of the semi-lithified composition of these intraclasts as well as the forces involved during transport. As suggested by the hyperconcentrated debris flow model the concentrated nature of the debris flow allowed, upon cessation of flow, the matrix to rapidly freeze in place, preserving clasts preserved in the phase of breaking up.

Within both channel fills and debris flows, the coarser clasts would have been supported within the body of the flow by a variety of mechanisms, including the cohesive strength of the matrix, dispersive pressures (Lowe, 1982; Kessler and Moorhouse, 1984; Amy *et al*, 2005) such as grain to grain contact, traction turbulence within the matrix and fluid pore pressures. Since the flows are matrix-supported, the intraclasts were not supported within the flow by clast to clast collisions, rather the flows were supported by the finer constituent grain to grain collisions that generated important dispersive pressures within the flow. These dispersive pressures created frictional strength within the flow creating the preferred orientation of tabular clasts (within channel fills), suggesting that dispersive pressure orientated these larger clasts within the flow preferentially indicating the probable direction of palaeoflow.

The incorporation of clasts signifies the importance of early lithification in the carbonate shelf edge and upper slope environment as well as quantifying the amount of energy produced within flows and channels needed to rip up segments of the underlying strata. It is interpreted that the fluid in the flow had no cohesion but grain to grain interaction created the energy to erode into the seafloor. Due to the generally structureless nature of the debris flows they probably did not flow for a long distance or have a high water content allowing for surging or sorting, whilst channel fills contain finer intraclasts that probably travelled into distal environments i.e. depositing their load further downslope. Gravity is the main factor that drives these flows, whose velocity and character were a response to the steepness of the slope that the flows ran down. This facies originated in the shelf edge environment where early lithification allowed intraclasts to be incorporated into flows.

4.1.2 FACIES 2 (GRADED PEBBLE CONGLOMERATE):

Field Description: The graded pebble conglomerate occurs as beds that as a whole fine-up and is <45 cm in thickness and characteristically contains > 20% clasts and very coarse peloids. The conglomerate is very poorly sorted and contains inverse clast grading and coarse tail matrix grading. The main constituents are medium sand grade allochems that form the matrix, and coarse sand sized to gravel sized peloids and sub-rounded to rounded pebbles (which have a wackestone texture), which form the remains of the sediment. The characteristic features of this facies are the dominance of large peloids compared with matrix peloids creating a bimodal sorting, the limit of clasts to the base of the facies and the occurrence of coarse tail grading. The coarse peloids commonly show coarse tail grading that commonly occurs in the basal 5 cm of the graded pebble conglomerates. This calcirudite is associated with subtle erosive basal contacts with the underlying strata (Figure 4.6A and C).

Sedimentary Structures: A subtle erosive base characterises this facies type (Figure 4.6A and C). Coarse tail grading of the coarsest peloids dominates the facies, which shows normal grading of ooids and intraclasts whilst the matrix remains massive in nature (Figure 4.6B).



Figure 4.6. Outcrop image of Facies 2 in comparison to background sedimentation at location C002. B- graded pebble conglomerate; note the hammer is 30cm in length (C002 approx 475-510 cm). Detail of erosive basal contact between Facies 2 and finer background sediments (C001 approx. 600cm).

Microfacies: This is a bimodal, very poorly sorted, packstone-grainstone assemblage of abundant very coarse to pebble sized, subrounded to subangular clasts and coarse peloids, which are found within a finer, medium to fine sand grade matrix of deformed radial-fibrous ooids, micritic ooids (with a tangential fabric recognisable in peripheral parts) and aggregate grains (Figure 4.7). Bioclasts most frequently occur as ooid nuclei which include rare poorly preserved microgastropods, foraminifera, disarticulated and abraded bivalve fragments and other very rare fine sand grade rounded shelly fragments (Appendix B, C001, 515).

Clasts have a similar composition to those in facies 1 and consist of two types. Both clast types are wackestones with clast type 1 consisting of a relatively diverse assemblage of micro-ooids and peloids, fine echinoderm fragments, sponge spicules and fine abraded (unidentifiable) shell debris where the muddy matrix is dark grey-green in PPL. Clast type 2 has an allochem assembly that is almost completely dominated by well orientated disarticulated and abraded thin shelled bivalves (?*Posidonia*), small quantities of fine micropeloids coated fine echinoderm debris and silt sized abraded calcite debris. CL indicates that clast type 1 has a dull orange luminescence whilst clast type 2 is brightly luminescent.

Within this facies, ooids have a variety of forms from being completely micritised to showing clear internal structure. Many ooids and other grains have been broken, and show changes in colour from alternating concentric ooid laminae and micritic laminae.



Figure 4.7 Thin section scan of typical Facies 2 microfacies (C001 515cm). Note the abundance of micritic clasts throughout the sample and finer oolitic-peloid matrix.

Interpretation: The variable clast size, poor sorting, matrix-supported nature of this facies all point to mixture of processes shared by gravity flow deposits (Mulder and Alexander, 2001; Flügel, 2004; Amy *et al.*, 2005; Felix *et al.*, 2009). This facies forms the basal divisions of turbidites in the Cutri Formation representing the coarsest section of turbidites, which show parts of the Bouma (Ta, Tb) and Lowe (R2 and R3) turbidite sequences.

This clast-dominated horizon conforms to the R2 and R3 divisions of Lowe's (1982) model for high density and coarse-grained turbidites. It represents deposition by the head of turbidity flows, which were highly erosive and surging in nature (Aalto, 1976; Lowe, 1982), capable of eroding fine-grained muddy slope sediments and integrating them into the body of the flow both as unconsolidated sediment and as semi-lithified slope clasts (e.g. Kano and Takeuchi, 1989; Middleton and Neal, 1989). The clasts within the facies tend to be concentrated towards the base of the flow, though not the very bottom, possibly due to clasts not being able to travel higher in the flow than the turbidite's highest rate of flow (Kano and Takeuchi, 1989), the boundary between suspended turbulent flow and higher density grain: grain contacts. The orientation of clasts (WNW-ESE) points to a possible easterly source for the turbidites.

The basal inverse and coarse tail grading may be due to hydrodynamic phenomena creating a traction carpet (as visible in Lowe, 1982 classification. The inverse grading and separation of finer and coarser clasts is typical of the R2 division and is explained via dispersive pressures that stratified clasts creating a much coarser layer (Lowe, 1982).

This facies is classified as a conglomerate due to its grain size, but forms the first division of carbonate turbidites in the Cutri Formation, which is transitional with graded calcarenites forming the rest of the Lowe sequence. This basal division is interpreted in the same way as Lowe (1982) as R2 and R3, which involves frictional freezing at the base which was driven along by shear strength of the flow, followed by a bombardment of grain: grain suspension fall out leading to the overlying graded features of the following facies type.

4.1.3 FACIES 3 (GRADED PELOIDAL OOID PACKSTONE):

Field Description: Facies 3 forms distinctive beds that commonly occur above facies 2 but also occur individually. The beds weather proud and tend to fine up section, ranging from 5 m to tens of centimetres in thickness.

Sedimentary Structures: The base of facies 3 is commonly represented by a gradational contact with the boulder-pebble conglomerate (Facies 2) or a very subtle erosive base. Facies 3 characteristically consists of two principal alternating sedimentary structures as well as an overall grain size decrease up section. The two principal alternating sedimentary structures are concentrated layers of stratified coarse peloids and fine to medium sand grade wackestone clasts which alternate with coarse tail grading found amongst coarse peloids (ranging from 2.5 mm to <250 µm). Flute marks, cross stratification and other sedimentary features common in siliciclastic turbidites are not noted in this facies.

Microfacies: The calcarenites of this facies are characteristically wacke-packstones to packstones that characteristically contain very little bioclastic material with the exception of *Posidonia* bivalves which occasionally form aligned accumulations at the very top of the calcarenite facies just below the finest portions of this facies (Figure 4.8B and C; Appendix B, C001 560). Other bioclasts that form constituent parts of the matrix are large benthic foraminifera, abraded echinoderm fragments (that all have syntaxial calcitic overgrowths), microgastropods and other shelly fragments. These bioclasts almost always have a micritic coat and commonly form the nuclei of coated grains. This microfacies contains a general fining up sequence that consists of very coarse to coarse sand grade ooid-peloidal sediment near the base (where they contrast with facies 2) and grade normally to massive coarse-medium to medium-fine sand grade muddy ooid-peloidal sediments where this facies generally grades up to muds that limit the facies. The calcarenites have alternating structures that consist of stratified medium to coarse sand grade mud, coarse sand grade wackestone intraclasts and concentrated beds of stratified oversized peloids of coarse sand grade size and are capped by fine laminations of coarse tail grading and inverse grading of ooids and peloids.

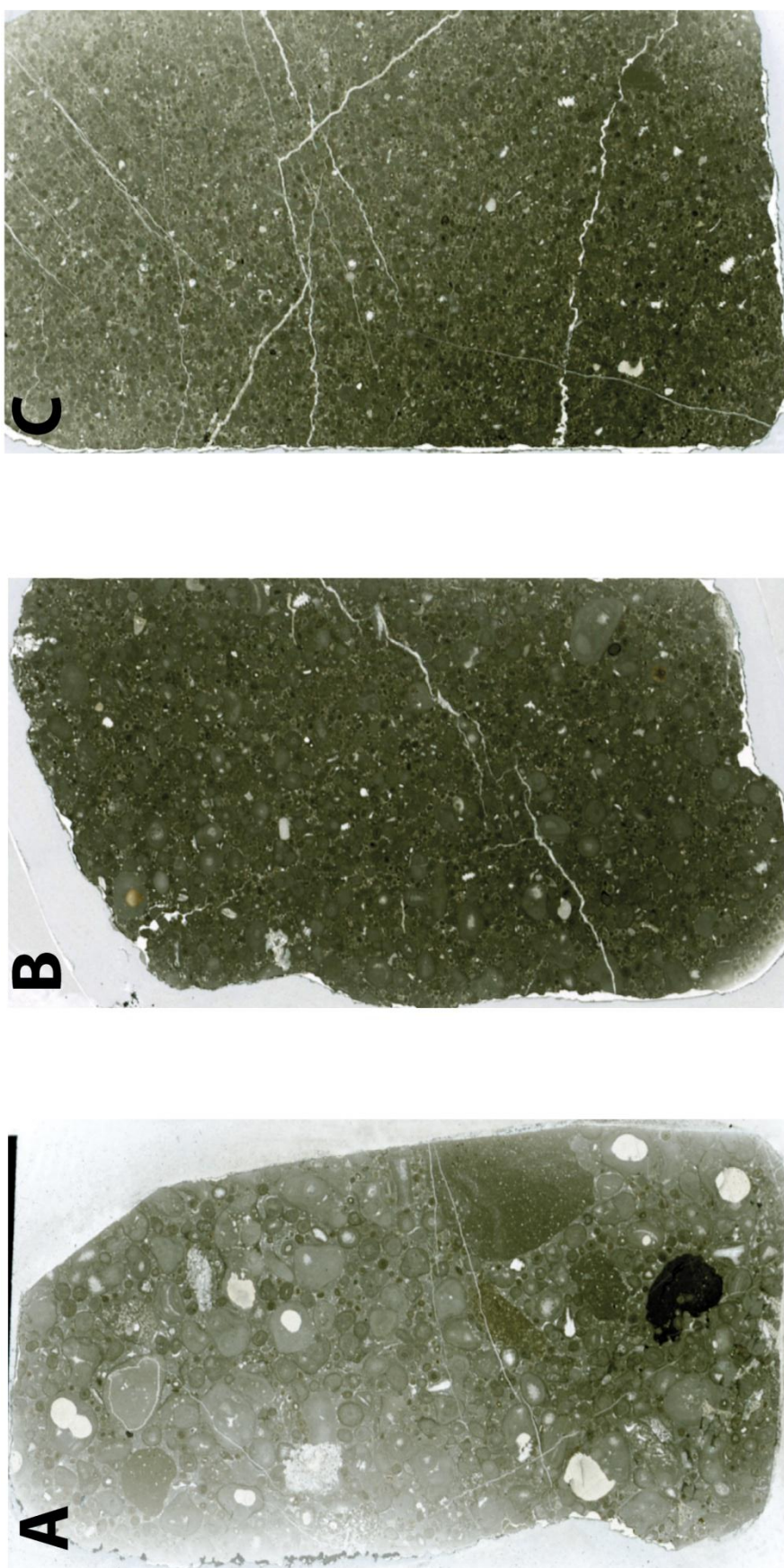


Figure 4.8. Comparison of microfacies 2 and 3. (A) S1 division of Lower (1989) facies 2, (B) S2 and (C) S3 division of Lower (1989) within facies 3. Note the change in grain size from A-C.

Interpretation: Divisions S1, S2 and S3 calcarenites consist of graded peloidal-oolid packstones, which are interpreted to be of Lowe (1982) coarse-grained turbidite classification (Figure 4.8). The presence of Lowe's (1982) sequences, and less well developed Bouma sequences, meets the criteria to characterise calcarenites attached to graded pebble conglomerates as coarse grained proximal turbidite deposits and much thinner graded low density ooid-peloid packstones. This facies sometimes occurs on its own or grades up from the graded conglomerate.

These sediments are interpreted by their graded nature, succession of sedimentary features including grading of peloids, inclusion of mud-wackestone clasts and stratification of grains to reflect the deposition of sediments by high-density turbidity flows. Suspension was by a combination of dispersive pressure and turbulence. This facies is represented by the 'S3' division of Lowe's (1982) classification of coarse-grained turbidites.

The concentration of graded coarse peloids and other finer sand grade grains at the base of this facies are related to the S1 division of the Lowe (1982) classification (Figure 4.8). The S1 division is characterised by coarse tail grading and stratification of peloids in the Cutri Formation and indicates the changing hydrodynamic conditions after deposition of the graded pebble conglomerates. The S2 division overlies S1 and consists of a massive fine to medium sand-grade ooid matrix with continued inverse coarse tail grading of oversized peloids. The continuation of coarse tail grading was probably caused by the increased dispersive pressures created after initial deposition of the S1 division. The change in sedimentary divisions associated with S1 and S2 indicate a change in energy levels within the turbidity current, which probably represents surging. The S1 and S2 alternating sequences are repeated up through the turbidite, becoming thinner up section resulting in a gradual reduction in coarse peloids compared to the oolite portions that themselves show little change in grain size.

The interpreted pulses of material can be seen in outcrop as thin traction carpets (S1) overlain by thicker suspension sediment (S2) horizons which were deposited via acceleration and deceleration of the turbidity current. This sequence grades, with eventual loss of pulsing energy, into final deposits of finer grade subtly laminated peloidal-oolitic material; this is interpreted as the S3 division of the turbidite and

represents the dwindling of dispersive energy with the increasing dominance of suspension as a depositional mechanism (Figure 4.8). Intraclasts that have a composition similar to those described in the boulder pebble conglomerate are only seen in the S1 and S2 divisions of this facies. They have a mudstone-wackestone fabric and host an assortment of very fine to fine grade bioclastic material that includes disarticulated bivalve fragments, foraminifera and shell material. The clasts in this facies are aligned to the direction of flow and help define sedimentary structures from their distribution.

The S3 division contains a subtly planar laminated to massive fine- to medium-sand grade sediment with subtle water-escape features (noted by Abbots, 1989) and subtle wavy laminations. This division is interpreted as the transition from high density sediments to lower density of sediments within the turbidity current. Suspension has overtaken other depositional mechanisms and accumulated rapidly as the growing surface of the bed coincided with the suspended cloud leading to very rapid deposition (Abbots, 1989), as suggested by water-escape features. The planar laminations may have been created via the deposition of clouds of suspended sediment that flowed by gravity downslope, influenced by the overall turbidity current, and produced the force to cut into the underlying sediments (Abbots, 1989). The remaining S3 division consists of a fining up sequence to a mudstone that caps the turbidites, where sand to silt grade suspended particles ceased to be deposited and the finest mud-grade sediments were deposited as a fissile mud.

Lack of sedimentary structures otherwise common in clastic turbidites (i.e. flute casts, grooves, cross stratification etc) is likely due to the thixotropic (Flügel, 2004) nature of carbonate mud and the relatively soft sediment the turbidites eroded, or the structureless nature of these may be the result of liquefaction or dewatering.

Proximal turbidite deposits within this facies are typically thick with grain-supported fabrics. The coarsest grained deposits are usually distributed in proximal parts of a carbonate apron (e.g. Cook, 1983; Melim and Scholle 1995; Whalen *et al.*, 2000b; Drzewiecki and Simo, 2002). The sequence of events and processes above is indicative for the sequence first described by Lowe (1982) which indicates the sediments of the Cutri Formation were deposited through high density turbidites. The coarsest grains are deposited in this sequence and were therefore deposited first by a decelerating flow.

4.1.4 FACIES 4 (GRADED OOLITES):

Field Description: This calcarenite has a fine to medium sand grade oolitic-peloidal matrix and occurs as thin beds (always <1 m). The beds are commonly less than half a metre thick with both tops and bases being planar (Figure 4.9). Normal grading occurs from a basal medium to coarse sand fining up to fine sand to silt-grade sediment. This sequence is capped by a laminated mud.

Sedimentary Structures: Normal grading of the coarsest material (medium to fine-sand grade allochems) and subtle dispersive grading of the coarse material has blurred the clarity of normal grading.

Microfacies: This calcarenite is commonly a wackestone packstone and is characterised by subtle normal grading of sparse fine sand to medium sand grade peloids and ooids that consists of a micrite matrix, which often consists of 50-70% of the rock. Allochems are laminated subparallel to bedding with the most widespread bioclasts being fine to medium sand-grade disarticulated and abraded thin shelled bivalves (?*Posidonia*), fine echinoderm debris, rare biserial foraminifera, and other shelly debris. In CL these microfacies are always a dull brown-orange luminescence.



Figure 4.9 Outcrop of facies 4.

Interpretation: This facies represents distal turbidites that consist of much finer material than facies 3 and distribution grading, which indicates deposition by minimal turbulence and dispersive pressures between grains (Lowe, 1982). This facies is characterised by the upper part of the Bouma graded bed sequence and some features of the Lowe S3 division. These turbidite sediments were most likely deposited at the margins of submarine fans some distance from their source. The bioclast assemblage is very similar to facies 3 suggesting that these facies may have a similar source.

4.1.5 FACIES 5 (CALCILUTITES):

Field Description: Thick muddy beds intervene between the coarser facies of facies 1, 2, 3 and 4 and consist of silt to very fine to fine sand grade mudstones, wackestones and fissile often cherty pelagic mudstones. They appear in outcrop as accumulations of weathered grey, brown and orangey-brown lithologies. The units range from 1 m to 2.5 m thick and are made up of 2-5 cm thick beds and laminations of light brown-yellow and grey muds. Beds consist of fine wavy laminations (1-10 mm; Figure 4.10) and have common inverse grading, particularly within the coarsest sediments.

Bioturbation is abundant in this facies typically consisting of distinct *Chondrites* and *Planolites* type burrows as well as rarer *Zoophycos*. Other larger bioturbation structures are noted that truncate laminations (Figure 4.10b). Amongst the wavy laminations chert nodules are common, found following the bedding planes.

Sedimentary Structures: Normal grading (Figure 4.11A), lenticular and wavy laminations, cross bedding, ripples and abundant bioturbation also characterise this facies (Figure 4.10). The largest sedimentary structures are large ripples with a 1 to 2 metre wavelength and 10-30 cm amplitude (Figure 4.10C). Within these large ripples are another set of smaller ripples that are between 20 and 30cm in wavelength occurring subtly within individual beds (Figure 4.10A, B and D).

Microfacies: A variety of microfacies are found within the calcilutites of the Cutri Formation. These vary from mudstones to well-orientated *Posidonia* dominated wackestones (see Appendix B, C002: 320, 350) to strongly graded calcisilte (see Appendix B, C002 480) that contain rare silt grade peloids, rare poorly preserved foraminifera and other shelly fragments (Figure 4.11B). The majority of the laminations consist of 50-70% micritic matrix with occasional accumulations of *Posidonia* bivalves that make up >50% of the bed (Figure 4.11B; Appendix B 350). All microfacies are commonly disrupted by bioturbation (Figure 4.11C). Fossil types are most commonly *Posidonia* thin shelled bivalves with rare occurrences of single foraminiferas and other thin shelled bivalve species.

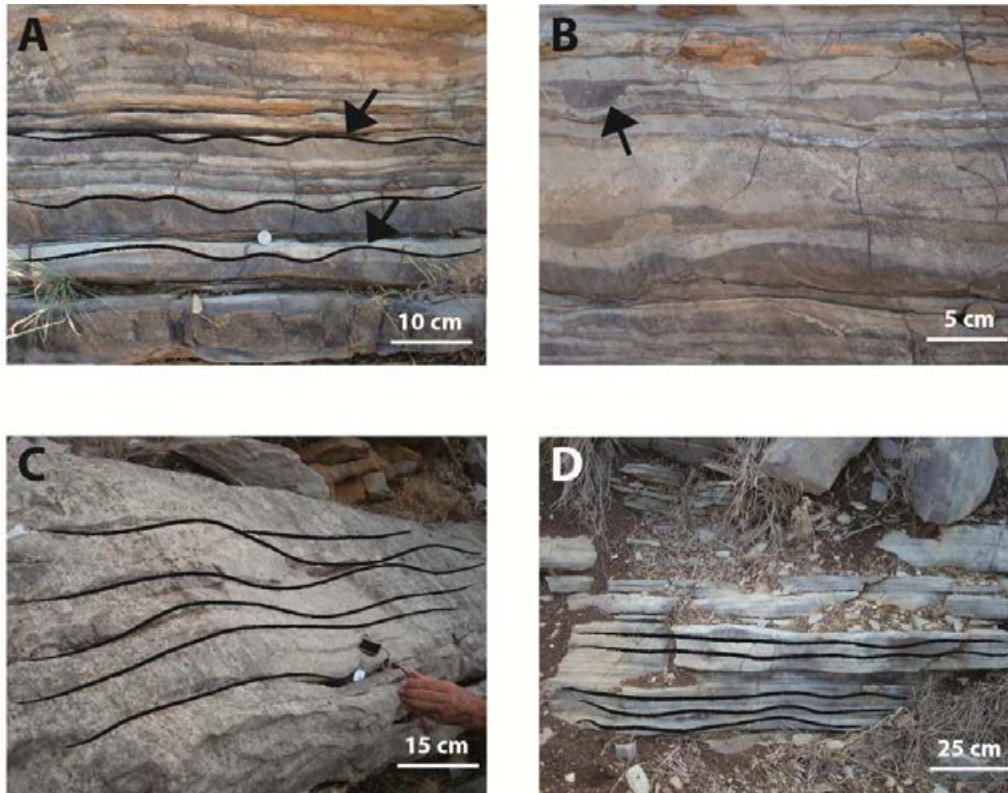


Figure 4.10 Sedimentary structures of facies 5. All Figures consist of part of a succession of subtle ripples (1-2m wavelength) that dampen up section where planar laminations prevail (note D). Ripple features (10-40 cm wavelength). Top left arrow in image B indicates a large burrow that truncates underlying laminations.

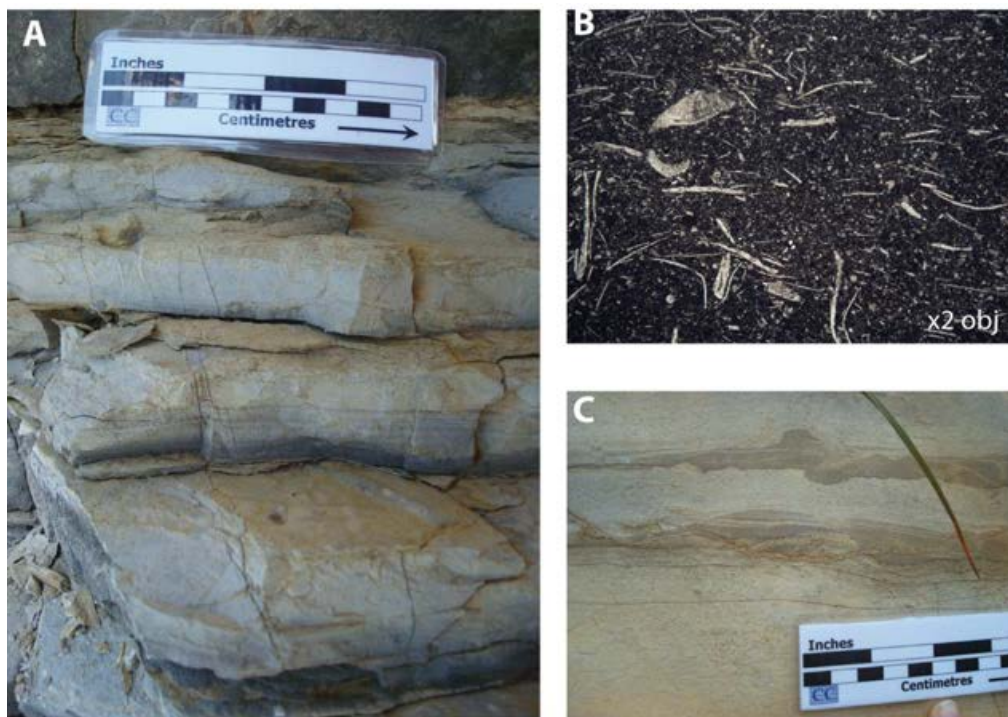


Figure 4.11 A and C Outcrop image of facies 5 note the very clear graded sequences in A and bioturbation, wispy laminations and cross bedding in C. B is a photomicrograph of facies 5 note the change in orientation of allochems in off centre position; this is due to bioturbation (FoV 5.78 x 4.31 mm).

Interpretation: Normal grading, ripples, cross stratification and laminations distinguish this facies as a contourite. The entire facies hosts a general fining-up sequence with individual beds showing fining-up in grain size, suggesting an decreasing influx of coarser sediment that may have been deposited via an accumulation of dilute turbidity flows and suspended fines from the developing carbonate apron complex higher up the carbonate platform, which resulted in the deposition of turbidity flows that commonly overlie this facies.

The facies is distinguished by its large ripples containing laminations that have preserved cross stratification and smaller ripples within the much larger ripples; this deposit is characterised as C4 of Stow's (2002) classification. Overlying these silty deposits are massive and fissile structureless mudstones that are interpreted as originating as pelagic mud deposits (Abbots, 1989) and as C1/C6 of Stow's (2002) classification, whilst the peloidal wackestones and packstones were likely derived from a number of sources, that were mixed in a current swept basin are interpreted as C5 of Stow's (2002) classification. This mixture of sedimentary process probably includes dilute low density turbidites as well as winnowing and redeposition of peri-platform sediment in response to storms although this is not distinctly derived from the classification of Stow, (2002) it is regarded as C5 due to its grain size and granular/sandy nature.

Dominance of burrowing activity throughout the deposit is observed to have taken place by *Chondrites* and *Planolites*. A hydrogen sulphide scent given off upon crushing the rocks, indicating there is probably a relatively high organic content. Large 2-7cm wide features that truncate underlying laminations filled by overlying sediments (Figure 4.10b); could have been created by bottom-dwelling fish or other large organisms (Pomar, 2011 Pers com). Facies 5 shows similarities to tidalites of the Los Molles Formation of Chile (Bell and Suárez, 1995).

4.1.6 FACIES 6 (COQUNIA):

Field Description: Notable accumulations of bivalves occur within this facies and are found only within calcilutites deposits forming flat bottom lens-shaped banks with dimensions of 30 m wide by 10 m height. These bivalve coquinas consist of accumulations of the bivalve ?*Posidonia* and possibly ?*Bositra* (Figure 4.12), with a matrix of dark brown to black carbonate mud and have a wackestone to packstone texture (modified by compaction) and are found with rare echinoderm debris, ?aptychi, calcified radiolarian and occasional peloids. These accumulations are commonly interbedded with thin beds of massive carbonate mud forming in association with facies 5. These accumulations are moderately well-sorted and occasionally show a rhythmic gradation with mud-rich laminations becoming more frequent up section.

Sedimentary Structures: Pseudo-laminations characterise this facies; however, this is caused by the alignment of bivalves within the rock.

Microfacies: Strongly-orientated parallel to bedding *Posidonia* or ?*Bositra* bivalves, coarse ?apatchi and abraded echinoderm fragments that are lined with dark brown to black mud forming laminations that this facies (Figure 4.12A). Note that the packstone nature seen in Figure 4.12A is likely a product of compaction. The *Posidonia* bivalve fragments are up to 1 cm in length and very thin, averaging about 0.05 mm, and are a uniform thickness along their length. The majority of bivalves are broken and disarticulated, with boring being rare. Bioturbation is common and disturbs the laminations most often being *Chondrites* and *Planolites* type burrows. Compaction has been intense and made it difficult to judge how the bivalves were orientated during deposition. The bivalves are preserved with calcite crystals oblique to the outer and inner shell surfaces (Figure 4.13). The bivalves show an orientation which is parallel to sub parallel to bedding.

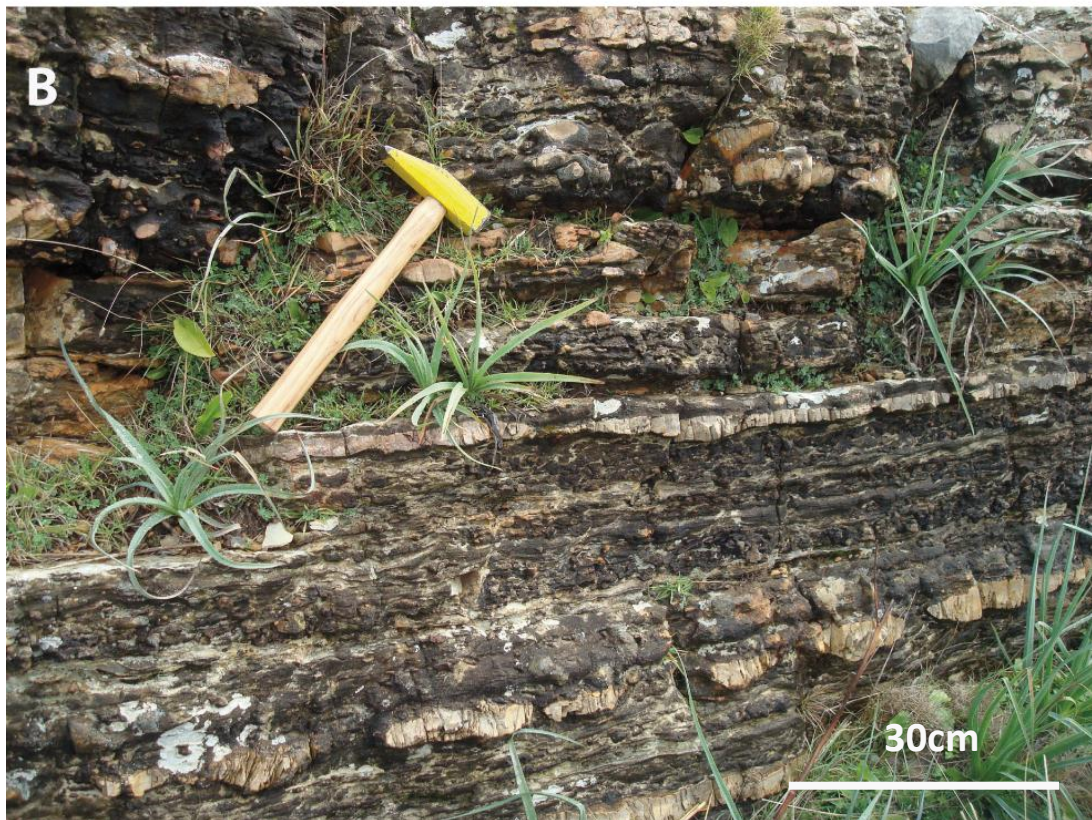


Figure 4.12 Photomicrograph (FoV 2.89 x 2.15 mm) and outcrop photograph of facies 6.

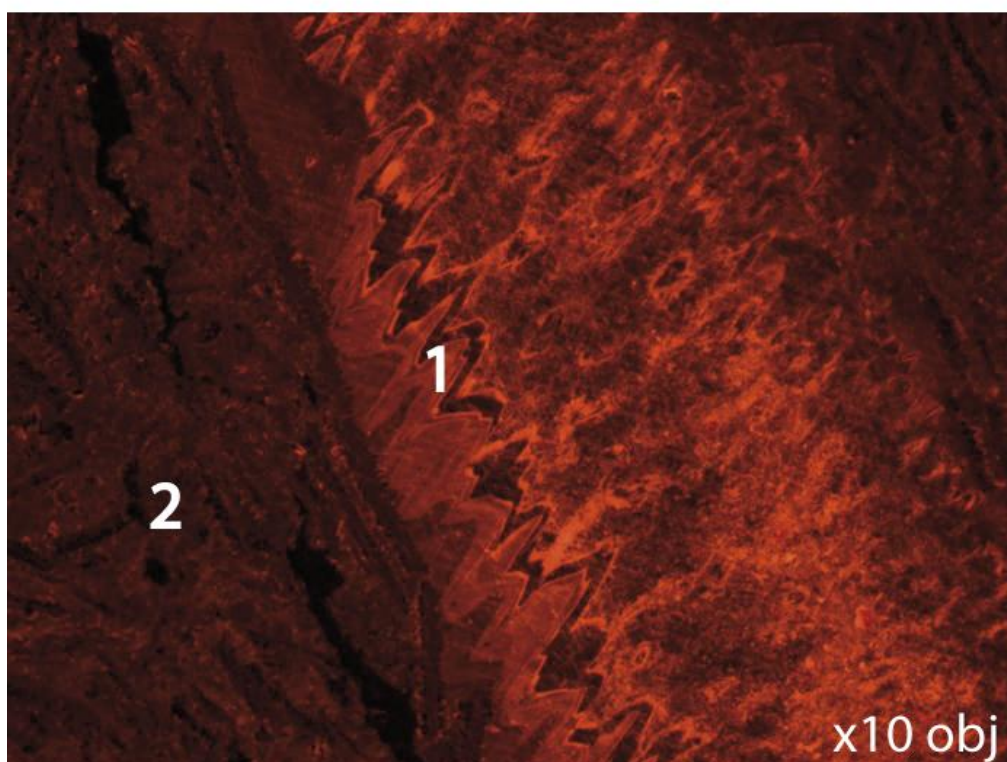
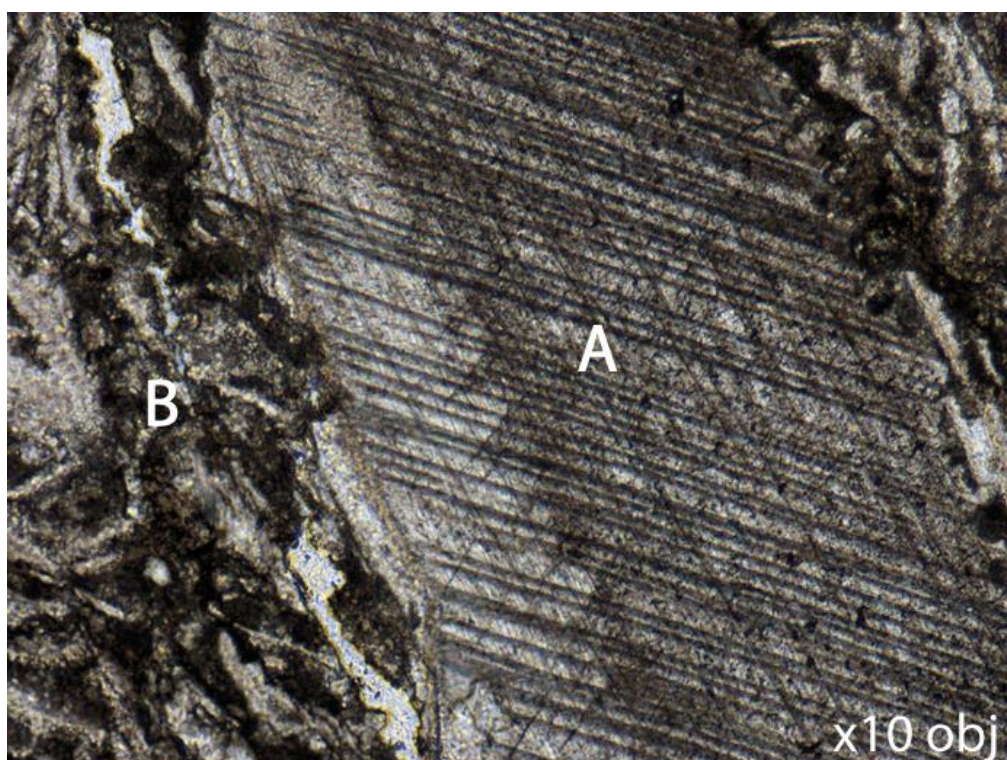


Figure 4.13 Photomicrograph and cathodoluminescence view of a *Bositra* bivalve amongst fine bivalve debris. A and 1 indicate the internal structure of a shell, consisting of calcite crystals oblique to the outer and inner shell surfaces. B and 2 indicate matrix composition (FoV 1.16 x 0.86mm).

Interpretation: *Posidonia* bivalves are characteristic of deeper water environments (Navarro *et al.*, 2009) and were probably nektonic in nature. In the Cutri Formation they have been observed to occur alongside other faunal remains characteristic of deep water environments such as radiolaria (Abbots, 1989), a planktonic fauna, and ?aptychi, which preserved in their original calcite form. The constituent grains are commonly aligned parallel to the bedding (Figure 4.12B), this orientation was likely to have been created by deposition and enhanced through compaction. These coquina accumulations locally alternate with thin layers of pelagic mud (Figure 4.14). This pelagic mud, found compacted between individual bivalves, gives the coquinas a black colour in outcrop. Burrowing occasionally disturb the fine laminations, with *Planolites* and *Chondrites*-type burrows occurring in outcrop, the low diversity of ichnotraces suggesting a restricted environment within the area of deposition (Seilacher, 2007).

Complete specimens of the bivalves were not found in the outcrop, only disarticulated bivalves were seen. *Posidonia* are the most commonly reported in the Subbetic (e.g. Colom 1962, Linares and Vera 1966; Azema *et al.*, 1971, Gonzalez-Donoso *et al.*, 1971, Rivas 1975, Rivas *et al.*, 1997) suggesting that the bivalve was widespread across that part of the Tethys Ocean.

Rivas (1975) described the distinctive features of *Bositra* compared with *Entolium*. Unfortunately, fossil characteristics were insufficient to identify the bivalves as either *Bositra* or *Entolium* genera. However, *Bositra* is commonly found within resedimented facies in this setting during the Jurassic (e.g. Portugal (Wright and Wilson, 1984); Subbetic Cordillera (Mamet and Pr  at, 2006); France (Olivero and Gaillard, 1996); Southern Alps, Italy (Cobianchi and Picotti, 2001).

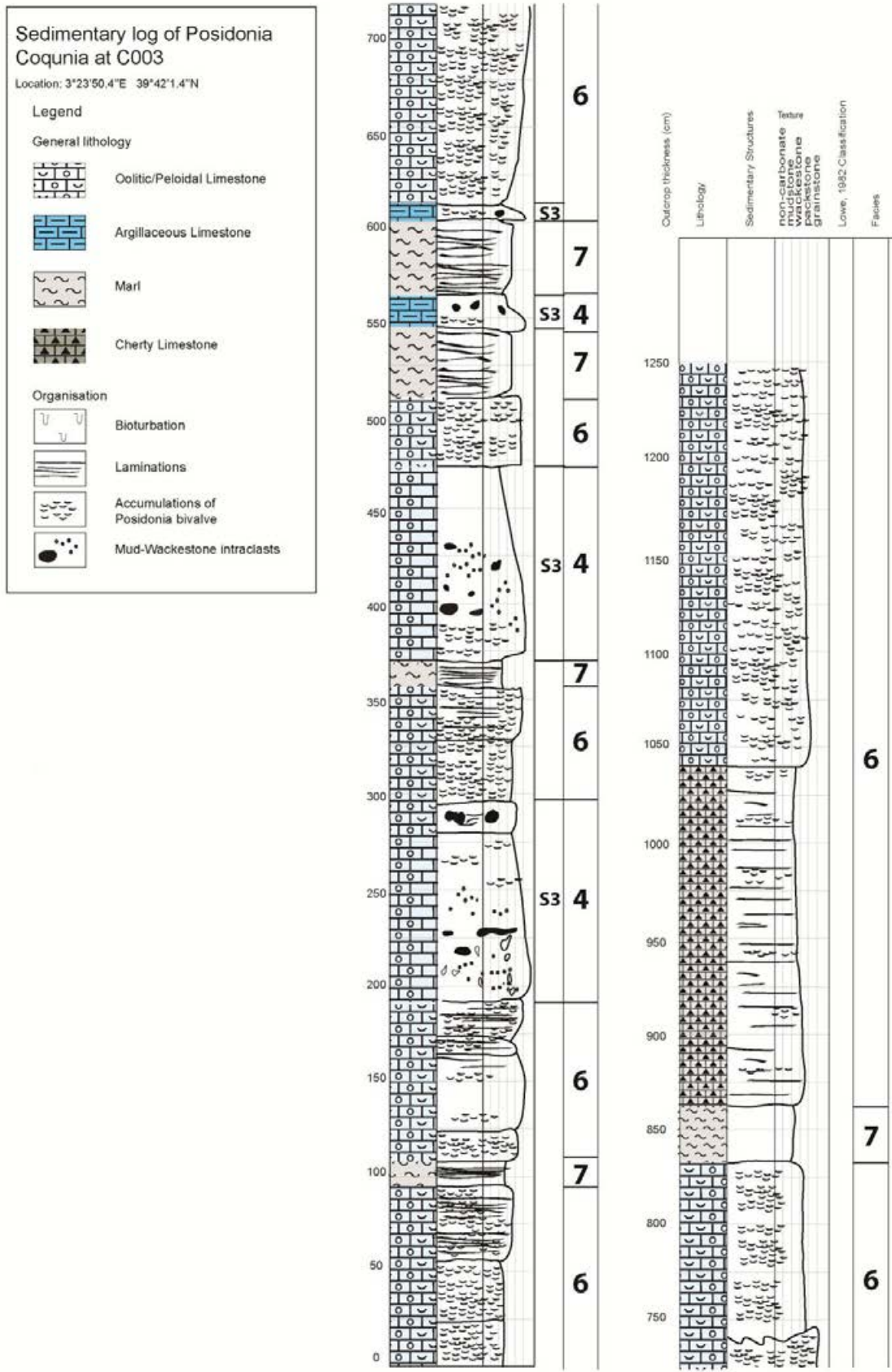


Figure 4.14 Sedimentary log of accumulation of facies 6 and annotated facies at Location C003.

4.1.7 FACIES 7 (MUDSTONES):

Field Description: Mudstones occur locally up to 2m thick (Figure 4.15), but more commonly are cm thick. Consisting of micrites and rare wackestones this facies is mainly found overlying the Cutri Formation, most notably at Puig Cutri. It is also interbedded between the occurrences of facies 2 and 3, especially at location C001.

Sedimentary Structures: Chert nodules dominate the facies and follow bedding planes. The nodules are commonly up to 10 cm in length. Subtle laminations are noted in a few locations that run parallel to bedding often hosting chert nodules. The mudstones have a planar contact with the underlying sediments.

Microfacies: Varying from well-orientated carbonate mud-wackestone that consists mainly of well-rounded poorly-preserved silt-sized calcite grains (probably disarticulated and eroded bivalve fragments) to complete mud-dominated accumulations (see Appendix B; C001, 1450, 1848 C003, 1190). Abbots (1989) noted the presence of radiolarian in this facies; however only rare quantities were seen in this study. The microfacies often exhibit burrows and an abundance of chalcedony grains. Bioturbation is common and consists of *Planolites* burrows and other general mixing of the sediment.

Interpretation: The presence of radiolarians in this study and the inclusion of fine grained poorly preserved calcite material, similar to grains in facies 5, suggests that this facies may represent very fine sediments being transported into the deep basin by suspension. These were therefore deposited alongside pelagic and periplatform sediments rather than representing true pelagic deposition which characterise the Puig de Ses Fites Formation.



Figure 4.15 Outcrop of facies 7. Note the abundance of chert nodules that follow bedding planes. Hammer 30cm in length.

4.2 FIELD LOCATIONS

The Puig Cutri has been divided into geographical 'regions' (Figure 4.16) where distinctive geometries differ, these are separated by the E-W strike-slip fault found immediately north of Puig Cutri. South of this fault the area is divided into two. The '*Puig Cutri Area*' is dominated by a massive oolitic gully fill that cuts into underlying strata and is capped by resedimented rocks and a small quantity of the overlying formation, whilst the 'Puig Cutri Southern Section' consists of a series of high density turbidites; this has been coined 'The Cutri Formation mega-sequence' by Abbots (1989). Areas north of the E-W strike-slip fault are divided into two areas named after their peaks; the 'Puig Poloni to Puig de Ses Fites' and the 'Puig Poloni South'. The 'Puig Poloni to Puig de Ses Fites' has a very similar geology compared to the southern section whilst the 'Puig Poloni East' is a unique outcrop which represents a deposition within in more proximal settings when compared to the other outcrops.

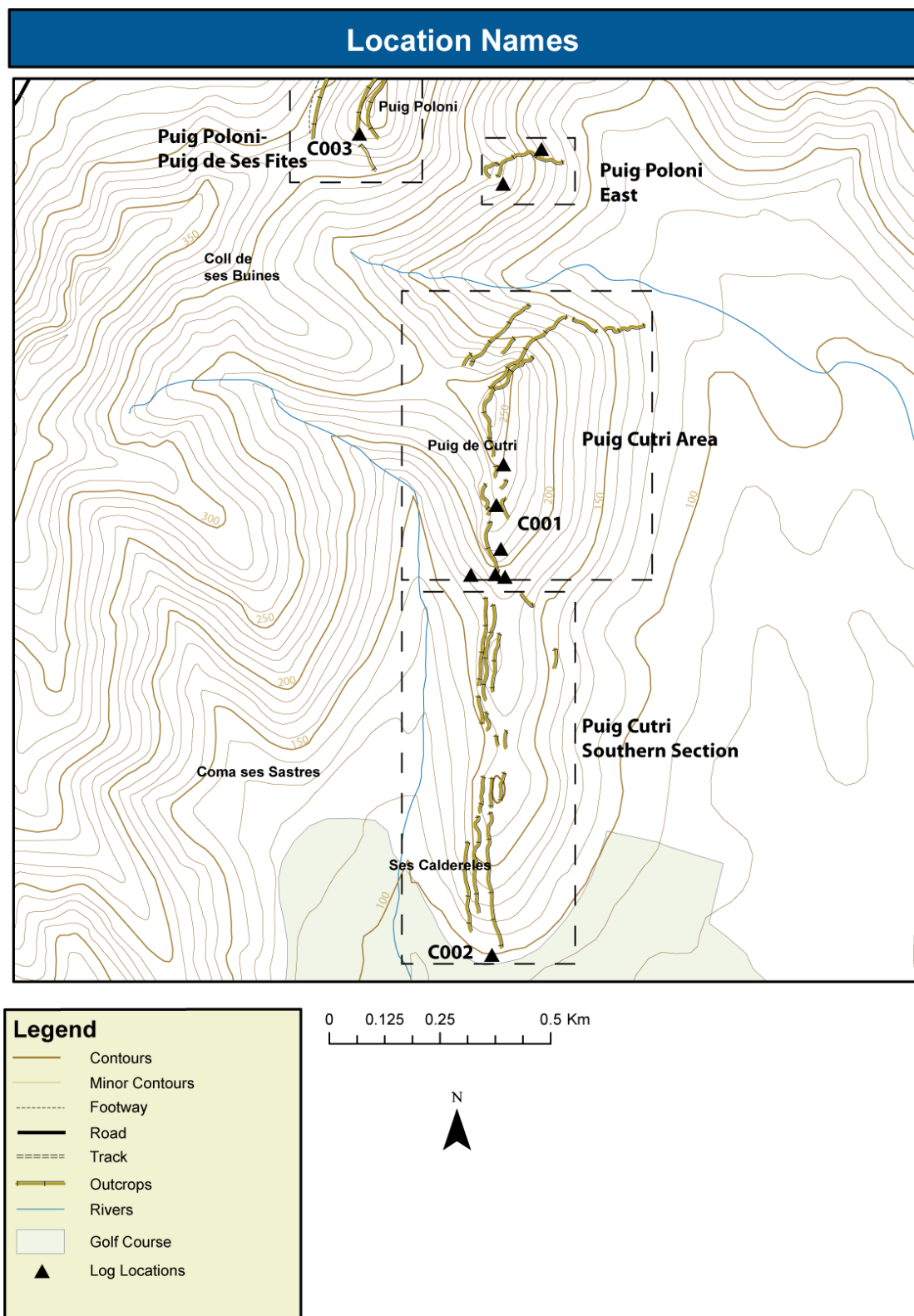


Figure 4.16 Location names found in this report with logging locations. Triangles indicate individual start log locations (sedimentary logs are presented as composite). Based on CNIG (Divisi3n 672-IV Art3).

4.2.1 PUIG CUTRI AREA (C001)

The Puig Cutri Area is the area immediately surrounds the Puig Cutri, and is dominated by a sub-vertical cliff of massive oolitic packstone grainstones that are up to 30 m thick and is capped by separate turbidite deposits (Figure 4.17; Figure 4.18a-b). These pack-grainstones are observed to erode into the underlying Cuber Formation (see 500, 600 and 1200 cm on Figure 4.18a), incorporating semi-lithified clasts into turbidity currents. This erosional unit consists of compacted oolitic pack-grainstones, and is 30 m wide and 20 m high with no large boulders or blocks being observed and has a geometry showing a channel infilled with high-density turbidite sands (Alvaro *et al.*, 1984a; Abbots, 1989). This channel was interpreted to have transported oolitic material out onto the inner apron (Abbots, 1989). The muddy oolitic sediment was transported with the incorporation of slope-derived muds, which supported dispersive pressures between the grains and dampened grain destruction during transport. The channel is orientated E-W and cuts downwards in a westerly direction, suggesting an eastward source direction. Additionally within facies 5 large ripples and cross stratification are always orientated perpendicular to the overlying orientation suggesting that currents were likely coming down the slope into deeper water.

Similar U-shaped back-filled channels cutting across the proximal apron have been described by Mullins *et al.* (1984), Phelps and Kerans, (2007), Noda and Toshimitsu (2009), and Sami *et al.* (2010). Comparable gully fills that cut into slope mudstone and which are similarly plugged with sediment coarser than the slope material are described from the Oligo-Miocene Numidian Flysch, Tunisia, where the channels are 500-1500 m wide (Sami *et al.*, 2010), the Devonian Prongs Creek Formation, Yukon, where they are 50-100 m deep and 100-200 m wide (Mullins and Cook, 1986), and other gully fills that have been described in other ancient apron sequences by Cook (1979b), Cook *et al.* (1972), Hüneke and Krienke (2004), and Noda and Toshimitsu (2009). U-shaped gullies are also common on clastic aprons and often cut across the proximal apron (Stow, 1985a).

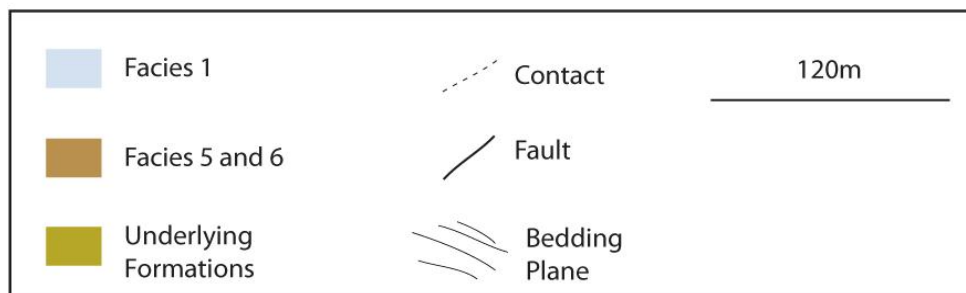
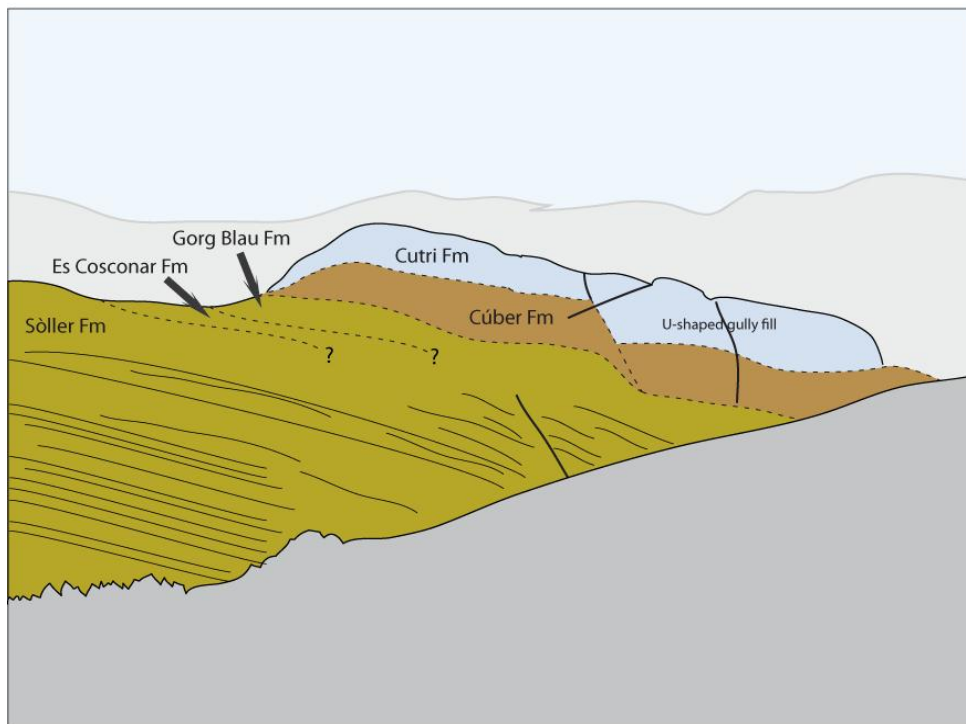
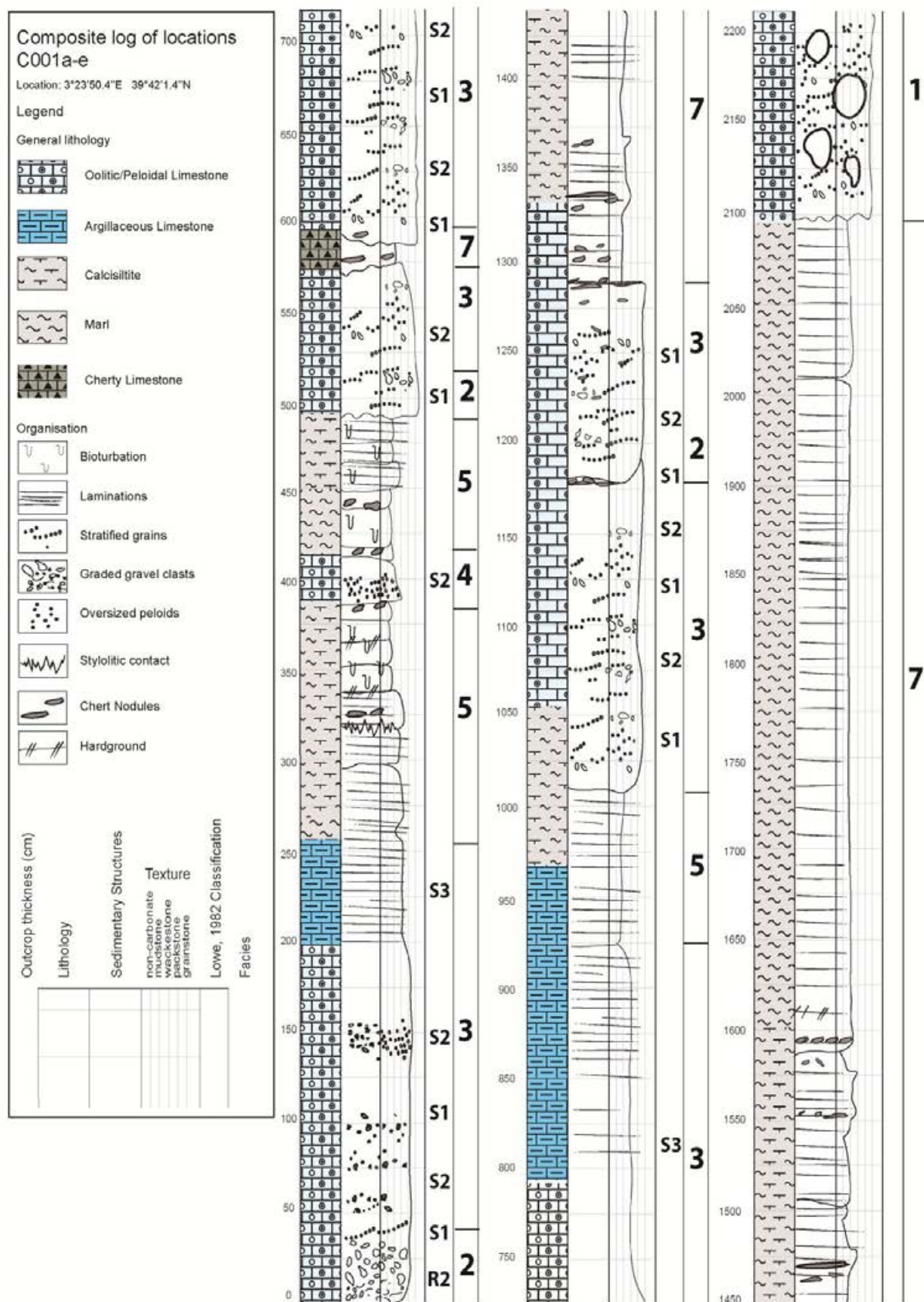


Figure 4.17 Photograph and field sketch of Abbots, (1989) *Puig Cutri* Area. Facing ESE.



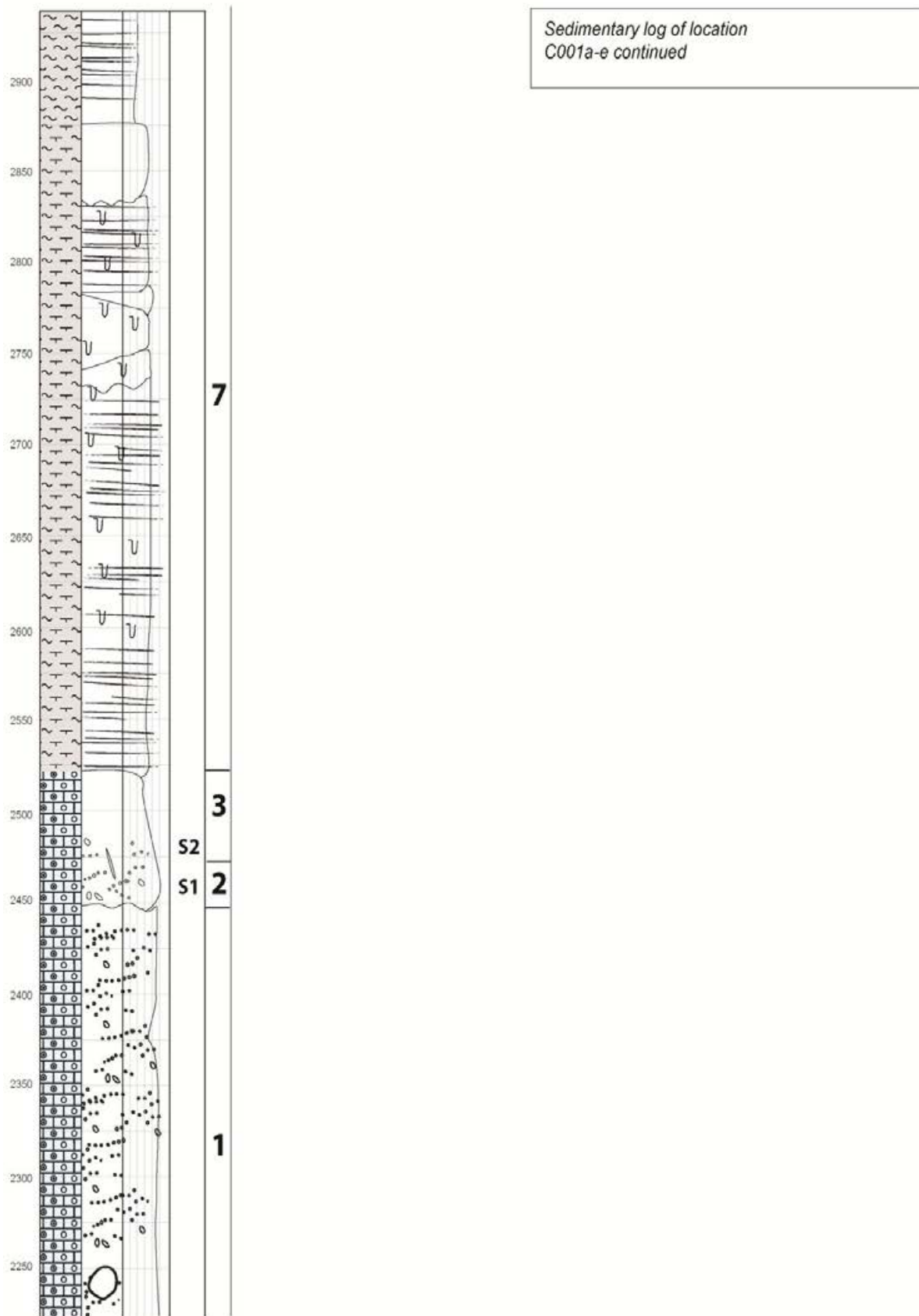


Figure 4.18b Sedimentary log of *Puig Cutri Area* continued.

4.2.2 PUIG CUTRI SOUTHERN SECTION (C002)

The 'Puig Cutri Southern Section' (Figure 4.19) displays a complete succession through the Cutri Formation (Figure 4.20). Normal faults serve to downthrow the section progressively to the SE where a more complete apron sequence is displayed. Proximal turbidites grade into more distal turbidite deposits and gradually record greater quantities of muddy deposition (facies 5). The section is characterised by thick packstone-grainstone turbidite units that thin up-section with a smaller proportion of resedimented grains. This is represented as thin dilute turbidite packages consisting of wacke-packstones that are interspersed with muddy facies that consist of mud-wackestones and coquinas.

The succession records a progression from inner-apron proximal facies to distal outer-apron and basin-plain facies. The facies of these apron-belt divisions correspond to the apron models of Mullins and Cook (1986) with the notable absence of debris flows in this part of the study area. The facies described are interpreted as resulting from deposition within a sandy turbidite deposition apron, dominated by the resedimentation of unconsolidated oolitic sands (Abbots, 1989; Hüneke and Krienke, 2004).

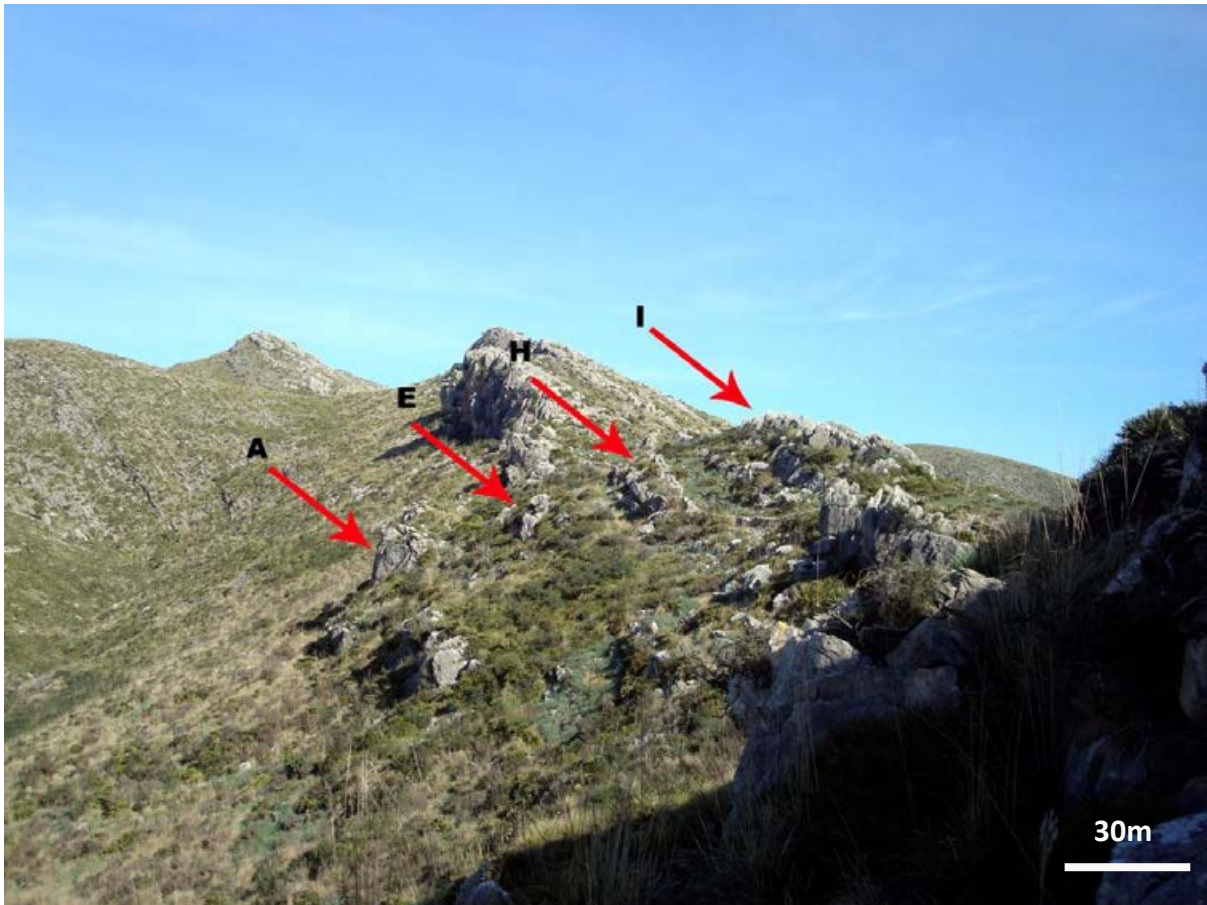


Figure 4.19 Photograph of major turbidite units found in Puig Cutri Southern Section. Facing NE.

Each turbidite unit has been given a letter from A to Q (A being the oldest Q being the youngest) by Abbots (1989); Figure 4.19. The major turbidite units are letters A, E, H and I as indicated in Figure 4.19, smaller, more dilute, turbidite units make up the remaining intervals. As suggested above the units thin up section eventually giving way to dark fissile mudstone pelagic facies (see composite log C002; Figure 4.21) of the Puig de Ses Fites Formation.



Figure 4.20 Photograph and field sketch of Puig Cutri Southern Section. Facing ESE.

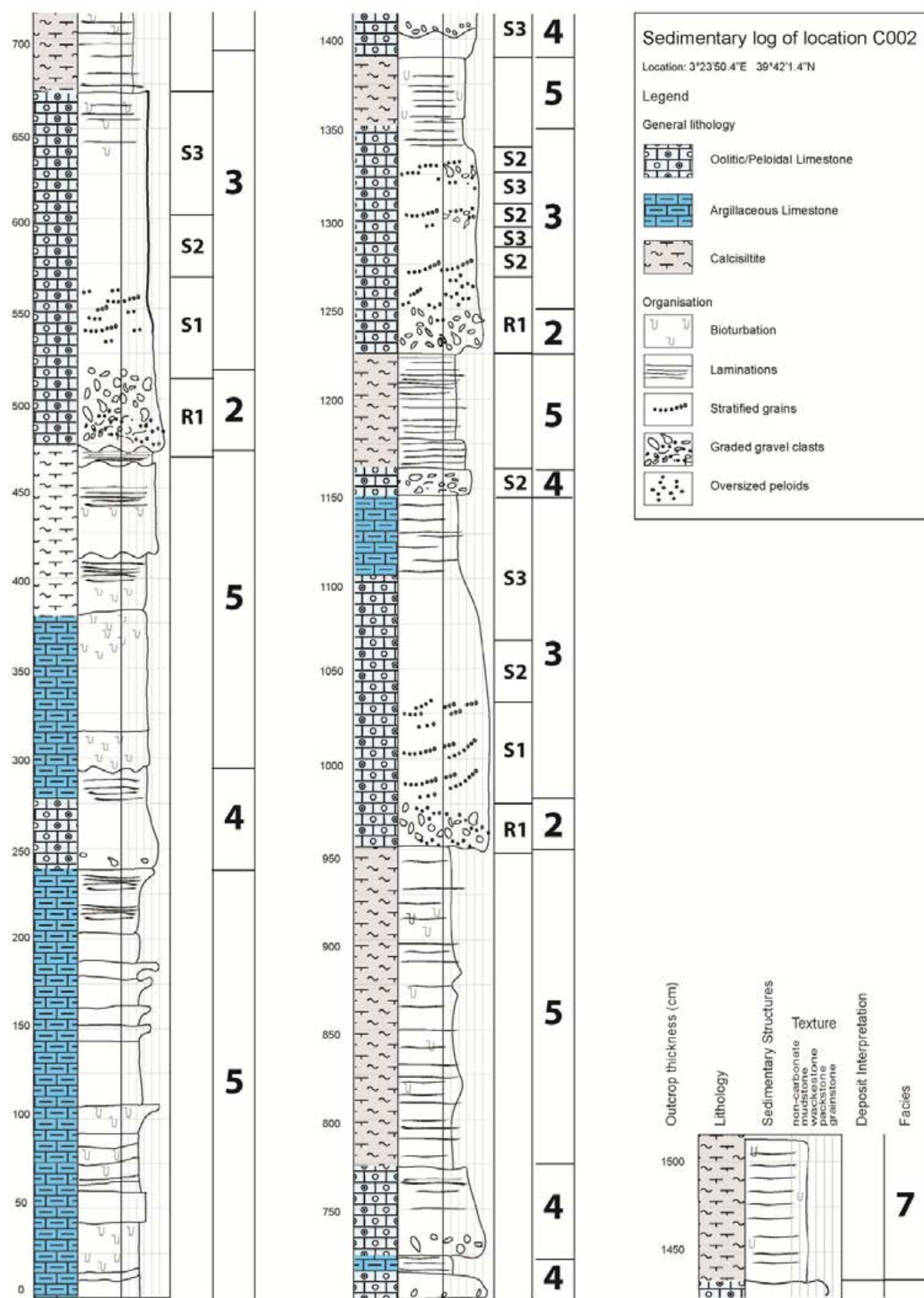


Figure 4.21 Sedimentary log of Puig Cutri Southern Section.

4.2.3 PUIG POLONI-PUIG DE SES FITES (C003)

This locality marks a SW-NE oriented extension of the Puig Cutri Area. It is separated from the Puig Cutri by a WNW-ESE trending strike-slip fault and by similar bounding faults to the NE, these faults allowing movement of the Puig Poloni-Puig de Ses Fites further to the WNW.

At this location the Cutri Formation forms a series of well-exposed near vertical cliff-type outcrops that sit on top of the bare Puig Poloni-Puig de Ses Fites ridge. These outcrops present a similar sequence to that of the southern section. However, a *Posidonia coquina* drift deposit characterises the location suggesting that the palaeotopography differed to the southern section of the apron complex (Figure 4.22; 4.23). A debris flow is noted in the outcrop (2050-2150 cm Figure 4.24a) suggesting slightly different sedimentary processes may have been in action in this area.

Due to the near vertical outcrop, and time constraints, as well as parts of the location coming under a protected area, detailed sedimentological study was not carried out; particularly towards the north. These distinctive oolitic units characterise the Puig Poloni-Puig de Ses Fites area and these units are also associated with hyperconcentrated flows.

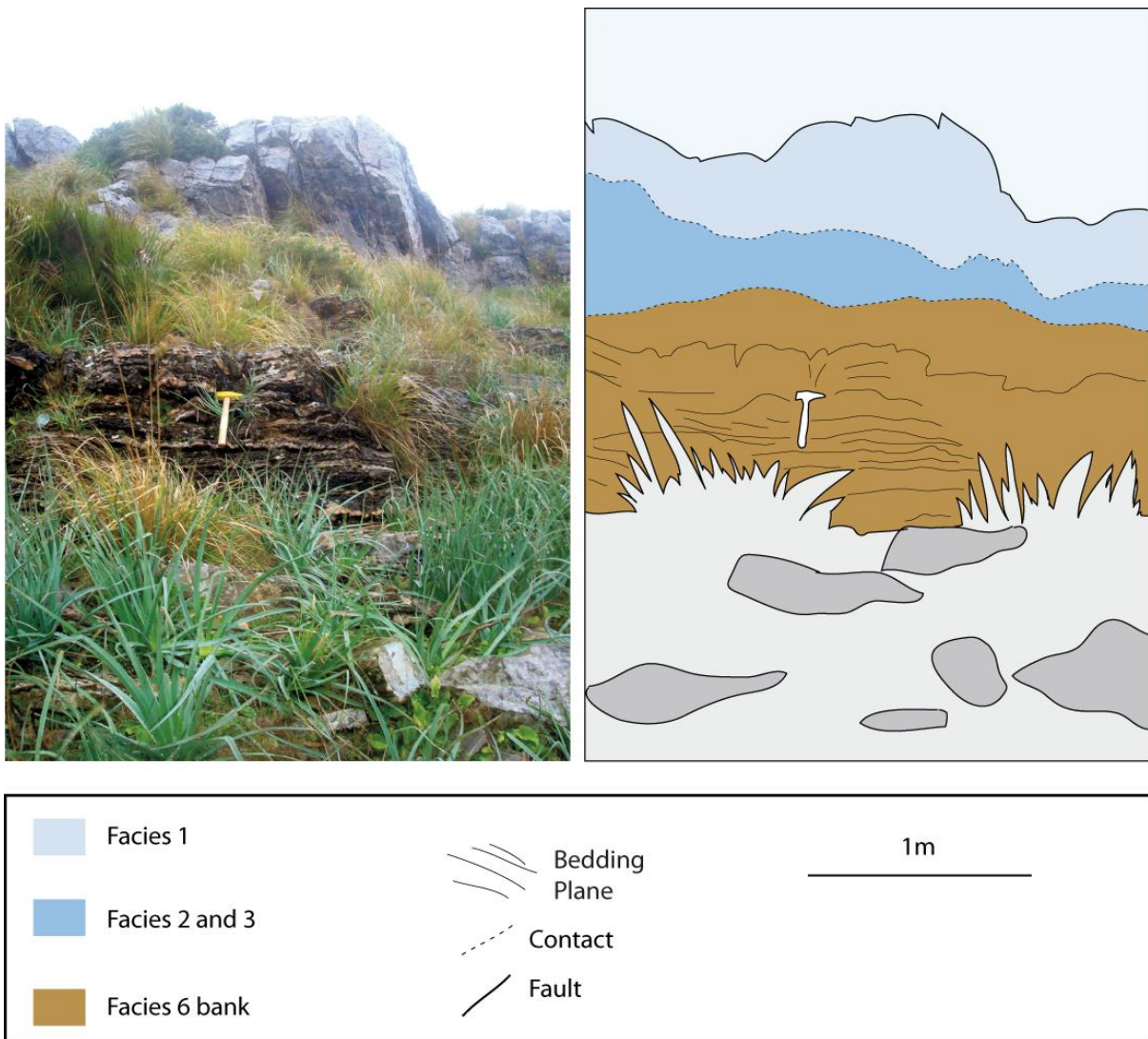


Figure 4.22 Photograph and field sketch of the Puig Poloni-Puig de Ses Fites outcrop. Note the dark coquina facies overlain by much lighter coloured turbidite packages. Facing NE.

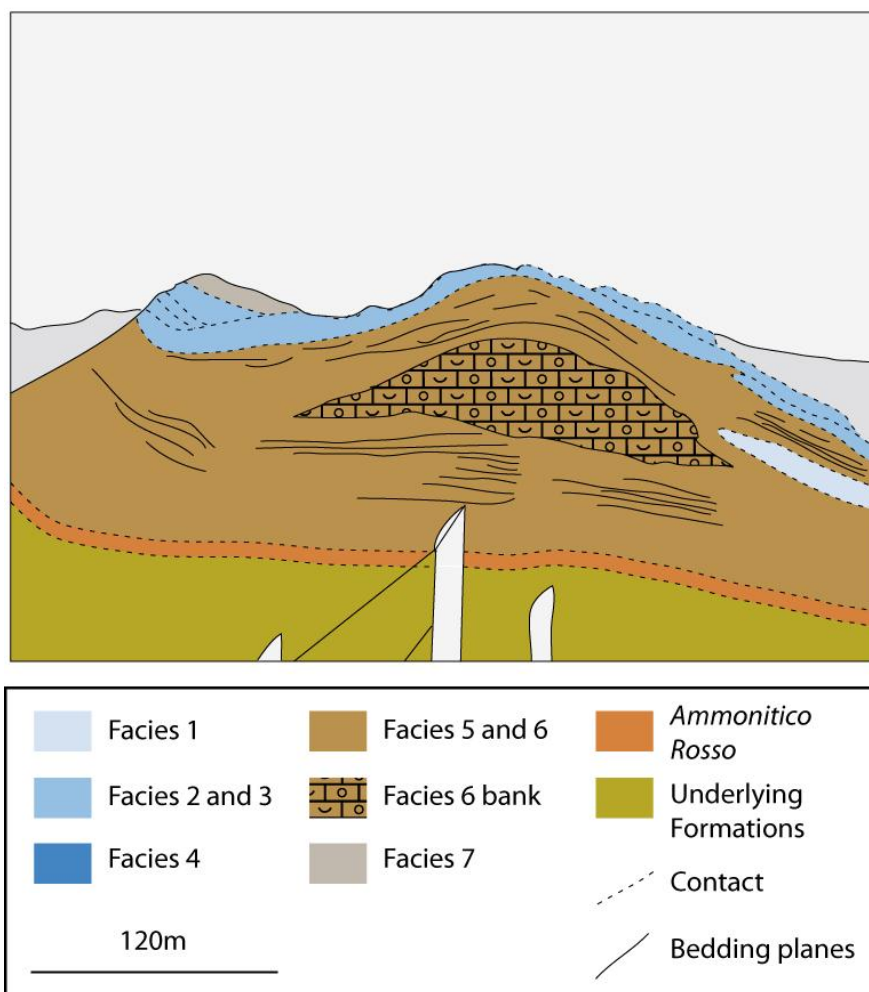


Figure 4.23 Photograph and field sketch of the Puig Poloni-Puig de Ses Fites. Facing NE.

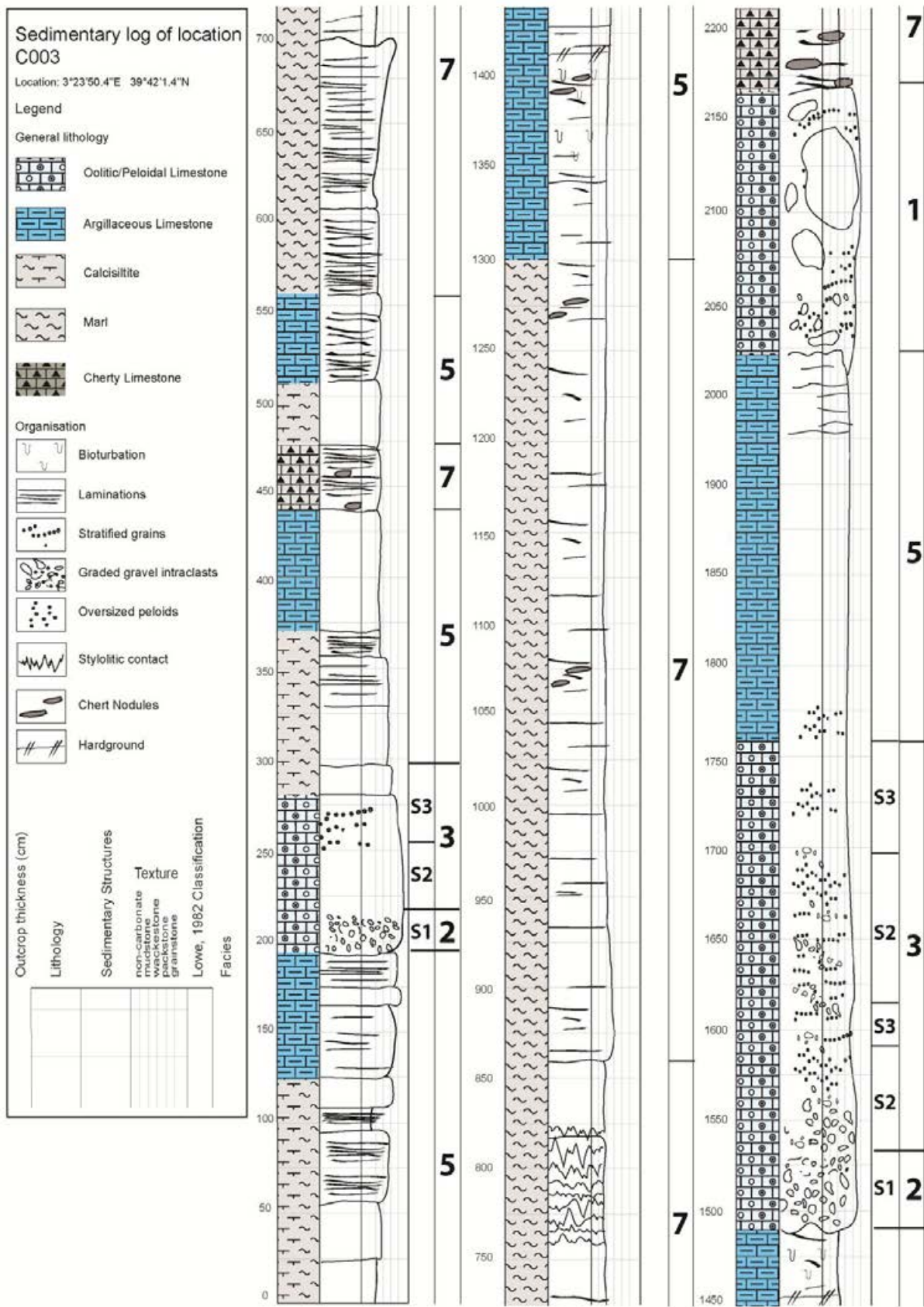
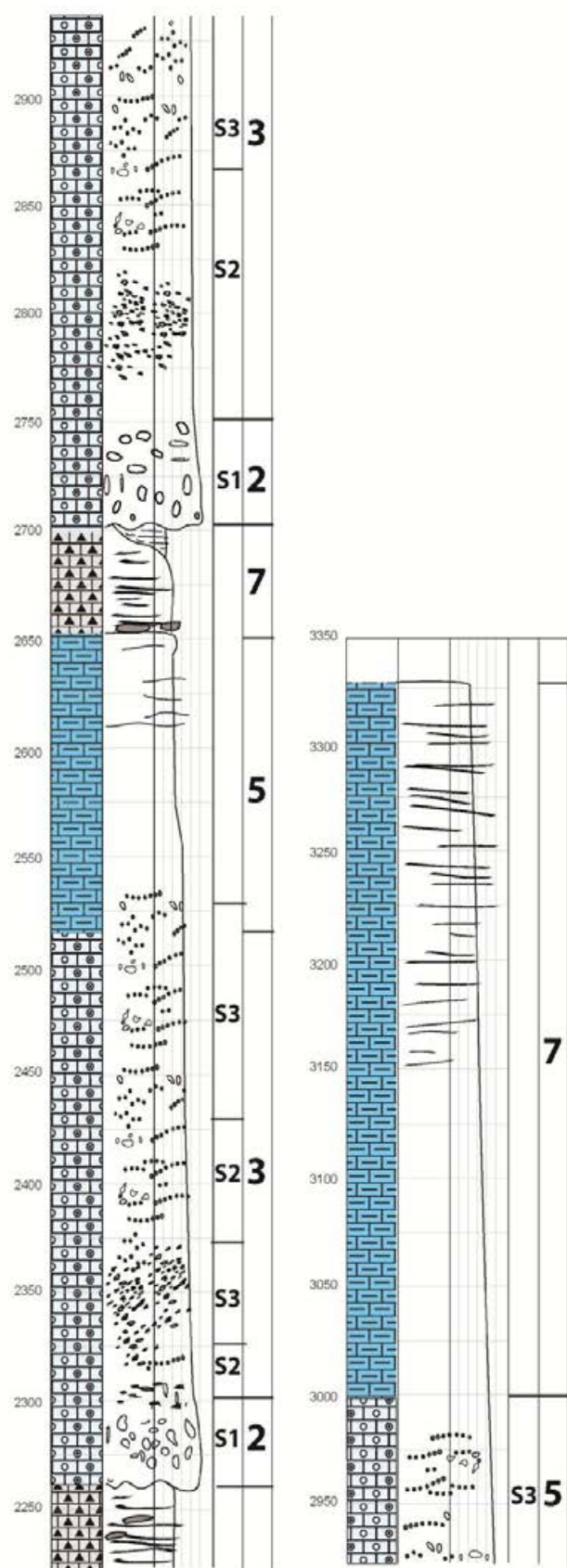


Figure 4.24a Sedimentary log of Puig Poloni-Puig de Ses Fites.



Sedimentary log of location
C003 continued

Figure 4.24b Sedimentary log of Puig Poloni-Puig de Ses Fites continued.

4.2.4 PUIG POLONI EAST (C003s)

The outcrop is found to the south east of Puig Poloni-Puig de Ses Fites outcrops, being thrust towards the NW, and has a unique composition compared to other outcrops in the area as it gives a stratigraphic representation towards the east (Abbots, 1989), and hence is a more proximal to source location.

This outcrop has a similar sequence to the southern section, showing a development of proximal turbidites and debrites interbedded with deeper water type facies. This outcrop has an overall coarser composition containing much more of facies 1, 2 and 3 in comparison to other areas (Figure 4.25, 4.26a and 4.26b). This is most likely due to the more proximal location of this outcrop compared to other areas.

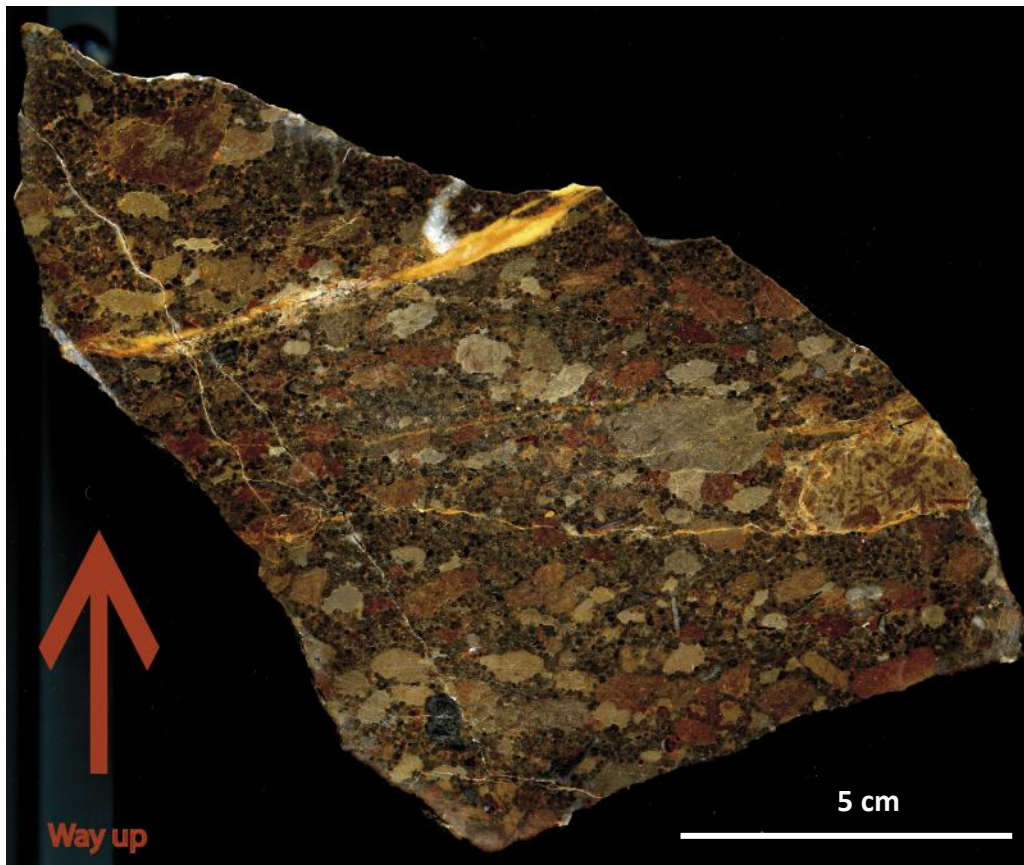


Figure 4.25 Polished slab of facies 1 in Puig Poloni east outcrop (Appendix B Hand Specimen 350). Note the variety of clast colours indicating a shallow water origin.

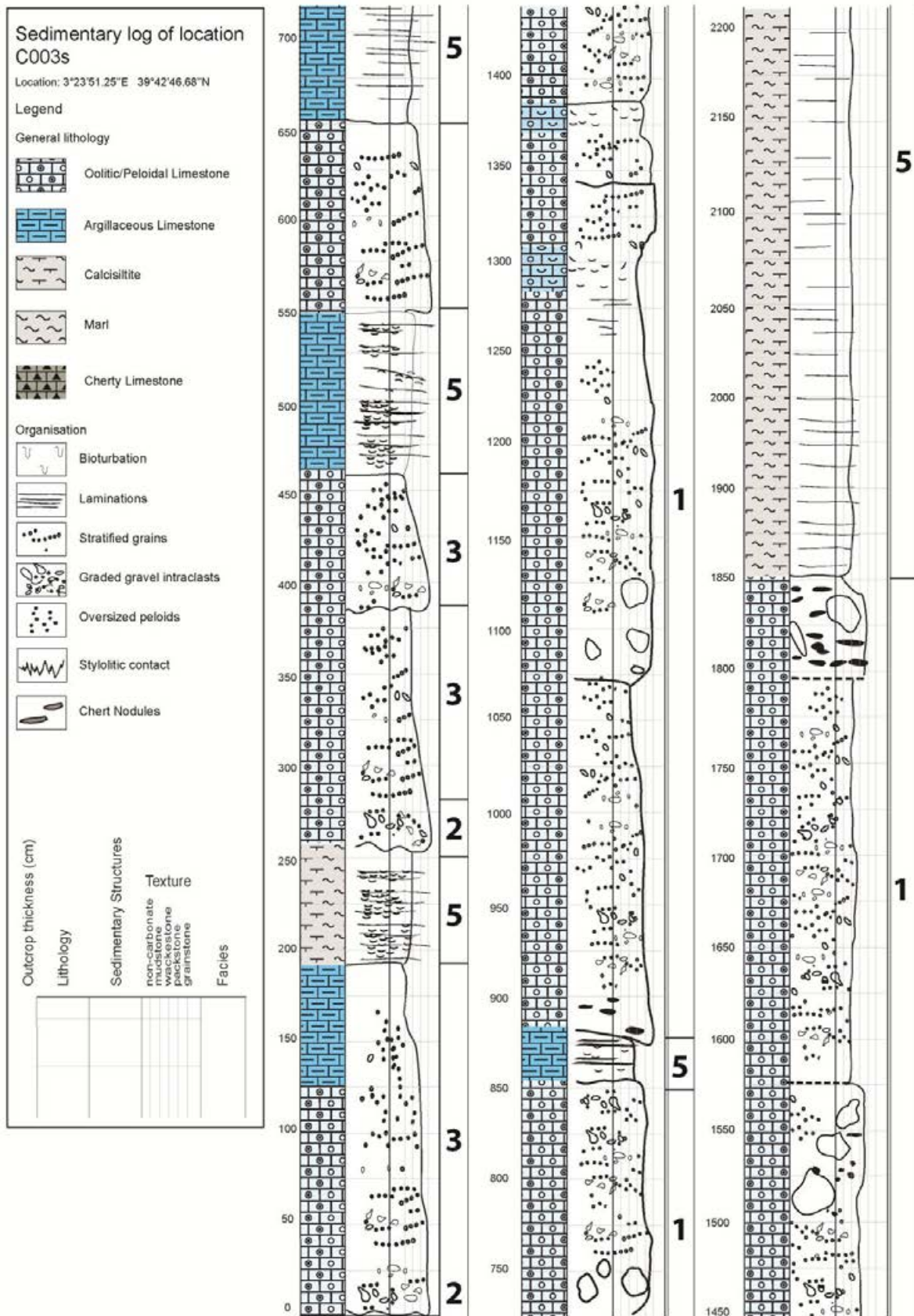
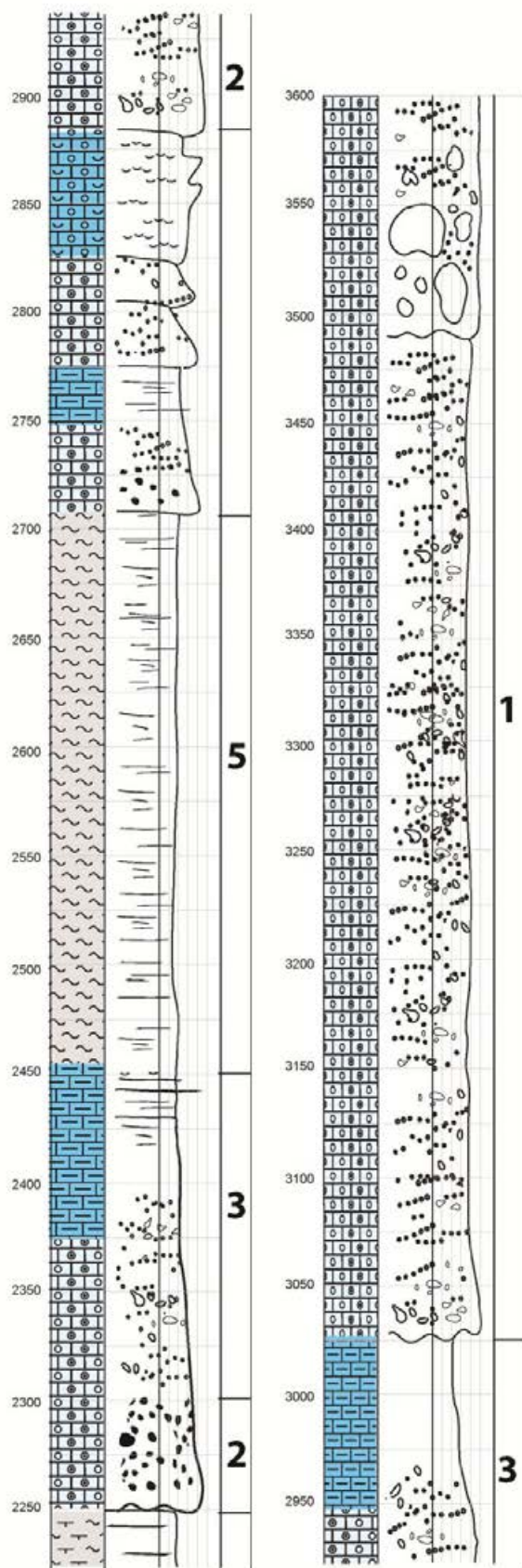


Figure 4.26a Sedimentary log of Puig Poloni east.



Sedimentary log of location
C003s continued

Figure 4.26b Sedimentary log of Puig Poloni east continued.

4.3 DISCUSSION

Overall, the Cutri Formation is a grain-rich turbidite system, with turbidites becoming increasingly distal up section, whilst always being interbedded with silty bioclastic mudstones and wackestones. The overall domination of muds and fine suspended sediments suggests that this sedimentary body was probably formed on the windward margin of the platform where sands from the platform top were being deposited on-bank. This is a characteristic feature of windward margins where transport of resedimented grains and finer muds and silts dominate the slope and base-of-slope environment. Ancient examples of windward margins include the eastern side of the Valles-San Luis Potosi; Minero, (1991) and Tuxpan Platforms; Enos and Stephen, (1991).

Similar ancient examples of these types of successions are seen in the Los Molles Formation, Chile (Bell and Suárez, 1995), Poza Rica field, Mexico (Janson *et al.*, 2011) and Wolfcampian/Leonard carbonates in the Midland Basin, U.S.A (Dutton *et al.*, 2004). The domination of muds and silts of facies 5 indicate an origin from either from the platform edge (through fine-grained shedding), or from background sedimentation from the water column. It is likely that these sediments were dispersed via wave, tidal and storm currents that transport fine grained material off-bank into the basin. Grain dominated elements (i.e. debrites and turbidites) are considered to be derived from shallow platform-top environments which were generating unconsolidated sands into the basin due to direct interaction with wave base and storm events. It is this continuous wave action and regular storm that drove shallow water sands into the basin.

The allochems found within debrites and turbidite facies suggest an origin in shallow water, with a mix of high-energy and lower-energy type allochems, where the development of ooids and aggregate grains took place in high energy settings and peloids and micritised grains lower-energy settings. The high energy setting of the sediment source is further suggested by the inclusion of semi-lithified intra- and exoclasts that are abundant in more proximal deposits (see location C003s). Their inclusion indicates that erosion due to both wave energy and gravity flows were

eroding the slope. Other locations (C001, C002 and C003) represent those deposits further downslope where a finer, although coarse grade sediment, is preserved.

Turbidity flows are interpreted to have been derived from a shallow water environment to a base-of-slope environment. Without any of the platform being preserved it is impossible to say, with a high degree of certainty, what was the sediment source environment. However, it is discussed in Abbots (1989) that upper slope deposits occur on the island of Cabrera, geologically part of the Sierra de Levante but separated from Mallorca to the SSW.

Abbots (1989) reinterpreted what was described as a “conjugate olistolith” by Arbona et al. (1984-1985) as being an upper slope gully fill, plugged with oolitic limestones, forming part of the grain-rich succession of the Middle Jurassic and is recognised as being equivalent to the Cutri Formation. This succession is interpreted to be the upper slope environment of the platform. Furthermore, Abbots’ (1989) upper slope deposits are described as consisting of “thin-bedded oolitic grainstones and wackestones with *Posidonia*...overlain by... [erosive]...carbonate conglomerates” forming gully fills and Aurell et al (2002) as having a wackestone packstone microfacies rich in filaments of *Boistra*. This succession of oolitic grainstones and wackestones characterises the studied strata. Additionally, *Posidonia* rich wackestones are observed in this study as forming exoclasts within facies 1 and 2. This suggests that the exoclasts are possibly the preserved upper slope/source area of the Cutri Formation deposits. Since only exoclasts remain of the platform it is assumed, due to the high proportion of ooids within the turbidites, that the source of the Cutri Formation was probably from high-energy environments or from spill-over of such environments near the platform top.

The predominance of ripples, fining-up sequences, strong alignment of allochems, and parallel-laminated beds within facies 5 indicates a gentle reworking by bottom currents and deposition of a muddy to sandy contourite. The inclusion of allochems that characterise facies 1, 2 and 3 within these contourites suggests that mixing of turbidity current material took place. These contourites are possibly deposited from a mixture of suspended sediments, dilute turbidites and probable storm events that incorporated platformal grains into the system. *Posidonia* bivalves form a bank in

one location and are commonly found amongst facies 5; the bioclasts are sorted by current reworking. These *Posidonia* coquina banks crop out at Puig de Ses Fites suggesting this area had a combination of unique currents compared to the rest of the area, which accumulated the bivalves into a bank.

Facies 7 was first interpreted by Abbots (1989) to represent the Puig de Ses Fites Formation that overlies the Cutri Formation partly based on the occurrence of radiolarians that reflect the continuous widening of the Neotethys Ocean. The boundary between these two formations is represented by a hiatus during the Bathonian-Oxfordian. However, the inability to correlate the boundary between the Cutri and Puig de Ses Fites Formation by contact types or biostratigraphy (due to the resedimented nature of these sediments) leaves open to interpretation the timing of deposition and whether this facies was associated with the resedimented facies of the Cutri Formation or the true pelagic sediments of the Puig de Ses Fites Formation. The above mentioned relationships between facies types and their geometries is summarised in Figure 4.27. Figure 4.27 illustrates the sedimentary geometries and relationships between the above discussed facies. Note the relatively extensive linear accumulation of turbidites between C001 and C002, this is the Cutri Megasequences. Within these outcrops the strike-slip fault noted to occur between C001 and C003 and C003s enables a view of more proximal deposits that represent more proximal (hence coarser grained) sediments.

The Cutri Formation is suggested to be a base-of-slope apron where a mixed turbidite/contourite system developed (e.g. Rebesco *et al.*, 1996, 1997, 2002; Pudsey, 2000; Escutia *et al.* 2002). The coarsest resedimented rocks are found in the base of slope environment and the finer, more distal, deposits are found within the toe-of-slope environment where they begin to incorporate basinal/pelagic type sediments like those seen in facies 7.

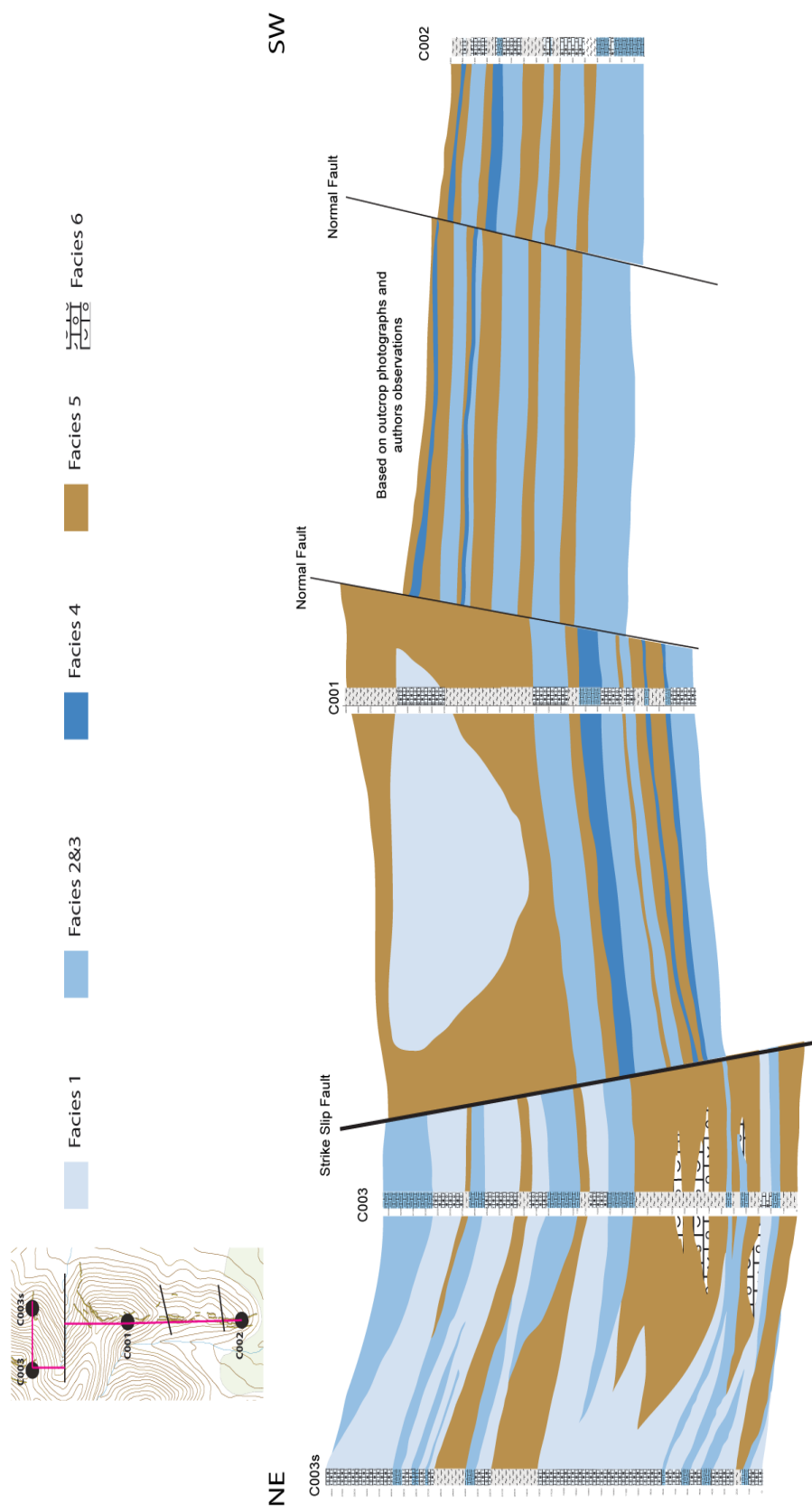


Figure 4.27. Fence diagram summarizing the 2D associations between facies.

4.3.1 DEPOSITION MODEL

The slope characteristics and proximity to the slope break probably have the greatest influence on what type of deposits occur at the base-of-slope and further beyond at the toe-of-slope and basin floor. Steep, unstable slopes are ideal for debrites, rock falls and coarse grain flows whilst gentle slopes are probably more likely to produce turbidites and soft sediment slumps. The Cutri Formation consists of debrites and turbidites, which contain two types of extraclasts of semi-lithified origin, suggesting that these deposits were formed on a heterogeneous carbonate slope dominated by the *Posidonia* bivalve, rather than further downslope in the probably more homogeneous mud-rich lower slope and basinal areas.

The Cutri Formation is regarded here as a good example for “Walther’s Law of Facies” (Stanley, 1999). Moving up the stratigraphic sections the rocks display continuously deepening and increasingly distal sedimentary environments that are related to the rifting Neotethys Ocean. The mixture of facies within the formation has also been described in other examples (e.g. Mullins and Cook, 1986; Reading and Richards, 1994) and points to the Cutri Formation most likely representing a base-of-slope carbonate apron (Figure 4.28 and 4.29) rather than a fan type deposit (e.g. Wright and Wilson, 1984), with its origin probably created by the changing tectonic and palaeogeographical events. As discussed at the end of chapter 2 the Cutri Formation is considered to have formed between 25-30°N suggesting that it had a subtropical, seasonal climate where a high pressure zone is postulated to have sat over the area, and most of western Tethys, during the northern hemisphere winter (see section 2.8). During the northern hemisphere summer low pressure is considered to have migrated south from Laurasia creating a more humid and wet climate and possibly more unstable weather, with storms becoming common during the season (Arias, 2008). The study area had a distinctively seasonal climate and a sensible modern comparison is the subtropical Caribbean Sea, where winters are dry and warm whilst summers are hot, humid and stormy (hurricanes). It is understood that a NE prevailing wind swept the Tethys Ocean during this time. Hurricanes are recognized to have played an important role in sediment transfer throughout the region.

In classic apron and fan models, sediments are transported via submarine canyons forming a fan deposit at the canyons mouth. But an apron complex is differentiated by the presence of a series of channels and small gullies that cut the slope (e.g. Mullins and Cook, 1986; Hüneke and Krienke, 2004), and feed sediment into a distinctively linear apron complex that forms parallel to the platform (e.g. the modern Bahamas slope, Mullins *et al.*, 1984 and the Tuxpan Platform, Janson *et al.*, 2011). This apron system is characterised by multiple sources along a margin rather than a single point source. This difference between point and linear source deposits have been described by Mullins and Cook (1986) and Colacicchi and Baldanza (1986), which has led to the development of carbonate apron models (e.g. Reading and Richards, 1994).

Rifting of the Neotethys Ocean created unstable platform tops due to localised subsidence causing oversteepening. Further, eustatic control and storm events resulted in increased instability that encouraged gravity flow sedimentation into current swept platform slope areas. The carbonate apron complex has slope sediments that form an extensive; basinwards thinning accumulation of resedimented carbonate sediment (see models in Figure 4.28 and 4.29). This retrogradational pattern (overall decrease in coarseness and thickness) seen in the Cutri formation is suggestive of a subsidence regime.

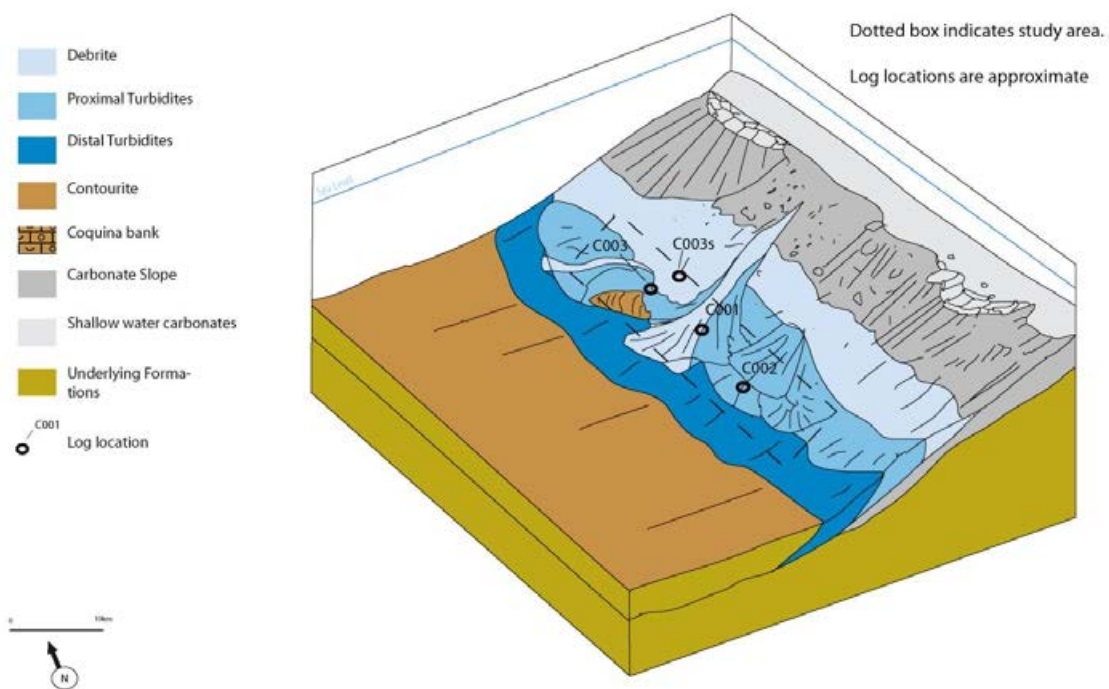


Figure 4.28 Depositional model for final deposition of the Cutri Formation. Note the location of logs which have been incorporated to indicate the spatial distribution of sedimentary geometries illustrated in 2D from Figure 2.27.

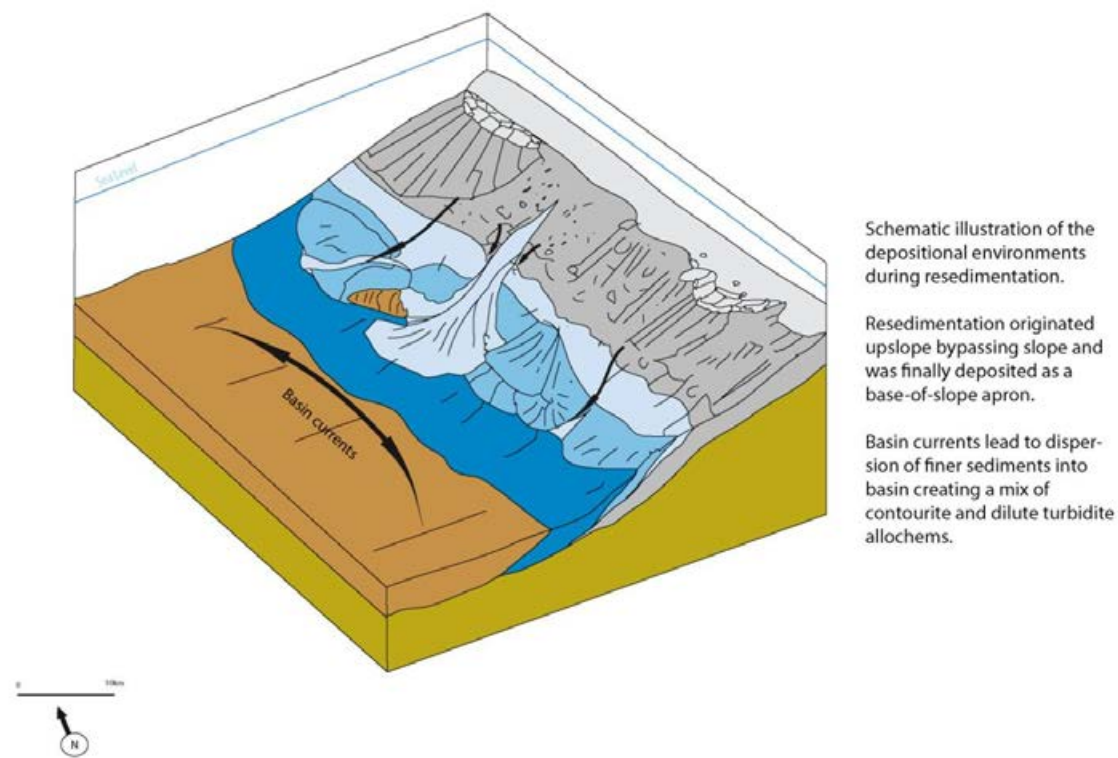


Figure 4.29 Depositional models for periods during deposition with arrow indicators for flow directions. See key in Figure 4.28.

4.3.2 EUSTASY AND THE CUTRI FORMATION: A SEQUENCE STRATIGRAPHIC FRAMEWORK

Sequence stratigraphy provides the methodology for the analysis of sediments based on a succession of units by chronostratigraphically defined surfaces such as unconformities and flooding surfaces. The lithofacies of the Cutri Formation consist of mainly coarse-grained platform-top derived detritus (ooids, peloids etc) and fine-grained slope and basinal muds and calcisilts. The lithofacies form a characteristic succession where a relationship between strata and sequence stratigraphy can be seen. With Abbots (1989) study of the upper slope on Cabrera it is possible to show that significant elements of deposition were created solely from sea level fluctuations and local alterations to the sedimentary environment (e.g. tectonics, shifting currents).

The Cutri Formation was deposited during a period of rising sea level as a part of the Lower Zuni II Megasequence, a period of long-term 1st-order rise in global sea level (Figure 4.30). Significant continental margin flooding occurred, together with submergence of both carbonate platforms and the central Lurasian rift basins (Golonka *et al.* 1994). Sea level reached its Jurassic maximum during Oxfordian-Kimmeridgian time (see Figure 4.30). Large continental shelves were established on the Tethyan margins, in Europe and in the Arctic (Golonka *et al.*, 1994, 1996, 2000) of which Cutri Formation was deposited as part.

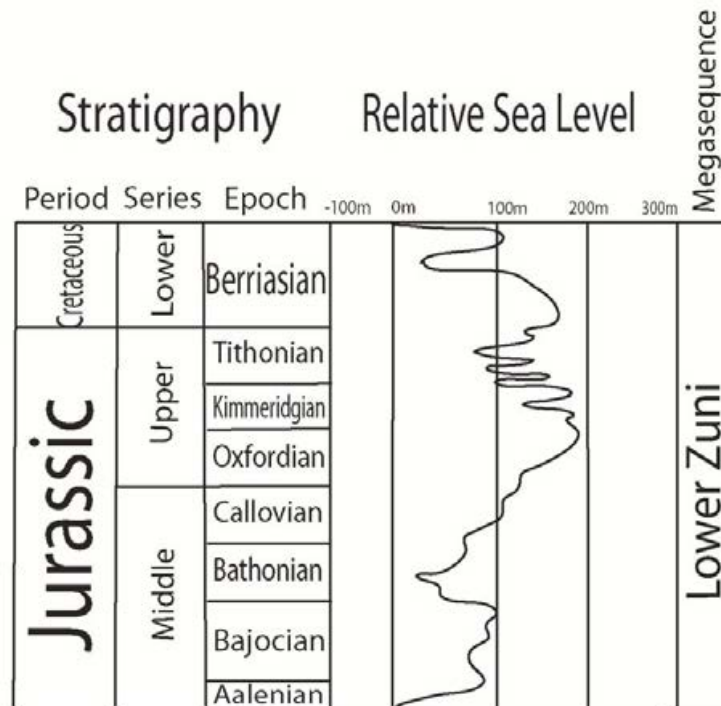


Figure 4.30 Global relative sea level chart from Haq et al. (1987).

In Figure 4.30, 2nd-3rd order sequences (sea level changes over 1-10 million years) are seen forming within the Callovian (165-161Ma; Walker *et al.*, 2009), when the Cutri Formation is believed to have been deposited. These sea level falls are temporary reductions in the rate of 1st order sea level rise throughout the late-Middle Jurassic. These short-lived changes in eustasy may have had a control on the deposition of the Cutri Formation. A brief summary of theoretical slope and base-of-slope deposits is described for lowstands, highstands and transgressive system tracts and applied to the Cutri Formation succession.

LOWSTAND

A lowstand is the lowermost depth reached by sea level during a specified period of time. The composition of lowstand sediment gravity deposits differs from highstand deposits and can be used as a key to interpreting the relative sea level during deposition. Lowstand carbonate turbidites often contain skeletal grains and clasts shed from older, possibly exposed, shelf edge. Schlager (1991) suggests that ooids and peloids are scarce in lowstand turbidites because ooid and peloid formation requires flooded well-circulated platform tops, whereas skeletal sands can be

produced at shelf edges. It is these skeletal-rich sediments that are deposited downslope (e.g. Vecsei and Sanders, 1997). The Cutri Formation is dominated by ooid-peloidal rich and skeletal poor system only containing locally abundant homogenous skeletal accumulations of *Posidonia* bivalves suggesting that the turbidites and debrites were sourced from a well-circulated platform top.

TRANSGRESSIVE

A marine transgression is a period of time where sea level rises relative to land. Posamentier and Vail (1988) postulate that the retrogradational succession of parasequences would probably form during a transgression towards highstand in the slope environment. This is a conclusion that Abbots (1989) reached for this formation; and is possibly due to continual back stepping of the carbonate platform during increasing sea level. Handford and Loucks (1990) imply that reaching maximum sea level possibly leads to the development of condensed facies over the slope and base-of-slope environments due to the deposition of hemipelagic and pelagic sediments (i.e. the deposition of Puig de Ses Fites Formation). In the Cutri Formation the youngest exposed rocks are of pelagic origin and have been identified as representing the opening of the Neotethys and Proto-Atlantic when true basinal environments prevailed over the region. It is possible that the platform associated with the Cutri Formation migrated with the widening Neotethys leading to an abandonment of the apron. This is seen in the deposits studied by a generally increasing distal nature of resedimented carbonates and increasing pelagic influence over deposition.

The type of deposits developed during a transgression depends on the type of platform (rimmed, isolated) and climate (arid, humid) since climate effects the deposits developed during exposure, if exposure occurred. However, no evaporites (associated with arid conditions) were found nor any evidence of karstification since no remains of the platform are preserved. This suggests that the platform was probably not exposed but was strongly influenced the rifting of the Tethys Ocean and the platform migrating away from the area of deposition.

HIGHSTAND

Highstand deposits typically contain a progradational parasequence set. Since a highstand is the period when sea level is at its highest, sediments consist of the greatest carbonate production including the growth of shoals and sandbars commonly made-up of ooids and other grains. It is noted that periplatform oozes tend to form in these times, where storm events and other high energy events transport suspended sediment into the basins covering the slope and basin floor (Handford and Loucks, 1990). Furthermore basin currents are probably likely to push into shallower water (i.e. higher up slope) increasing rates of erosion on the slope.

Both lowstand and highstand deposits represent the two extremes of relative sea level. The Cutri Formation does not comply with either of these described deposits, where the system has a general fining up sequence indicating a general deepening of the sedimentary environment agreeing with the general sea level rise noted in Figure 4.30.

Palaeogeographical study of the depositional system points to other local controls such as tectonics, which were active during this time. The rifting of the Neotethys led to the segregation of platforms, with the remnants forming small isolated platforms within the Neotethys Ocean. The continuing widening of the ocean pushed proximal sources of resedimentation further away until pelagic sedimentation prevailed over the region. This pattern of increasingly distal environments is clearly recognized, and seems to be the best interpretation of the facies evolution within the sequence stratigraphic framework.

TECTONIC INFLUENCE

The Jurassic of the Western Mediterranean is characterised by regional rifting of the Neotethys Ocean and consequently localised subsidence. The retrogradational pattern seen in the Cutri formation is indicative of a subsidence regime where an overall decrease in turbidite coarseness and thickness is observed. Tectonic influence is further signified by the abrupt sedimentological disparity between the coarser facies (1, 2 and 3) and finer grained facies (5 and 7). This disparity is

indicted by a sharp contrast between coarse and fine grained bodies suggesting that resedimentation events occurred as single events rather than being an accumulation of sediment derived from high-stand shedding for example (e.g. Adabi et al. 2010; Gawthorpe et al., 1994). Furthermore, the inclusion of semi-lithified clasts within facies 1 and 2 is evidence that the slope was unstable and debrites and turbidites carried fragments of this unstable material down-slope. Oversteepening is the probable reason for this instability, caused by tectonic activity on the platform edge. Evidence discussed from Cabrera by Abbots (1989) suggests that the margin was formed on a footwall and was tectonically active during the time of deposition. This margin formed part of the rifting zone and therefore is characterised as a normal fault where the base-of-slope apron formed at the bottom of the footwall.

5. DIAGENESIS AND RESERVOIR PROPERTIES

5.1 INTRODUCTION

The diagenesis and petrography of the Cutri Formation was investigated by means of standard petrographic techniques including acetate peels, unstained polished thin sections and cathodoluminescence.

5.2 DIAGENETIC HISTORY

5.2.1 MICRITISATION, MICRITE COATS AND SEAFLOOR MICRITE

In the Cutri Formation samples, most of the interparticle pore-space is filled by micrite matrix. This is a combination of pelagic carbonate mud and carbonate silt grade sediment that consists of abraded and disarticulated thin-shelled bivalve fragments of benthic soft mud dwellers, micropeloids and other abraded grains of shell material.

Micritised grains are the dominant allochems in the turbidite facies. Micritisation is the first diagenetic process that occurs at the sediment water interface (Adams and Mackenzie, 1998). It is essentially a near-surface process where grains have been bored by algal and fungal fauna and flora in low energy shallow-marine environments (Bathurst, 1975; Flügel, 2004). Commonly, internal structures have been destroyed through the process. The composition of the calcirudites in the Cutri Formation suggests that micritisation of grains was probably common prior to transport.

Micritisation of grains ranges from pervasive (i.e. destroyed the internal structures of grains) to a thin dark outer layer of micrite. The micritisation of these allochems possibly started to develop in shallow water, high energy conditions where peloids and ooids probably formed by being rolled around an accumulating material.

Micrite coats are found only in calcirudite facies where the majority of coated grains probably developed their coatings through transport (Flügel, 2004).

The Cutri Formation contains only small amounts of fossil material, which were particularly susceptible to micritisation, these include: corals, foraminifera, molluscs and bryozoan. Micritised grains commonly have a dull brown to orange luminescence under CL (Figure 5.1).

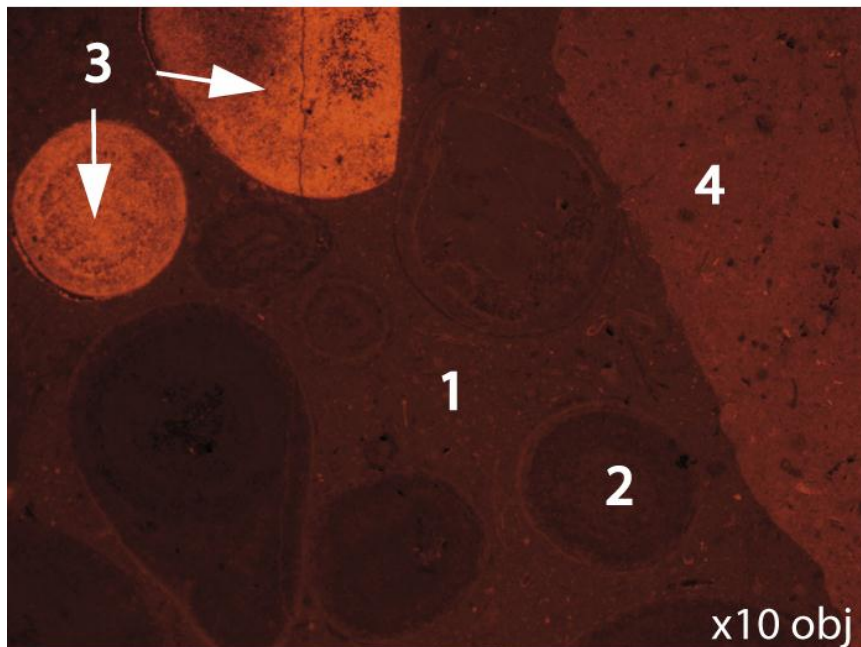
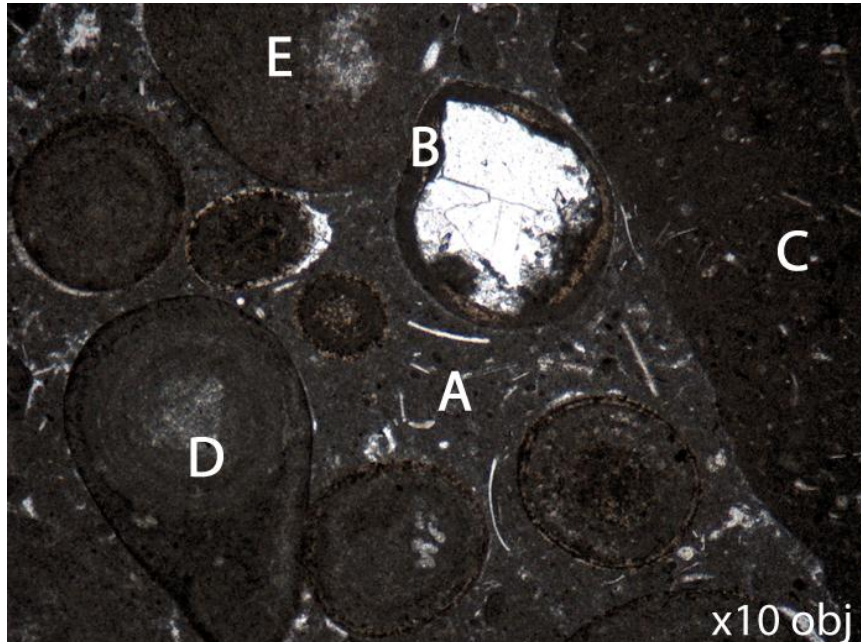


Figure 5.1. Photomicrograph (x10 obj.) and CL image illustrating host micrite matrix and micrite coats. A- Microcrystalline matrix hosting calcisiltite sediment displaying a dull luminescence. B- A micritised abraded bivalve fragment. C- Rip-up clast containing a different matrix to host deposit. D- Aggregate grains. E- Micritic ooid with a poor concentric structure. 2-Darker micrite of ooids and other allochems 3-A much brighter luminescence found in other allochems 4- intraclasts derived from the shelf edge. FoV 1.16 x 0.86mm. Appendix B C003 590cm.

5.2.2 EARLY ISOPACHOUS FRINGE CEMENTS

Early fringing cements are only observed in one facies type, the *Posidonia coquinas*. These early marine cements show a dull brown-orange catholuminescence and are predominantly non-ferroan calcite (seen by means of peels). These cements have reduced the severity of compaction in the bivalve-rich sediments.

5.2.3 SILICIFICATION

Three morphologies of chert occur in the Cutri Formation, they include: nodule beds, scattered nodules (which contain microquartz mosaics) and microquartz in the form of replacive chalcedony, which is visible in thin section (Figure 5.2). Nodule beds and scattered nodules are found amongst marls and calcisilts often following bedding planes and are probably derived from the nucleation of chert nodules on some allochems (e.g. Maliva and Siever, 1988).

Replacive chalcedony is highly selective and replaced only the cores of the coarsest of ooids and peloids and few other biogenic carbonate fragments such as coarse abraded and disarticulated oysters and other bivalves. Chalcedony forms only a small fraction of the sediments being mainly restricted to calcirudites. In silicified parts allochems are less compacted than in surrounding non-silicified regions, indicating that silicification occurred prior to or at least synchronously with significant compaction. With very minor quantities of quartz and no observable opaline silica it is unlikely that replacive silica could have originated from these sources; however, there are common radiolarian tests and less common sponge spicules found amongst the rocks (e.g. Bustillo and Ruiz Ortiz, 1987; Hesse, 1987). The dissolution of these tests and spicules is the likely source for replacive silica. Indeed, silicification is noted to be more abundant stratigraphically towards the top of the Cutri Formation, getting more abundant the closer to the overlying Puig de Ses Fites Formation (radiolarian mudstones). Chalcedony commonly occurs as grains with a grey-brown core in PPL. Chalcedony is non-luminescent (Figure 5.3).

Timing of silicification is noted in Figure 5.4 where fluids expelled from finer sediments were enriched in silica, possibly due to their clay content, as well as dissolution of radiolaria and sponge spicules, silicification was concentrated in the grain-supported turbidites where the latter acted as flow conducts in a host poorly-permeable sediment.

Radiolarians are now preserved with fine crystalline calcite. The majority of radiolarians do not appear to have moved from their primary deposited location and as such they must have been recrystallised without a void stage. In theory silica and calcite must have exchanged sites simultaneously with calcite from those areas

being replaced. The thin solution film can be seen in Figure 5.3 where an interface is now found, this is likely the exchange site for silica and calcite.



Figure 5.2 Chert accumulations in the Cutri Formation. A (1175 cm C001), chert forms large isolated nodules (>30 cm in length) and B (1600, C001) forming nodular beds which are rarely over 2 cm thick. Chalcedony is relatively common as replacement and detrital grains in thin section. XPL, FoV 2.89 x 2.15 mm, Appendix B C002 530cm

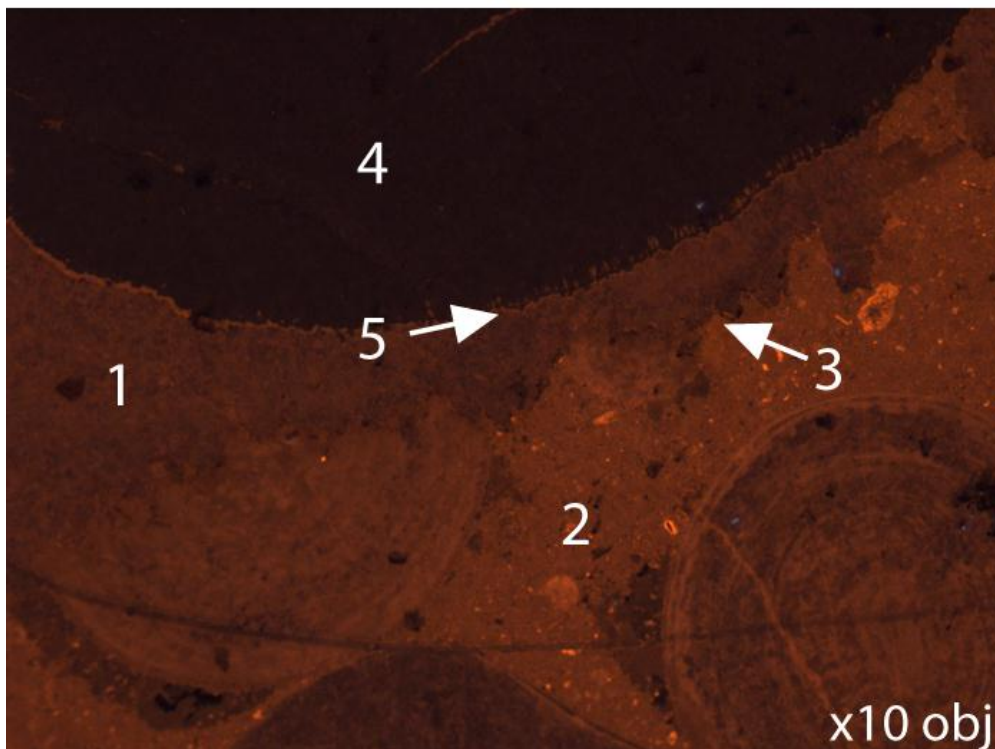
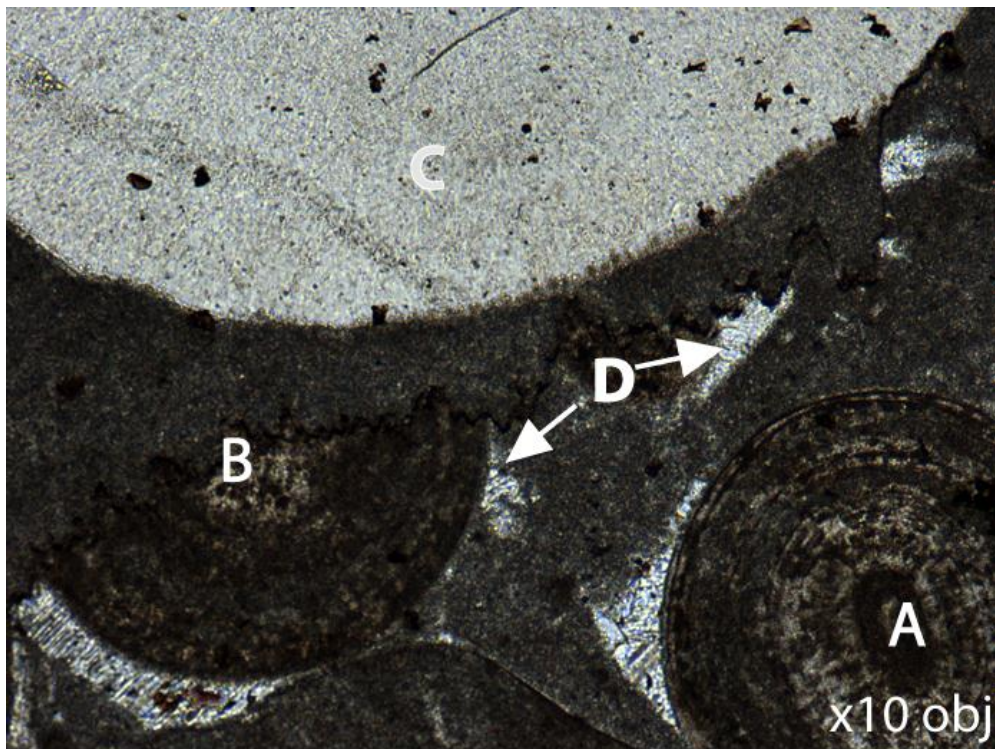


Figure 5.3 Ooids (A), dissolved ooid (B) and silica (C) amongst a micrite matrix and pore filling cement (D). Note the cements associated with stylolite display a different luminescence compared to the host calcisiltite matrix. A silica grain is found at (4) and (5) is the migrating replacing front between silica and calcite. FoV 1.16 x 0.86mm. Appendix B C003 590cm.

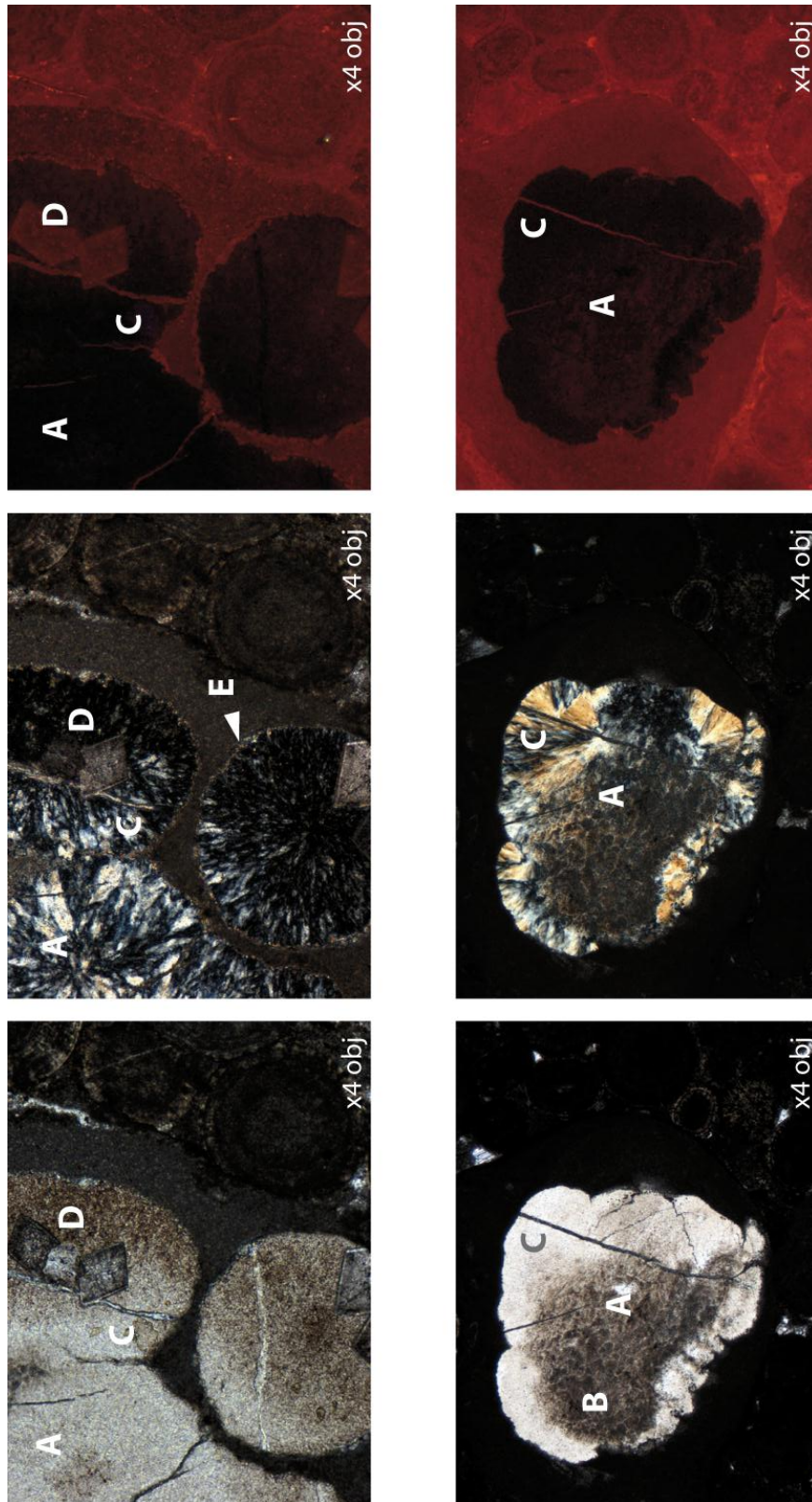


Figure 5.4 Note the common calcite fringe that is the replacing front for calcite to silica and ghosts within some silica grains. Dolomite postdates microfractures. A=Chalcedony B=Ghost of replaced allochem C=Microfracture D=Dolomite E=Calcite rim. FoV 2.89 x 2.15 mm. Appendix B C001 1250cm.

5.2.4 COMPACTION

INTRODUCTION

The most significant diagenetic feature of the Cutri Formation is the influence compaction has had on the occlusion of porosity and the enhancement of pore water chemistry due to dissolution by means of compaction. During the turbidites' deposition via suspension into unconsolidated muds of deep water origin, and a lack of evidence for either extensive early marine cements or fresh water cementation and/or stabilisation, both mechanical and chemical compaction have been maximised. As the sediment settled under its own weight and subsequent addition of sediments on top of them, plastic deformation, seen as longitudinal contacts and plastically deformed grains increased. Chemical compaction then took over mechanical compaction as the characterising features of these rocks through the abundance of sutured contacts and pressure solution seams. The small quantities of total cement and the associated close packing of the grains indicate extensive compaction (Figure 5.5) and seem to be a characteristic diagenetic feature of deep water diagenesis (e.g. Scholle, 1971). Moreover, most of the observed burial cements are closely associated with stylolites, indicating a rather closed system during diagenesis.

MECHANICAL COMPACTION

The quantity of plastic grain deformation seen in the Cutri Formation and the relative rarity of brittle deformation (Figure 5.5) suggests that the sediment originally contained mud that softened grain to grain impacts during transport. However, the grains were slightly lithified as indicated by the presence of micro-fracturing (See section 5.2.6).

The most considerable mechanical grain compaction effect is noted as plastic deformation which forms as longitudinal grain contacts (Figure 5.5). This was created by the slow increase in pressure from overburden, which promoted 'bending' of the allochems. Brittle ooid deformations, where ooids and other grains are split,

buckled or crushed are relatively rare; however, internal fracturing is observed to be frequent (See section 5.2.6). Broken grains are most often smaller allochems associated with much larger allochems; this is possibly related to the poorly sorted nature of the sediments and the effort associated with movement of larger rigid grains compared to those of a smaller size leading to damage to smaller grains.

CHEMICAL COMPACTION

Sutured seams, stylolites and solution seams, which originate from chemical compaction, are common in the Cutri Formation. Chemical compaction is a continuous process throughout burial; sutured grains are one of the earliest products of chemical compaction, occurring in as shallow as 400 m of overburden in carbonates (e.g. Moore, 2001). Sutured grain contacts are common with these microstylitic contacts (e.g. Figure 5.5) between individual grains and wackestone clasts and oolitic packstone matrix being widespread.

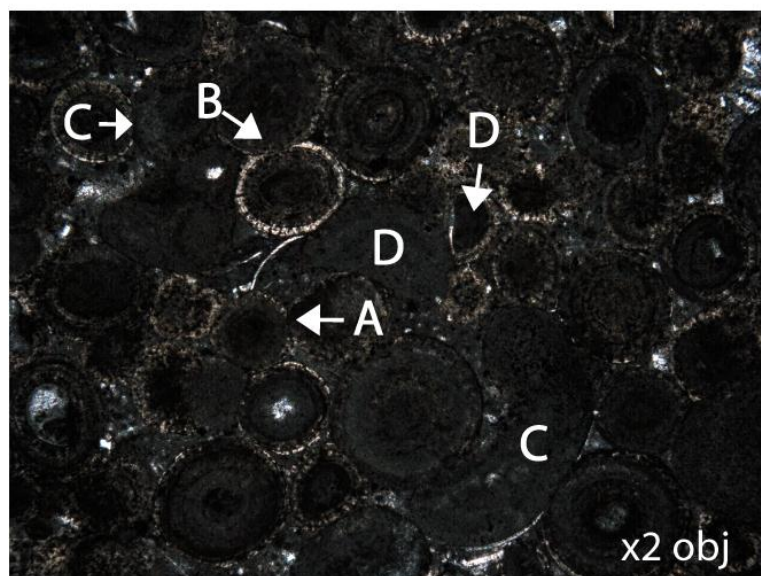
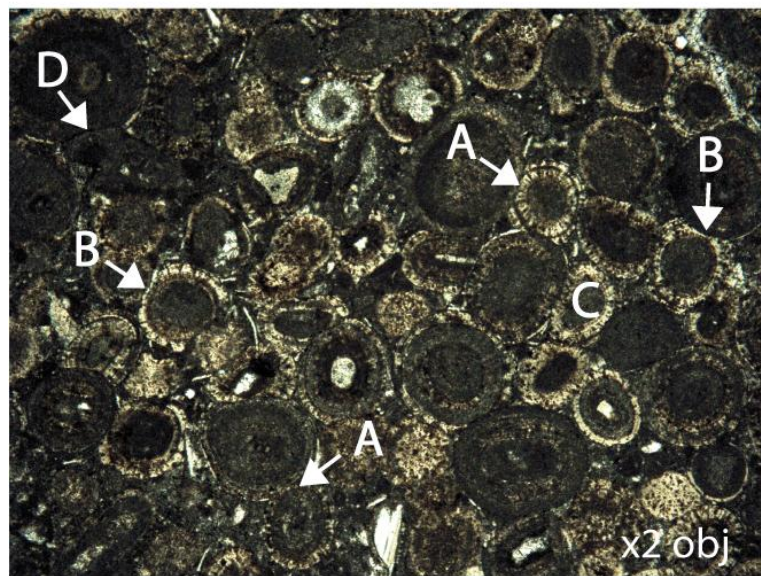
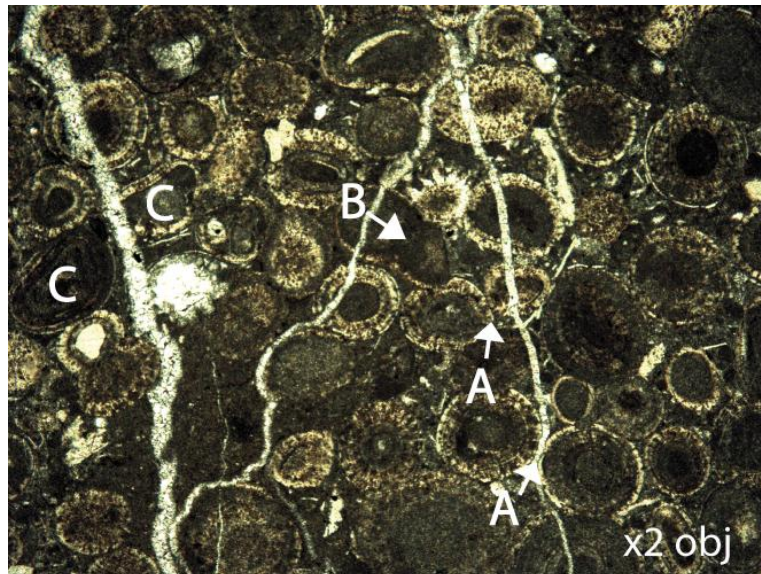


Figure 5.5. Mechanical compaction. A-Point contacts, B-Longitudinal contacts, C- concavo-convex contacts D- Deformed grains. FoV 5.78 x 4.31 mm. Appendix B C001 560cm.

5.2.5 BURIAL CEMENT 1 AND CONTINUED CHEMICAL COMPACTION

The earliest cement type within the Cutri Formation is a rare intergranular pore filling cement that is associated with stylolites and microstylolites that have developed with increased overburden (Figure 5.6). This cement, a calcite spar, fills intergranular pores and ranges from clear to cloudy calcite crystals up to 1mm across that fill intergranular pore space. The cements were probably deposited via fluids issued from chemical compaction. The dissolved carbonate would most likely have been moved a tiny distance from their source, i.e. pressure-solution features, before being reprecipitated, 'autocementing' the rock (Plummer *et al.*, 1976).

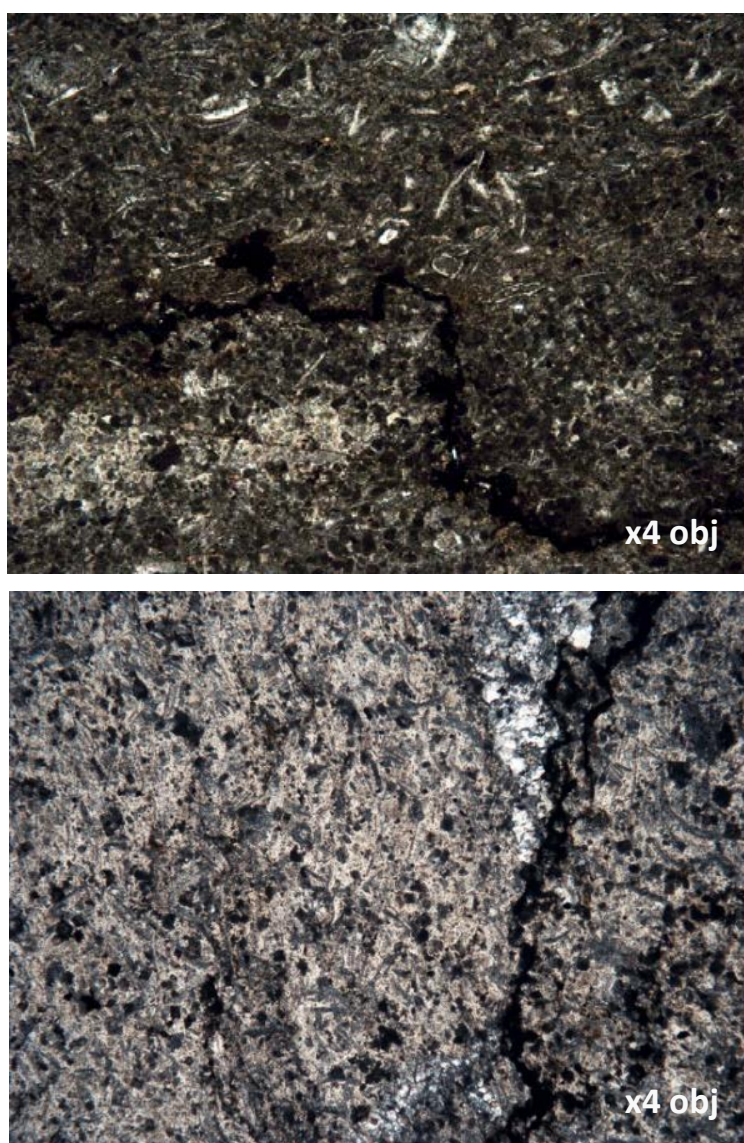


Figure 5.6 Burial cement filling intergranular pore space in close proximity to stylolites cutting across the matrix. FoV 2.89 x 2.15 mm. Appendix B C001 1450cm

5.2.6 MICROFRACTURES

Microfracturing, associated with increasing pressure, pressure solutions and stylolites that cut indiscriminately through the rock are less common than minor sutured contacts. They suggest that the development of pressure solution seams and stylolites occurred as part of a continuing process that continued into the later diagenetic environment that carried pore fluids around the rock, leading to the development of intergranular cements and final lithification of the sediment.

Microfractures commonly follow grain contacts and cut through grains and cements (Figure 5.5). Internal microfracturing occurs most prominently within replacive silica grains as well as other micritised allochems these microfractures are cemented with a microcrystalline equant calcite that has a dull brown luminescence. These fractures are always <0.5 mm in diameter and are filled with an equant calcite fill that is yellow to brown luminescent. The fractures occur parallel and oblique to bedding and do not persist for great distances. They are often associated with stylolites that are found at the margins of allochems. This suggests that at least part of these microfractures could be interpreted as tension gashes.

A second microfracture set that cuts across the first fracture set and all allochems and cements is much more persistent and can run the whole length of thin sections. These microfractures occur both parallel and vertical to bedding, suggesting that further burial of the sediment was characterised by increasing overburdening of the rock, possibly from fluid overpressure.

5.2.7 DOLOMITISATION

Dolomitisation in the Cutri formation occurs in coarse-grained sediments commonly along fractures and dissolution seams. They are scattered inconsistently within fine-grained samples as associated to dissolution seams and occur as individual very fine to fine euhedral-anhedral grains. Dolomites display a clear core with calcified later stages of dolomite growth (e.g. Taylor and Sibley, 1986; Figure 5.8). Dolomite patches are commonly associated with iron oxide cement (Figure 5.8). Dolomites are seen in CL as dull orange-red-brown coloured crystals (Figure 5.7).

Faults are known to control flow paths of dolomitising fluid, although the fluid source is commonly not well known (e.g. Fu *et al.*, 2008; Callot *et al.*, 2010). In the case of the Cutri Formation, dolomite crystals are most often associated with fracturing and stylolites, where dolomites have replaced patches of calcite cements and have occluded porosity by overgrowing into remaining pore space (Figure 5.7).

The dolomites are possibly a product of the continuous process of chemical compaction where calcite cements are first precipitated by the redistribution of carbonates, and after a period of time and considerable pressure-solution resulted in the concentration of significant amounts of insoluble material along solution seams and stylolites, where dolomite precipitated.

The grain-dominated packstones and grainstones of the Cutri formation are typically composed of coarse grains, so partial replacement by dolomite has not affected pore sizes thus not altering/enhancing poor porosity and permeability observations suggesting dolomitisation has no significant effect on reservoir quality in this formation.

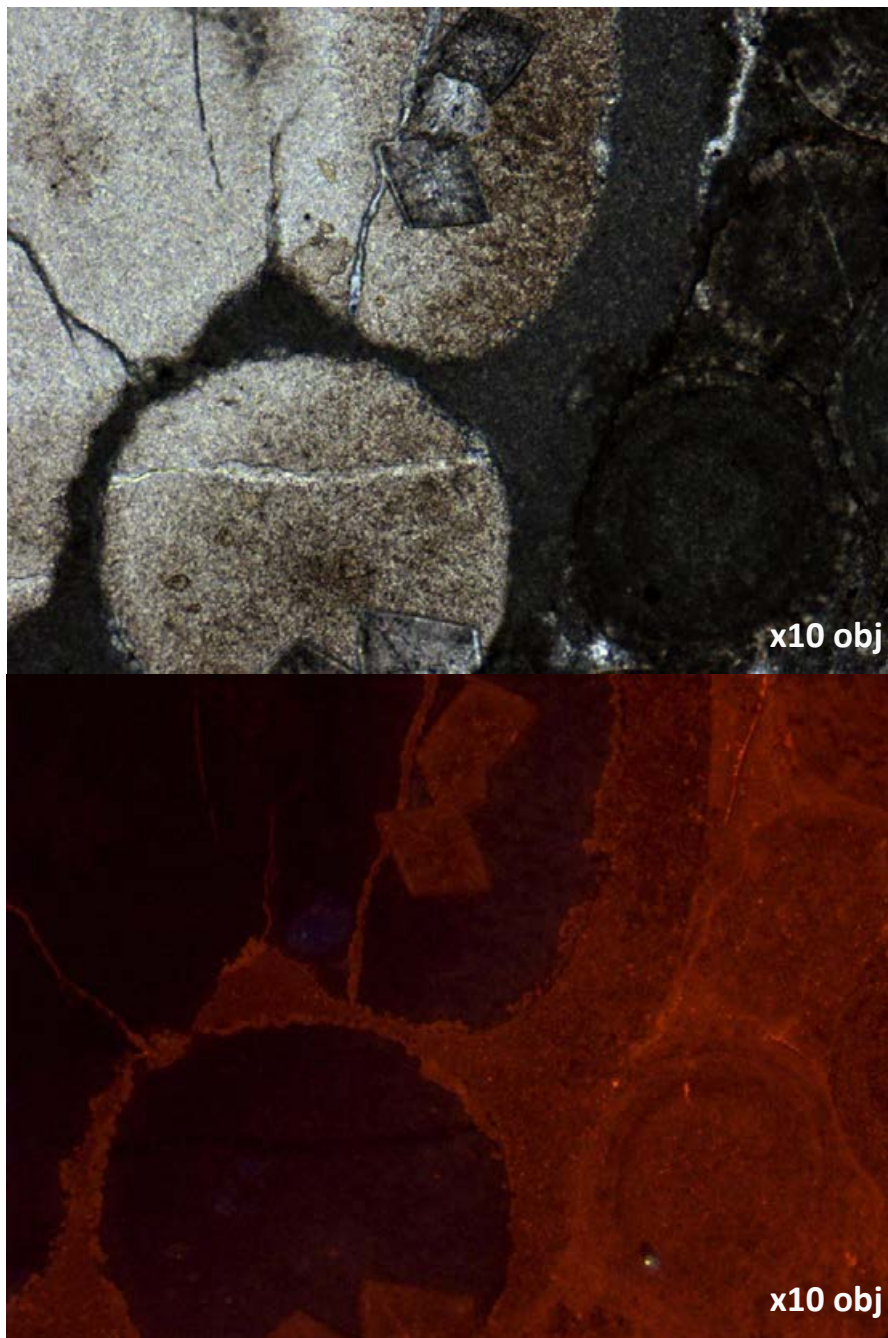


Figure 5.7 Microfractures that cut the dolomites and any remaining porosity are often filled with dull to non-luminescent calcite that rarely contains bright yellow micropatches. Note the predominance of dolomite crystals along grain edges, microfractures and dissolution seams. FoV 1.16 x 0.86mm. Appendix B C001 2450 cm

5.2.8 FRACTURING- CALCITE VEINS

Large calcite veins that are <5 cm thick cut across all components of the rocks and form both obliquely and vertical to bedding. These calcite veins show evidence of shear fracturing, through displacement and micro-brecciation within the fracture cements. Calcite veins are associated with patches of calcified dolomites and commonly contain intercrystal porosity and at hand specimen scale contain unconnected intra-fracture vugs, which probably created through recent dissolution.

These calcite veins post date inter-particle cementation and dolomitisation of the sediments and are dated to more recent tectonic events, (probably in the Tertiary Alvaro *et al.*, 1989). The calcite veins of the Cutri Formation were caused by brittle failure of the rock during tectonic fracturing of the lithified rocks caused by stress and shear displacement, where these fractures were filled with a coarse equant calcite spar.

5.2.9 CALCIFICATION (DEDOLOMITISATION)

Dedolomitisation is the diagenetic replacement or dissolution of dolomite, which may occur under various conditions such as a near-surface process or in deep burial diagenesis followed by precipitation of calcite (Flügel, 2004). Calcification, has partly affected all dolomites in the Cutri Formation, and probably occurred during the flow of calcite-saturated fluids in later fractures.

Calcification is an important process in the Cutri Formation as the cores of dolomite rhombs are rarely preserved. Calcification affected the outer rims of dolomite, releasing iron that precipitated as iron-oxides in the surrounding matrix. This signifies why the dolomites are found hosted in an iron-rich outer rim (Figure 5.8).

The preferential occurrence of dedolomitisation along fractures and adjacent areas as fracture/void-filling calcite indicates that dedolomitising fluids utilised fractures for flow, suggesting that fractures probably acted as permeable conduits to channel dedolomitising fluids, i.e. probably Tertiary fresh water during the Langhian when a major orogenic phase occurred producing the Sierra Norte and Sierra de Levante mountainous regions (Alonso-Zarza *et al.*, 2002). Calcification has led to ferroan calcite replacing patches where dedolomite rhombs were clustered. The replacive calcite in these samples is bright yellow in CL.

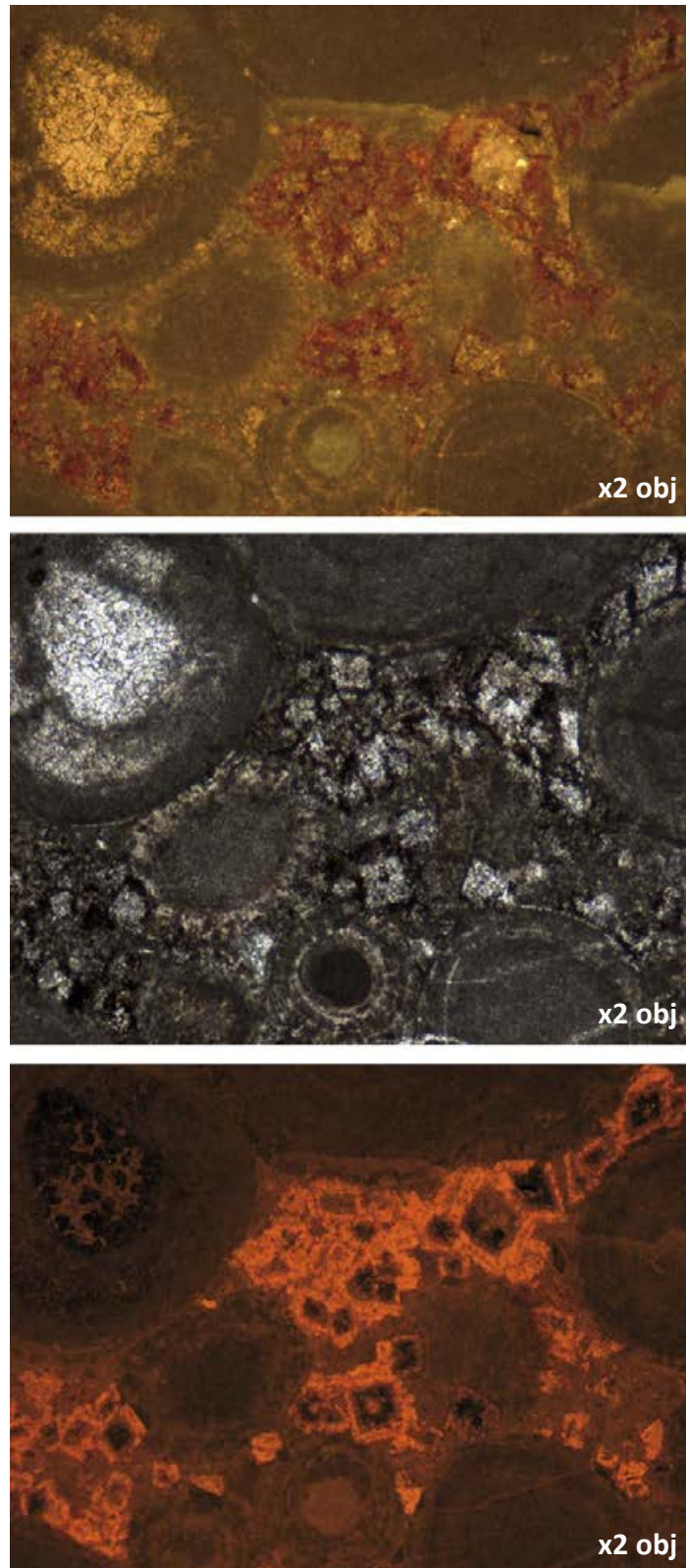


Figure 5.8 Top image is a cross polar reflective photomicrograph indicating the dominance of iron oxide deposits in the matrix. The middle image, PPL, and bottom image, CL, illustrate selective replacement of dolomite rims has occurred giving the orange luminescence in CL. The cloudy luminescence of the outer bright orange rims is due to the presence of small red spots that are dolomite remnants. FoV 5.78 x 4.31 mm. Appendix B C002 520 cm.

5.3 DIAGENETIC CONCLUSIONS

The Cutri Formation is typified by the prevalence of oolitic-peloid sediments and a very small quantity of skeletal debris making up the debrites and turbidites that interrupt fine grained background sedimentation. Extensive micritisation throughout the samples is interpreted to have been a shallow water process where allochems acquired micritic coats in shallow-water environments. A seafloor micrite is interpreted to have been present in the base-of-slope environment where the resedimented allochems settled. Seafloor micrite is suggested to have originated from suspended sediments being shed off the margin of the platform. This succession (suspension-dominated) is characteristic of windward margins where net on-bank transport of sands results in the majority of sediments on the platform margin consisting of fine-grained accumulations that are only interrupted by infrequent gravity flow deposits.

Furthermore, the platform margin was situated in a relatively open area of shallow seas to the west and north and sheltered from the open Tethys Ocean to the south and east (Figure 2.2 and 2.4). As suggested by the sedimentological characteristics, this was a predominantly windward margin where winds and currents were coming from the west through the opening “Nova Scotia-Gibraltar Corridor” (see Figure 2.2).

After resedimentation (eogenesis) a lack of early cementation allowed considerable compaction to occur, at a shallow burial depth, which systematically reduced the vast majority of porosity and created a close-packed texture with small quantities of cement. Mechanical compaction reduced original porosity by rearrangement and deformation of grains.

The mesogenesis stage is characterised by the continued compaction and remobilisation of unstable silica, which was derived from radiolarian tests and sponge spicules where larger, likely organic-rich allochems, were replaced by chalcedony. Later mesogenesis includes the development of extensive calcite cementation, interpreted to have been derived through autocementation processes and associated with microfracturing and dolomite precipitation.

Weathering has resulted in dedolomitisation and iron oxide deposition during telogenesis. Minor karstification is common in the outcrops.

Porosity within the formation was reduced most extensively by compaction and was further reduced by intergranular pore filling cements, interpreted mainly to be derived from chemical compaction. Dissolved carbonate from dissolution and chemical compaction of allochems has locally reprecipitated forming calcite cement in adjacent pore space leading to autocementation, which has completely occluded porosity removing any reservoir potential.

A possible diagenetic history of these deep-marine sediments consistent with the observed petrography is summarised in Figure 5.9. However the sequence is based partly on petrographic relationships and partly by comparison with literature reviews, and so contains uncertainties. Many processes take place simultaneously and the exact paragenetic sequence cannot be determined precisely.

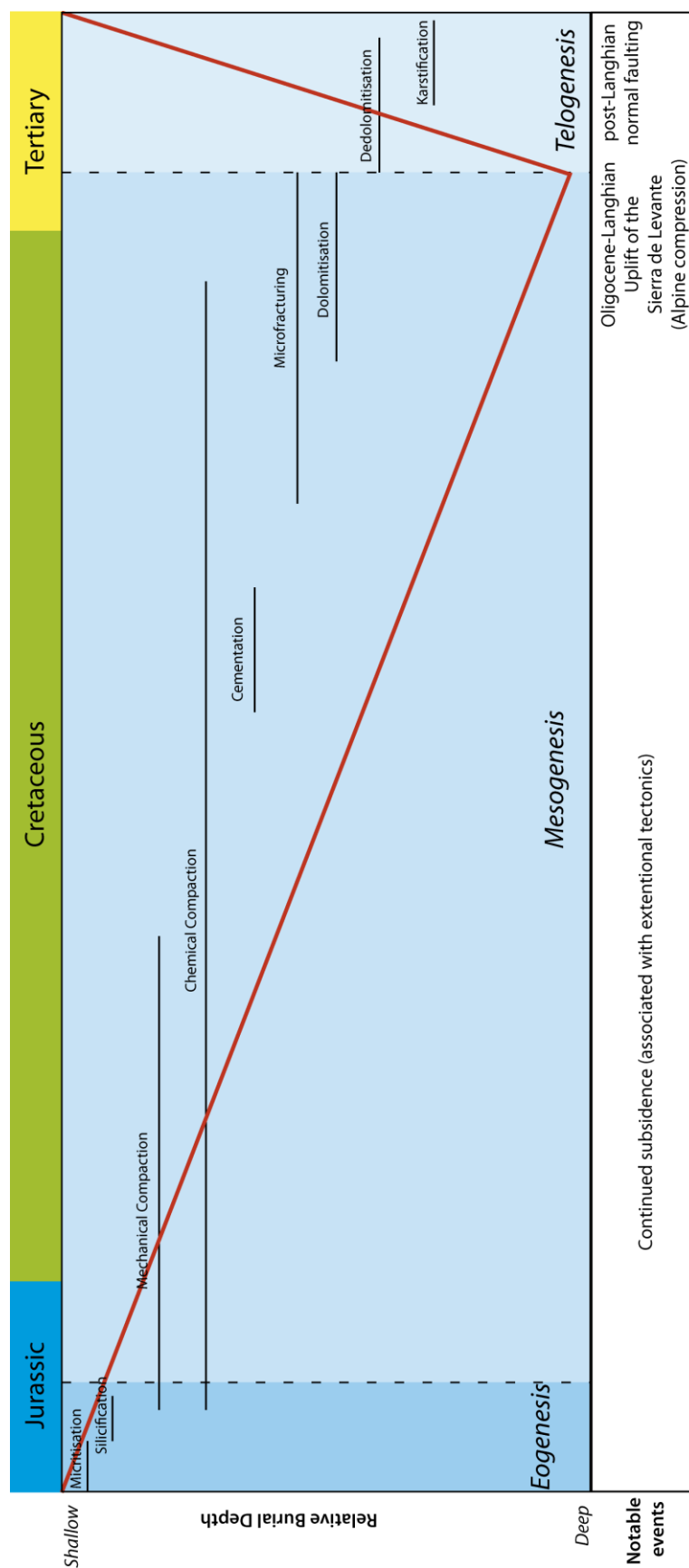


Figure 5.9 Diagenetic history of the Cutri Formation.. Red line indicates burial curve.

6. PETROLEUM RESERVOIR PROPERTIES AND CONCLUSIONS

6.1 INTRODUCTION

Finding new hydrocarbon reserves is becoming increasingly difficult, risky and expensive, due to the finite nature of hydrocarbon and fossil fuels and the economic revival of smaller fields. However, high demand in the world today is forcing exploration into deeper waters and smaller more subtle reservoirs due to these resources becoming more economically viable. As exploration becomes more risky research into new play types and new reservoir models are becoming more and more common. One of the reasons for research into carbonate turbidites is the success that siliciclastic turbidites have provided for hydrocarbon reservoirs and the possibility that carbonate turbidites may prove a new play type.

6.2 DISCUSSION OF KEY PRODUCING FIELDS

There are few hydrocarbon reservoirs producing from resedimented carbonates presently and these include such fields as: Apulia Field, Italy (Cretaceous); Tengiz field, Kazakhstan (Devonian-Permian); and several fields in the U.S. Permian basin, such as Central Glasscock, Credo and Triple-M fields (Permian).

MIDLAND AND DELAWARE PERMIAN BASINS

Forty-one fields produce from resedimented carbonates (Dutton *et al.*, 2004) within the Midland and Delaware basins in Texas and New Mexico (USA). These rocks are associated with the Wolfcamp Platform during the Guadalupian Series and consist of deposits that were derived from several processes including debris flows, turbidity currents, and bottom currents on lower slope areas and the basin floor (Hobson *et al.*, 1985). In the Midland Basin, Pacht *et al.* (1995) concluded that the majority of carbonate debris was deposited during highstand time, but porous debris flows were best developed in lowstand systems tract.

APULIA PLATFORM

The Apulia Platform is found in the SE of Italy near the Gargano Promontory. The platform formed on the southern margin of the Tethys Ocean during the Jurassic-Cretaceous. Resedimented facies are found on the Gargano Promontory where resedimented rudists and megablocks were derived from several processes including debris flows, turbidity currents, and bottom currents. Thick deposits of breccias containing typically dolomitic megablocks represent lowstand deposits whilst highstand bioclastic base-of-slope deposits represent highstand deposits (Borgomano, 2000). These highstand deposits contain the best reservoir potential.

TENGIZ FIELD

The Tengiz field is found in Kazakhstan on the NE shore of the Caspian Sea. The field produces from a Late Devonian isolated platform where resedimented facies surround the platform. The most significant sediments derived from resedimentation processes are found during the Late Visean and Bashkirian (Ulmishek, 2007) where turbidite aprons form on seaward ramps as bioclastic turbidites. Other turbidites are noted to occur within the lower slope of the platform which shows very little permeability (Weber *et al.*, 2008). It is noted that these rocks produce from fractures.

6.2.1 RESERVOIR PROPERTIES

MIDLAND AND DELAWARE PERMIAN BASINS

Conglomeratic carbonate debrites and calcarenite turbidites are reservoirs in the Permian basin (Cook and Mullins, 1983). Clasts of shallow-water origin including skeletal grainstones, wackestones and ooid grainstones (Hobson *et al.*, 1985) characterise the rocks. In addition to these components are large detached blocks of dolomites which are particularly prevalent in proximal parts of debris flows (Mazzullo and Reid, 1987). It is noted that porosity ranges from 6-22% in this play where debrites having the highest porosity readings containing recrystallised bioclast-lithoclast floatstones (Hobson *et al.*, 1985). Porosity in these rocks includes intercrystalline, solution enlarged biomouldic (primarily through lithoclast dissolution),

intraskelatal and fracture. It is suggested that carbonate components were leached from lithoclasts before the original sediment was broken up into lithoclasts and that post-burial leaching also held some importance due to the preservation of a wide variety of porosity.

APULIA PLATFORM

Around the Apulia Platform it is thick sheets of resedimented grainstones (dominated by rudists) that present the highest hydrocarbon potential whilst megablock dominated debrites have the lowest reservoir potential (Borgomano, 1987). The grainstones are characterised by high percentages of intergranular and mouldic porosities, Borgomano (1987) suggested that this high mouldic porosity is possibly due to skeletal aragonite being deposited (i.e. radiolutid rudists). Interestingly, the lowstand deposits have a low reservoir potential due to their diagenetic history which resulted in a lot of compaction and cementation, which is similar to the situation in the Cutri Formation.

TENGIZ FIELD

Resedimented carbonates surround the Tengiz Platform and are commonly found as packstones (Weber *et al.*, 2008) and bioclastic turbidite aprons rich in *Tubiphytes*-algae and bryozoan accumulations (Ulmishek, 2007). However, resedimented upper slope sediments (therefore probably coarser strata) are noted to have been heavily influenced by marine cementation where it occurs as isopachous linings and intergranular cements (Zempolich, 1995). This marine cementation limits primary depositional porosity and therefore porosity-enhancing diagenetic processes or fracturing contribute to any reservoir potential in these sediments.

6.2.2 CONCLUSIONS

In summary, it is notable that the prevalence of good reservoir quality within highstand deposits makes this one of the important areas for further research. Observations suggest the Cutri Formation likely belong to a transgressive system where the oolitic units are deposited into predominately mud-rich sediments and

have been heavily compacted and cemented; occluding porosity almost completely. These allochems may have originated as winnowed uncoated grains that only gained a muddier texture through resedimentation into fine grained sediments downslope. This would have removed almost any potential to have developed into a reservoir since this blocked pore space. The Cutri Formation is an interesting study for research into the hydrocarbon properties of resedimented carbonates because carbonate turbidites are among the few carbonates that have been transported significant distances that could potentially preserve reservoir properties far from source within basinal environments.

7. FINAL CONCLUSIONS

7.1 SYNOPSIS

The Cutri Formation is interpreted as a base-of-slope apron deposit characterized by a thinning up-wards sequence indicating increasing distality from source. The apron is composed of distinct oolitic turbidite units that are laterally extensive, interbedded by mudstones and packstones interpreted to be of contourite origin.

The turbidites are high-density turbidites that are identified to have been sourced from an easterly location. Slope deposits are noted to occur further to the south on the Island of Caberera suggesting that this platform was a significant size.

The apron is suggested to have formed during the Callovian, a period of sea level rise which may explain the overall thinning-up sequence as the carbonate platform migrated away from its original location as it increased the intensity of carbonate growth towards the rising sea level. However tectonic control is considered to have taken a more direct role in initiating deposition of the Cutri Formation where Abbots (1989) investigation of the Island of Caberera indicated the proximity of a normal fault to the platform edge.

The overall fine-grained nature of the formation indicates that these deposits were formed on the windward margin of a carbonate platform. The orientation of the platform to winds (i.e. windward vs. leeward) provides a fundamental control on sediment type being deposited and hence its diagenetic potential.

A diagenetic investigation suggests that reservoir potential for the Cutri Formation was minimized by the rapid porosity loss due to compaction and autocementation processes. In fact, it is noted that porosity in resedimented carbonates is formed commonly due to mineralogical composition (i.e. aragonite vs. calcite dissolution) or secondary porosity formation such as fracturing.

7.1 FURTHER STUDY

This study of the Cutri Formation has resulted in several ideas that are of interest for future study including:

- Understand the regional context of contourite/turbidite systems in the Tethys Ocean during the Mid-Late Jurassic.
- Comparison of other examples of resedimented carbonates that are or have produced hydrocarbons with other non-producing rocks to determine the main causes for reservoir properties being preserved in some resedimented carbonates and not others.
- Review of all reservoirs producing from resedimented carbonates, these include debrites, turbidites, contourites and other resedimented rocks to determine their reasons for reservoir quality.
- Further diagenetic study is appropriate to determine actual timing of events and therefore their impact on the reservoir properties within the Cutri Formation and whether this can be developed into a diagenetic model applicable to resedimented carbonates in general.
- Study into whether turbidite packages such as the Cutri Formation are visible using current exploration technologies such as seismic techniques and whether it is possible to map potential plays in carbonate slope deposits.

REFERENCES

- Aalto, K. R., 1976. Sedimentology of a mélange: Franciscan of Trinidad, California. *Journal of Sedimentary Petrology* **46** p913-929
- Aas, T. E., Howell, J. A., Janocko, M., Midtkandal, I., 2010. Re-created Early Oligocene seabed bathymetry and process-based simulations of the Peira Cava turbidite system. *Journal of the Geological Society* **167**(5) p857-875
- Abbots, F. V., 1989. Sedimentology of Jurassic syn-rift resedimented carbonate sandbodies. PhD Thesis, University of Bristol pp 403.
- Adams, A.E., Mackenzie, W.S., (1998) *A color atlas of carbonate sediments and rocks under the microscope*. Manson Publishing, London, p 180
- Adabi, M. H., Salehi, M. A., and Ghabeishavi, A., 2010. Depositional environment, sequence stratigraphy and geochemistry of Lower Cretaceous Carbonates (Fahliyan Formation), south west Iran. *Journal of Asian Earth Sciences* **39**(3) 148-160
- Ahr, W. M., 2008. Geology of Carbonate Reservoirs: The identification, description and characterization of hydrocarbon reservoirs in carbonate rocks. John Wiley & Sons pp.277
- Akhurst, 1993. Aspects of late Quaternary sedimentation in the Faeroe-Shetland Channel, NW UK continental margin. British Geological Survey Technical Report. WB/91/2.
- Allen, J. R. L., 1985. *Principles of Physical Sedimentology*. Allen and Unwin, London
- Alonso-Zarza, A. M., Armenteros, I., Braga, J. C., Muñoz, A., Pujalte, V., Ramos, E., Aguirre, J., Alonso-Gavilán, Arenas, C., Baceta, J. I., Carballeira, J., Calvo, J. P., Corrochano, A., Fornós, J., González, A., Luzón A., Martín, J. M., Pardo, G., Payros, A., Pérez, Pomar, L., Rodríguez, J. M., Villena, J. 2002 Tertiary In: Gibbons, W., and Moreno, M. T. (eds) *The Geology of Spain*. Geological Society, London.
- Álvaro , M., Barnolas, A., Del Olmo, P., Ramírez del Pozo, J., and Simó, A., 1984a. Estratigrafía del Jurásico. In: Álvaro , M., Barnolas, A., Del Olmo, P., Ramírez del Pozo, J., and Simó, A. (eds) *Sedimentología del Jurásico de Mallorca*. GEM-IGME-CGS, pp. 43-71
- Álvaro, M., Barnolas, A., Cabra, A *et al.*, 1989. El Jurásico de Mallorca (Islas Baleares). *Cuadernos de Geología Ibérica*, **13**, 67-120
- Amante C., and Eakins, B.W., 2009. ETOPO1 1 Arc-Minute Global Relief Model: Procedures, Data Sources and Analysis, *NOAA Technical Memorandum NESDIS NGDC24* pp.19
- Amy, L.A. and Talling, P.J. 2006. Anatomy of turbidites and linked debrites based on long distance (120 × 30 km) bed correlation, Marnoso Arenacea Formation, Northern Apennines, Italy, *Sedimentology* **53**, pp. 161–212.
- Amy, P.J. Talling, J. Peakall, R.B. Wynn and R.G. Arzola Thynne, 2005. Bed geometry used to test recognition criteria of turbidites and (sandy) debrites, *Sedimentary Geology* **179**, pp. 163–174.

- Arbona, J., Fontboté, J., -M., González-Donoso, J., M et al., (1984-1985). Precisiones bioestratigráficas y aspectos sedimentológicos del Jurásico-Cretácico basal de la isla de Cabrera (Balears). *Cuadernos de Geología, Universidad de Granada*, **12**, 169-186.
- Argyriadis, I., De Graciansky, P. C, Marcoux, J. & Ricou, LE 1980. The opening of the Mesozoic Tethys between Eurasia and Arabia-Africa. In: Auboin, J., Debelmas, J. & Latreille, M. (eds) *Geology of the Alpine chains born of the Tethys*. Mémoires du Bureau de Recherches Géologiques et Minières, **115** p200-213
- Arias, C., 2008. Palaeoceanography and biogeography in the Early Jurassic Panthalassa and Tethys Oceans. *Gondwana Research* **14** 306-315.
- Aurell, M., Badneas, B., Bosence, D. W. J., and Waltham, D> A. 1998. Carbonate production and offshore transport on a late Jurassic carbonate ramp (Kimmeridgian, Iberian Basin, N. E Spain); evidence from outcrop and computer modeling. In: Wright, V. P., and Burchette, T. P. (eds) *Carbonate Ramps*, Geological Society Special Publication 149, 137-161. Geological Society of London.
- Aurell, M., Meléndez, G., Bádenas, B., Pérez-Urresti, I. And Ramajo, J. 2002. Sequence Stratigraphy of the Callovian-Berriasian (Middle Jurassic-Lower Cretaceous) of the Iberian basin (NE Spain). *GeoResearch Forum*, **5**, pp. 281-292.
- Azañón, J. M., Galindo-Zaldívar, J., García-Deñas, V., and Jabaloy A. 2002. Alpine Tectonics II: Betic Cordillera and Balearic Islands. In: Gibbons, W., and Moreno, M. T. (eds) *The Geology of Spain*. Geological Society, London.
- Azéma, J., Champetier, Y., Foucault, A., Fourcade, E., Rangheard, J. 1971. Le Jurassique dans le partie oriental des Zones Externes des Cordillères Bétiques: essai de coordination. *Cuadernos de Geología Ibérica*, **2**, 91-110.
- Bagnold, R. A., 1954. Experiments on a gravity-free dispersion of large solid spheres in a Newtonian fluid under shear. *Proceedings of the Royal Society of London A* **225**(1160) p49-63
- Bagnold, R.A. 1962. Auto-suspension of transported sediment; turbidity currents. *Proceedings of the Royal Society of London A* **265**, p315-319.
- Banda, E., Gallart, J., García-Deñas, V., Dañobeitia, J. J., Makris, J., 1993. Lateral variation of the crust in the Iberian peninsula: new evidence from the Betic Cordillera. *Tectonophysics* **221** p53-66
- Barker, S. P., P.D.W. Haughton, W.D. McCaffrey, S.G. Archer and B. Hakes., 2008. Development of rheological heterogeneity in clay-rich high-density turbidity currents: Aptian Britannia Sandstone Member, U.K. Continental shelf, *Journal of Sedimentary Research* **78** p 45–68.
- Barnolas, A., Simon, A., 1987. La sedimentación oolítica del Dogger de Mallocra: Un modelo de bajada carbonática de pie de talud retrogradacional. *Geogaceta* **3** p31-34
- Barron, E.J., Fawcett, P.J., 1995. The climate of Pangaea: a review of climate model simulations of the Permian. In: Scholle, P.A., et al.,. (Ed.), The Permian of Northern Pangaea. *Paleogeography, Paleoclimates, Stratigraphy*, **1**. p37–52.

- Barron, E.J., Petersen, W.H., 1990. Model simulation of the Cretaceous ocean circulation. *Science* **244**, 684–686.
- Bathurst, R.G. C., 1975. *Carbonate Sediments and their Diagenesis*. Developments in Sedimentology (12). Elsevier, 658pp
- Baudin F, Dercourt J, Herbin JP, Lachkar G (1988) Le Lias supérieur de la zone ionienne (Grèce) une sédimentation riche d'Épire (zone ionienne, Grèce): le Membre de Paliambela. *C R Acad Sci* **311** : II, 421-428
- Baudin F, Lachkar G (1990) Géochimie organique et palynologie du Lias supérieur en zone ionienne (Grèce): Exemple d'une sédimentation anoxique dans une paléo-marge en distension. *Bull Soc géol France* **8** 6:1, p123–132
- Bein, A., Weiler, Y., 1976. The Cretaceous Talme Yafe Formation, a contour current shaped sedimentary prism of carbonate debris at the continental margin of the Arabian Craton. *Sedimentology* **23**, 511-532.
- Belderson, R. H., and Laughton, A. S. 1966. Correlation of some Atlantic Turbidites. *Sedimentology* **7** p103-116
- Bell, C. M. and Suárez, M., 1995. Slope apron deposits of the Lower Jurassic Los Molles Formation, Central Chile. *Revista Geologica de Chile*. **22**(1), p103-114
- Benedicto, A., Ramos, E., Casas, A., Sábat, F., and Barón, A. 1993. Evolución tectonosedimentaria de la cubeta neógena de Inca (Mallorca). *Revista de la Sociedad Geológica de España*, **6** p167-176
- Bennetts, K.R., Pikley, O.H., 1976. Characteristics of three turbidites, Hispaniola-Caicos Basin. *Geological Society of America Bulletin*, **87**, p1291-1300
- Bergman, K., L., Westphal, H., Janson, X., Poiriez, A., and Eberli, G. P., (2010) Controlling Parameters on Facies Geometries of the Bahamas, and Isolated Carbonate Platform Environment. In: H. Westphal, B., Riegl, G. P., Eberli (eds) *Carbonate Depositional Systems: Assessing Dimensions and Controlling Parameters*. Springer, London pp 235.
- Bernoulli, D. and Jenkyns, H.C. (1974). Alpine, Mediterranean and Central Atlantic Mesozoic facies in relation to the early evolution of the Tethys. In: R.H. Dott and R.H. Shaver, Editors, *Modern and Ancient Geosynclinal Sedimentation*, a Symposium, Special Publication Soc. econ. Paleont. Miner., **19**, p129-160.
- Bill, M., O'Dogherty, L., Guex, J., Baumgartner, P.O., Masson, H., 2001. Radiolarite ages in Alpine–Mediterranean ophiolites: constraints on the oceanic spreading and the Tethys–Atlantic connection. *Geological Society of America Bulletin* **113**, p129– 143.
- Bjorlykke, K., Y.G. Gundersen, and J. Jahren, 2004, Compaction driven fluid flow in overpressured compartments: Annual Meeting Expanded Abstracts AAPG, **13**, p14.

- Bju-Duval, B., Dercourt, J., Le Pichon, X., 1977. From the Tethys ocean to the Mediterranean Sea: a plate tectonic model of the evolution of the western alpine system. International Symposium of Structure Historian of Mediterranean basins, Spilt, 1976. Technip edit, Paris pp 134-162
- Blendinger, W., and Blendinger, Eva. 1989. Windward-leeward effects on Triassic carbonate bank margin facies of the Dolomites, northern Italy. *Sedimentary Geology* **64**(1-3) p143-166
- Borgomano, J. R. F., 1987, La plate-forme et le talus carbonates du Cretace Superieur du Gargano et des Murges (Italie Meridionale), Ph.D. thesis, University of Provence, Marseille, France, 626 p.
- Borgomano, J. R. F., 2000. The Upper Cretaceous carbonates of the Gargano-Murge region, southern Italy: A model of platform-to-basin transition. *AAPG Bulletin* **84** (10) pp 1561-1588
- Bosellini, A., Masetti, D., Sarti, M., 1981a. The Vajont Limestone: an oolitic deep sea fan, Middle Jurassic, Venetian Alps. Excursion 8 IAS Excursion Guidebook, 2nd European Regional Meeting (1981) p305-342
- Bouma, Arnold H. (1962) *Sedimentology of some Flysch deposits: A graphic approach to facies interpretation*, Elsevier, Amsterdam, 168 p.
- Bourgeois, J., 1980. Pre-Triassic fit and alpine tectonics of continental blocks in the Western Mediterranean: Discussions and reply. *Geological Society of America Bulletin*, Part I, **91** p632-634
- Bourroilh, R. 1973. *Stratigraphie, sedimentology et tectonique de l'île de Minorque et du Nord-East de Majorque (Baléares). La terminación nord-orientale des Cordillères Bétiques en Méditerranée occidentale*. PhD Thesis, Univeristy of Pierre and Marie Curie, Paris.
- Brunet, M. F., 1986. The influence of the evolution of the Pyrenees on adjacent basins. *Tectonophysics*, **129**, pp. 343-354
- Bryn, P. Berg, K. Stoker, M.S. Haflidason, H. Solheim, A. 2005. Contourites and their relevance for mass wasting along the Mid-Norwegian Margin, *Marine and Petroleum Geology*, **22**(1-2) p85-96
- Bryn, P., Berg, K., Stoker, M. S., Haflidason, H and Solheim, a. 2010. Contourites and their relevance for mass wasting along the Mid-Norwegian Margin. *Marine and Petroleum Geology* **22**(1-2) pp. 85-96
- Bustillo, M. A., and Ruiz-Ortiz P. A., 1987. Chert occurrences in carbonate turbidites: examples from the Upper Jurassic of the Betic Mountains (southern Spain). *Sedimentology*, **34**, pp. 611-621
- Callot, J-P., Breesch, L., Guilhaumou, N., Roure, F., Swennen, R., Vilasi, N. 2010. Palaeo-fluids characterisation and fluid flow modeling along a regional transect in Northern Arab Emirates (UAE). *Arabian Journal of Geosciences* **3**(4) p413-437
- Caracuel J. E., Khalil, E. L., Oloriz F., 1995. Faciès radiolaritiques et discontinuités à la limite Dogger-Malm dans la formation Puig d'en Paré (Sierra Norte, Majorque) = Radiolarian facies and discontinuities around the Dogger-Malm boundary in the Puig d'en paré Formation (Sierra Norte, Mallorca). *Geobios*, **28** (6).
- Carracedo, J., C., Torrado, F., J., P., Ancoches, E., Meco, J., Hernán, F., Cubas, C., R., Casillas, R., Badiola, E., R., and Ahijado, A. Cenozoic volcanism II: the Canary Islands. In: Gibbons, W., and Moreno, M. T., (eds) 2002. *The Geology of Spain*. Geological Society, London.

- Chandler, M.A., Rind, D., Ruedy, R., 1992. Pangaeen climate during the Early Jurassic: GGCM simulations and the sedimentary record of paleoclimate. *Geological Society of American Bulletin* **194**, 543–559.
- Chuhan, F. A., Kjeldstad, A., Bjørlykke, K and Høeg, K., 2002. Porosity loss in sand by grain crushing-experimental evidence and relevance to reservoir quality. *Marine and Petroleum Geology* **19 (1)** 39-53
- Cobianchi, M., and Picotti, V., 2001. Sedimentary and biological response to sea-level and palaeoceanographic changes of a Lower-Middle Jurassic Tethyan platform margin (Southern Alps, Italy). *Palaeogeography, Palaeoclimatology, Palaeoecology*, **169**(3-4), p219-244
- Colacicchi, R. and Baldanza, A., 1986. Carbonate turbidites in a Mesozoic pelagic basin: Scaglia Formation, Apennines. Comparison with siliciclastic depositional models. *Sedimentary Geology*, **48**, p81-105.
- Collins, L.B, 2010. Controls on Morphology and Growth history of Australia's Western Margin. In: Morgan, W. A., George, A. D., Harris, P. M., Kupecz, J. A., and Sarg, J. F (eds.) *Cenozoic Carbonate Systems of Australia*. SEPM Special Publication 95 p. 195-217
- Colom, G., 1975. *Geología de Mallorca*, Vol 1. Instituto de Estudios Baleáricos, Palma de Mallorca, p40-84
- Colom, G., and Escandell, B., 1962. L'évolution du geosynclinal Baléare. Livre Mémoire. *P. Fallot, Soc. Géol. France*, **1**, p.125-136.
- Comas, M. C., García Dueñas, V., Jurado, M. J., 1992. Neogene tectonic evolution of the Alborán basin from MCS data. *GeoMarine Letters* **12** p157-164
- Comas, M. C., Platt, J. P., Soto, J. I., Watts, A. B., 1999. The origin and tectonic history of the Alborán Basin: Insights from Leg 161. In: Zahn, R., Comas, M. C., Klaus, A (eds.) *ODP Proceedings, Scientific Results*, **161** p555-579
- Cook, H. E., 1979b. Generation of debris flows and turbidity current flows from submarine slides (abs). *AAPG Bulletin* **63**, p435
- Cook, H. E., 1983. Ancient carbonate platforms, slopes and basins. In: H. E. Cook and H. T. Mullins (eds) *Platform margin and deep water carbonates*. Society for Sedimentary Geology (SEPM) Short Course **12** p189
- Cook, H. E., McDaniel, P. N., Mountjoy, E.W., Pray, L. C., 1972. Allochthonous carbonate debris flows at Devonian bank ("reef") margins, Alberta, Canada. *Bulletin of Canadian Petroleum Geology* **20**, p439-497
- Crevello, P.E. and Schlager, W., 1980. Carbonate debris sheets and turbidites, Exum Sound, Bahamas. *Journal of Sedimentary Petrology* **50**, p1121–1148.
- Croizé, D., K. Bjorlykke, D.K. Dysthe, F. Renard, and J. Jahren, 2008, Deformation of carbonates, experimental mechanical and chemical compaction: Geophysical Research Abstracts, **10**.

Crowley, T.J., Hyde, W.T., Short, D.A., 1989. Seasonal cycle variations on the supercontinent of Pangaea: implications for Early Permian vertebrate extinctions. *Geology* **17**, 457–460.

Curnelle, R., Dubois, P., Seguin, J. C., Whitaker, D., Matthews, D. H., Roberts, D. G., Peter Kent, Laughton, A. S. and Kholief M. M. The Mesozoic-Tertiary Evolution of the Aquitaine Basin. *Philosophical Transactions of the Royal Society of London. Series A, Mathematical and Physical Sciences*, **305 (1489)**, p63-84

Danelian, T., Baudin, F., (1990) Découverte d'un horizon carbonaté, riche en matière organique, au sommet des radiolarites en carbone organique. *C R Acad Sci* **307**: 985–990

Debiche, M.G., Cox, A., Engebretson, D., 1987. The motion of allochthonous terranes across the North Pacific basin. *Geological Society of America Special Paper* **207**, p1–49.

Dercourt, J., L.P. Zonenshain, L.-E. Ricou, V.G. Kazmin, X. Le Pichon, A.L. Knipper, C. Grandjacquet, I.M. Sbertshikov, J. Geyssant, C. Lépvrier, D.H. Pechersky, J. Boulin, J.-C. Sibuet, L.A. Savostin, O. Sorokhtin, M. Westphal, M.L. Bazhenov, J.P. Lauer, B. Biju-Duval., 1986. Geological evolution of the tethys belt from the atlantic to the pamirs since the Lias. *Tectonophysics*, **123**(1-4) p241-315

Dercourt, J., Ricou, L. E., and Vrielynck, B (eds), 1993. *Atlas Tethys Palaeoenvironmental Maps*. Gauthier-Villars, Paris.

Dewey, J.F., Helman, M.L., Turco, E., Hutton, D.H.W., Knott, D., 1989. Kinematics of the western Mediterranean. In: Coward, M.P., Dietrich, D., Park, R.G. (Eds.), *Alpine Tectonics*. Special Publication-Geological Society, **45**, p265– 283.

Drzewiecki, P. A., & Simo`, J. A., 2002. Depositional processes, triggering mechanisms and sediment composition of gravity flow deposits: examples from the Late Cretaceous of south-central Pyrenees, Spain. *Sedimentary Geology*, **146**, p155–189.

Duan, T., Gao, T., Zeng, Y., Stow, D.A.V., 1993. A fossil carbonate contourite drift on the Lower Ordovician paleocontinental margin of the middle Yangtze Terrane, Jiuxi, northern Hunan, southern China. In: Stow, D.A.V., Faugbres, J.-C. (Eds.), *Contourites and Bottom Currents*. Sedimentary Geology **82**, p271- 284.

Dutton, S. P., E. M. Kim, R. F. Broadhead, C. L. Breton, W. D. Raatz, S. C. Ruppel, and C. Kerans, 2004, *Play analysis and digital portfolio of major oil reservoirs in the Permian basin: Application and transfer of advanced geological and engineering technologies for incremental production opportunities*: University of Texas at Austin, Bureau of Economic Geology p408.

Eberli, G.P., 1987. Carbonate turbidite sequences deposited in rift-basins of the Jurassic Tethys Ocean (eastern Alps, Switzerland). *Sedimentology* **34**, 363–388.

Eberli, G.P., and Ginsburg, R.N., 1989, Cenozoic progradation of northwestern Great Bahama Bank, a record of lateral platform growth and sea level fluctuations. In: Crevello, P., Wilson, J.L., Sarg, J.F., and Read, J.F., eds., *Controls on carbonate platform to basin development*. Society of Economic Paleontologists and Mineralogists Special Publication **44**, p. 339-352.

- Eberli, G. P., and Westphal, H., 2010. The Depositional Systems of the Bahamas, Belize Lagoon and The Gulf Compared. *In: Carbonate Depositional Systems: Assessing Dimensions and Controlling Parameters*. Springer, Netherlands, pp 229
- Edwards, D. A., Leeder, M. R., Best, J., Pantin, H. M., 1994. On experimental reflected density currents and the interpretation of certain turbidites. *Sedimentology* **41**(3) p437-461
- Einsele, G., 1998. Event stratigraphy: recognition and interpretation of sedimentary event horizons. *In: Doyle, P., Bennett, M. R (eds) Unlocking the stratigraphic record*. Wiley, p193
- Einsele, G., 2000. *Sedimentary Basins: Evolution, Facies and Sediment budget*. Springer, p795
- Engelbreton, D.C., Cox, A., Gordon, R.G., 1985. Relative motions between oceanic and continental plate in the Pacific basin. *Geological Society of America, Special Paper* **206**, p1–59.
- Enos, P., and Stephens, B. P., 1991. Basin-margin carbonates, mid-Cretaceous, Mexico. *In: Bourrouilh, R., and Doyle, L. J. (eds). Carbonate Gravity Deposits*. International Association of Sedimentologists, Special publication.
- Escutia, C., Nelson, C. H., Acton, G. D., Eitrem, S. L., Cooper, A. K., Warnke, D. A., Jaramillo, J. M., 2002. Current controlled deposition on the Wilkes Land continental rise, Antarctica. *In: Stow, D. A. V., Pudsey, C. J., Howe, J. A., Faugères, J. -C., Viana, A. R. (eds.) Deep-Water Contourite Systems: Modern Drifts and Ancient Series, Seismic and Sedimentary Characteristics*. Geological Society of London Memoir, **22** p373-384.
- Faugères, J.-C., Imbert, P., Mézerais, M. L., Crémer, M., 1998. Seismic patterns of a muddy contourite fan (Verma Channel, South Brazilian Basin) and a sandy distal turbidite deep-sea fan (Cap Ferret system, Bay of Biscay): a comparison. *Sedimentary Geology* **115** (1-4) p 81-110
- Faugères, J.-C., Zaragosi, S., Mézerais, M. L., and Massé, L., 2002. The Vema contourite fan in the South Brazilian Basin. *In: Stow, D. A. V., Pudsey, C. J., Howe, J. A., Faugères, J.-C. & Viana, A. R. (eds) Deep-Water Contourite Systems: Modern Drifts and Ancient Series, Seismic and Sedimentary Characteristics*. Geological Society, London, Memoirs, **22**, p289-303.
- Faulp, P and A., Beran, (1983) Diagenetische Veränderungen von Radiolarium und Schwamm-spicula führenden Gesteinen der Strubbergsschichten. *Neues Jh. Geol. Paläont. Mh.*, **3**, p129-140
- Favre, P. & Stampfli, G. 1992. From rifting to passive margin: the Red Sea, the central Atlantic and the Alpine Tethys as examples. *Tectonophysics*, **215**, p69–97.
- Fawcett, P.C., Barron, E.J., Robinson, V.D., Katz, B.J., 1994. The climate evolution of India and Australia from the Late Permian to mid-Jurassic; a comparison of climate model results with the geological record. *Geological Society of America Special Paper* **228**, 139–157.
- Felix, M., Leszczyński, S., Ślaczka, A., Uchman, A., Amy, L., Peakall, J. 2009. Field expressions of the transformation of debris flows into turbidity currents, with examples from the Polish Carpathians and the French Maritime Alps. *Marine and Petroleum Geology*, **26** p2011-2020
- Fenner, D. P., 1988. Some Leeward Reefs and Corals of Cozumel, Mexico. *Bulletin of Marine Science*. **42**(1) p 133-144

Flügel, F. 2004. *Microfacies of Carbonate Rocks: Analysis, Interpretation and Application*. Springer p976

Ford, D., and Golonka, J., 2003. Phanerozoic palaeogeography, palaeoenvironments and lithofacies maps of the circum-Atlantic margins *In*: Golonka, J. (ed) Thematic set on palaeogeographic reconstruction and hydrocarbon basins: Atlantic, Caribbean, South America, Middle East, Russian Far East, Arctic. *Marine and Petroleum Geology*, **20** p249-285

Friedman, G. M., 1998. Rapidity of marine carbonate cementation-implications for carbonate diagenesis and sequence stratigraphy: perspective. *Sedimentary Geology*. **119** (1-2) p1-4

Fruth, L. S., Orme, G. R., and Donath, F. A., 1966. Experimental compaction effects in carbonate sediments. *Journal of Sedimentary Research*. **36**(3) 747-754

Fu, Q., Quing, H., Bergman, K. M., Yang, C. 2008. Dedolomitization and calcite cementation in the Middle Devonian Winnipegosis Formation in Central Saskatchewan, Canada. *Sedimentology*. **55**(6) p1623-1642.

García Dueñas, V., Balanyá, J. C., 1986. Estructura y naturaleza del Arco de Gibraltar. *Mollee Boletim Informativo da Sociedade Geológica de Portugal* **2** p23

García-Hernandez, M., López-Garrido, A. C., Rivas, P., Sanz de Galdeno, C and Vera, J. A. 1980. Mesozoic palaeogeographic evolution of the External Zones of the Betic Cordillera. *Geologie en Mijnbouw*, **59**, p155-168.

Gaudin, M., Berne, S., Jouanneau, J.-M. Palanques, A., Puig, P., Mulder, T., Cirac, P., Rabineau, M., Imbert, P., 2006. Massive sand beds attributed to deposition by dense water cascades in the Bourcart canyon head, Gulf of Lions (northwestern Mediterranean Sea), *Marine Geology*, **234** (1-4) p111-128

Gawthorpe, R. L., Fraser, A. J., and Collier, R. E., 1994. Sequence stratigraphy in active extensional basins: implications for the interpretation of ancient basin fills. *Marine Geology* **11** (6) p642-658.

Gee, M. J. R., Masson, D. G., Watts A.B. and Allen P.A., 2001. Passage of debris flows and turbidity currents through a topographic constriction: seafloor erosion and deflection of pathways, *Sedimentology* **48**, p1389–1411.

Gelabert-Ferrer, B. 1998. *La estructura geológica de la mitad occidental de la Isla de Mallorca*. PhD Thesis, University of Barcelona

Giménez, J., Gelabert, B and Sabat, F., 2007. El relieve de las Islas Baleares. *Enseñanza de las Ciencias de la Tierra* **15** (2) p175-184.

Goldhammer RK 1997 Compaction and decompaction algorithms for sedimentary carbonates. *Journal of Sedimentary Research* **67**, 1:26-56

Golonka, J, 2007. Late Triassic and Early Jurassic palaeogeography of the world. *Palaeogeography, Palaeoclimatology, Palaeoecology* **244**. 297-307

- Golonka, J., 2004. Plate tectonic evolution of the southern margin of Eurasia in the Mesozoic and Cenozoic. *Tectonophysics*, **381**, 235-273
- Golonka, J., and Kiessling, W. 2002. Phanerozoic time scale and definition of time slices. In: Kiessling, W., Flügel, E., Golanka, J. (Eds.), *Phanerozoic Reef Patterns*. *SEPM Special Publication* **72**, 1-20.
- Golonka, J., Bocharova, N.Y., 2000. Hot spot activity the break-up of Pangea. *Palaeogeography, Palaeoclimatology, Palaeoecology* **161**, 49– 69.
- Golonka, J., Edrich, M. ., Ford, D. W., Pauken, R. B., Bocharova, N. Y. & Scotese, C. R., 1996. Jurassic Paleogeographic Maps of the World. In: M. Morales. (ed.), *The Continental Jurassic. , Museum of Northern Arizona Bulletin*, **60** p1-5.
- Golonka, J., Ford, D.W., 2000. Pangean (late Carboniferous – Middle Jurassic) paleoenvironment and lithofacies. *Palaeogeography, Palaeoclimatology, Palaeoecology* **161**, 1– 34.
- Golonka, J., Ross, M.I., and Scotese, C.R., 1994. Phanerozoic paleogeographic and paleoclimatic modeling maps. In: A.F. Embry, B. Beauchamp, and D.J. Glass (eds.), *PANGEA: Global Environments and Resources*, *Canadian Society of Petroleum Geology Memoir* **17**, p 1-48.
- Gómez, J. J., and Fernández-López, S. R., 2006. The Iberian Middle Jurassic carbonate-platform system: Synthesis of the palaeogeographic elements of its eastern margin (Spain). *Palaeogeography, Palaeoclimatology, Palaeoecology* **236** (3-4), 190-205
- Gonthier, E. G., Faugères, J. –C., Stow, D. A. V. 1984. Contourite facies of the Faro Drift, Gulf of Cadiz. *Geological Society, London, Special Publications*. **15** p275-292
- Gonzalez-Donoso, J. M, Linares, A., Lopez-Garrido, A. C., Vera, J. A., 1971. Bosquejo estratigráfico del Jurásico de las Cordilleras Béticas. *Cuad Geol Iberica* **2** p55–90
- Goy, A., Martínez, G., Ureta, M. S., 1995. Ammonitina (Hammatoceratidae) of the Toarcian and Aalenian in the Serra de Llevant (Isle of Mallorca, Spain). *Hantkeniana*, **1**, p97-104
- Goy, J. L., Zazo, C., Cuerda, J., 1997. Evolución de las areas margin-litorales de la Costa de Mallorca (I. Baleares) durante el Ultimo y Presente Interglacial: Nivel del mar Holoceno y clima. *Boletín Geológico y Minero*, **108** p127-135
- Grammer, G.M., and Ginsburg, R.N., 1992, Highstand versus lowstand deposition on carbonate platform margins: Insight from Quaternary foreslope in the Bahamas. *Marine Geology*, **103**, p. 125-136.
- Grammer, G.M., Ginsburg, R.N., and Harris, P.M., 1993, Timing of deposition, diagenesis, and failure of steep carbonate slopes in response to a high-amplitude/high frequency fluctuation in sea level, Tongue of the Ocean, Bahamas. In: Loucks, R.G. and Sarg, J.F., eds., *Carbonate Sequence Stratigraphy*: American Association of Petroleum Geologists Memoir, 57, p. 107-131.
- Guerrera, F., Martín-Algarra, A., Perrone, V., 1993. Late Oligocene-Miocene syn-/late-orogenic successions in Western and Central Mediterranean Chains from the Betic Cordillera to the Southern Apennines. *Terra Nova*, **5**, p525-544.

Gutiérrez-Elorza, M., García-Ruiz, J. M., Goy, J. L., Gracia, F. J., Gutiérrez-Santolalla, F., Martí, C., Martín-Serrano, A., Pérez-González, A., and Zazo, C. 2002. Quaternary. In: Gibbons, W., and Moreno, M. T. (eds) *The Geology of Spain*. Geological Society, London.

Hallam, A. 2002. How catastrophic was the end-Triassic mass extinction? *Lethaia* **35**, 147–157.

Halley, R.B., Harris, P.M., 1979. Freshwater cementation of a 1,000 year old oolite. *Journal of Sedimentary Petrology* **49**, 969–988.

Hamlin, H. S., 2009. Ozona sandstone, Val Verde Basin, Texas: Synorogenic stratigraphy and depositional history in a Permian foredeep basin. *AAPG bulletin* **93** (5) 573 -594

Handford, C. R., and Loucks, R. G. 1990. Dynamic response of carbonate systems tracts to relative sea level changes and the development of carbonate depositional sequences in platforms and ramps (abstract): *AAPG Bulletin* **75** p 669

Haq, B.U., Hardenbol, J., and Vail, P.R., 1987. Chronology of fluctuating sea levels since the Triassic (250 million years ago to present). *Science*, **235**, p1156–1167.

Haughton, P., Davis, C., McCaffrey, W., Barker, S. 2009. Hybrid sediment gravity flow deposits- Classification origin and significance. *Marine and Petroleum Geology* **26** p1900-1918

Haughton, P.D.W. 1994. Deposits of deflected and ponded turbidity currents, Sorbas Basin, Southeast Spain, *Journal of Sedimentary Research* **A64**, pp. 233–246.

Haughton, P.D.W. Barker S.P. and McCaffrey, W.D. 2003. ‘Linked’ debrites in sand-rich turbidite systems – origin and significance, *Sedimentology* **50** , pp. 459–482.

Haughton, P. Davis, C., McCaffrey, W., Barker, S., 2009. Hybrid sediment gravity flow deposits- Classification, origin and significance. *Marine and Petroleum Geology* **26** 1900-1918.

Heezen, B. C, Ewing, M., 1952. Turbidity currents and submarine slumps and the 1929 Grand Banks earthquake. *American Journal of Science* **250** p849–873.

Heezen, B. C., Ericson, D. B., Ewing M., 1954. Further evidence for a turbidity current following the 1929 Grand Banks earthquake. *Deep Sea Research* **1** p193–202.

Heezen, B.C., Hollister, C. D., Ruddiman, W.F., 1966. Shaping of the continental rise by deep geostrophic contour currents. *Science* **152** p502–508.

Hernández-Molina, F. J., Llave, E., Stow, D. A. V., García, M., Somoza, L. Vázquez, J.T. Lobo, F.J. Maestro, A. Díaz del Río, V. León, R. Medialdea T. and Gardner J. 2006. The contourite depositional system of the Gulf of Cadiz: A sedimentary model related to the bottom current activity of the Mediterranean outflow water and its reaction with the continental margin. *Deep Sea Research Part II: Topical Studies in Oceanography*. **53** (11-13) p. 1420-1463

Hernández-Molina, F. J., Paterlini, M., Violante, R., Marshall, P., de Isasi, M., Somoza, L., Rebesco, M., 2009. A contourite depositional system on the Argentine slope: an exceptional record of the influence of Antarctic water masses, *Geology* **I37** (6), p507–510.

- Hesse, R., 1987. Selective and reversible carbonate-silica replacements in Lower Cretaceous carbonate-bearing turbidites of the Eastern Alps. *Sedimentology*, **34** p.1055-1077
- Hine, A. C., 1977. Lily Bank, Bahamas: history of an active oolite sand shoal. *Journal of Sedimentary Petrology*. **47** p 1554-1581
- Hine, A.C., Wilber, R.J., Bane, J.M., Neumann, A.C. and Lorenson, K.R., 1981. Offbank transport of carbonate sands along open, leeward bank margins: northern Bahamas. *Marine Geology*. **42** p327-348.
- Hobson, J. P., Caldwell, C. D., Toomey, D. F., 1985. Early Permian Deep-Water Allochthonous Limestone Facies and Reservoir, West Texas. *AAPG Bulletin* **69** (12) p2130-2147
- Hodgson, D. M., 2009. Distribution and origin of hybrid beds in sand-rich submarine fans of the Tanqua depocentre, Karoo Basin, South Africa. *Marine and Petroleum Geology*. **26**(10) p1940-1956
- Hodgson, D. M., and Haughton, P. D. W., 2004. Impact of syn-depositional faulting on gravity current behaviour and deep-water stratigraphy: Tabernas–Sorbas Basin, SE Spain. In: S. Lomas and P. Joseph, Editors, *Confined Turbidites Systems*, Geological Society, London, *Special Publications* vol. **222**, pp. 135–158
- Hollister, C.D. (1993). The concept of deep-sea contourites. *Sedimentary Geology* **82**: 5–11.
- Hooke, R.LeB. and Schlager, W., 1980, Geomorphic evolution of the Tongue of Ocean and the Providence Channels, Bahamas. *Marine Geology*, **35**, p. 343-366.
- Howe, J.A., Stoker, M.S., Stow, D.A.V., 1994. Late Cenozoic sediment drift complex, northeast Rockall Trough, North Atlantic. *Paleoceanography* **9**(6), p 989-1000.
- Hsu, L., Dietrich, W. E., Sklar, L. S. 2008. Experimental study of bedrock erosion by granular flows. *Journal of Geophysical Research* **113** (F2) p 21
- Hüneke, H., and Krienke, K. 2004. Toe-of-slope deposits of a Givetian reef-rimmed platform: provenance of calcareous density-flow deposits (Rabat-Tiflet-Zone, Morocco). *Facies* **50** (2) p 327-346.
- Huppertz, T. J., and Piper, D. J. W., 2010. Interbedded Late Quaternary turbidites and contourites in Flemish Pass, off southeast Canada: Their recognition, origin and temporal variation. *Sedimentary Geology* **228** (1-2) p 46-60
- Huvenne, V. A. I., Masson, D. G., and Wheeler, A. J., 2009. Sediment dynamics of a sandy contourite: the sedimentary context of the Darwin cold-water coral mounds, Northern Rockall Trough. *International Journal of Earth Science*, **98** pp 865-884
- IGME, 2010. Mapa Geológico de España a escala 1:50.000 (accessed via <http://www.igme.es/internet/cartografia/cartografia/magna50.asp>)
- Ineson J, Surlyk F., 1995. Carbonate slope aprons in the Cambrian of North Greenland: geometry stratal patterns and facies. In: Pickering KT, Hiscott RN, Kenyon NH, Ricci Lucchi F, Smith RDA (eds)

Atlas of deep water environments: architectural style in turbidite systems. Chapman and Hall, London, pp 56–62

Jackson, C.A.-L., Adli Zakaria, A. Johnson, H. D., Tongkul, F., Crevello, P. D., 2009. Sedimentology, stratigraphic occurrence and origin of linked debrites in the West Crocker Formation (Oligo-Miocene), Sabah, NW Borneo. *Marine and Petroleum Geology*, **26** (10)

James, N.P. and Ginsburg, R.N., 1979, The seaward margin of Belize barrier and atoll reefs. *Special Publication of the International Association of Sedimentologists*, **3**, p 191

Jan Sverre Laberg, Martyn S. Stoker, K.I. Torbjorn Dahlgren, Henk de Haas, Haflidi Haflidason, Berit O. Hjelstuen, Tove Nielsen, Pat M. Shannon, Tore O. Vorren, Tjeerd C.E. van Weering, Silvia Ceramicola, Cenozoic alongslope processes and sedimentation on the NW European Atlantic margin, *Marine and Petroleum Geology*, **22** (9-10) pp1069-1088

Janson, X., Kerans, C., Loucks, R., Marhx, M., A., Reyes, C., and Murguia, F. 2011. Seismic architecture of a lower Cretaceous platform-to-slope system, Santa Agueda and Poza Rica fields, Mexico. *AAPG Bulletin*. **95** (1) p 105-146.

Jassim, S. Z., and Goff, J. C. 2006. *The Geology of Iraq*. Geological Society of London. p 341

Jenkyns, H. C., Sellwood, B. W., Pomar, L., 1990. *A field excursion guide to the island of Mallorca*. The Geologists Association **42** p93

Johnson, A. M., 1970. *Physical Processes in Geology*. Freeman Cooper, San Francisco, 577pp

Johnson, D. A., and Rasmussen, K. A., 1984. Late Cenozoic turbidite and contourite deposition in the Southern Brazil basin. *Marine Geology*. **58**, 225-262

Jolivet, M., Brunel, M., Seward, D., Xu, Z., Yang, J., Roger, F., Tapponnier, P., Malavieille, J., Arnaud, N., Wu, C., 2001. Mesozoic and Cenozoic tectonics of the northern edge of the Tibetan plateau: fission-track constraints. *Tectonophysics* **343**, 111-134.

Jones, E. W., and Okada, H. Abyssal circulation in the equatorial Atlantic: Evidence from Cenozoic sedimentary drifts off West Africa. *Marine Geology* **232** (1-2) p49-61

Kano, K., and Takeuchi, K., 1989. Origin of mudstone clasts in turbidites of the Miocene Ushikiri Formation, Shimane Peninsula, Southwest Japan. *Sedimentary Geology* **62** p79-87

Kenny, R., 1992. Origin of disconformity dolomite in the Martin Formation (Late Devonian, northern Arizona). *Sedimentary Geology*, **78** pp137-146

Kenter, J.A.M., 1990. Carbonate platform flanks: slope angle and sediment fabric. *Sedimentology*, **37**, p777-794

Keppie, J.D., Dostal, J., 2001. Evaluation of the Baja controversy using paleomagnetic and faunal data, plume magmatism, and piercing points. *Tectonophysics* **339**, pp427–442.

Kessler, L.G. and Moorhouse, K. 1984. Depositional processes and fluid mechanics of upper Jurassic conglomerate accumulations, British North Sea. In: Koster, E.H. and Steel, R.J. (eds) *Sedimentology of gravels and conglomerates. Canadian Society of Petroleum Geologists Memoir* **10**, 383-398.

Kiessling, W., Flügel, E., Golonka, J., 1999. Paleoreef maps: a comprehensive database of Phanerozoic reefs with graphic presentations. *AAPG Bulletin* **83**, pp1552–1587.

Kiessling, W., Flügel, E., Golonka, J., 2003. Patterns of Phanerozoic carbonate platform sedimentation. *Lethaia* **36 (3)**, pp195-225.

Krause, F. F. and Oldershaw, A. E., 1979. Submarine carbonate breccia beds-a depositional model for two-layer, sediment gravity flows from the Sekwi Formation (Lower Cambrian), Mackenzie Mountains, Northwest Territories, Canada. *Canadian Journal of Earth Sciences*, **16**, 189-199.

Kutzbach, J. E., and Gallimore, R. G., 1989. Pangaeen climates: megamonsoons of the megacontinent. *Journal of Geophysical Research*. **94**, pp3341-3357

Kutzbach, J. E., Guetter, P. J., Washington, W. M., 1990. Simulated circulation of an idealized ocean for Pangaeen time. *Palaeoceanography* **5**, pp299-317.

Kuvaas, B., Kristoffersen, Y. K. Guseva, J., Leitchenkov, G., Løvås, O., Sand, M. and Brekke, H. 2005. Interplay of turbidite and contourite deposition along the Cosmonaut Sea/Enderby Land margin, East Antarctica. *Marine Geology* **217**, pp143–159.

Lagabrielle, Y., Polino, R., Auzende, J. –M., Blanchet, R., Caby, R., Fudral, S., Lemoine, M., Mevel, C., Ohnenstetter, M., Robert, D., Tricart, P., 1984. Les témoins d’une tectonique intra-océanique dans le domaine téthysien: analyse des rapports entre les ophiolites et leur converture métasédimentaire dans la zone piémontaise des Alpes franco-italiennes. *Ofioliti* **9** p67-88

Laubscher, E., Bernoulli, D., 1977. Mediterranean and Tethys. In: Nairn, A. E. M., Kanes, W. H., Stethi, F. G., (eds.) *The Ocean Basins and Margins*. **4A** Plenum Press, New York pp1-28

Leeder, M. R., 1982. Upper Palaeozoic basins of the British Isles-Caledonide inheritance versus Hercynian plate margin processes. *Journal of the Geological Society, London* **139**, p479-491

Leinfelder, R.R., Schmid, D.U., Nose, M. & Werner, W. 2002. Jurassic reef patterns - The expression of a changing globe. In: Flügel, E., Kiessling W. & Golonka, J. (eds), *Phanerozoic Reef Patterns, SEPM Special Publication*. **72**, pp. 465-520.

Lemoine, M., Tricart, P., Boillot, G., 1987. Ultramafic and gabbroic ocean floor of the Ligurian Tethys (Alps, Corsica, Apennines): in search of a genetic model. *Geology*, **15**, 622–625.

Lima, A. F., Faugeres, J. C., Machiques, M. 2009. The Oligocene-Neogene deep-sea Columbia Channle system in the South Brazilian Basin: Seismic stratigraphy and environmental changes. *Marine Geology* **266** (1-4) pp18-41

Linares, A., Vera, J. A., 1966. Precisiones estratigráficas sobre in serie mesozoíca de Sierra Gorda, Cordilleras Béticas (provincial de Granada). *Estudios geológicos* **XII** p65-99,

- Llave, E., Hernández-Molina, F.J., Somoza, L., Díaz-del-Río, V., Stow, D.A.V., Maestro, A. and Alveirinho Dias, J.M. (2001) Seismic stacking pattern of the Faro-Albufeira contourite system (Gulf of Cadiz): a Quaternary record of paleoceanographic and tectonic influences. *Marine Geophysical Researches*, **22** (5-6), p487-508.
- Lovell, J.P.B. and Stow, D. A. V., (1981) Identification of ancient sandy contourites, *Geology* **9**, pp 347–349.
- Lowe, D. R., 1976. Grain flow and grain flow deposits. *Journal of Sedimentary Research* **46**(1) p188-199
- Lowe, D. R., and Guy M., 2000. Slurry-flow deposits in the Britannia Formation (Lower Cretaceous), North Sea: a new perspective on the turbidity current and debris flow problem, *Sedimentology* **47**, p31–70.
- Lowe, D.R., 1982. Sediment gravity flows: II. Depositional models with special reference to the deposits of high-density turbidity currents, *Journal of Sedimentary Petrology* **52**, p279–297.
- Lucia, F. J., 2007. *Carbonate Reservoir Characterization. An Integrated Approach*. 2nd ed. Springer-Verlag, Berlin.
- Maliva, R. G., Siever, R., 1989. Nodular chert formation in carbonate rocks. *Journal of Geology* **97** (4) p421-433
- Mamet, B., and Préat,., 2006. Jurassic microfacies, Rosso Ammonitico limestone, Subbetic cordillera, Spain. *Revista Española de Micropaleontología*, **38**(2-3), p219-228
- Marchès. E., Mulder, T., Gonthier, E., Cremer, Hanquiez. V., Garlan, T., Lecroart. P. 2010 Perched lobe formation in the Gulf of Cadiz: Interactions between gravity processes and contour currents (Algarve Margin, Southern Portugal). *Sedimentary Geology* **229** (3-1) p81-94.
- Martin-Rojas, R. Somma, F. Delgado, A. Estévez, A. Iannace, Perrone, V. and Zamparelli, V. 2009. Triassic continental rifting of Pangaea: direct evidence from the Alpujarride carbonates, Betic Cordillera, SE Spain. *Journal of the Geological Society*. **166**, p447-458
- Marzoli, A., H. Bertrand, K.B. Knight, S. Cirilli, N. Buratti, C. Vérati, S. Nomade, P.R. Renne, N. Youbi, R. Martini, K. Allenbach, R. Neuwerth, C. Rapaille, L. Zaninetti, G. Bellieni, 2004, Synchrony of the Central Atlantic magmatic province and the Triassic-Jurassic boundary climatic and biotic crisis. *Geology*, **32** (11) p 973–976.
- Marzoli, A., Renne, P. R., Piccirillo, E, M., Ernesto, M., Bellieni, G., and Min, A, D., 1999. Extensive 200-Million-Year-Old Continental Flood Basalts of the Central Atlantic Magmatic Province. *Science*, **284**, p616-618.
- Mazzullo, L. J., 1987, Stratigraphy of the Bone Spring Formation (Leonardian) and depositional setting in the Scharb Field, Lea County, New Mexico. *Society of Economic Paleontologists and Mineralogists* **87** (27), p. 107-111.
- McCaffrey, W., and Kneller, B. C., 2001. Process controls on the development of stratigraphic trap potential on the margins of confined turbidite systems and aids to reservoir evaluation, *Bulletin of the American Association of Petroleum Geologists* **85**, pp. 971–988.

- McDonnell, A., and Shannon, P. M. 2001 Comparative Tertiary stratigraphic evolution of the Porcupine and Rockall Basins. *In*: P.M. Shannon, P.D.W. Haughton and D.V. Corcoran, Editors, *The Petroleum Exploration of Ireland's Offshore Basins*, Geological Society, London, Special Publication **188** p323–344.
- Meischner, D. (1964): Allodapische Kalke, Turbidite in riffnahen Sedimentations-Becken. - *In*: Bouma, A.H. and Brouwer, A. (eds.): *Turbidites*. Developments in Sedimentology, **3**, 156-191, Amsterdam
- Melim, L. A., and Scholle, P. A., 1995. The foreereef facies of the Permian Capitan Formation: the role of sediment supply versus sea-level changes. *Journal of Sedimentary Research*. **B65** p 107-118
- Melim, LA, Anselmetti, FS, Eberli, GP 2001 The importance of pore type on permeability of Neogene carbonates, Great Bahama Bank, In Ginsburg, RN (ed) *Subsurface geology of a prograding carbonate platform margin, Great Bahama Bank: Results of the Bahamas drilling project*. SEPM Special Publication **70** p217-240
- Metcalf, I. 1994. Gondwanaland dispersion, Asian accretion and evolution of Eastern Tethys (abs.). 12th Australian Geological Convention, Perth, 1994, *Geological Society of Australia*, **37**, p287.
- Michard, A., Chalouan, A., Feinberg, H., Goffe, B., and Montigny, R. 2002 How does the Alpine belt end between Spain and Morocco? *Bulletin of the Geological Society of France*. **173** (1), 3-15
- Michels, K. H. Kuhn, G. Hillenbrand, C.-D. Diekmann, B. Futterer, D. K. Grobe H. and Uenzelmannneben, G., 2002. The southern Weddell Sea: combined contourite-turbidite sedimentation at the south eastern margin of the Weddell Gyre. *In*: Stow, D. A. V., Pudsey, C. J., Howe, J. A., Faugères, J.-C. & Viana, A. R. (eds) *Deep-Water Contourite Systems: Modern Drifts and Ancient Series, Seismic and Sedimentary Characteristics*. Geological Society, London, Memoirs, **22**, 289-303.
- Michels, K. H., Rogenhagen, J and Kuhn, G., 2001. Recognition of contour-current influence in mixed contourite-turbidite sequences of the Western Weddell Sea, Antarctica. *Marine Geophysics Researches* **22** p465-485
- Middleton, G. V., and Neal, W> J., 1989. Experiments on the thickness of beds deposited by turbidity currents. *Journal of Sedimentary Petrology* **59**, 297-307
- Minero, C. J., 1991. Sedimentation and diagenesis along open and island-protected windward carbonate platform margins of the Cretaceous El Abra Formation, Mexico, *Sedimentary Geology*. **71** (3–4), p261-288
- Moore, C. H., 2001. Carbonate Reservoirs: Porosity Evolution and Diagenesis in a Sequence Stratigraphic Framework. Elsevier pp 444
- Moore, E.M., Fairbridge, R.W. (eds.), 1998: *Encyclopedia of European and Asian Regional Geology*. Encyclopedia of Earth Sciences Series, London, p. 825
- Morata, D., 1993. Petrología y geoquímica de las ofitas de las Zonas Externas de las Cordilleras Béticas. PhD Thesis, University of Granada.

- Moshier, S. O., 1989. Development of microporosity in a micritic limestone reservoir, Lower Cretaceous, Middle East. *Sedimentary Geology* **63** (3-4) p217-240
- Mulder, T., and Alexander, J., 2001. The physical character of subaqueous sedimentary density flows and their deposits, *Sedimentology* **48**, p269–299.
- Mullins, H. T, Heath, K. C., Van Buren, H. M., and Newton, C. R., 1984. Anatomy of a modern open-ocean carbonate slope: Northern Little Bahama Bank. *Sedimentology*. **31** p141-168
- Mullins, H. T., and Cook, H. E., 1986. Carbonate apron models: Alternatives to the submarine fan model for palaeoenvironmental analysis and hydrocarbon exploration. *Sedimentary Geology*. **48** p37-79
- Navarro, V., Molina, J. M., Ruiz-Ortiz, P. S., 2009. Filament lumachelle on top of Middle Jurassic oolite limestones: event deposits marking the drowning of a Tethysian carbonate platform (Subbetic, southern Spain). *Facies*, **55** p89-102
- Nelson, C. H., and Baraza, J., and Maldonado, A., 1993. Mediterranean undercurrent sandy contourites, Gulf of Cadiz, Spain. *Sedimentary Geology*. **82** (1-4) p103-131
- Nelson, C.H. Twichell, D.C. Schwab, W.C. Lee H.J. and Kenyon, N.H. 1992. Late Pleistocene turbidite sand beds and chaotic silt beds in the channelized distal outer fan lobes of Mississippi Fan, *Geology* **20**, p 693–696.
- Noda, A., and Toshimitsu, S. 2009. Backward stacking of submarine channel-fan successions controlled by strike-slip faulting: The Izumi Group (Cretaceous), southwest Japan. *Lithosphere* **1**(1) p 41-59
- Olivero, D., and Gaillard, C., 1996. Palaeoecology of Jurassic *Zoophycos* from south-eastern France. *Ichnos*, **4**, p249-260
- Olóriz, F. 2000. Time averaging and long-term palaeoecology in macroinvertebrate fossil assemblages with ammonites (Upper Jurassic). *Revue de Paléobiologie*, Volume Spécial **8** p123-140.
- Olsen, P. E. 1997. Stratigraphic record of the early Mesozoic breakup of Pangea in the Laurasia-Gondwana rift system. *Annual Reviews of Earth and Planetary Science* **25**, p. 337-401
- Osete, M. L., Villalaín, J. J., Osete, C and Gialanella, P. R., 2000. Evolución de Iberia durante el Jurásico a partir de datos paleomagnéticos. *Geotemas*. **1**, 116-119.
- Pacht, J. A., Brooks, L., Messa, F., 1995, Stratigraphic analysis of 3D and 2D seismic data delineate porous carbonate debris flows in Permian strata along the northwestern and eastern margins of the Midland Basin. In: Martin, R. L., ed., *In search of new Permian Oil and Gas Fields: using today's technologies and tomorrow's ideas for Exploration, Development and 3D Seismic in a Mature Basin*. WTGS Special Publication (95-98) p111-132
- Pálfi, J., Mortensen, J. K., Carter, E. S., Smith, P., L., Friedman, R. M., and Topper, H., W. 2000. Timing the end-Triassic mass extinction: First on land, then in the sea? *Geology* **28**(1) 39-42

- Parrish, J.T., Curtis, R.L., 1982. Atmospheric circulation, upwelling and organic rich rocks in the Mesozoic and Cenozoic eras. *Palaeogeography, Palaeoclimatology, Palaeoecology* **40**, 31–66.
- Patacca, E., Scandone, P., Giunta, G., Liguori, V. 1979. Mesozoic paleotectonic evolution of the Ragusa zone (Southeastern Sicily). *Geologica Romana*, **18** 331-369.
- Payros, A., Pujalte, V., Orue-Etxebarria, X., 2007. A point-sourced calciclastic submarine fan complex (Eocene Anotz Formation, western Pyrenees): facies, architecture, evolution and controlling factors. *Sedimentology* **54**, 137-168
- Phelps, R. M., and Kerans, C. 2007. Architectural characterisation and three-dimensional modelling of a carbonate channel-levee complex: Permian San-Andres Formation, Last Chance Canyon, New Mexico, USA. *Journal of Sedimentary Research*. **77** (11-12) pp 939-964
- Piccardo, G. B. & VISSERS, R. L. M. 2007. The preoceanic evolution of the Erro–Tobbio peridotites (Voltri Massif—Ligurian Alps, Italy). *Journal of Geodynamics* **43**, 417–449.
- Piccardo, G. B. 2006. The pre–oceanic evolution of the Jurassic Ligurian Tethys: a fossil slow/ultra-slow spreading ocean: the mantle perspective. EOS Transactions, American Geophysical Union, Fall Meeting Supplement, abstract.
- Piccardo, G. B., 2008. *The Jurassic Ligurian Tethys, a fossil ultraslow-spreading ocean: the mantle perspective*. Geological Society, London, *Special Publications*. **293**, 11-34
- Pickering, K.T., Hiscott, R.N., Hein, F.J., 1989. *Deep Marine Environments: Clastic Sedimentation and Tectonics*. Unwin Hyman Ltd, London, 416 pp.
- Pierson, T. C., and Costa, J. E., 1987. A rheologic classification of subaerial sediment-water flows. In: Costa, J. E., and Wieczorek, G. F. (eds.) *Debris Flows/Avalanches: Processes, Recognition and Mitigation*. Geological Society of America Reviews Engineering Geology, **7**, 1-12
- Playton, T., E., 2008. Characterization, Variations, and Controls of Reef-rimmed Carbonate Foreslopes. PhD Thesis, University of Texas at Austin p.302
- Plummer, L.N., Vacher, H.L., Mackenzie, F.T., Bricker, O.P., and Land, L.S., 1976, hydrogeochemistry of Bermuda: a case history of groundwater diagenesis of biocalcarenes. *Geological Society of America Bulletin*, **87**, p.1301-1316.
- Posamentier, H. W., and Vail, P. R, 1988. Eustatic controls on clastic deposition II- sequence and systems tract models. In: Wilgus, C. K., Hastings, B. S, Kendall, C. G. St. C, Posamentier, H. W., Van Wagoner, J. C (eds.) *Sea Level Changes: An Integrated Approach*. SEPM Special Publication **42** pp 125-154
- Pudsey, C. J., 2002. The Weddell Sea: contourites and hemipelagites at the northern margin of the Weddell Gyre. In: Stow, D. A. V., Pudsey, C. J., Howe, J. A., Faugères, J.-C. & Viana, A. R. (eds) 2002. *Deep-Water Contourite Systems: Modern Drifts and Ancient Series, Seismic and Sedimentary Characteristics*. Geological Society, London, *Memoirs*, **22**, 289-303.

- Puga, E., 1980. Hypothèses sur la genèse des magmatismes calcoalcalins, intraorogéniques et postorogéniques alpins dans les Cordillères Bétiques. *Bulletin de la Société Géologique de France* **22** p243-250
- Puga, E., Díaz de Federico, A., Demant, A., 1995. The eclogitized pillows of the Betic Ophiolitic Association: relics of the Tethys Ocean floor incorporated in the Alpine chain after subduction. *Terra Nova* **14** p1-188
- Puga, E., Díaz de Federico, A., Molina-Palma, J. F., Nieto, J. M and Tendero-Segovia, J. A., 1993. Field trip to the Nevado-Filabride Complex (Betic Cordilleras, SE Spain). *Ofioliti*, **18**(1), 37-60.
- Racki, G and Cordey, F., 2000. Radiolarian palaeoecology and radiolarites: is the present the key to the past? *Earth-Science Reviews*. **52**(1-3) p83-120
- Rasmussen, S. Lykke-Andersen, H. Kuijpers, A. and Troelstra, S. R. 2003. Post-Miocene sedimentation at the continental rise of Southeast Greenland: the interplay between turbidity and contour currents. *Marine Geology* **196**, pp. 37–52.
- Reading, H. G. (1996). *Sedimentary Environments and Facies*. Blackwell Scientific Publications.
- Reading, H. G., & Richards, M. (1994). Turbidite systems in deep-water basin margins classified by grain size and feeder system. *AAPG Bulletin*, **78**, 792-822
- Rebesco, M., Larter, R. D., Camerlenghi, A., Barker, P. F., 1996. Giant sediment drifts on the continental rise west of the Antarctic Peninsula. *Geo-Marine Letters*, **16**, p65-75
- Rebesco, M., Pudsey, C., Canals, M., Camerlenghi, A., Barker, P., Estrada, F., Giorgetti, A., 2002. Sediment drift and deep-sea channel systems, Antarctic Peninsula Pacific Margin *In: Stow, D. A. V., Pudsey, C. J., Howe, J. A., Faugères, J. C., Viana, A. R. (eds) Deep-water Contourite Systems: Modern Drifts and Ancient Series, Seismic and Sedimentary Characteristics*. Geological Society, London, Memoirs, **22**, p353-371
- Rebesco, M., Larter, R. D., Barker, P. F., Camerlenghi, A., Vanneste, L. E., 1997. The history of sedimentation on the continental rise west of the west of the Antarctic Peninsula. *In: Cooper, A. K., and Barker, P. F. (eds) Geology and Seismic Stratigraphy of the Antarctic Margin 2*. American Geophysical Union, Antarctic Research Series, **71**, p29-50
- Reijmer, J. J. G., and Andresen, N. 2007. Mineralogy and grain size variations along two carbonate margin-to-basin transects (Pedro Bank, North Nicaragua Rise). *Sedimentary Geology*, **198** p327-350
- Richter, D. K., Götze, Th., Götze, J., Neuser, R. D. 2003. Progress in application of cathodoluminescence (CL) in sedimentary petrology. *Mineralogy and Petrology* **79** 127-166
- Ríos, J., M. The Mediterranean coast of Spain and the Alboran Sea. *In: Nairn, A. E. M., Kanes, W. H., and Stehli, F., G. (eds.) 1978. The Ocean Basins and Margins Volume 4B Plenum Press, London pp. 447*
- Rivas, P., 1975. Calizas de Wlamentos en el Lias Medio de la Zona Subbética. *Cuad Geol* **6** p137–142

- Rivas, P., Aguirre, J., Braga, J. C., 1997. Entolium beds: Hiatal shell concentrations in starved pelagic settings (Middle Liassic, SE Spain). *Eclogae Geol Helv* **90** p293–301
- Rooji, D., V. Iglesias, J. Hernández-Molina, F. J., Ercila, G. Gomez-Ballesteros, M., Casas, D., Llave, E., De Hauwere, A., Garcia-Gil, S., Acosta, J., Henriët, J. –P. 2010. The Le Danois contourite depositional system: Interactions between the Mediterranean Outflow Water and the upper Cantabrian slope (North Iberian margin). *Marine Geology*. **274** pp. 1-20
- Ruiz-Ortiz, P. A., 1983. A carbonate submarine fan in a fault controlled basin of the Upper Jurassic, Betic Cordillera, southern Spain. *Sedimentology*, **30**(1) p33-48
- Sàbat, F., 1986. Estructura geològica de les Serres de Llevant de Mallorca (Balears). PhD Thesis p128
- Sàbat, F., Muñoz, J. A., Santanach, P., 1988. Transversal and oblique structures at the Serres de Llevant thrust belt (Mallorca Island). *Geologische Rundschau*, **77**, 529-538
- Salles, T. Marches, E. Dyt, C. Griffiths, C. Hanquiez, V. Mulder, T. 2010. Simulation of the interactions between gravity processes and contour currents on the Algarve Margin (South Portugal) using the stratigraphic forward model Sedsim. *Sedimentary Geology* **229**(3) pp. 95-109
- Sami, R., Mohamed Soussi, Boukhalfa Kamel, Ben Ismail Lattrache Kmar, Dorrik Stow, Khomsi Sami, Bedir Mourad, 2010. Stratigraphy, sedimentology and structure of the Numidian Flysch thrust belt in northern Tunisia, *Journal of African Earth Sciences*, **57**(1-2), p109-126
- Sander, N. J., 1970. Structural Evolution of the Mediterranean Region during the Mesozoic Era. *In*: Sonnenfeld, P., (ed.) 1981. *Tethys*. Benchmark Papers in Geology **53** p100-189
- Sanders, J. E., 1965. Primary sedimentary structures formed by turbidity currents and related resedimentation mechanisms. *In*: Middleton, G. V. (ed) *Primary sedimentary structures and their hydrodynamic interpretation*. Special publication of the Society of Economic Palaeontologists and Mineralogists **12**, p192-217
- Sandoval, J., 1994. The Bajocian stage in the Island of Mallorca: Biostratigraphy and ammonite assemblages. *Miscellanea del Servizio Geológico Nazionale* **5** p203-215
- Savary, B., 2005. Calcareous turbidity current emplacement as an initiation mechanism for substrate brecciation and deformation. *In*: Hodgson, D. M., Flint, S. S (eds.) *Submarine Slope Systems: Processes and Products*. Geological Society of London Special Publication **244** pp207-220
- Schlager, W. and Chermak, A., 1979, Sediment facies of platform-basin transition, Tongue of the Ocean, Bahamas, in, Doyle, L.J. and Pilkey, O.H., eds., *Geology of continental slopes*. *Society of Economic Paleontologists and Mineralogists Special Publication* **27**, p. 193-208.
- Schlager, W., 1991. Depositional bias and environmental change-important factors in sequence stratigraphy. *Sedimentary Geology*. **70** p109-130
- Schlager, W., Reijmer, J. J. G., Droxler, A. 1994. Highstand shedding of carbonate platforms. *Journal of Sedimentary Research*. **64** p. 270-281

Schmoker JW, Halley RB 1982 Carbonate porosity versus depth: a predictable relation for south Florida. *AAPG Bulletin* **66**(12) p2561-2570

Scholle, P. A., 1971. Diagenesis of deep-water carbonate turbidites, Upper Cretaceous Monte Antola Flysch, Northern Apennines, Italy. *Journal of Sedimentary Petrology* **41**(1) p233-250

Schwab, W.C. Lee, H.J. Twitchell, D.C. Locat, J. Nelson, C.H. McArthur W.G. and Kenyon, N.H., 1996. Sediment mass-flow processes on a depositional lobe, outer Mississippi Fan, *Journal of Sedimentary Research* **66**, p916–927.

Scotese, C. R., 2002. Plate Tectonic animation, Jurassic to Quaternary. <http://www.scotese.com>

Scotese, C.R., and Summerhayes, 1986. A computer model of paleoclimate to predict upwelling in the Mesozoic and Cenozoic. *Geobyte*, **1** p28-42.

Scotese, R., 1994, Phanerozoic paleogeographic and paleoclimatic modeling maps. In: Embry, A. F., Beauchamp, B. & Glass, D. J., (eds.), *Pangea: Global environment and resources*. Canadian Society of Petroleum Geologists, Publication **95-98** p83–86.

Seilacher, A., 2007. *Trace Fossil Analysis*. Springer pp 226.

Sengör, A. M. C. & Natalin, B. A. 1996. Palaeotectonics of Asia: fragments of a synthesis. In: Yin, A. & Harrison, M. (eds) *The Tectonic Evolution of Asia*, Cambridge University Press, 443–486.

Sengör, A. M. C. 1984. The Cimmeride Orogenic System and the Tectonics of Eurasia, Special Paper, **195**, Geological Society of America

Sengör, A.M.C., Natalin, B.A., 1996. Paleotectonics of Asia: fragment of a synthesis. In: Yin, A., Harrison, T.M. (Eds.), *The Tectonic Evolution of Asia*. Cambridge University Press, Cambridge, pp. 486–640.

Smith, A. G., Briden, J. C., Drewry, G. F., 1973. Phanerozoic world maps. In: Huges, N. F. (ed), *Organisms and Continents Through Time*. Special Paper in Palaeontology, **12** p 1-39

Smith, J. A., Hillenbrand, C.-D., Pudsey, C. J., Allen, C. S and Graham, A. G. C., 2010. The presence of polynyas in the Weddell Sea during the Last Glacial Period with implications for the reconstruction of sea-ice limits and ice sheet history. *Earth and Planetary Science Letters*. **296** (3-4) p287-298

Solli, K.; Kuvaas, B.; Kristoffersen, Y.; Leitchenkov, G.; Guseva, J.; Gandjukhin, V., 2008. The Cosmonaut Sea wedge. *Marine Geophysical Researches* **29** (1) p51

Stampfli, G. M and Borel G. D., 2004. A plate tectonic model for the Paleozoic and Mesozoic constrained by dynamic plate boundaries and restored synthetic oceanic isochrones. *Earth and Planetary Science Letters*. **196** (1-2) 17-33.

Stampfli, G.M., Mosar, J., Favre, P., Pillevuit, A., Vannay, J.-C., 2001. Late Palaeozoic to Mesozoic evolution of the western Tethyan realm: the Neotethys – East Mediterranean basin connection. In: Ziegler, P.A., Cavazza, W., Robertson, A.H.F., Crasquin-Soleau, S. (Eds.), Peri-Tethys Memoir 6. *Peri-*

Tethyan Rift/ Wrench Basins and Passive Margins, **186**. Mémoires du Museum National d'Histoire Naturelle, Paris, pp. 51–108.

Stanley, S.M. (1999). *Earth System History*. New York: W.H. Freeman and Company. pp. 134.

Steiner, C. W., Hobson, A. Favre, P. Stampfli, G. M. & Hernandez, J. 1998. The Mesozoic sequence of Fuerteventura (Canary islands): witness of an Early to Middle Jurassic seafloor spreading in the Central Atlantic. *Geological Society of America Bulletin*, **110**, 1304–1317.

Steinhauff, D.M., 1989, Marine Cements. *In*: Walker, K.R. ed., The fabric of cements in Palaeozoic limestones; a short course workshop held at the Geological Society of America annual meeting, Studies in Geology (Knoxville), **20**, p.37-53.

Stow, D. A. V and Lovell, J. P. B. 1979. Contourites: Their recognition in modern and ancient sediments. *Earth Science Review*. 14 p251-291

Stow, D. A. V. 1979. Distinguishing between fine-grained turbidites and contourites on the Nova Scotian deepwater margin. *Sedimentology* **26**, pp. 371–387.

Stow, D. A. V., and Shanmugam, G., 1980. Sequence of structures in fine-grained turbidites: comparison of recent deep-sea and ancient Flysch sediments. *Sedimentary Geology*. **25**, p23-42

Stow, D. A. V., Pudsey, C. J., Howe, J. A., Faugères, J.-C. & Viana, A. R. (eds). 2002. *Deep-Water Contourite Systems: Modern Drifts and Ancient Series, Seismic and Sedimentary Characteristics*. Geological Society, London, Memoirs, **22**, 289-303.

Stow, D.A.V., 1994. Deep sea processes of sediment transport and deposition. *In*: Kenneth, P. (Ed.), *Sediment Transport and Depositional Processes*. Blackwell, Oxford, pp. 257–291.

Stow, D.A.V., Faugères, J.C. (Eds.), 1993. Contourites and Bottom Currents. *Sedimentary Geology*, **82** (spec. issue).

Stow, D.A.V., Faugères, J.C., Gonthier, E., 1986. Facies distribution and textural variation in Faro Drift contourites: velocity fluctuation and drift growth. *Marine Geology* **72**, 71-100.

Taft, W.H., 1963, *Cation influence on diagenesis of carbonate sediments* (abs.). *Geological Society of America Special Paper* **76**, p172.

Takahashi, T., 1981. Estimation of potential debris flows and their hazardous zones: Soft countermeasures for a disaster. *Natural disaster science* **3**(1) p57-89

Talling, J. A.U., Wynn, P. J., Schmitt, R.B., Rixon, D. N., Sumner, R., Amy, L, 2010. How did thin submarine debris flows carry boulder-sized intraclasts for remarkable distances across low gradients to the far reaches of the Mississippi fan? *Journal of Sedimentary Research* **80** (9-10) pp 829-851

Talling, P.J. Amy, L. A., Wynn, R. B., Peakall, J., and Robinson, M. 2004. Beds comprising debrite sandwiched within co-genetic turbidite: origin and widespread occurrence in distal depositional environments, *Sedimentology* **51**, pp. 163–194.

- Taylor, T. R., and Sibley, D. F., 1986. Petrographic and geochemical characteristics of dolomite types and the origin of ferroan dolomite in the Trenton Formation, Ordovician, Michigan Basin, U.S.A. *Sedimentology*, **33** (1) pp61-86
- Tribuzio, R., Thirlwall, M. F. & Vannucci, R. 2004. Origin of the gabbro–peridotite association from the Northern Apennine ophiolites (Italy). *Journal of Petrology*, **45**, 1109–1124.
- Ulmishek, G. F., 2007. Overview of the North Caspian basin. *In*: Yilmaz, P. O., Isaksen, G. H (eds) *Oil and Gas of the Greater Area*. AAPG Studies in Geology **55** p157
- Van der Voo, R., 1993. *Paleomagnetism of the Atlantic, Tethys and Iapetus*. Cambridge University Press, Cambridge.
- Vecsei, A., and Sanders, D. G. K., 1997. Sea-level highstand and lowstand shedding related to shelf margin aggradation and emersion, Upper Eocene-Oligocene of Maiella carbonate platform, Italy. *Sedimentary Geology* **112**(3-4) p219-234
- Vera, J. A. 1998. El Jurásico de la Cordillera Bética: Estado actual de conocimientos y problemas pendientes. *Cuadernos de Geología Ibérica*, **24**, 17-42
- Verdicchio, G., and Trincardi, F. 2007. Mediterranean shelf-edge muddy contourites: examples from the Gela and South Adriatic basins. *Geo Marine Letters* **28** pp137-151
- Verdicchio, G., and Trincardi, F. 2008. Mediterranean shelf-edge muddy contourites: examples from the Gela and South Adriatic basins. *Geo-Marine Letters*. **28**(3) pp 137-151
- Viana, A. Figueiredo, A., Faugeres, J. C., Lima, A., Gonthier, E., Brehme, I., and Zaragosi, S. 2003. The Sao Tome deep-sea turbidite system (southern Brazil Basin): Cenozoic seismic stratigraphy and sedimentary processes. *AAPG Bulletin* **87**(5) pp 873-894
- Viana, A. R., and Rebesco, M. (eds) *Economic and Palaeoceanographic Significance of Contourite Deposits*. Geological Society, London, Special Publication. **276**, p95-110
- Viana, A. R., Faugères, J. C., and Stow, D. A. V., 1998. Bottom-current-controlled sand deposits- a review of modern shallow- to deep-water environments. *Sedimentary Geology*. **115**, 53-80.
- Viana, A., R., 2001. Seismic expression of shallow to deep water contourites along the south eastern Brazilian margin. *Marine Geophysical Researches*, **22**(5) p509-521
- Vigorito, M., Murru, M., Simone, L., 2005. Anatomy of a submarine channel system and related fan in a foramol/rhodalg carbonate sedimentary setting: a case study from the Miocene syn-rift Sardinia Basin, Italy. *Sedimentary Geology*, **174**, p1-30
- Vissers, R. L. M., Drury, M. R., Hoogerduijn, E. H., Strating and D., Van Der Wal, D. 1991. Shear zones in the upper mantle: a case study in an Alpine Lherzolite massif. *Geology*, **19**, 990–993.
- Walker, J.D. & Geiss, J.W. (2009) 2009 GSA Geologic Time Scale. *GSA today* p60-61
- Weber, L., Francis, B. P., Harris, P. M., Clark, M. 2008. Stratigraphy, Lithofacies, and Reservoir Distribution-Tengiz Field, Kazakhstan. Poster AAPG Annual Convention May 11-14, 2003

- Weissert, H., 1994. Super Sedimentological Exposures: Southern Ticino, Switzerland: Geological archive of the evolution of the Mesozoic alpine Tethys Ocean. *IAS Newsletter* 194.
- Whalen, M.T., Eberli, G.P., van Buchem, F.S.P., and Mountjoy, E.W., 2000, Facies architecture of Upper Devonian carbonate platforms, Rocky Mountains, Canada, *In: Homewood, P.W., and Eberli, G.P., (eds) Genetic stratigraphy on the exploration and production scales - Case studies from the Pennsylvanian of the Paradox Basin and the Upper Devonian of Alberta*. Bulletin, Centre Recherche Elf Exploration-Production, **24**, p139-178.
- Wilson, M. E. J., 2002. Cenozoic carbonates in SE Asia: implications for equatorial carbonate development. *Sedimentary Geology* 14(3-4) p295-428
- Winland, H.D., 1968, The role of high Mg calcite in the preservation of micrite envelopes and textural features of aragonite sediments. *Journal of Sedimentary Petrology*, **38**, p.1320-1325.
- Withjack, M.O., Schlische, R.W., and Olsen, P.E., 1998, Diachronous rifting, drifting, and inversion on the passive margin of central eastern North America: An analog for other passive margins. *AAPG Bulletin* **82**, p. 817-835.
- Woodberry, K. E., Luther, M. E., O'Brien, J. J., 1989. The wind driven seasonal circulation in the southern tropical Indian Ocean. *JGR-Oceans*, **94**(C12) p17985-18002
- Wright, V.P., Wilson, R.C.L., 1984. A carbonate submarine fan sequence from the Jurassic of Portugal. *Journal of Sedimentary Petrology*, **54/2**, p394-412
- Zempolich, W. G. Cook, H. E. Zhemchuzhnikov V. G., 1995. Distribution of Reservoir Facies in Devonian and Carboniferous Carbonates of Southern Kazakhstan: The Roles of Early Cementation, Dolomitization and Meteoric Diagenetic Processes. AAPG Abstract, AAPG Annual Convention, Houston, Texas
- Ziegler, P. A., 1988b. Post-Hercynian plate reorganization in the Tethys and Arctic-North Atlantic Domains. *In: Manspeizer, W (ed.) Triassic-Jurassic Rifting. Continental Breakup and the Origin of the Atlantic Ocean and Passive Margins, Part B, III Related Mesozoic Atlantic Rift Basins, Western Europe*. Elsevier, Amsterdam, p711-756.
- Ziegler, P.A., 1988. Evolution of the Arctic– North Atlantic and the western Tethys. *American Association of Petroleum Geologists* **43** p198.
- Zielger, P. A., 1990. *Geological atlas of western and central Europe*. Shell Internationale Petroleum Maatschappij BV, International Lithosphere Program, **148** p239

APPENDIX A

A.1 PREPARATION TECHNIQUES AND OBSERVATION TECHNIQUES

A.1.1 PRODUCTION OF ACETATE PEELS AND THIN SECTIONS

Rock samples were cut perpendicular to bedding (when possible) and coarse saw marks were removed with 80 grade carborundum powder, followed by increasingly fine powders (200, 400, 600 and 1000). The final polished surface was cleaned with distilled-water and not touched.

Two staining solutions were prepared: Alizarin Red S (ARS) with a concentration of 0.2g per 100 ml of 1.5% HCl and Potassium Ferricyanide (PF) with a concentration of 2g per 100 ml of 1.5% HCl the two solutions were then mixed ARS:PF = 3:2.

Then a shallow tray was filled with 1.5% HCl, a second with the combined ARS:PF solution and a third with the ARS. The polished samples were first held in the HCl for 45 seconds, and then in ARS/PF solution for 60 seconds and then rinsed with distilled water. Finally, the polished samples were seconds and rinsed again with distilled water.

The samples were left to dry. Samples were positioned with the polished etched and stained surface upwards on sand and flooded with acetone. Immediately the flooded surface was covered with an acetate sheet. Samples were left to dry for 24 hours. The peel was then removed and labelled. The acetate was trimmed as close to the impression of the sample as possible to prevent crinkling.

A.1.2 CATHODOLUMINESCENCE

Many petrographic and diagenetic features are revealed by cathodoluminescence, whereas they often remain invisible using conventional transmitted light microscopy. The method of cathodoluminescence (CL) microscopy involves electron bombardment of an uncovered thin section or rock slab in an evacuated sample chamber. This results in emission of electromagnetic radiation including visible light, which is characteristic for the material being bombarded.

The luminescence characteristics of the carbonate mineral are controlled primarily by the relative abundances of manganese, REE and iron. The Mn^{2+} ion and some trivalent REE ions appear to be the most important activator ions of extrinsic CL where as Fe^{2+} is the principal quencher (e.g. Richter *et al.*, 2003).

The CL characteristics of calcite are noted in the literature as being most commonly extrinsic luminescence colours of orange-yellow, yellow-orange and orange. The Mn^{2+} ion appears to be the most important activator in calcite although some REE ions may also be activators. CL provides information on the spatial distribution of trace elements, particularly Fe^{2+} and Mn^{2+} , in calcite, dolomite and other grains and cements. CL was most useful at delineating dolomite crystals, the wide variety of calcite cements and early marine fringes on such allochems as *Posidonia* bivalves. Cathodoluminescence responses in the samples are poorly luminescent, indicating an incorporation of Fe^{2+} compared to Mn^{2+} .

Poor and non-luminescent responses are a product of more oxidising environments in which the reduced forms of both Mn and Fe are less available for incorporation into the crystal lattice of calcite and dolomite precipitated. Oxidized forms of these elements are not incorporated into calcite or dolomite crystals and therefore there is nothing in the crystals to excite luminescence a great deal. Bright luminescence is not found in this location but is associated with relatively high Fe/Mn trace elements ratios, typically achieved under reducing conditions during early to intermediate stages of burial diagenesis.

Appendix B

Thin Section Microfacies Descriptions

TABLE OF CONTENTS

APPENDIX B	1
THIN SECTION MICROFACIES DESCRIPTIONS.....	1
LOCATION C001	3
C001 170 CM.....	4
C001 375 CM.....	6
C001 515 CM.....	8
C001 560 CM.....	11
C001 625 CM.....	14
C001 1250 CM.....	17
C001 1450 CM.....	22
C001 1848 CM.....	25
C001 2150 CM.....	27
C001 2150CM	29
C001 2295 CM.....	31
C001 2300CM	33
C001 2350 CM.....	36
C001 2500CM	38
LOCATION C002	41
C002 320 CM.....	42
C002 350 CM.....	44
C002 480 CM.....	46
C002 480 CM.....	48
C002 520 CM.....	51
C002 530 CM.....	55
C002 550 CM.....	60
C002 555 CM.....	62
C002 610 CM.....	64
C002 650 CM.....	66
C002 675 CM.....	67

LOCATION C003 AND C003S.....	69
C003 20 cm.....	70
C003 125 cm.....	72
C003 250 cm.....	74
C003 590 cm.....	76
C003 600 cm.....	82
C003 860 cm.....	84
C003 1190cm	86
C003 1560 cm.....	88
C003 1615 cm.....	90
C003 2050 cm.....	92
C003 2125cm	94
C003 OOLITIC CHANNEL	96
C003s 1150 cm	99
POLISHED SLAB DESCRIPTIONS	102
C002 525cm	103
C002 550cm	105
C002 645cm	107
C003 150cm	108
C003 230cm	110
C003 350cm	111
C003 350cm	113
C003 1550cm	115
C003 1700	116
C003 1850cm	118
C003s 380cm.....	120
C003s 1350cm.....	121
<i>AMMONITICO ROSSO</i>	122

Location C001

OF C001 170 cm



C001-170cm			
Texture	Ooid peloid grainstone		
Description	<p>Ooid peloid grainstone that contains a poorly sorted assemblage of abundant rounded to sub-rounded, superficial and micritic ooids, peloids, aggregate grains and fine sand grade mud-wackestone clasts. That consist of an assemblage of silt sized bivalve fragments and rare radiolarians.</p> <p>Bioclasts consist of common biserial foraminifera, abraded gastropod fragments, disarticulated thin shelled bivalves that commonly occur in clasts and rare echinoderm fragments that commonly have calcite overgrowths. Almost all bioclasts have a micrite coating. The most common coating on these bioclasts are concentric and micritic. Ooids are commonly completely micritised showing very subtle internal structure however, there are several ooids that have a clear fibrous internal structure. There is an abundance of peloids and less frequently occurring aggregate grains that tend to contain two or more ooids that are cemented by micrite.</p> <p>Grain Sizes: Max. 1,500µm [Ooid 1,200µm] Mode. 300µm [Ooid 600µm] Min. 60µm [Ooid 300µm]</p>		
Palaeoenvironment Interpretation	The dominance of rounded micrite coated grains and broken and abraded bioclasts suggests these sediments were deposited in a moderate to high energy environment.		
Diagenesis	<p>Compaction is widely seen with all allochems touching. These contacts are commonly point, longitudinal, concavo-convex or sutured contacts. Allochems rarely show micro-fracturing within the grain, suggesting mechanical compaction was crushing the grains and that the grains were not soft during deposition. This sample is cementated by a drusy calcite spar that has occluded any remaining pore space.</p> <p>A patch of recrystallised calcite is found the bottom left of the section scan. This is filled by a coarse equant calcite spar with microspar regions showing the shapes of allochems in the surrounding sediment. The areas of microspar may be relic patches of microcrystalline cement.</p> <p>A thin (<30µm) wide fracture cuts across all grains in the thin section. This is filled by microspar calcite.</p>		
Pore types	Inter-crystal		
Reservoir quality	None-Poor		

OF C001 375 CM



C001-375			
Texture	<i>Posidonia</i> peloidal grainstone		
Description	<p>This is a well orientated <i>Posidonia</i> and peloidal grainstone showing obvious laminations. The <i>Posidonia</i> thin shelled bivalves dominate the thin section and are cemented by a coarse calcite spar overgrowth in addition some laminae consist of a dark brown-black micrite. There are occasional unidentified larger bivalves that have small calcite overgrowths. Accumulations of micro-peloids are found along occasional laminae.</p> <p>The <i>Posidonia</i> bivalves are typically 2.4 mm in length.</p>		
Palaeoenvironment Interpretation	<p>The strong orientation of allochems and overall lack of mud indicates that this sediment was probably deposited in a moderate to high energy environment where currents winnowed mud away from the accumulating bivalves. This may have been part of a <i>coquina</i> bank.</p>		
Diagenesis	<p>The <i>Posidonia</i> bivalves have been compacted and are broken and deformed along with peloids that have been deformed with long axis aligned to bedding planes. Calcite spar cement developed on the bivalves and peloids show a mottled appearance possibly due to micritisation.</p> <p>There are denticular stylolites that occur singularly and periodically widen exposing areas of fine calcite spar within the stylolites. These stylolites run parallel to the orientation of the <i>Posidonia</i> bivalves (and hence bedding) this is probably due to overburden pressure leading to chemical compaction.</p> <p>Thin 150 µm fractures vertical to bedding are discontinuous and show evidence of shearing suggesting these were created through shear stresses. The largest fracturing is observed as single sharp edged equant calcite filled 900µm wide fracture that cuts vertical to oblique to bedding (top right of the thin section scan).</p>		
Pore types	None		
Reservoir quality	None		

OF C001 515 cm

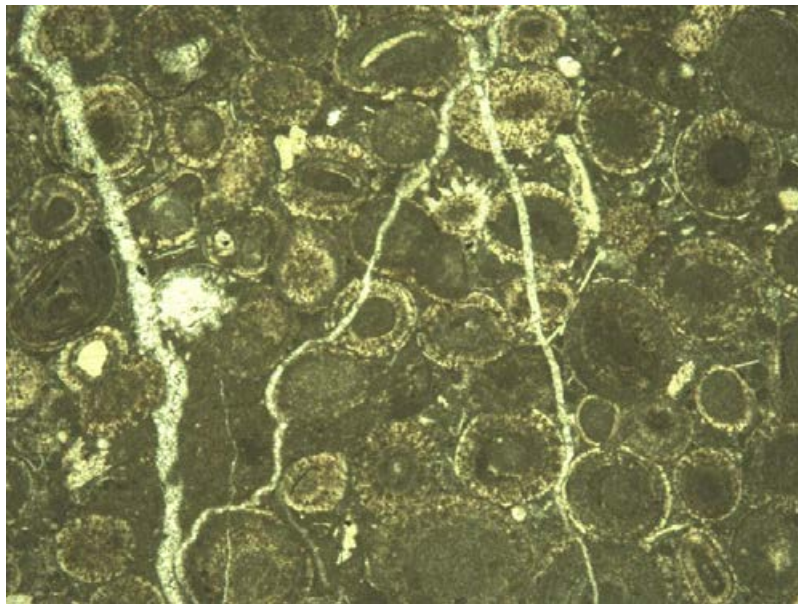


C001 515				
Texture	Dolomitised oolitic aggregate grainstone			
Description	<p>This is a bimodal poorly sorted assemblage of abundant very coarse sand to fine gravel sized deformed peloids, aggregate grains, mud-wackestone clasts and medium to coarse sand grade superficial ooids, echinoderm fragments, peloids and mudstone clasts.</p> <p>Bioclasts are rare and are poorly preserved; they are mainly found in aggregate grains and rarely as ooid nuclei but there is a common occurrence of coarse abraded echinoderm fragments. Only silt sized bivalve fragments are preserved within clasts. Ooids occur as a mixture of completely micritised to poorly developed ooids. The majority of allochems have been deformed but are rarely broken. Ooids comprise a light grey micritic centre and a darker laminate edge. There is an abundance of large peloids and less frequently occurring aggregate grains that tend to contain two to three ooids cemented by a micrite coat. These peloids and aggregate grains are often an order of magnitude large than the ooid matrix.</p> <p>Total grain sizes range: Max. 1,500 µm [Ooid 900 µm] Mode. 300 µm [Ooid 600 µm] Min. 60 µm [Ooid 300 µm]</p>			
Palaeoenvironment Interpretation	<p>The dominance of rounded coarse rounded peloids and finer superficial ooids and abraded bioclasts suggests these sediments were deposited in a moderate to high energy environment. The mixture of allochem types and sizes suggest this sample represents an allochthonous limestone with the larger peloidal component representing a higher energy of flow during transport.</p>			
Diagenesis	<p>Many of the grains are plastically deformed with point, longitudinal and concave-convex contacts being common. There are rare broken grains. Chemical compaction is evident through sutured contacts and evidence of dissolution of grains.</p> <p>Silica replacement occurs in two forms with chalcedony replacing grains nuclei and microcrystalline quartz replacing small quantities of calcite grains, particularly within patches associated with fracturing. Chalcedony often contains the ghost of what it has replaced and has a spherical replacive structure as the silica grew from a single point.</p> <p>The rock is cemented with a dusty equant calcite spar. Dolomite has replaced much of the original cement and selective parts of the replacive chalcedony with rhombic crystal invading from the chalcedony grains edge.</p> <p>Calcite veins cut across all grains and are seen in the bottom left of the thin section sample. These veins consist of equigranular calcite and contain breccias of the host rock.</p> <p>The second fractures form a conjugate set and have a calcite fill of equant calcite spar (and rare quartz) often lined with iron oxide. Patches of neomorphosed inequigranular replacive quartz and calcite occur throughout the sample. These patches are associated with thin fractures that cut across all allochems and the calcite veins. Dedolomitization (calcification), found in neomorphosed patches, where the outer edges of dolomite crystals are part filled by calcite whilst retaining a dolomite core occurring as a late diagenetic process. An iron oxide coats the calcified dolomites; this is likely due to the release of iron from ferroan dolomite during calcification.</p>			

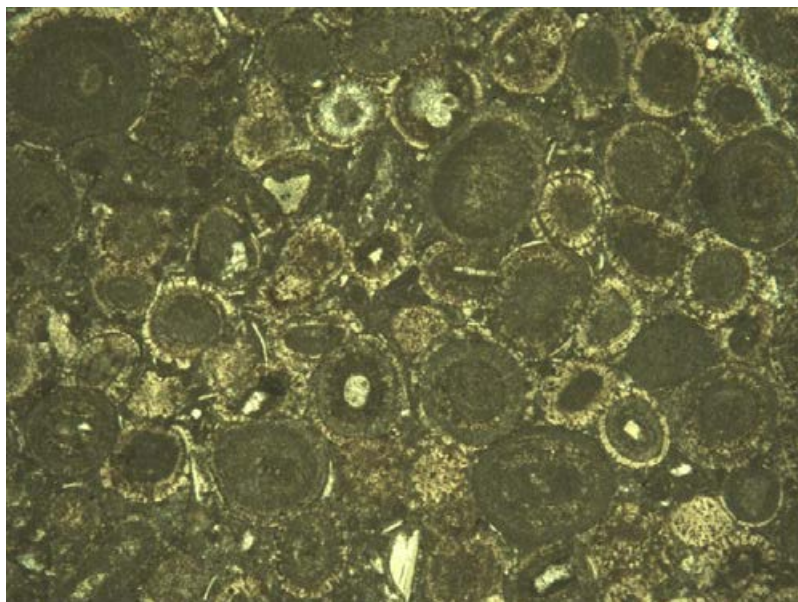
Pore types	None
Reservoir quality	None

OF C001 560 cm





Microphotograph 2 The abundance of different types of ooids suggests ooids of different maturity were incorporated into turbidites. FoV 2.89 x 2.15 mm.



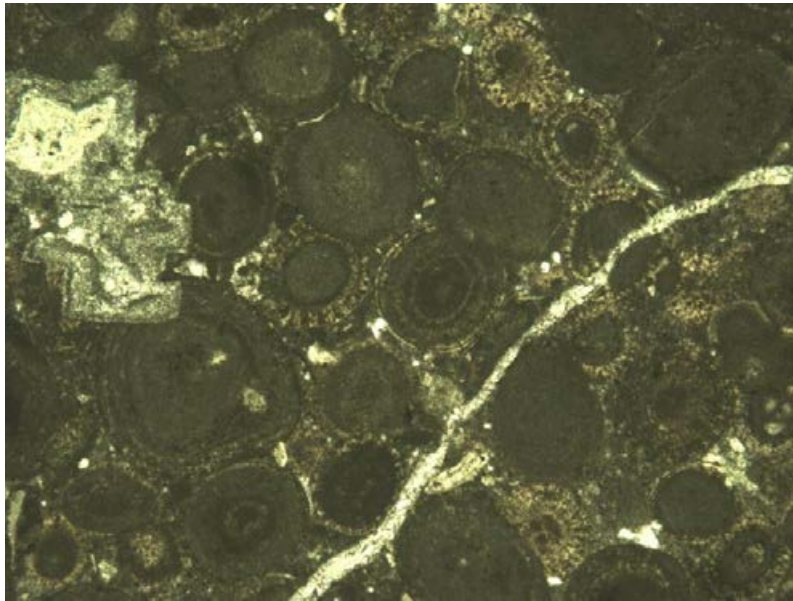
Microphotograph 1 Assemblage of grains, with superficial, micritic and fibrous ooid structures. Note the dominance of compaction as a diagenetic feature. FoV 2.89 x 2.15 mm.

C001 560cm			
Texture	Ooid pack-grainstone		
Description	<p>This shows a moderately well sorted assemblage of whole, broken and deformed superficial ooids and clearly defined ooids that are no more than 1 mm in diameter. Bioclasts are found most commonly as ooid nuclei or rarely as fine debris. Bioclasts that do occur are commonly well rounded grains of calcite, which are probably from abraded and disarticulated bivalves and brachiopods as, in addition there are very rare poorly preserved micrite coated ?uniserial foraminifera.</p> <p>The ooids in this sample show a variety of ooid types from 450µm mean diameter superficial ooids with clear thin radial-fibrous outer coating with a subtle micritic layered to structureless centre to 600µm mean diameter micritic ooids that range from largely coated micrite spheres with pervasive micritisation of the cortex to occurrences of subtle thinly laminated tangential cortices.</p>		
Palaeoenvironment Interpretation	<p>The mixture of ooid type, sizes, and thicknesses of the cortices, associated grains and abrasion of laminae is suggestive that the ooids are allochthonous ooids. Some ooids that have a clear structure have a thick micrite outer core; this may have been acquired during transport. The well defined ooid structures are characteristic of formation in quiet-water low turbulence environments (Flügel, 2004), this may possibly be due to ooids being transported from below the wave base or a lagoonal environment.</p>		
Diagenesis	<p>All allochems have been compacted leading to point contacts, sutured contacts and plastic deformation between allochems. Thin stress fractures run through cement and allochems. Chalcedony has replaced the centre of several of the larger grains and has an iron oxide coat. A microcrystalline calcite cements the rock. This micrite also contains micro-peloids and fine accumulations of calcite. Dolomites are rare throughout the sample but are found in patches associated with fractures.</p> <p>These neomorphosed patches contain calcified dolomites are scattered through the sample.</p> <p>The sample has two sets of thin irregular calcite filled fractures that cut across all allochems and features with some fractures moulding around harder grains. The thinner fracture set runs obliquely to thicker fractures.</p>		
Pore types	None		
Reservoir quality	None		

OF C001 625 cm



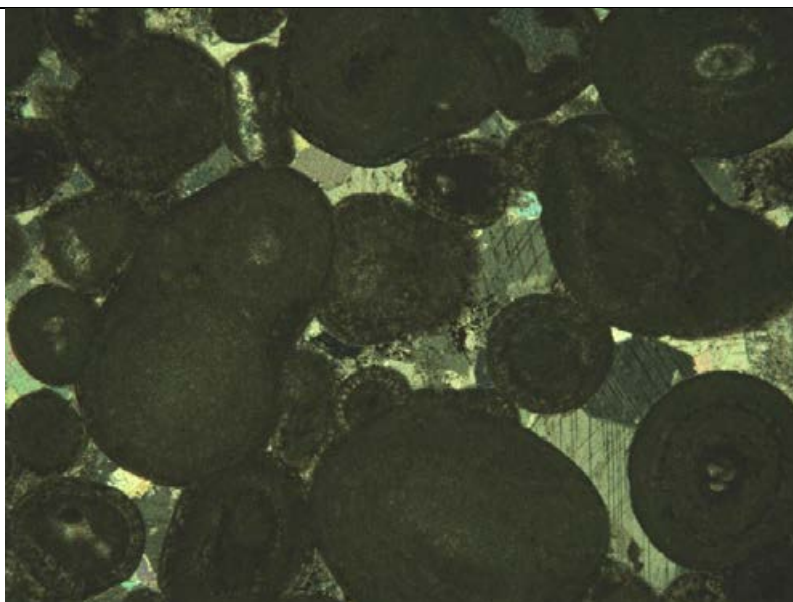
1 cm



Microphotograph 3. An assemblage of ooids in this section, with superficial, micritic and fibrous ooid structures visible. Note the neomorphosed patch of calcite that contains replacive microcrystalline quartz and calcite. FoV 2.89 x 2.15 mm.



Microphotograph 4. The nuclei of ooids can be varied. A microgastropod forming the nuclei of superficial ooid. Note microfractures cutting all allochems. FoV 1.16 x 0.86mm.

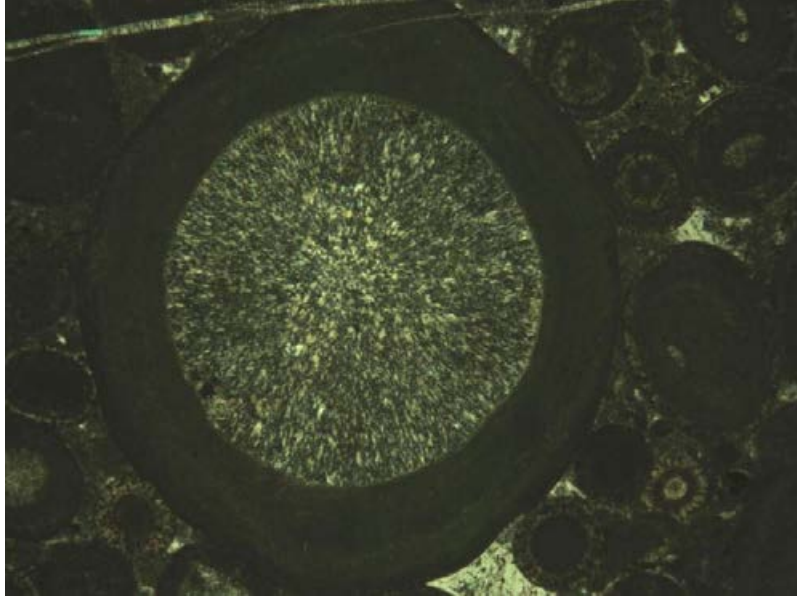


Microphotograph 5. A rare patch pore filling coarse equant calcite spar. FoV 2.89 x 2.15 mm.

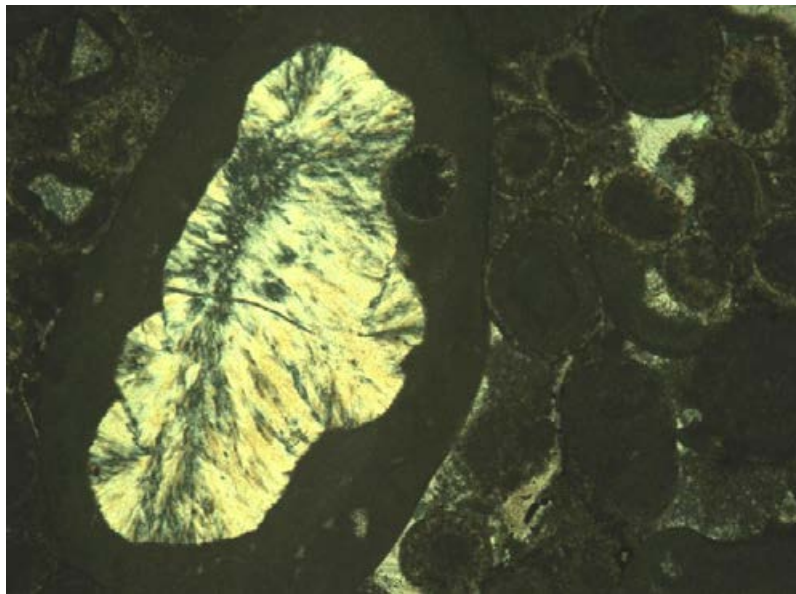
C001 625				
Texture	Dolomitised oolitic aggregate grainstone			
Description	<p>This is a poorly sorted bimodal pack-grainstone, which contains an assortment of plastically deformed to rare broken radial-fibrous ooids, superficial ooids, aggregate grains and much coarser micritic ooids (with a tangential fabric recognisable in peripheral parts) and coarse peloids.</p> <p>Bioclasts most frequently occur as ooid nuclei and include rare microgastropods, poorly preserved biserial foraminifera and other very rare fine rounded shelly fragments. Only echinoderm fragments are found as individual grains.</p>			
Palaeoenvironment Interpretation	The mixture of different ooid types and compaction features suggests this sediment was transported downslope in a turbidity flow.			
Diagenesis	<p>Grains within this sample are plastically deformed with point, longitudinal and concave-convex contacts being common. There are rare broken grains. Chemical compaction is evident through sutured contacts and evidence of dissolution of grains. The rock is cemented by locally common coarse calcite spar, which has occluding porosity. However, the majority of the rock cement is microcrystalline. Stylolites follow sutured grain contacts and cut through the cements but around micritic ooids and larger clasts. This stylolite is filled with iron oxide.</p> <p>Dolomitisation has replaced parts of recrystallised patches equant calcite spar. A scattering of anhedral rhombic crystals are found amongst the rock particularly close to fractures. A secondary ferroan dolomite has filled regions of previous dolomitisation; this is coated in iron oxide. Many calcite filled sharp edged fractures span the sample and cut across all allochems.</p> <p>Two fracture sets are observed in the sample. Thin calcite filled fracture are seen running parallel to bedding and likely represent compression fractures. Thick calcite veins cut across the sample vertical to bedding, they consist of equant calcite spar.</p>			
Pore types	None			
Reservoir quality	None			

OF C001 1250 CM

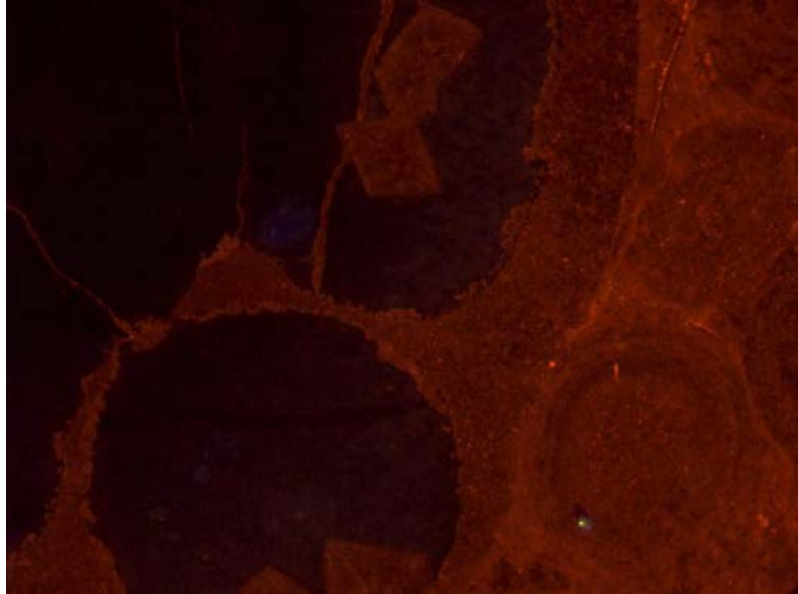




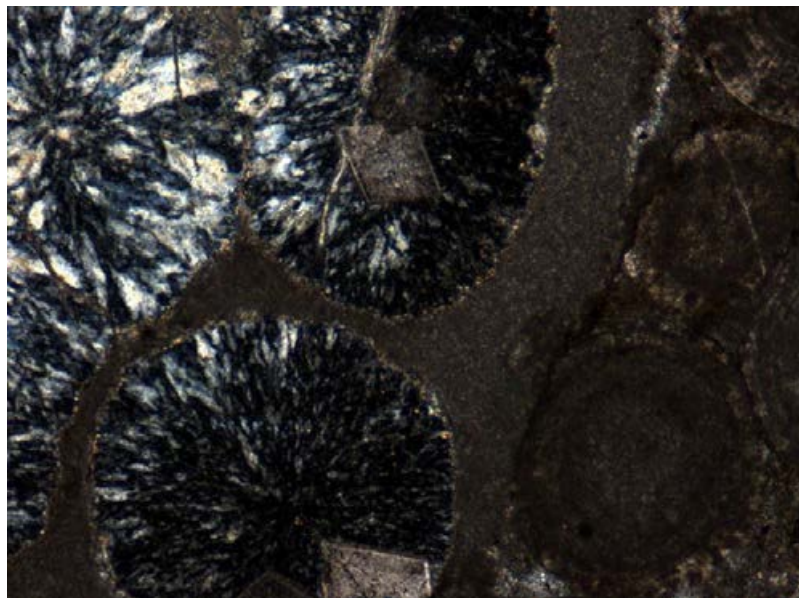
Microphotograph 6 Highly rounded coated chalcedony grain. FoV 2.89 x 2.15 mm.



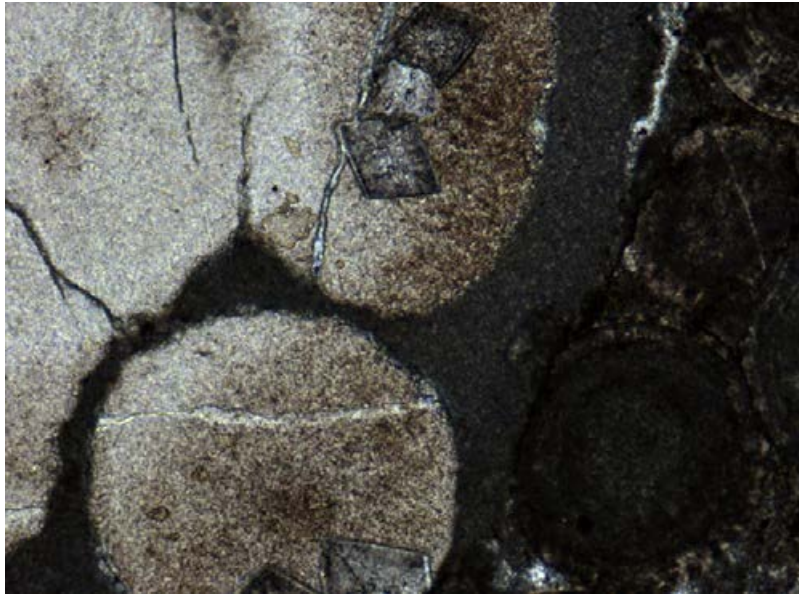
Microphotograph 7. Chalcedony only replaces large micritic grains, which were probably organic rich. Note the lack of compaction around large chalcedony grains. Smaller grains may have been protected from full compaction effects. FoV 2.89 x 2.15 mm.



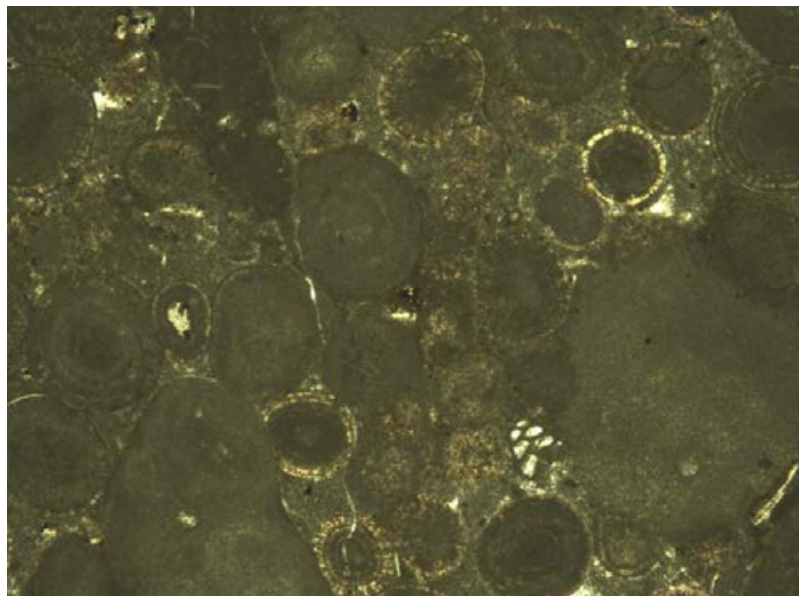
Microphotograph 8. CL detail of replacive chalcedony that have been dolomitised. Note the calcification of dolomite associated with fracturing. FoV 1.16 x 0.86mm.



Microphotograph 9. XPL of chalcedony detail. FoV 1.16 x 0.86mm.



Microphotograph 10. PPL of chalcedony detail. note the different fracture fill cements, which suggest changing stress over time. FoV 1.16 x 0.86mm.

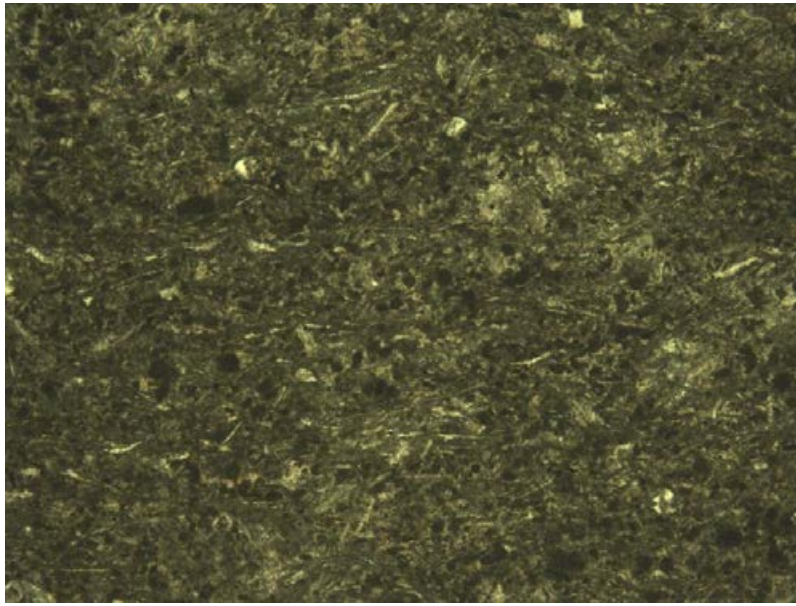


Microphotograph 11. PPL of over sized peloid characterise this section. Very coarse peloids and exoclasts dominate the sediment texture; however, the oolitic matrix keeps a constant grain size. FoV 2.89 x 2.15 mm.

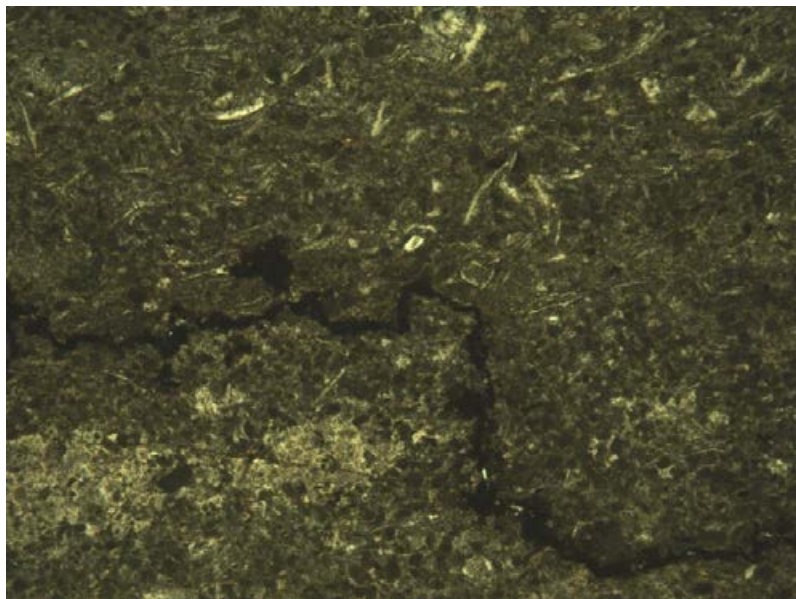
1250	C001			
Texture		Ooid aggregate grainstone		
Description		<p>This grainstone consists of a poorly sorted bimodal assemblage of medium to coarse sand grade plastically deformed to broken superficial ooids, radial-fibrous ooids and micritic ooids along with much coarser fine to medium gravel sized aggregate grains that commonly consist of two or more micritised ooids and wackestone clasts. A single subangular very fine sand grade detrital quartz grain is noted. Wackestone clasts consist of sparse bivalve fragments radiolarians and other silt particles that are rounded.</p> <p>Bioclasts rarely occur as ooid nuclei. Those that do occur in the sample include poorly preserved foraminifera, bivalves, and other very rare fine rounded shelly fragments.</p>		
Palaeoenvironment Interpretation		The mixture of different ooid types and compaction features suggests this sediment was transported downslope in a turbidity flow. The incorporation of detrital quartz suggests the proximity to shore.		
Diagenesis		<p>This sample was compacted as evidenced through the plastic deformities of ooids, sutured and point contacts to broken ooids. Chalcedony occurs in this sample in a spherical form, suggestive of radiolarians tests. It is of light brown colour in plane polarised light and carbonate crystals that have a rhombic shape are found amongst the chalcedony. An equant calcite spar occludes porosity and cements the rock. Dissolution seams and stylolites frequently cut through both cement and around allochems.</p> <p>Single calcite filled sharp edged fractures that span the sample and cut across all allochems.</p>		
Pore types		None		
Reservoir quality		None		

OF C001 1450 CM

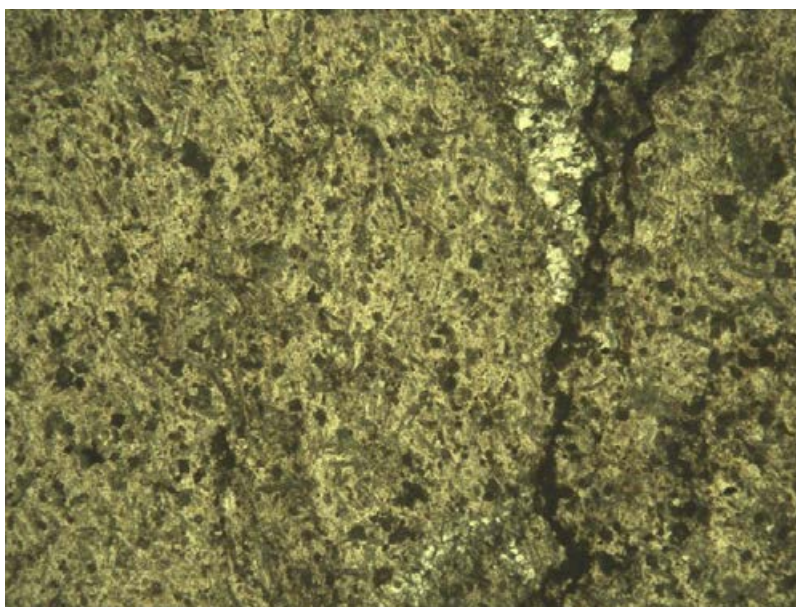




Microphotograph 13. Part of dissolution seam with patch of microcrystalline calcite cementing rocks components. Note the prevalence of micro-peloids compared to microphotography 16 and the less severe alignment of bioclast debris. FoV 2.89 x 2.15 mm.



Microphotograph 12. Orientated accumulations of thin shelled bivalves and other shell material. FoV 2.89 x 2.15 mm.



Microphotograph 14. Part of dissolution seam with calcite cement patch amongst strongly aligned allochems that are cemented by a microcrystalline calcite spar. FoV 2.89 x 2.15 mm.

C001 1450			
Facies	?Coquina		
Texture	Dolomitised <i>Posidonia</i> peloidal packstone		
Description	This is a well orientated <i>Posidonia</i> and peloidal packstone, which has patches of micrite rich and lighter areas which have less micrite. The sample includes abraded echinoderms and other fine shell fragments. <i>Posidonia</i> thin shelled bivalves are well orientated and found throughout the thin section with peloids commonly found between laminations. The <i>Posidonia</i> bivalves are typically 2.4 mm in length.		
Palaeoenvironment Interpretation	This sediment was probably deposited in a moderate energy environment where mud was winnowed out of parts of the rock whilst bivalves accumulated on top of each other. Peloids probably entered the sediment by high energy environments up slope.		
Diagenesis	The bivalves have been compacted since they are broken and crushed under weight. Stylolites follow the contacts between some bivalves. Dissolution seams cuts across the sample oblique-to-vertical to bedding. A scattering of replacement subhedral-euhedral dolomite crystals are found throughout the sample but are more densely populated in micritic areas and seem to preferentially replace peloids and other micritic regions. The dolomite crystals are polymodal (varying in size). A recrystallised patch is found associated with a large dissolution seam; this suggests that younger meteoric water may have used these dissolution seams as paths to alter the mineralogy of the sample. The majority of dolomites have been completely calcified only the largest dolomites have retained their dolomitic core and have a calcified coat.		
Pore types	None		
Reservoir quality	None		

OF C001 1848 CM



C001 1848				
Texture	Bivalve Wackestone			
Description	This wackestone is cemented by a micritic matrix. There is a strong orientation of allochems that consist of thin shelled bivalves, microgastropods, coral fragments and other fossil material. There is a scattering of rounded peloids that have a mottled appearance.			
Palaeoenvironment Interpretation	The orientation of allochems may have been caused by gentle current flows or compaction. Muddy composition suggests this was a low energy environment of deposition.			
Diagenesis	A fine fracture cuts across part of the thin section and is infilled by microspar calcite.			
Pore types	None			
Reservoir quality	None			

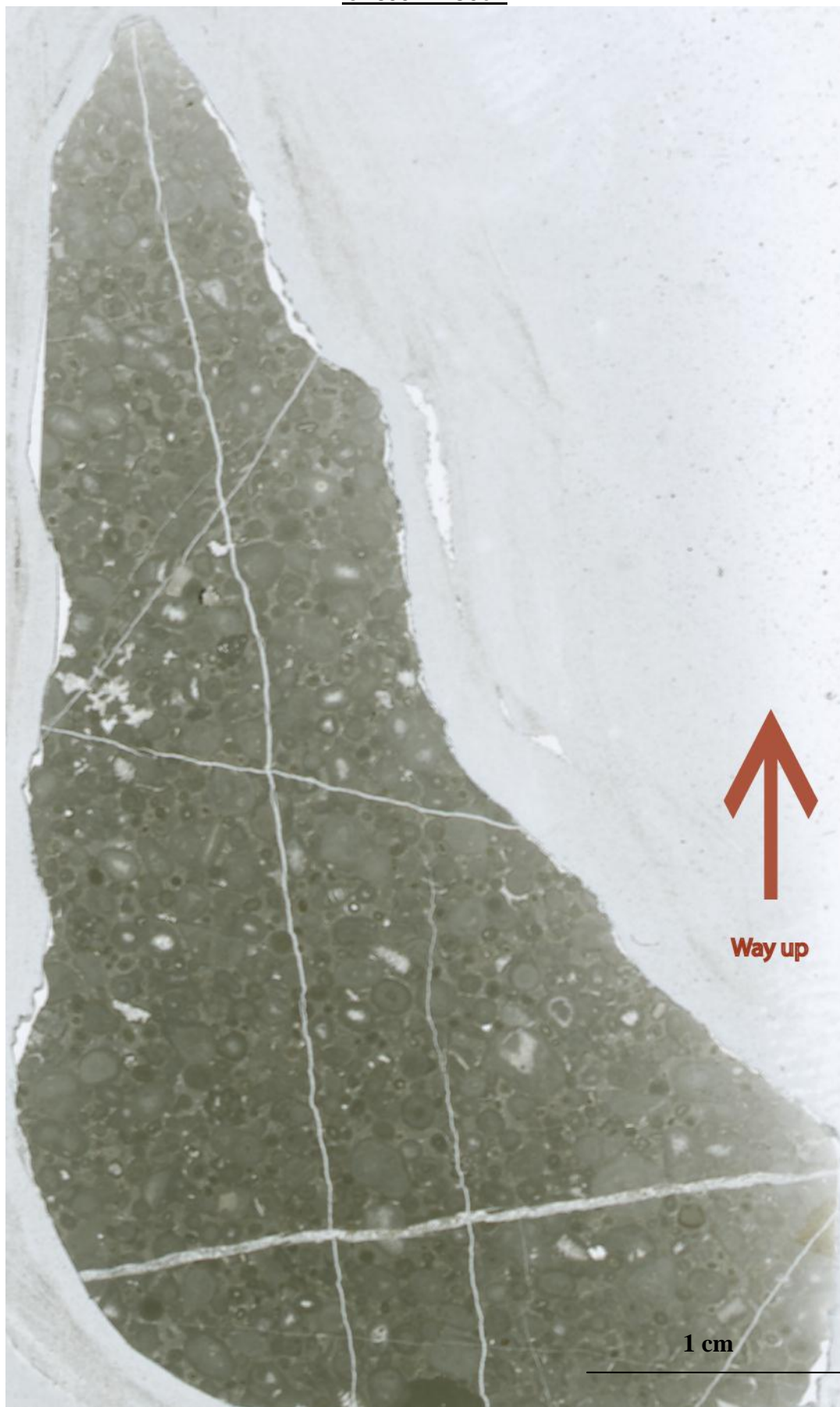
OF C001 2150 CM



1 cm

2150 cm	C001			
Texture		Ooid aggregate grainstone		
Description		This grainstone a poorly sorted assortment of mostly uniformly sized, plastically deformed to broken radial-fibrous ooids and micritic ooids (with a tangential fabric recognisable in peripheral parts) along with much coarser aggregate grains that commonly consist of two or more micritised ooids and coarse peloids. Bioclasts consist of microgastropods, poorly preserved foraminifera, green algae and other very rare fine rounded shelly fragments.		
Palaeoenvironment Interpretation		The mixture of different ooid types and compaction features suggests this sediment was transported downslope as an allochthonous limestone.		
Diagenesis		<p>This sample was compacted as evidenced through the plastic deformities of ooids, sutured and point contacts to broken ooids. Dissolution seams and smooth stylolites frequently occur around micritic ooids and larger clasts indicating chemical compaction. Intergranular porosity was occluded by a microcrystalline calcite spar. Discontinuous thin calcite filled stress fractures cut through all allochems and cements.</p> <p>Patches of neomorphosed calcite spar contain a equant calcite spar that is similar to large fracture fills. Dolomitisation has altered equant calcite spar regions and a scattering of anhedral rhombic crystals are found in patches amongst the rock. This dolomite was further altered via calcification, which explains the morphology of some rhombic calcite crystals. Ferroan dolomite has lined regions of previous dolomitisation and lines some fractures, this is probably the product of calcification.</p> <p>Calcite filled sharp edged fractures that span the sample cut across all allochems. These fractures often have thinner fractures branching off them obliquely.</p>		
Pore types		None		
Reservoir quality		None		

OF C001 2150cm



2150 cm	C001			
Texture		Peloidal grainstone		
Description		<p>This pack-grainstone a poorly sorted assortment of coarse sand to fine gravel sized, coated grains than include radial-fibrous ooids, micritic ooids (with a tangential fabric recognisable in peripheral parts) aggregate grains and rounded peloids. Small clasts form part of the assemblage and consist of a microcrystalline cemented assortment of micropeloids and fine sand grained ooids and calcitic debris.</p> <p>Bioclasts consist of large coated poorly preserved benthic foraminifera, abraded, rounded coated shelly fragments and echinoderm fragments.</p>		
Palaeoenvironment Interpretation		The mixture of different ooid types and compaction features suggests this sediment was transported downslope as an allochthonous limestone.		
Diagenesis		<p>This sample was compacted as evidenced through grain contacts that include point, concavo-convex and longitudinal contacts. Dissolution seams and smooth stylolites frequently occur around micritic ooids and larger clasts indicating chemical compaction. Thin discontinuous calcite filled fractures cut through allochems and are orientated vertical to bedding; these probably originate from compaction stress.</p> <p>Intergranular porosity was occluded by a microcrystalline calcite spar. A conjugate fracture set that consists of thin calcite filled fractures cut through all allochems and cements.</p> <p>Calcite filled sharp edged fractures that span the sample cut across all allochems running parallel to bedding. These fractures often have thinner fractures branching off them vertically to bedding.</p>		
Pore types		None		
Reservoir quality		None		

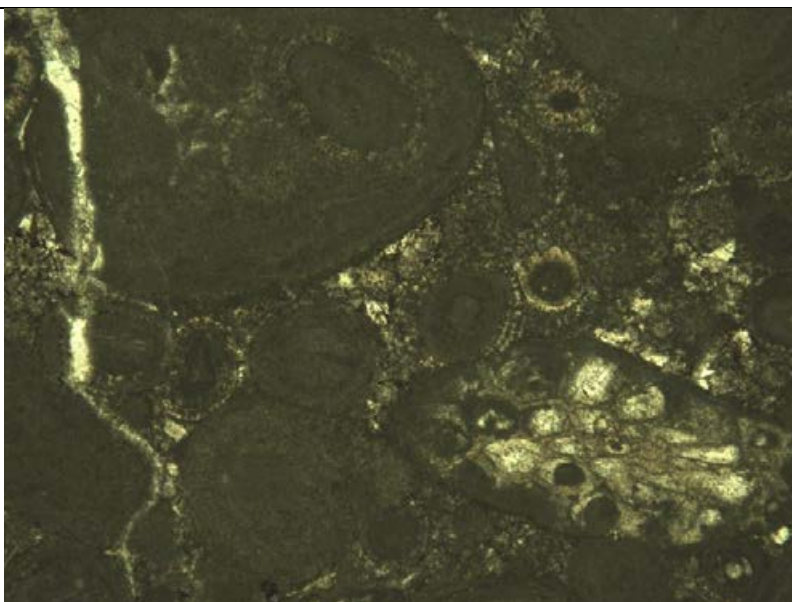
C001 2295 cm



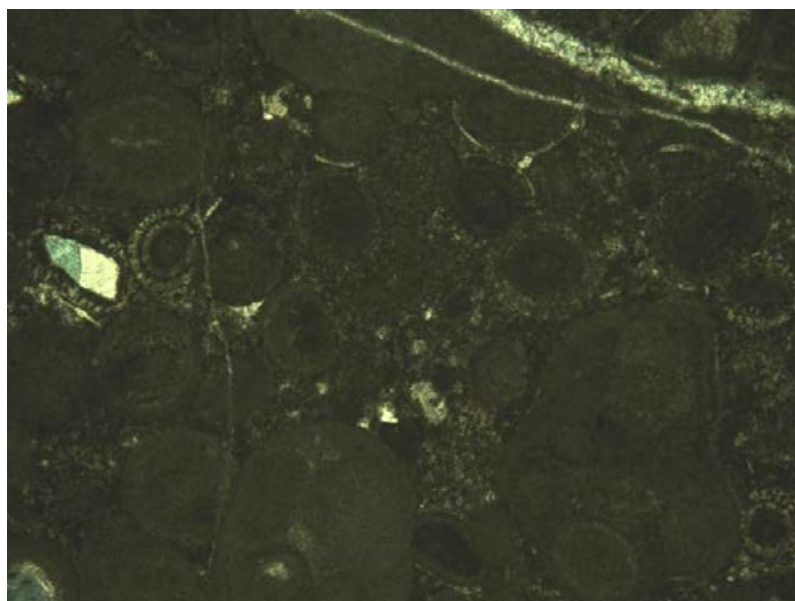
2295 cm	C001			
Texture		Ooid aggregate grainstone		
Description		<p>This is an ooid-peloidal grainstone which is a bimodal poorly sorted assortment of fine to medium gravel sized plastically deformed to broken aggregate grains and very coarse sand sized peloids and well rounded wackestone clasts. The second, finer assemblage consists of medium to coarse sand sized superficial ooids, radial-fibrous ooids and micritic ooids (with a tangential fabric recognisable in peripheral parts).</p> <p>The mud-wackestone clast consists of rounded dark green-grey clasts that consist of principally mud with a sparse quantity of thin shelled bivalve fragments and calcisiltite debris.</p> <p>Bioclasts rarely occur as ooid nuclei. Those that do occur in the sample include: poorly preserved foraminifera, green algae and other very rare fine, rounded shelly fragments.</p>		
Palaeoenvironment Interpretation		The mixture of different ooid type's compaction features and grain sizes suggests this sediment was transported downslope as an allochthonous limestone.		
Diagenesis		<p>This sample was compacted as evidenced through the plastic deformities of ooids, sutured and point contacts to broken ooids. Chalcedony has replaced the centre of large micritic ooids. There are calcite microspar microfractures that run at regular intervals parallel to each other; these are a result of mechanical compaction. Any remaining porosity is occluded by coarse equant calcite spar cement.</p> <p>Calcite filled sharp edged fractures that span the sample cut across all allochems. These fractures often have thinner fractures branching obliquely off them.</p>		
Pore types		None		
Reservoir quality		None		

C001 2300cm





Microphotograph 15. Very coarse peloids, aggregate grains and a bryozoan. FoV 2.89 x 2.15 mm.

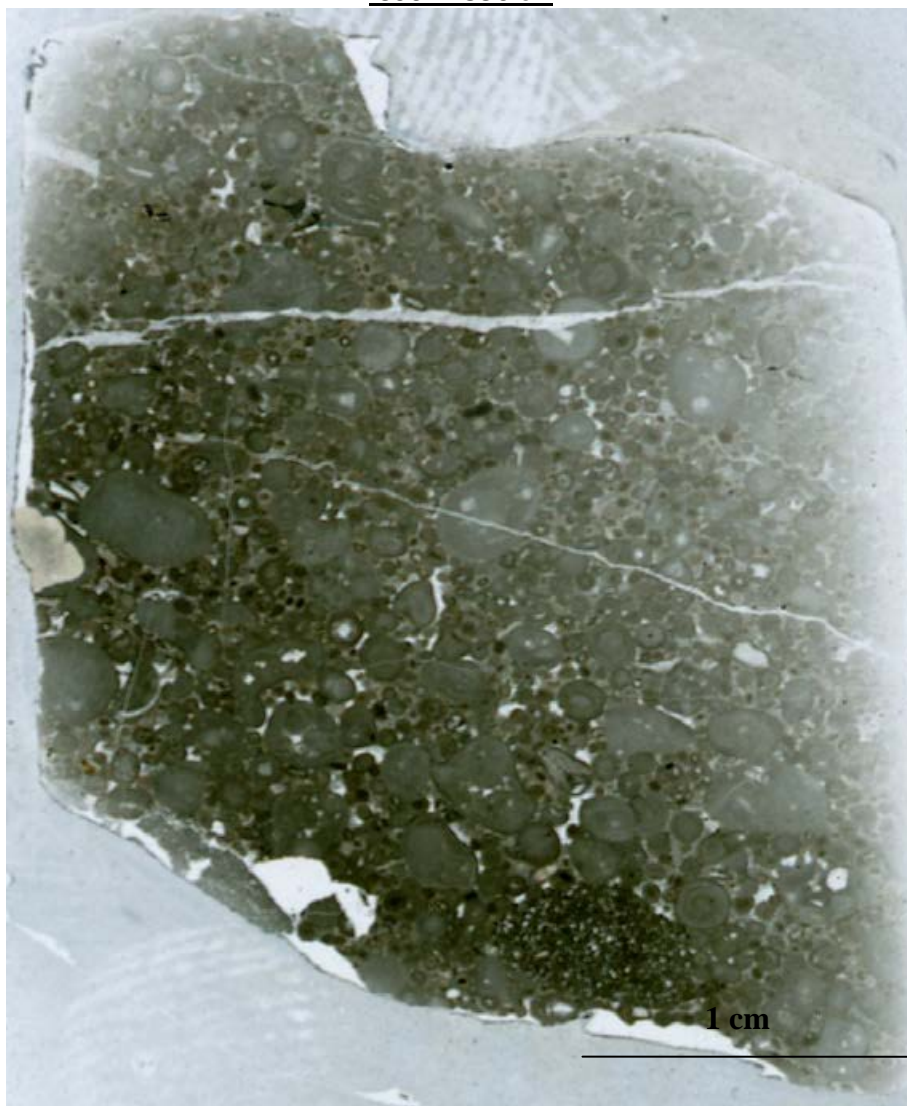


Microphotograph 16. Very coarse peloids, aggregate grains within an oolitic host sediment. Note the quartz grain that is forming the nucleus of a fibrous ooid. FoV 2.89 x 2.15 mm.

2300	C001			
Texture		Ooid aggregate grainstone		
Description		<p>This grainstone is bimodal assortment of plastically deformed to broken radial-fibrous ooids, micritic ooids (with a tangential fabric recognisable in peripheral parts) along with much coarser medium grained to coarse sized aggregate grains and well rounded coarse sand sized peloids and gravel wackestone clasts clasts. The clasts contain fine abraded calcite shell fragments, and other well rounded debris that includes micropeloids and algae.</p> <p>Bioclasts rarely occur as ooid nuclei. Those that do occur in the sample</p>		

	include: poorly preserved foraminifera, bryozoan fragments, green algae and other very rare fine rounded shelly fragments.
Palaeoenvironment Interpretation	The mixture of different ooid type of compaction features and grain sizes suggests this sediment was transported downslope as an allochthonous limestone.
Diagenesis	<p>This sample was compacted as evidenced through plastic deformities of grains such as point, concavo-convex and longitudinal contacts as well as, sutured contacts that indicate chemical compaction. The rock was cemented by a microcrystalline calcite spar. Very fine calcite filled stress fractures run through all allochems.</p> <p>Dolomite has replaced much of the microcrystalline cement giving rhombic shapes to crystals. These have been dedolomitised through calcification. Patches of recrystallised calcite that contain rhombic crystals, are associated with fractures that probably introduced calcifying water to the rock in recent times. An iron oxide is deposited around the majority of dolomite crystals.</p> <p>Calcite filled sharp edged fractures span the sample and cut across all allochems. These fractures often have thinner fractures branching off them at an oblique angle.</p>
Pore types	None
Reservoir quality	None

C001 2350 cm

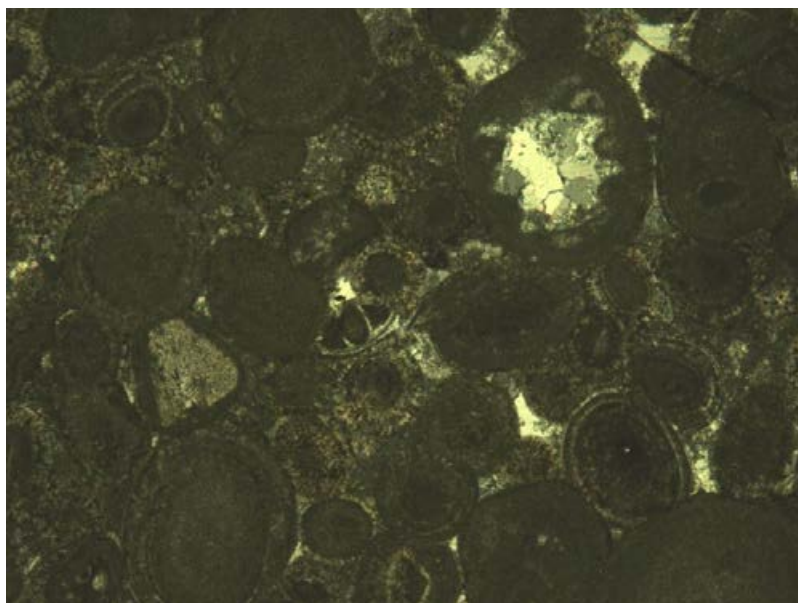


2350 cm	C001			
Texture		Ooid aggregate grainstone		
Description		<p>This is a bimodal grainstone which consists of a poorly sorted assortment of fine grained plastically deformed to broken superficial, radial-fibrous and micritic ooids (with a tangential fabric recognisable in peripheral parts) along with much coarser medium gravel to coarse gravel sized aggregate grains and peloids and well rounded coarse sand sized wackestone clasts. The clasts consists of micrite that hosts fine debris of rounded calcite grains and disarticulated and abraded shells.</p> <p>Bioclasts rarely occur in the sample but those that do occur include: poorly preserved foraminifera, and other rare fine rounded bivalve and other shelly fragments.</p>		
Palaeoenvironment Interpretation		The mixture of different ooid type's compaction features and grain sizes suggests this sediment was transported downslope as an allochthonous limestone.		
Diagenesis		<p>This sample was compacted as evidenced through plastic deformities of ooids, point, concavo-convex and longitudinal contacts as well as sutured contacts. Large peloidal grains have had their cores replaced by chalcedony.</p> <p>Equant calcite spar has occluded intergranular porosity and cemented the</p>		

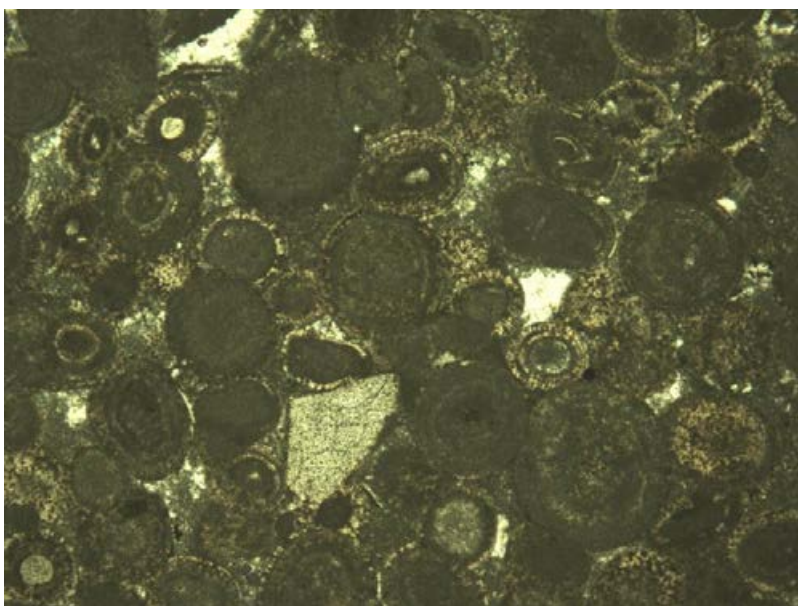
	<p>rock together.</p> <p>Calcite filled sharp edged fractures that span the sample cut across all allochems and run parallel to each other.</p>
Pore types	None
Reservoir quality	None

OF C001 2500cm





Microphotograph 18. Poorly sorted grainstone with coated echinoderm fragment. FoV 2.89 x 2.15 mm.



Microphotograph 17. Note the echinoderm fragment amongst a diverse suite of peloids and ooids. FoV 2.89 x 2.15 mm.

2500cm	C001			
Texture		Ooid aggregate grainstone		
Description		This grainstone a poorly sorted assortment of uniformly sized, plastically deformed to broken radial-fibrous ooids and micritic ooids (with a tangential fabric recognisable in peripheral parts) along with much rare coarse sand sized grains these often contain chalcedony. Bioclasts rarely occur in the sample but those that do occur include: poorly preserved green algae, and other rare fine rounded bivalve and other shelly fragments. Chalcedony forms the nuclei of some ooids.		
Palaeoenvironment		The mixture of different ooid type's compaction features and grain sizes		

Interpretation	suggests this sediment was transported downslope as an allochthonous limestone.
Diagenesis	<p>This sample was compacted as evidenced through the plastic deformities of ooids which have point, concavo-convex and longitudinal contacts as well as sutured contacts. Sutured contacts and dissolution seams occurred during chemical compaction. A microcrystalline calcite spar filled porosity with small patches of equant calcite spar. Stylolites cut across both cements and allochems.</p> <p>Chalcedony has replaced the cores of large micritic ooids; in this sample one grain is most prominent. It is light brown colour in plane polarised light and contains replacive carbonate crystals that have a rhombic shape occur in the chalcedony. Dolomites are very rare and are seen only to replace silica and are scattered very sparsely throughout the sample.</p> <p>Small patches of recrystallised calcite are found connected to fractures. These patches contain equant calcite spar regions and anhedral rhombic calcite crystals which are coated in iron oxide. Dedolomitisation has created via calcification a release of iron from ferroan dolomite to create an iron oxide coat.</p> <p>Single fine calcite filled sharp edged fractures cut across all allochems in a small section of the sample.</p>
Pore types	None
Reservoir quality	None

Location C002

OF C002 320 CM



C002	320			
Texture		Bivalve wackestone		
Description		This wackestone consists of calcite grains, very fine peloids, poorly preserved rare foraminifera and other shelly fragments. The thin section is dominated by the well orientated presence of two types of disarticulated and abraded bivalves; a thin <i>Posidonia</i> bivalve (30 µm) and a much thicker (300 µm) ? <i>Aptychi</i> mollusc bivalves. A strong orientation is indicated by the bioclasts long axis direction. All of the allochems sit in a dark green-brown micritic matrix.		
Interpretation		The muddy nature of the sediment and strong orientation points to an environment of moderate to high energy deposition where strong currents further away have transported allochems into the sediment. Areas of a chaotic organisation are possibly created by bioturbation. Evidence of bioturbation indicates probable deposition in a low energy, aerobic environment.		
Diagenesis		<p>The common orientation of allochems is partly due to compaction as suggested by the presence of stylolites. Stylolites are irregular anastomosing sets that cut through the matrix and are sometimes concentrated creating stained brown regions. Some stylolites and dissolution seams show porosity</p> <p>There are a very few scattered calcite crystals with a rhombic morphology, which suggests possible dedolomitization.</p> <p>There are several single equant calcite filled fractures that cut across the thin section.</p>		
Pore types		Styloporosity		
Reservoir quality		None		

OF C002 350 CM



C002	350 cm			
Texture	Bivalve wackestone			
Description	This wackestone is dominated by the presence of two types of disarticulated and abraded bivalves; a thin <i>Posidonia</i> bivalve (30 µm) and a much thicker <i>Apytchi</i> (150 µm) bivalves, there is also a common presence of finer calcitic shelly debris, very fine peloids, micrite coated algae and rounded calcite grains. The allochems and bioclasts are strongly orientation, which can be picked out by the bioclasts long axis direction. All of the allochems sit in a micritic matrix.			
Interpretation	The muddy nature of the sediment and strong orientation points to an environment of low energy deposition where strong currents further away have transported allochems into the sediment. Areas of mixed bivalve orientation may possibly have been created by bioturbation. Evidence of bioturbation indicates probable deposition in a low energy, aerobic environment.			
Diagenesis	<p>Compaction has lead to a strongly orientated sample and few broken bivalves. There is a common occurrence of irregular broken anastomosing sets of stylolites that cut through the muddy matrix of the rock.</p> <p>There are a very few scattered calcite crystals in the shape of rhombs, these may be dedolomites.</p>			
Pore types	None			
Reservoir quality	None			

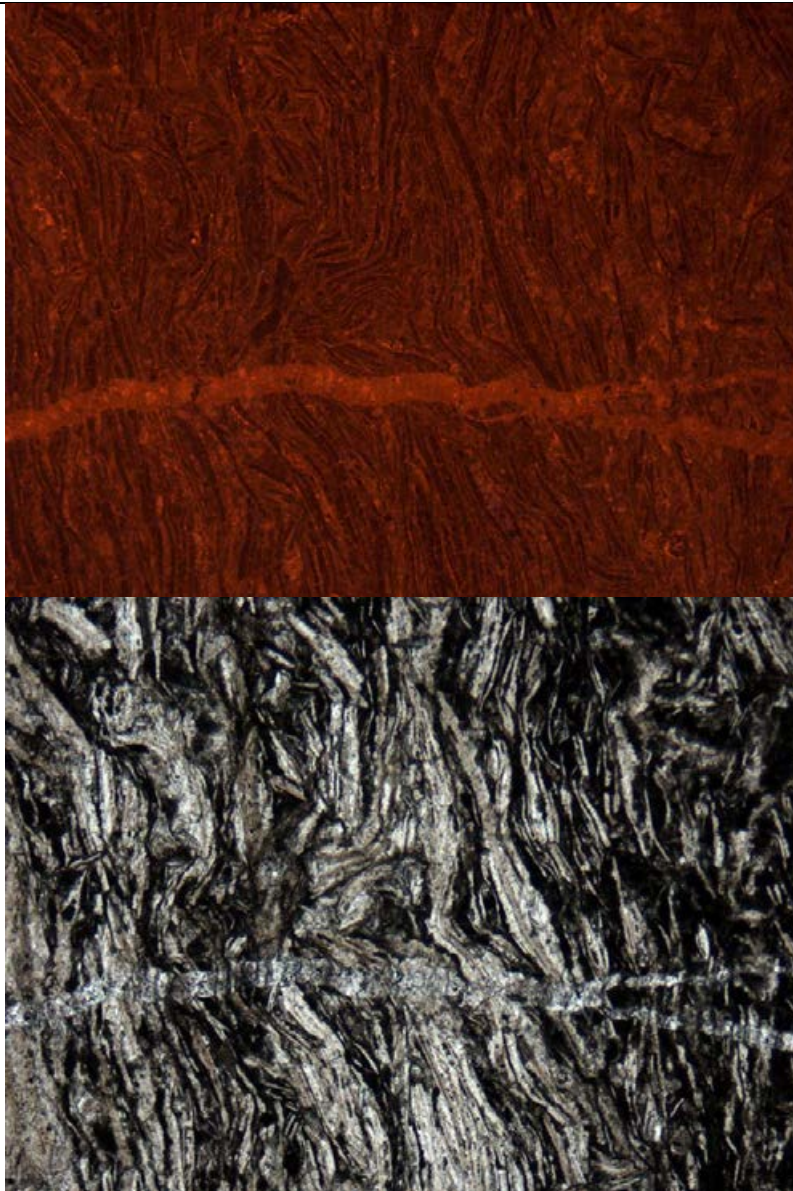
OF C002 480 cm



C002	480			
Facies				
Texture	<i>Posidonia</i> muddy pack-grainstone			
Description	<p>This is a well orientated and normal graded <i>Posidonia</i> pack-grainstone. The disarticulated <i>Posidonia</i> thin shelled bivalves are the main attribute of this thin section. The laminations of <i>Posidonia</i> are intermediately interrupted by concentrations of peloids, rare abraded brachiopod fragments and other slightly coarser bioclasts such as silicified echinoderm fragments. The <i>Posidonia</i> bivalves are typically 460 µm in length. Normal grading is clear in this sample showing a change from muddy facies including >5% pellets and other allochems to a more dominant calcite cemented <i>Posidonia</i> grainstone. There are common interruptions of grading by homogeneous laminations of highly spherical peloids. In the muddier sections of the sample <i>Posidonia</i> bivalves appear to have a varied size and have a much more disordered orientation compared to cleaner areas.</p>			
Interpretation	<p>The lack of variety of bioclasts suggests this was an ecological niche supporting a select few fauna. The gradation from muddier condition to a cleaner texture suggests that a current may have increased winnowing out fine mud-rich particles leaving a relatively mud-free fabric. If bioturbation has created disordered orientation in the muddier section then a decrease up the thin section would suggest a more limited environment of deposition over time. The appearance of undulose quartz suggests a terrain that has been eroded that has been tectonically deformed.</p> <p>Interruptions of <i>Posidonia</i> deposition by laminations of highly spherical peloids may be the result of distal resedimentation events.</p>			
Diagenesis	<p>The <i>Posidonia</i> bivalves are broken up through compaction and have a strong orientation, inside of laminations, forming the laminations seen in thin section.</p> <p>The rock is cemented with a calcite spar where the bioclasts have acted as centres of calcite growth. Echinoderms commonly have calcite overgrowths and rarely a silicified core. There is an increase in calcite cemented <i>Posidonia</i> bivalves in the mud-free regions. Areas with more micritic allochems are cemented by a microspar.</p> <p>Dolomite crystals are evident throughout the sample as scattered anhedral-euhedral rhombs to patches of anhedral rhombs binded in iron rich cement.</p> <p>Some very thin fractures cut through all allochems except patches of microspar and dolomite crystals.</p> <p>Patches of calcite microspar have filled any remaining porosity. These patches are associated with dolomites.</p> <p>A wide (120 µm) single fracture cuts perpendicular to laminations and is filled by a calcite spar. Thinner fractures, which are broken cut through all allochems parallel to laminations these are also filled by an equant calcite spar.</p>			
Pore types	Intercrystal			
Reservoir quality	None			

OF C002 480 CM



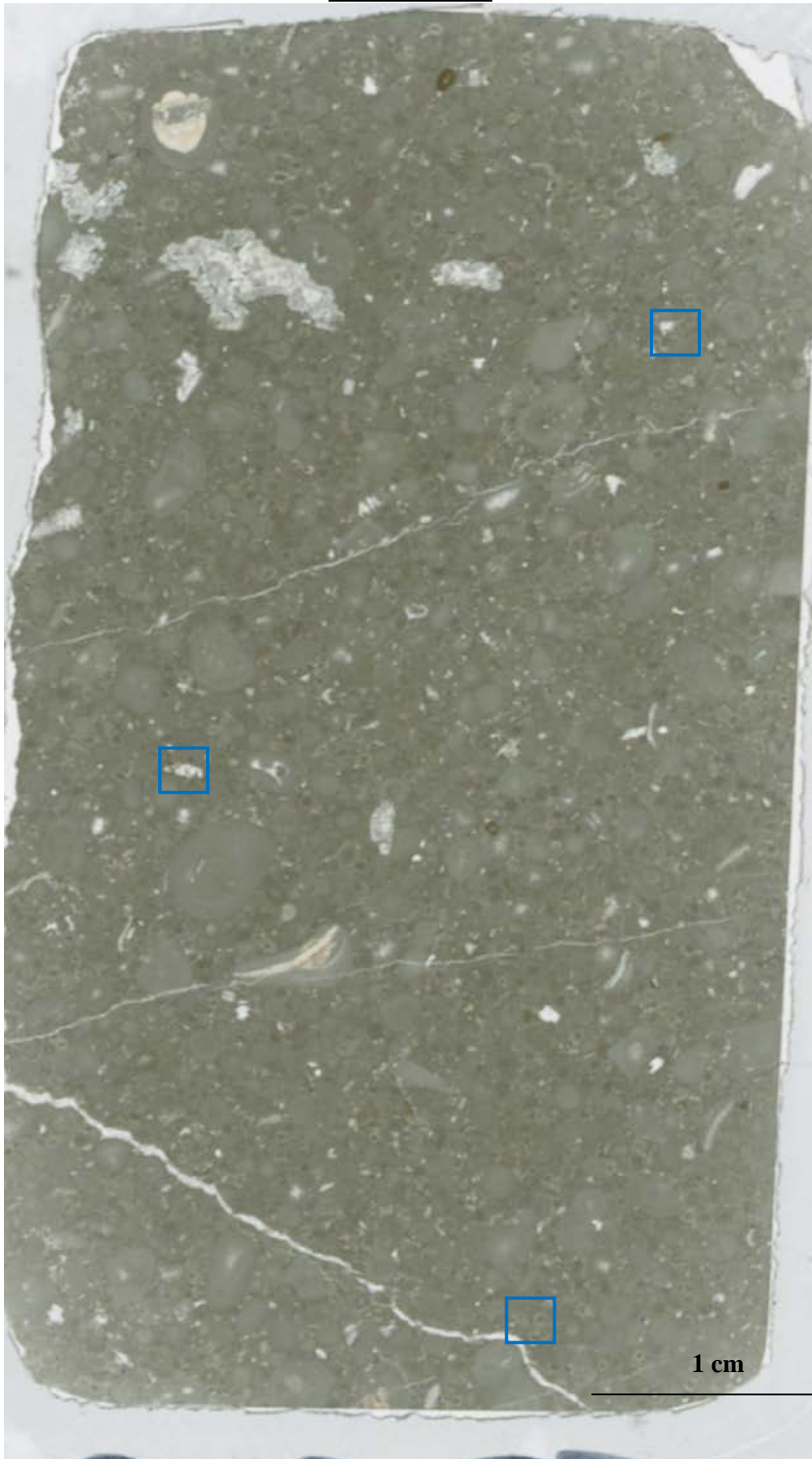


Microphotograph 19. CL and PPL microphotographs of *Posidonia* facies. Note the occurrence of early calcite fringe cements that prevented destruction during compaction. FoV 2.89 x 2.15 mm.

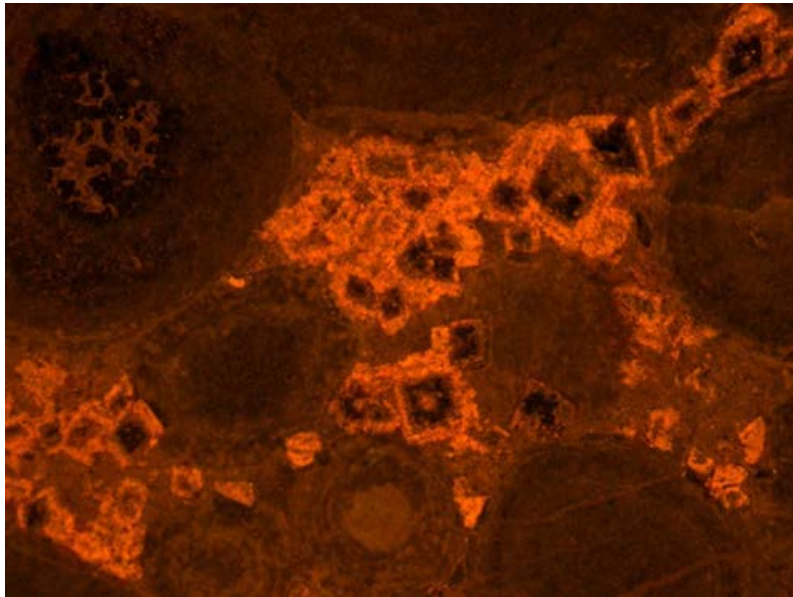
C002	480 cm		
Texture	<i>Posidonia</i> muddy pack-grainstone		
Description	<p>This is a well orientated <i>Posidonia</i> and bivalve mollusc pack-grainstone. The <i>Posidonia</i> thin shelled bivalves are the dominate bioclasts. Laminations of <i>Posidonia</i> are intermediately interrupted by much coarser abraded <i>Aptychi</i> bivalve molluscs. The thin shelled <i>Posidonia</i> bivalves include other introduced allochems of fine dark brown to black micritic rounded pellets.</p> <p>The <i>Posidonia</i> bivalves are typically 2.4 mm in length.</p>		
Interpretation	The lack of variety of bioclasts suggests this may have been an ecological niche that only supported a select few fauna. The lack of mud indicates that a current possibly winnowed out fine particles leaving a relatively mud-free fabric.		
Diagenesis	The <i>Posidonia</i> bivalves are broken up through compaction and have a strong orientation forming the laminations seen in thin section <i>Aptychi</i> bivalves are abraded and disarticulated. Singularly occurring smooth stylolites follow the laminations and show no muddy infill showing some porosity.		

	<p>The rock is cemented with a calcite spar where the bioclasts have acted as centres of calcite growth. There is an increase in calcite cemented <i>Posidonia</i> bivalves in the sheltered areas of the larger bivalves. Areas that include micritic allochems are cemented by a microspar.</p> <p>A wide (180 µm) single fracture cuts across the sample. The fracture is filled by a coarse equant calcite spar. The calcite has a dusty appearance. There is some minor intercrystal porosity in this fracture.</p>
Pore types	Intercrystal, styloporosity
Reservoir quality	None

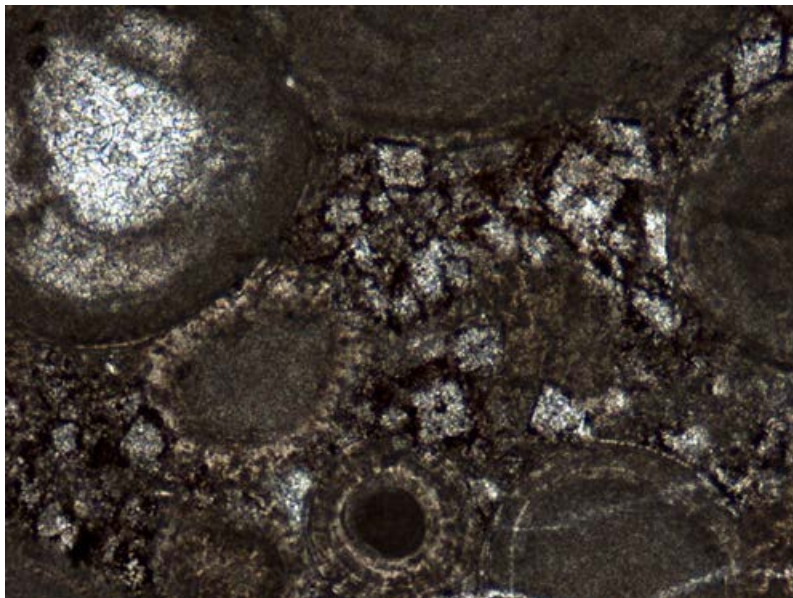
OF C002 520 cm



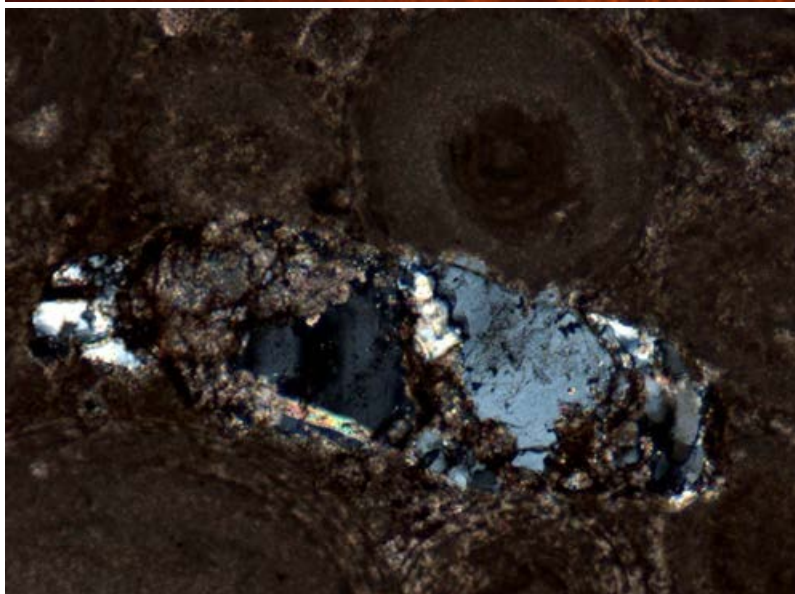
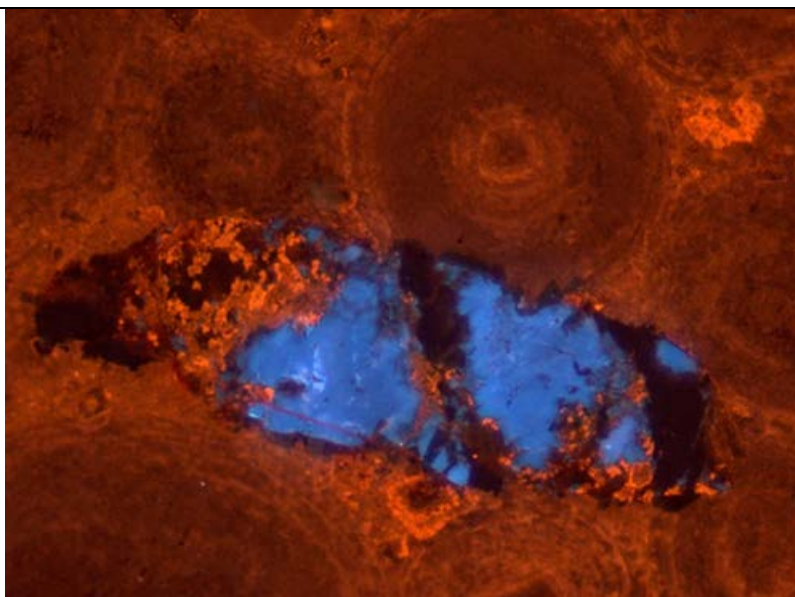
1 cm



Microphotograph 20. Calcified rhombohedral dolomite crystals. Calcite has replaced the outer zones of dolomite with a brightly luminescent calcite. Note the compression fractures in the bottom right; CL. FoV 2.89 x 2.15 mm.



Microphotograph 21. Calcified dolomites showing an iron rich coat, which probably formed during dedolomitisation. PPL. FoV 2.89 x 2.15 mm.



Microphotograph 22. K-Feldspar grain discovered amongst the grainstone matrix. FoV 2.89 x 2.15 mm.

C002	520 cm			
Texture		Ooid aggregate grainstone		
Description		<p>This is a poorly sorted grainstone. The main components are uniformly sized, plastically deformed to broken, radial-fibrous, superficial and micritic ooids (with a tangential fabric recognisable in peripheral parts) that are found amongst medium to coarse sand grade peloids and aggregate grains that commonly consist of two or more micritised ooids.</p> <p>Bioclasts rarely occur as ooid nuclei. Those that do occur in the sample include microgastropods, poorly preserved foraminifera and other very rare fine rounded shell fragments. Coral fragments rarely occur as clasts in their own right. Other ooid nuclei include chalcedony and dolomitised shell fragments. One coarse (1mm diameter) K-feldspar grain is found in this sample.</p>		
Interpretation		<p>The assortment of different grains types suggest the rocks components were developed in a high energy environment. This and plastic compaction features suggest the rock is a allochonthous limestone. The presence of K-</p>		

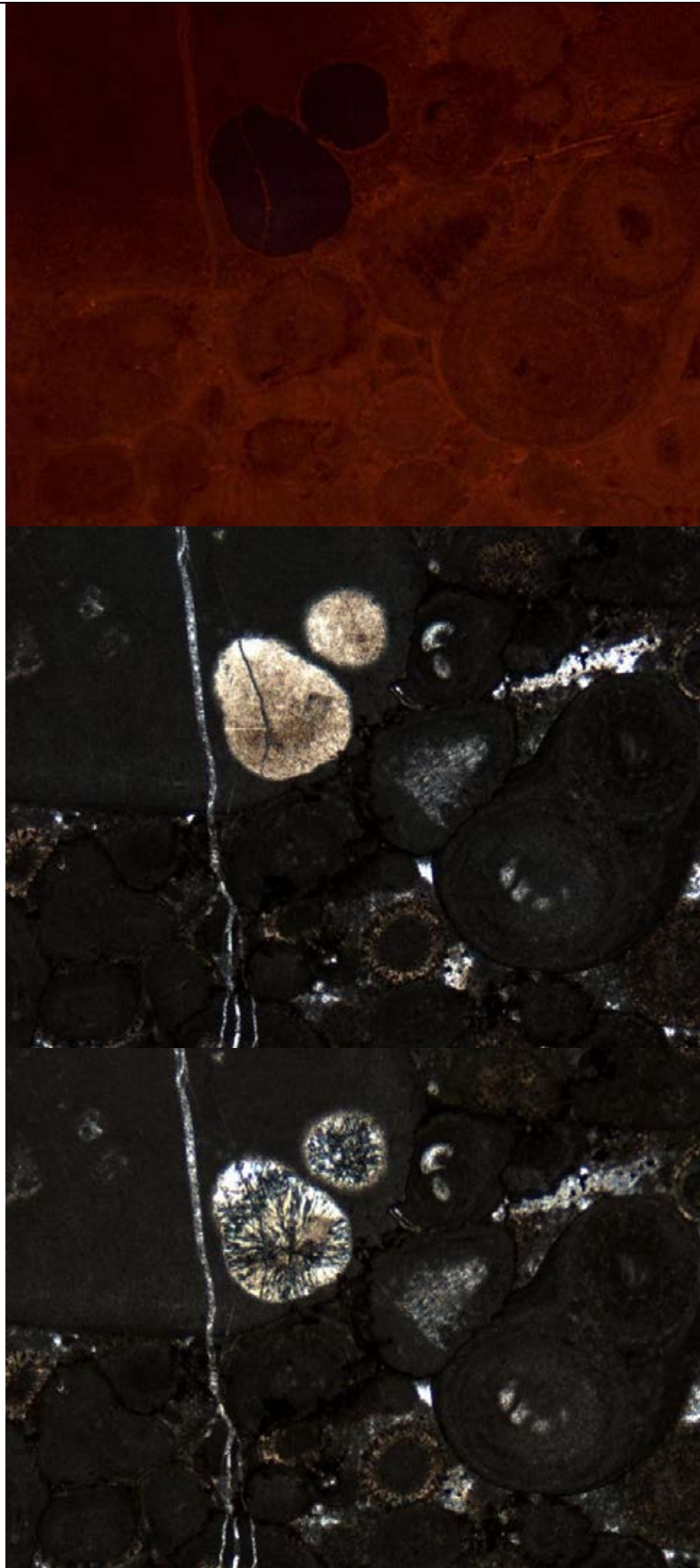
	feldspar suggests the proximity of the shoreline.
Diagenesis	<p>This sample was compacted as evidenced through the plastic deformities of grains, which have point, concavo-convex, longitudinal and sutured contacts as well as rare occurrences of broken ooids. Dissolution seams and smooth stylolites frequently occur around micritic ooids and larger clasts indicating chemical compaction. Chalcedony has replaced the nucleus of larger micritic grains. The rock is cemented by a microcrystalline calcite spar. A pore filling equant calcite spar has occluded porosity.</p> <p>Dolomitisation has altered equant calcite spar regions and a scattering of anhedral rhombic crystals are found in patches amongst the rock. This dolomite was further altered via calcification, which explains the morphology of some rhombic calcite crystals. A secondary ferroan dolomite has filled regions of previous dolomitisation; this is now an iron oxide (haematite). Single calcite filled sharp edged fractures span the sample and cut across all allochems.</p>
Pore types	None
Reservoir quality	None

OF C002 530 cm

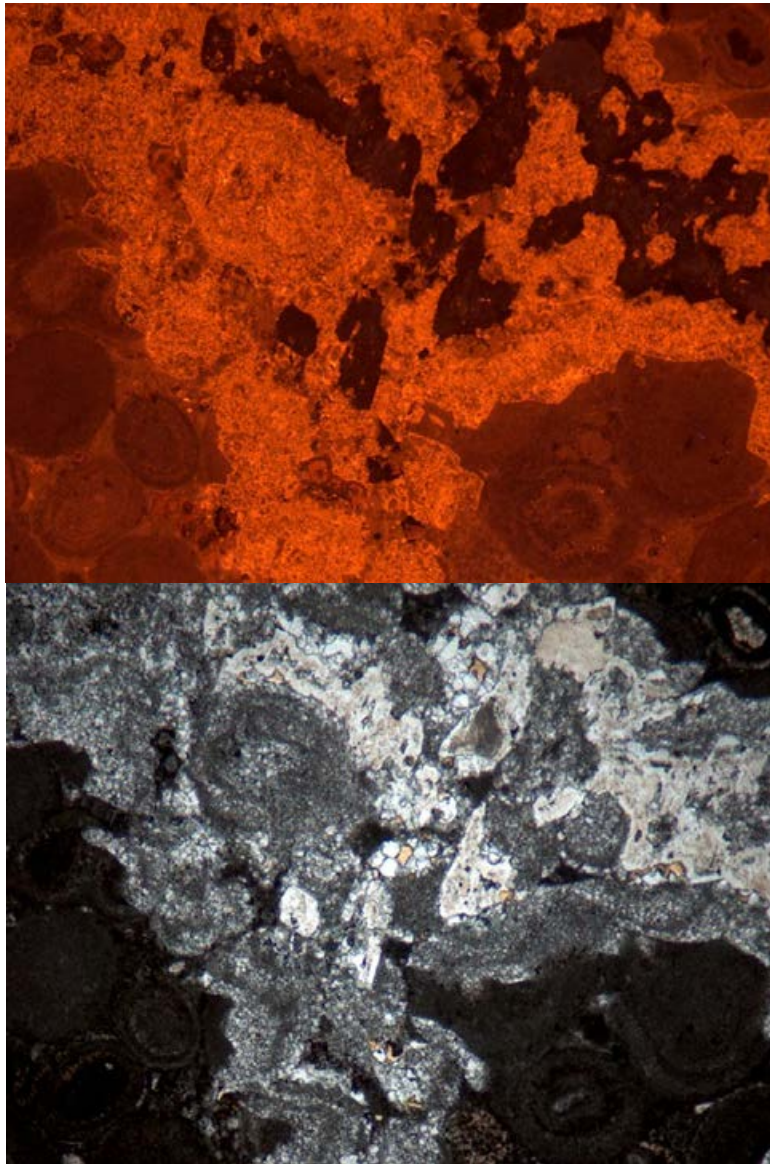


Way up

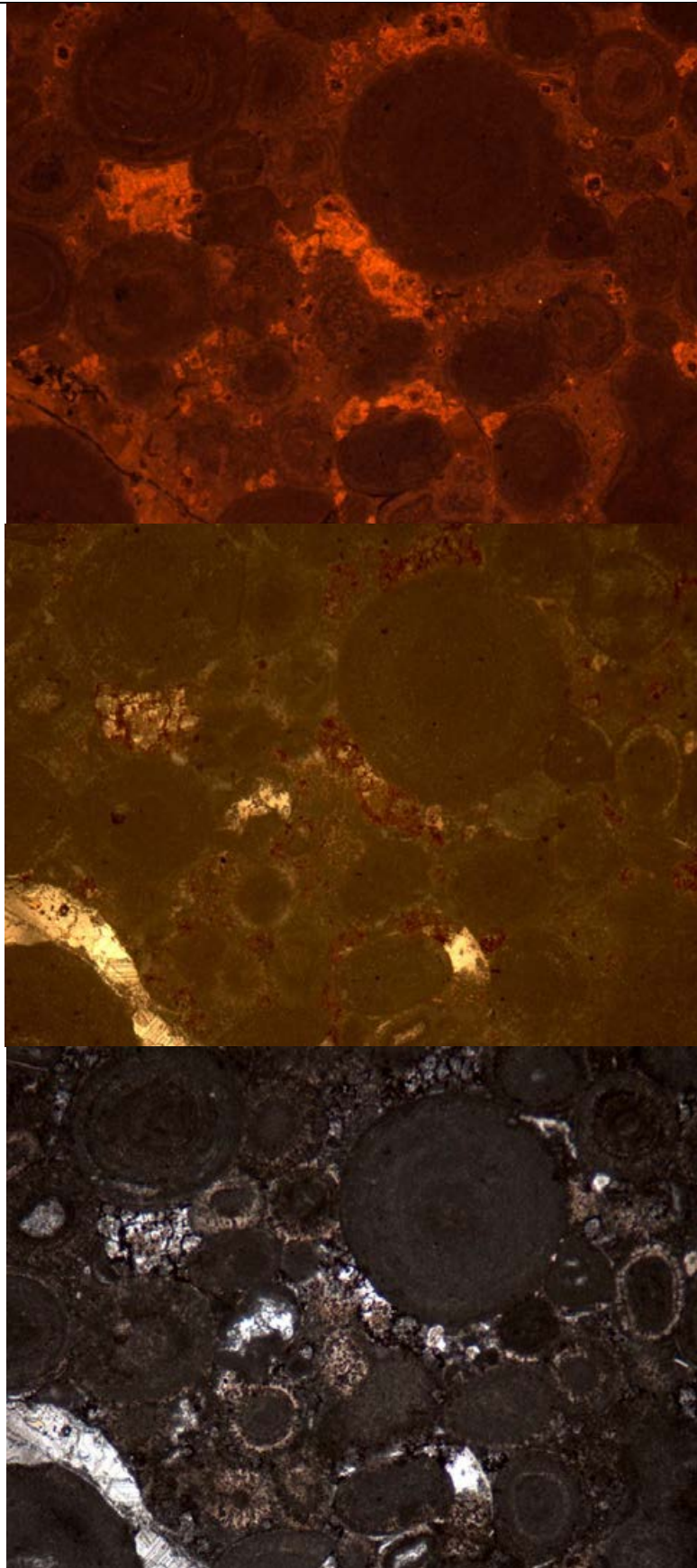
1 cm



Microphotograph 23 CL, PPL and XPL of a grainstone containing very coarse to gravel sand grade sized peloids that have had parts replaced by chalcedony. Note the abundance of stylolites that link up sutured grain contacts. FoV 2.89 x 2.15 mm.



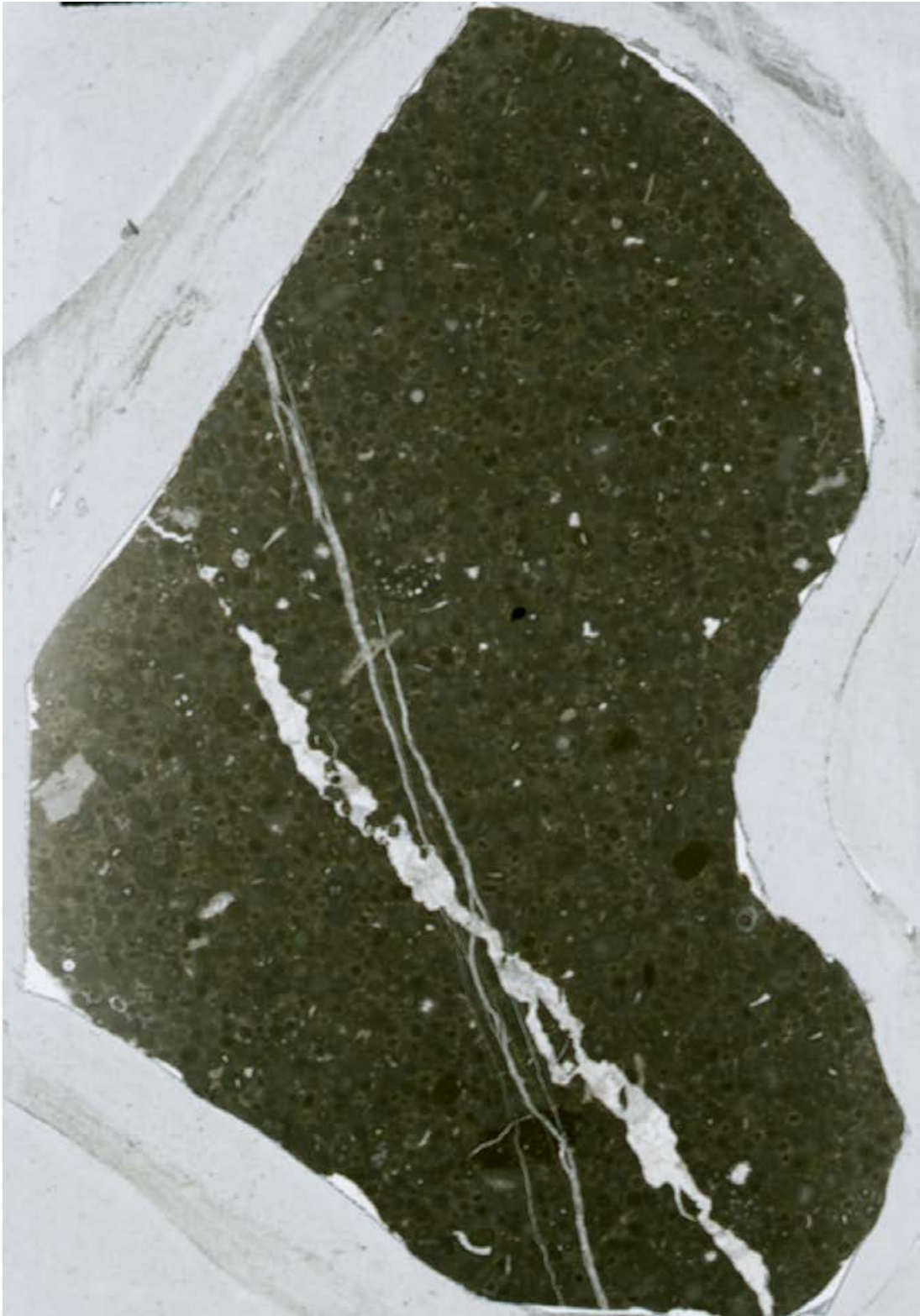
Microphotograph 24 CL and PPL of a neomorphosed cement that is host to silica crystals. FoV 2.89 x 2.15 mm.



Microphotograph 25 Scattered calcified dolomite crystals in an iron oxide matrix. Dedolomites clearly showing iron oxide deposits that formed as a product of dedolomitisation. XPL reflective light. FoV 2.89 x 2.15 mm.

C002	530 cm			
Texture		Ooid aggregate grainstone		
Description		<p>This is a bimodal grainstone with a poorly sorted assortment of medium sand-sized, plastically deformed to broken radial-fibrous ooids and micritic ooids (with a tangential fabric recognisable in peripheral parts) matrix that hosts much coarser grain sized aggregate grains that commonly consist of two or more micritised ooids and coarse peloids. Bioclasts consist of large benthic foraminifera, microgastropods, other poorly preserved foraminifera, green algae, and echinoderm fragments and other rare fine rounded shelly fragments.</p>		
Interpretation		<p>The mixture of different ooid types and compaction features suggests this sediment was transported downslope as an allochthonous limestone.</p>		
Diagenesis		<p>Compacted has created plastic deformities of the grains including; point, concavo-convex, longitudinal and sutured contacts. Styolites are rare and only occur with sutured contacts. Intergranular porosity was occluded by a microcrystalline calcite spar. Discontinuous thin calcite filled stress fractures cut through all allochems and cements. Larger peloids and micritic grains have been replaced by chalcedony.</p> <p>A large sheared calcite filled vein has cut across all allochems and has similar composition to a coarse equant calcite spar that has filled remaining intergranular porosity. There are small particles of iron oxide found throughout the sample this is likely a product of neomorphic alteration.</p>		
Pore types		None		
Reservoir quality		Poor		

OF C002 550 cm



1 cm

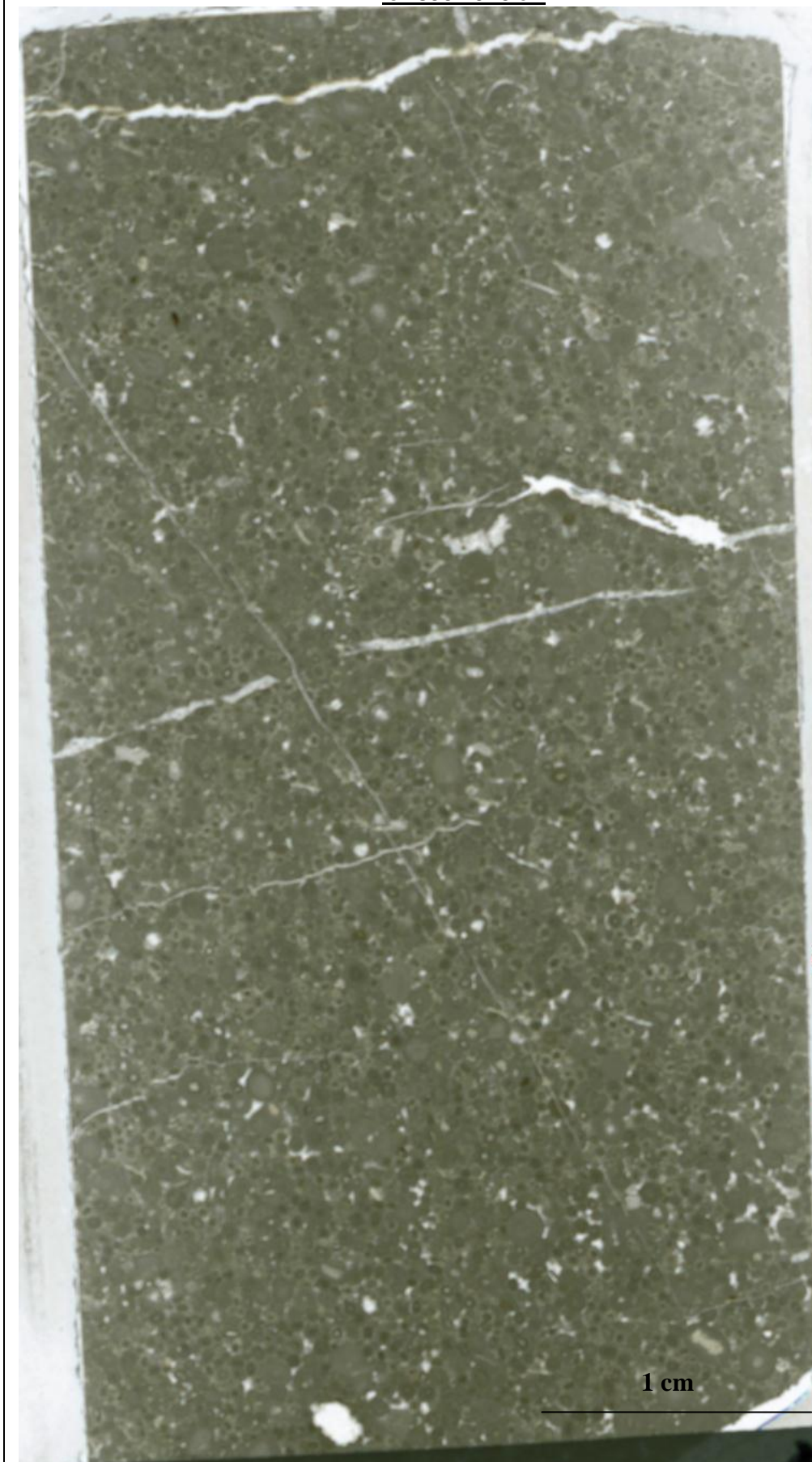
C002	550 cm		
Texture	Ooid intraclastic pack-grainstone		
Description	<p>This grainstone is a poorly sorted assortment of plastically deformed to broken radial-fibrous ooids, coarser micritic ooids (with a tangential fabric recognisable in peripheral parts), aggregate grains and intraclasts. The intraclasts are a dull green in colour and contain a micrite that is hosting fine shell material.</p> <p>Bioclasts include poorly preserved microgastropods, echinoderms, a single bryozoan and fine abraded bivalves and other very rare fine rounded shelly fragments. All of these allochems are found within a micrite matrix that hosts a fine assortment of abraded calcite fragments.</p>		
Interpretation	The mixture of different ooid types and plastic compaction features suggests this sediment was transported downslope in a muddy turbidite flow.		
Diagenesis	<p>Previously cemented wackestone clasts entered the sample through transportation of unconsolidated sediment. The sample was compacted as evidenced through the plastic deformities of ooids, sutured, point and concavo-convex contacts. Echinoderms have developed calcite overgrowths. The sediment was then cemented by a microcrystalline calcite.</p> <p>A calcite vein that is filled by coarse equant calcite cuts across the section. It shows shear fracturing and contains breccia of the host rock. Thinner fractures also span the sample and cut across the thicker calcite vein.</p>		
Pore types	None		
Reservoir quality	Poor		

OF C002 555 CM



555 cm	C002			
Texture		Ooid Intraclast Pack-Grainstone		
Description		<p>This grainstone is a poorly sorted assortment of uniformly sized, plastically deformed to broken radial-fibrous ooids and coarser micritic ooids (with a tangential fabric recognisable in peripheral parts). There is a noticeable presence of coarse wacke-packstone clasts, which appear plastically deformed.</p> <p>Bioclasts are rare and include poorly preserved microgastropods, foraminifera and other very rare fine rounded shelly fragments. Other ooid nuclei include rare chalcedony and common dolomitised shelly fragments.</p>		
Interpretation		The mixture of different ooid types and plastic compaction features suggests this sediment was transported downslope in a turbidity flow, with larger mud-wackestone clasts being incorporated into the sediment during transport.		
Diagenesis		<p>Previously cemented wackestone clasts entered the sample through transportation of unconsolidated sediment. The sample was compacted as evidenced through the plastic deformities of ooids, sutured and point contacts to broken ooids. Dissolution seams and smooth stylolites frequently occur around micritic ooids and larger clasts.</p> <p>The rock was then cemented by a micrite, which incorporates calcitic silt.</p> <p>After micritic cementation equant calcite spar filled porosity and overgrew some calcitic allochems. Dolomitisation has altered equant calcite spar regions creating porosity. These porous regions were filled by iron oxide cement. This dolomite was further altered via calcification, which explains the morphology of some rhombic calcite crystals.</p> <p>Single calcite filled sharp edged fractures span the sample and cut across all allochems implying fracturing took place after lithification.</p>		
Pore types		Very rare intercrystal porosity created through dolomitisation		
Reservoir quality		Poor		

OF C002 610 cm

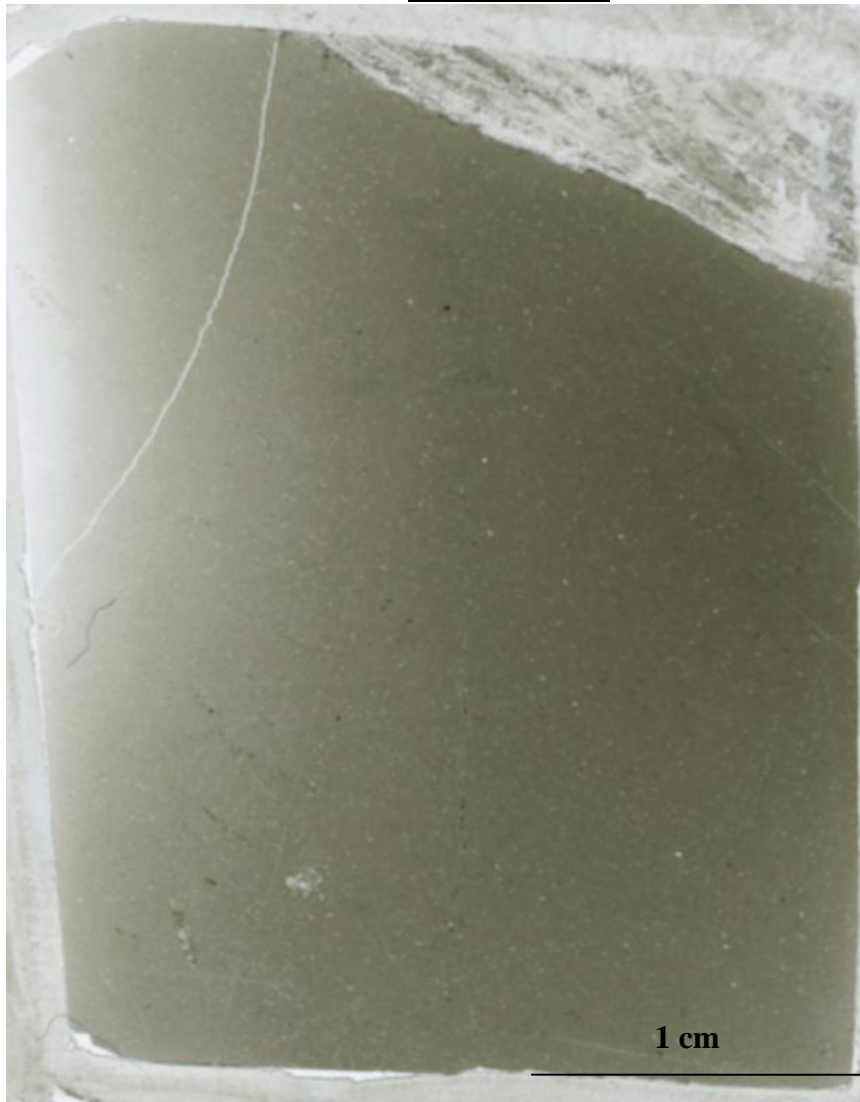


Way up

1 cm

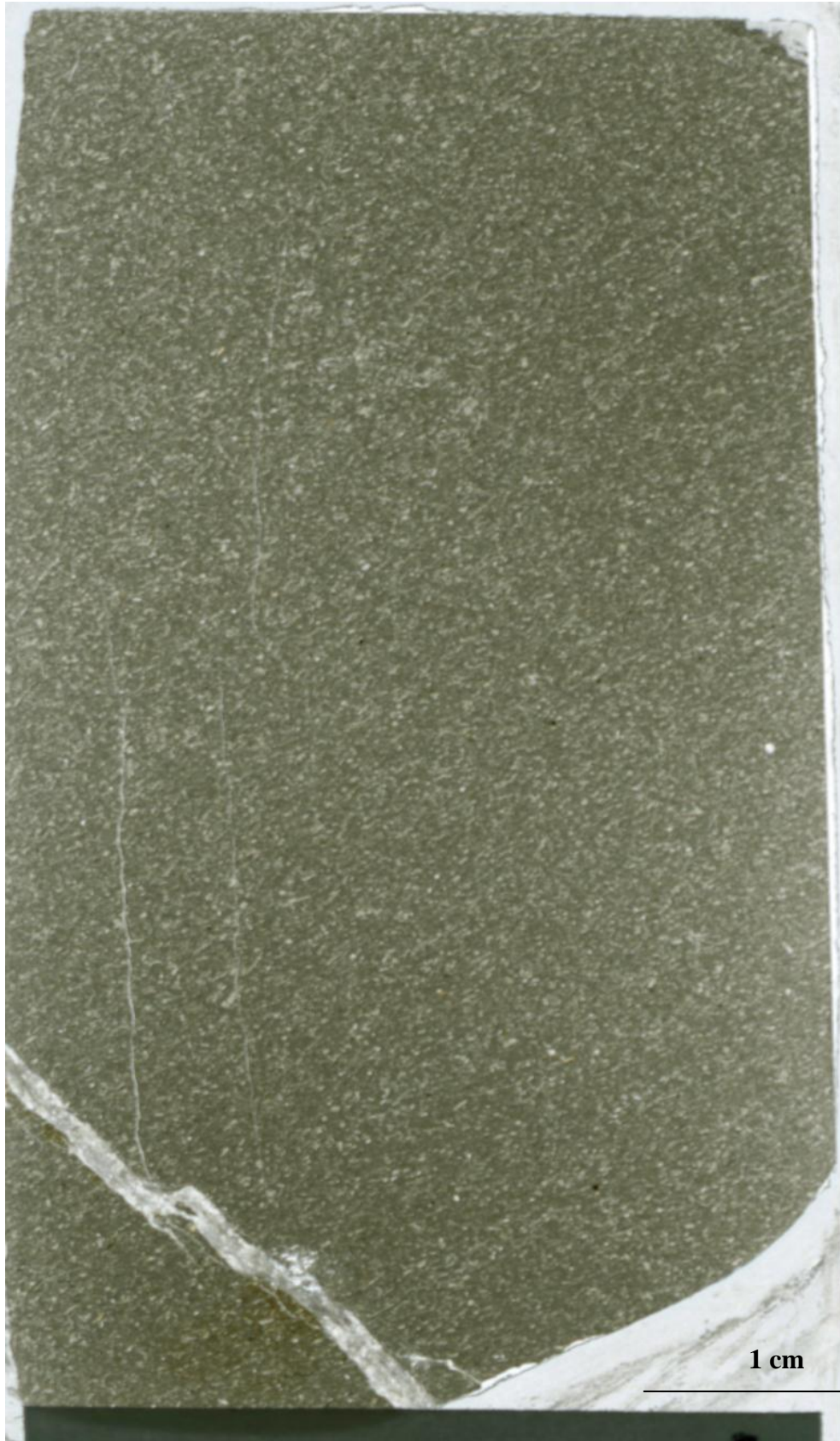
C002	610 cm			
Texture		Ooid aggregate grainstone		
Description		<p>This grainstone a bimodal poorly sorted assortment of plastically deformed to broken radial-fibrous ooids and much coarser micritic ooids (that have a tangential fabric recognisable in peripheral parts) and wackestone clasts. Bioclasts commonly occur as ooid nuclei including microgastropods, poorly preserved foraminifera and other very rare fine rounded shelly fragments. Echinoderm debris and thin shelled bivalves are found amongst the grains. Other ooid nuclei include microcrystalline quartz grains.</p>		
Interpretation		<p>The mixture of different ooid types and compaction features suggests this sediment was transported downslope in a turbidity flow.</p>		
Diagenesis		<p>This sample was compacted as evidenced through the plastic deformities of ooids, sutured and point contacts. Echinoderm syntaxial calcite overgrowths have filled intergranular porosity. Dissolution seams and smooth stylolites frequently occur around micritic ooids and larger clasts indicating chemical compaction. The rock was then cemented by a microcrystalline calcite spar.</p> <p>Dolomitisation has altered patches of equant calcite spar and a scattering of anhedral rhombic crystals are found in patches amongst the rock. A secondary ferroan dolomite has filled regions of previous dolomitisation; this is now an iron oxide (haematite). Calcite filled sharp edged fractures that span the sample and cut across all allochems parallel to bedding.</p>		
Pore types		Fracture		
Reservoir quality		Poor		

OF C002 650 cm



C002	650 cm			
Facies				
Texture	Bioclastic mud-wackestone			
Description	This is a mud-wackestone that contains a well orientated scattering of fine bioclast debris including thin shelled bivalves, echinoderm debris and a single occurrence of micrite walled uniserial foraminifera.			
Interpretation	The fine grained nature of the sediment suggests this was deposited in a low energy environment where mud was allowed to settle. However a strong orientation may have been formed by a weak current, which orientated the fine grained allochems.			
Diagenesis	The allochems of this sample were deposited in a micritic matrix. The strong orientation may have been caused by minor compaction. There are few occurrences of echinoderm syntaxial calcite overgrowths. Smooth stylolites are only evident over a small distance. Fine fractures cut across the thin section parallel to bedding; these are filled by a microcrystalline calcite.			
Pore types	None			
Reservoir quality	None			

OF C002 675 cm



Way up

1 cm

C002	675 cm			
Facies				
Texture		<i>Posidonia</i> peloid packstone		
Description		<p>This is a well orientated <i>Posidonia</i> pack-grainstone. Disarticulated and broken <i>Posidonia</i> thin shelled bivalves are the dominate bioclast in this thin section. Other allochems include widespread well rounded peloids, fine echinoderm debris, green algae, rare poorly preserved triserial foraminifera and other slightly coarser bioclasts such as heavily abraded brachiopod fragments. The <i>Posidonia</i> bivalves are typically 160 µm in length. Peloids are uniform in size, commonly 140 µm in diameter. Some regions of the sample have the strong orientation interrupted this may be due to bioturbation.</p>		
Interpretation		<p>Due to this samples position in terms of sedimentary processes seen in outcrop this is interpreted as a return from turbid conditions to background sedimentation.</p> <p>However, it is of note the higher quantity of rounded peloids compared to below the turbidites. This may be due to continuing fallout from turbid conditions suggesting this sample is not the truly 'pure' background sedimentation.</p>		
Diagenesis		<p>The strong orientation is most likely caused by early compaction. <i>Posidonia</i> bivalves are broken up through compaction and have a strong orientation, forming the direction seen in thin section. Minor smooth stylolites partially cross the thin section, these only cut through the muddy matrix.</p> <p>The rock is cemented with a microcrystalline spar (micrite) where the bioclasts have acted as centres of coarser calcite growth. Echinoderms commonly have calcite overgrowths.</p> <p>Some very thin incontinuous fractures (<5 µm in diameter) cut through all allochems, these are filled by a micro-equant calcite cement.</p> <p>A wide (900 µm) single fracture cuts across all allochems in the bottom right of the thin section scan this is filled by a equant calcite spar.</p>		
Pore types		None		
Reservoir quality		None		

Location C003 and C003s

OF C003 20 CM



C003	20			
Texture		Bivalve Peloid Packstone		
Description		<p>This is a strongly orientated laminated assortment of disarticulated abraded shelly fragments, thin shelled bivalves, echinoderm debris, pellets and very fine superficial ooids. Laminations alternate between a bioclasts assemblage and a muddier micritic microfacies. The top of the thin section scan shows a region of darker mud-wackestone texture. This is probably evidence of bioturbation in the substrate.</p> <p>The thin section cuts through a chert nodule that appears as the brighter region in the top right of the scan. The nodule has a chalcedonic form with a microcrystalline-quartz replacing a coarse mollusc fragment in the centre of the nodule.</p> <p>There are rare rusty red grains (<1 mm) of iron oxide that appear to show dark black clay laminations.</p>		
Interpretation		The alterations of muddy to fine granular calcitic texture indicates this microfacies represents an environment of alternating energy, probably between low and a moderate to high energy environment.		
Diagenesis		<p>The allochems have clearly been compacted showing strong orientation and very common dissolution grains and stylolites that cut through the micritic matrix. Echinoderm calcitic overgrowths and minor overgrowths on other bioclasts have resulted in minor porous sections been infilled.</p> <p>A nodule of crypto-quartz and chalcedony has selectively replaced a spherical area of the thin section. This may be due to the mollusc acting as a centre for chalcedony nucleation. Nodules of microcrystalline spar sit in an iron oxide rich matrix that are probably a by-product of calcification where dolomite crystals are observed.</p> <p>A very thick fracture filled with coarse equant calcite cuts everything in the section.</p>		
Pore types		Rare intercrystal		
Reservoir quality		None		

OF C003 125 cm



C003	125			
Texture		Bivalve mud-wackestone		
Description		<p>This is a well orientated mud-wackestone that consists mainly of disarticulated thin shelled bivalves that measure a mean 160µm in length as well as other poorly preserved echinoderm fragments and other well rounded shelly fragments. The thin section shows a concentration of burrows or nodules towards the top of the thin section scan these regions contain a packstone which consists of well orientated disarticulated bivalves and similar bioclasts as above. But this section includes a coarser element of well rounded chalcedony and dolomitised grains that may be superficial ooids or peloids.</p> <p>There are regions that may have resulted from bioturbation, which are found inside the finer facies. This region is filled by the coarser element of the thin section and disturbs the laminations created in the finer facies. There is a large bivalve mollusc fragment that only slightly displaces the surrounding laminations. The bioclast has been replaced by a micro-quartz.</p>		
Interpretation		This fine grained mud-wackestone was probably deposited in a low energy environment and consists of particles being deposited from currents distally.		
Diagenesis		<p>The strong orientation of bioclasts and allochems suggest mechanical compaction occur early on when the sediment was unconsolidated. The micritic matrix is has high concentrations of dissolution seams in both microfacies types implying chemical compaction occurred.</p> <p>Very fine bioclasts have been preserved with microcrystalline spar that appears mottled. Coarser bioclasts commonly have been replaced by chalcedony. Those allochems replaced with chalcedony often contain dolomite crystals.</p>		
Pore types		Some minor intercrystal and intergranular porosity		
Reservoir quality		None-Poor		

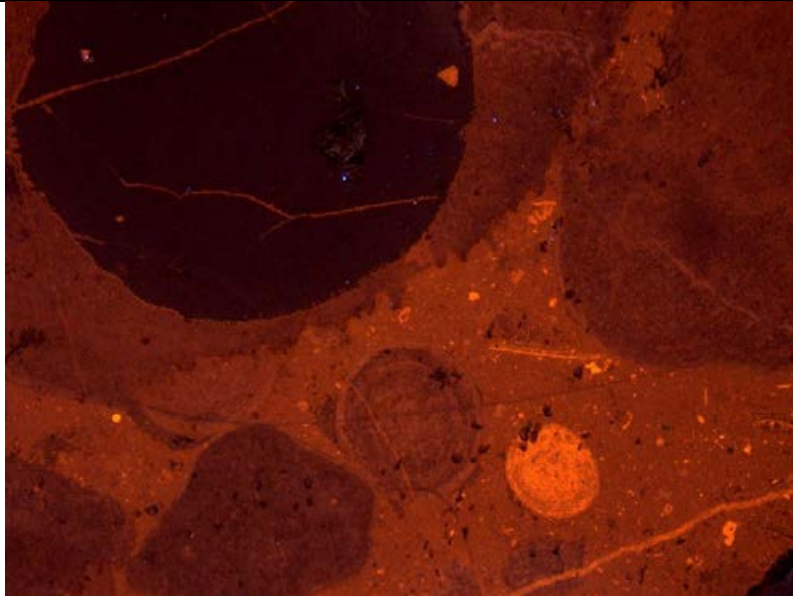
OF C003 250 cm



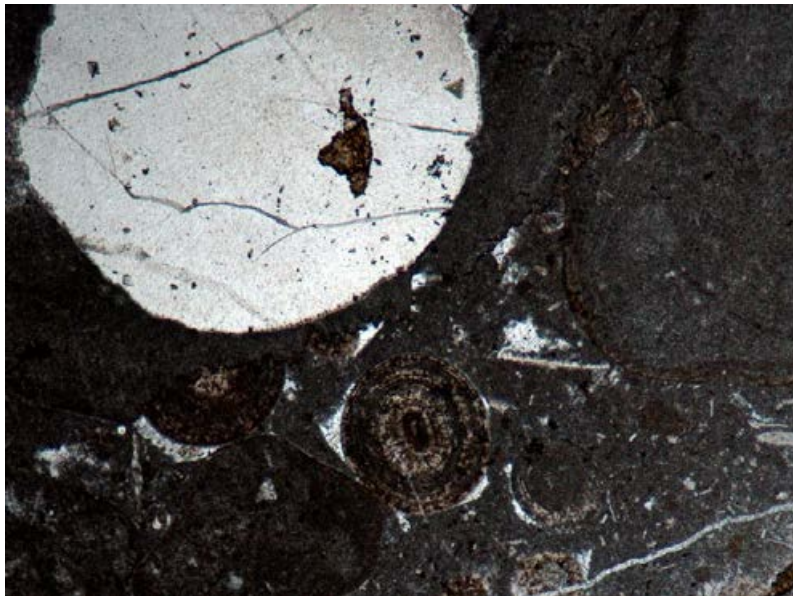
C003				
Texture	Peloidal-oid pack-grainstone			
Description	Oriented poorly sorted assemblage of gravel to medium sand grade whole and deformed ooids, peloids and fossil debris. Bioclasts include fine debris of shell material, abraded and disarticulated bivalves, biserial foraminifera, rare green algae and coated echinoderm fragments. A variety of allochems are found including ooid types that include superficial ooids to micritised ooids that containing a subtle thinly laminated tangential cortices.			
Interpretation	The mixture of ooid type, sizes, and thicknesses of the cortices, associated grains and abrasion of ooid laminae is suggestive that the ooids are allochthonous ooids (Chow and James, 1987).			
Diagenesis	All allochems have been compacted leading to point contacts, sutured contacts and plastic deformation. Dissolution seams and stylolite cut across the sample. Dissolution seams now contain anhydral dolomite rhombs that sit in iron oxide. Microfracture set that contains a euhedral calcite fill.			
Pore types	None			
Reservoir quality	None			

of C003 590 cm

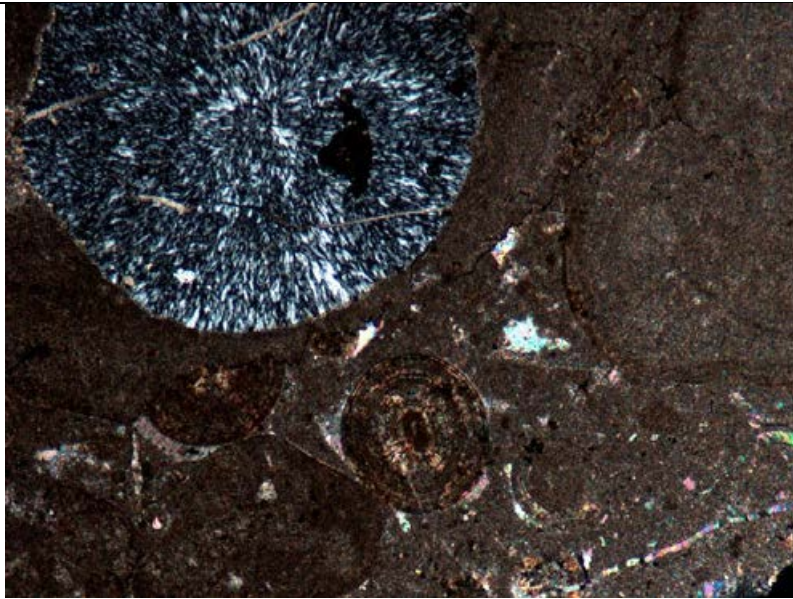




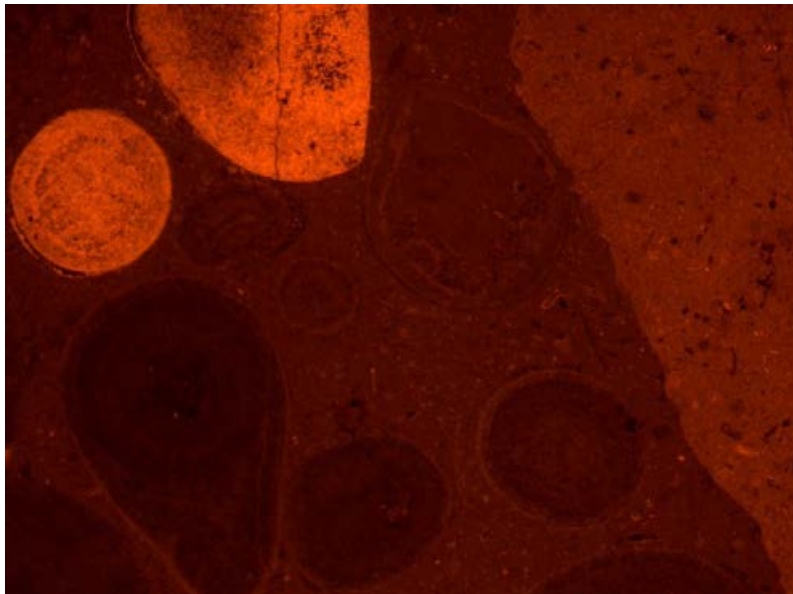
Microphotograph 26. Note the separate phases of cementation. The lighter pale yellow orange grains were probably deposited in a more porous state and are cemented via a younger phase compared to 'darker' cements, which appears to have had no porosity during resedimentation. FoV 2.89 x 2.15 mm.



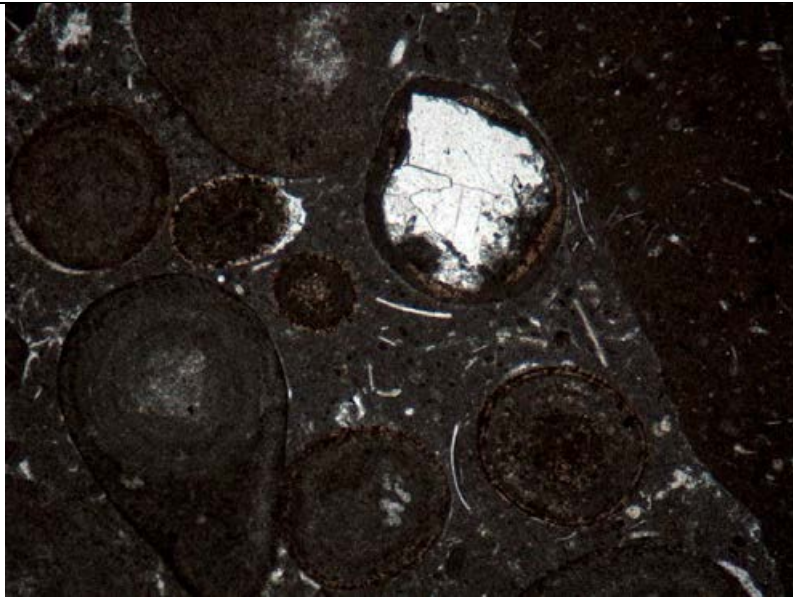
Microphotograph 27. Note the fractured chalcedony grain. This suggests that fracturing occurring before redeposition. FoV 2.89 x 2.15 mm.



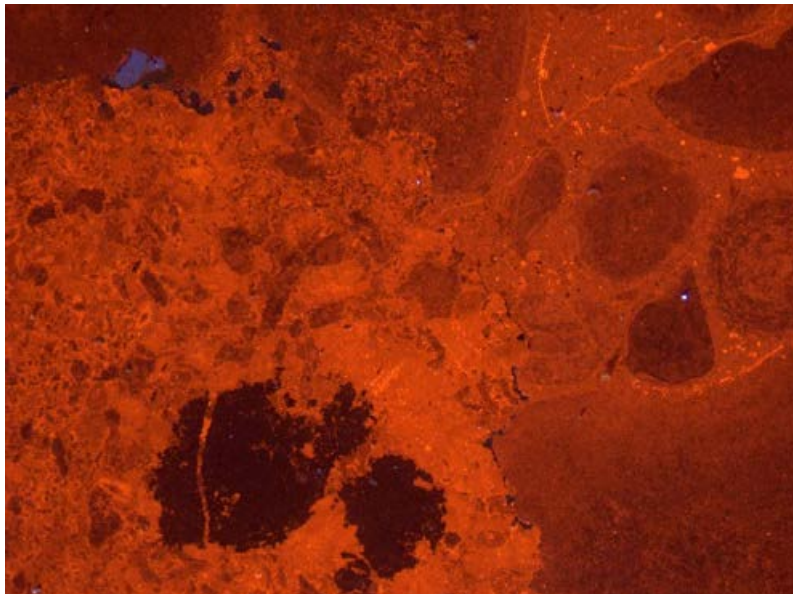
Microphotograph 28. A thin cement lining of the chalcedony grain indicates that this was created previous to resedimentation. FoV 2.89 x 2.15 mm.



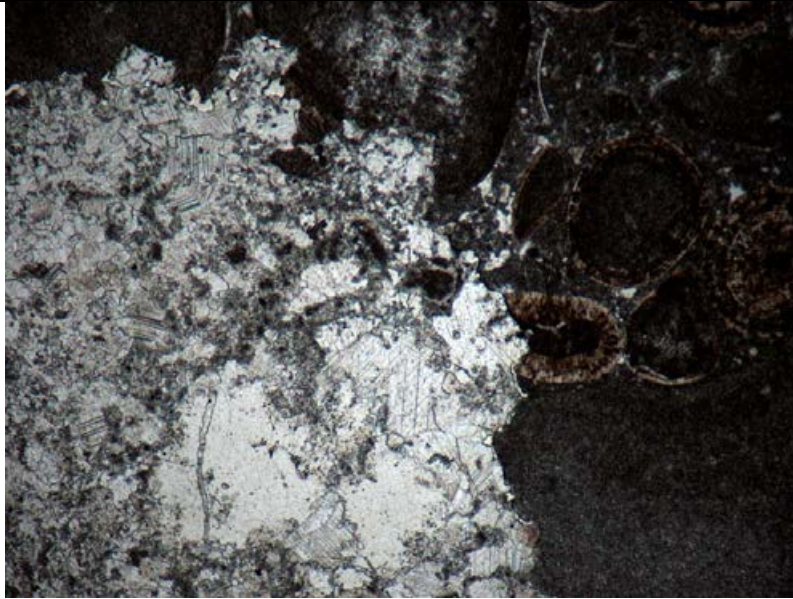
Microphotograph 29 Detail of allochems composition. Note the different luminescence colours of each allochems. FoV 1.16 x 0.86mm.



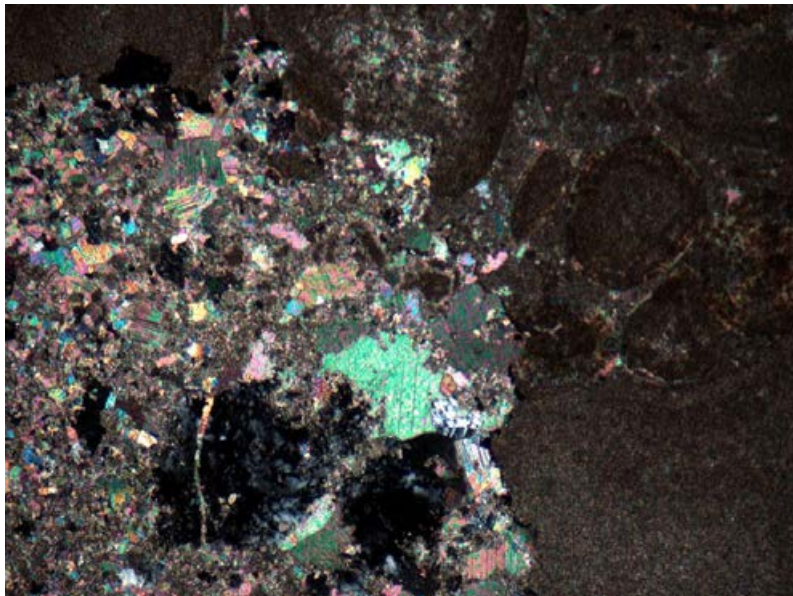
Microphotograph 30 Detail PPL of Microphotography 4. FoV 1.16 x 0.86mm.



Microphotograph 31 Detail of neomorphosed patch. Note the different colours suggesting that parts of the burial cement have been altered from silica to calcite



Microphotograph 32 PPL FoV 1.16 x 0.86mm.



Microphotograph 33 XPL FoV 1.16 x 0.86mm.

590 cm	C003			
Texture		Dolomitised ooid aggregate grainstone.		
Description		<p>This shows a poorly sorted assemblage of ooids, coarse aggregate grains, intraclasts that consist of very coarse wackestone clasts that contain <i>Posidonia</i> bivalves and other well rounded calcitic shelly fragments and a single 1mm grain of K-feldspar. The allochems have been compacted together creating sutured contacts and are commonly plastically deformed and rarely broken. Bioclasts include rare coral fragments, poorly preserved microgastropods, thin shelled bivalves and the possible remains of poorly preserved biserial foraminifera.</p> <p>The ooids in this sample show a mixture of ooid types and intraclasts ranging from 10mm to 200µm in diameter. Ooid types include superficial ooids and spherical clearly structured ooids to larger micritic ooids showing only subtle laminae as well as composite micritic ooids.</p>		

	<p>The outer structures of clear ooids consist of radial-fibrous structure. Micritic ooids are a mean 900µm in diameter and show obliterated laminations due to pervasive micritisation of the cortex. Superficial ooids and spherical clearly structured ooids are a mean 450µm in diameter and have a thin radial-fibrous outer coating with a subtle micritic layered to structureless centre. Some very coarse grains have a micritic make-up with several subtle laminae, this laminae is inclusion rich equant euhedral-anhedral calcite. Chalcedony is often found at the nuclei of allochem grains.</p>
Interpretation	<p>The mixture of ooid type, sizes, and thicknesses of the cortices, associated grains and abrasion of ooid laminae is suggestive that the ooids are allochthonous ooids (Chow and James, 1987). The mixture of ooid types, using the depositional sites in Flügel, 2004 [page 155] suggests that the ooids originate from high-Mg calcitic, saline environments from a moderately energetic environment such as a semi-open lagoonal system/semi closed sand bar. However, micritic ooids have thinly laminated tangential cortices and no fossils associated with them (possibly suggesting a more lagoonal environment), whilst ooids with a few fine-radial laminae occur as the dominant ooid type in this pack-grainstone.</p> <p>Ooid source location: Well defined ooid structures are characteristic of formation in quiet-water low turbulence environments (Flügel, 2004).</p>
Diagenesis	<p>The grains in this sample show moderate compaction and plastic deformation.</p> <p>This sample is cemented by a micritic matrix, which consists of a scattering of fine abraded calcite fragments and micro-ooids/pellets that often have a radial-fibrous structure.</p> <p>The nuclei of many this ooids appears mottled, due to early micritisation of grains. Dissolution seams and denticular stylolites occur frequently and span the whole thin section; they form around grains and do not cut through them.</p> <p>Chalcedony occurs as the centre of larger ooids, they commonly have a thick micrite coat and thin isopachous incomplete calcite coats of bladed calcite crystals. Chalcedony is commonly inclusion rich and/or shows ghosts of what it has replaced; it is possible that the chalcedony is associated with pronounced silicification of fossils or another carbonate grains. It is not clear if the chalcedony had formed previous to resedimentation or replaced allochems forming the allochems nuclei.</p> <p>Dolomitisation has selectively replaced areas of the sample creating shadows of previous elements including chalcedony grains and micritic grains. The dolomite does not luminous red and therefore suggest that calcification of the dolomite has removed any dolomititic material, this may have occurred during cementation of fracturing.</p> <p>Calcite patches have replaced and filled porosity with an equant calcite.</p> <p>Calcite filled fractures happen as sharp edged and occur regularly. These were created after deposition as they cut through all grains and cements.</p>
Pore types	None
Reservoir quality	None

OF C003 600 cm



C003	600 cm			
Texture		Ooidal-peloidal pack-grainstone		
Description		<p>Moderately well sorted assemblage of medium to coarse sand grade whole, broken and deformed ooids, peloids and fossil debris. Bioclasts include a fine debris of shell material, abraded and disarticulated bivalves, very rare poorly preserved biserial foraminifera.</p> <p>The ooids in this sample show a variety of ooid types that include superficial ooids to micritised ooids that often contain a subtle thinly laminated tangential cortices.</p>		
Interpretation		<p>The mixture of ooid type, sizes, and thicknesses of the cortices, associated grains and abrasion of ooid laminae is suggestive that the ooids are allochthonous ooids (Chow and James, 1987). The dominance of micritic ooids that have a thin tangential cortex and no fossils associated with them (possibly suggesting a more lagoonal environment).</p>		
Diagenesis		<p>All allochems have been compacted leading to point contacts, sutured contacts and plastic deformation, and rarely breakages between allochems. Micrite forms the matrix where a minor area of intergranular cement is formed of equant calcite spar. Fine microfracture set that contains a euhedral calcite fill. The fractures are parallel to each other.</p>		
Pore types		None		
Reservoir quality		None		

OF C003 860 cm



1 cm

860 cm	C003			
Texture		Dolomitised ooid pack-grainstone		
Description		<p>This shows a moderately well sorted assemblage of whole, broken and deformed ooids and rare compound ooids (no more than 1 mm in diameter). They have been compacted together creating sutured contacts. Allochems are commonly plastically deformed and more rarely broken.</p> <p>Bioclasts are only rarely found within ooids at their nuclei or rarely as fine debris. Bioclasts are commonly well rounded grains of calcite, which are probably from abraded and disarticulated bivalves and brachiopods; there are very rare poorly preserved biserial foraminifera. Other common ooid cortices include grains of chalcedony, micrite and euhedral-anhydral dolomite crystals (which have been calcified).</p> <p>The ooids in this sample show a variety of ooid types from 450µm mean diameter superficial ooids with clear thin radial-fibrous outer coating with a subtle micritic layered to structureless centre to 600µm mean diameter micritic ooids that range from largely coated micrite spheres with pervasive micritisation of the cortex to occurrences of subtle thinly laminated tangential cortices.</p>		
Interpretation		<p>The mixture of ooid type, sizes, and thicknesses of the cortices, associated grains and abrasion of laminae is suggestive that the ooids are allochthonous ooids. Some ooids that have a clear structure have a thick micrite outer core; this may have been acquired during transport. The well defined ooid structures are characteristic of formation in quiet-water low turbulence environments (Flügel, 2004), this may possibly be due to ooids being transported from below the wave base or a lagoonal environment.</p>		
Diagenesis		<p>All allochems have been compacted leading to point contacts, sutured contacts and plastic deformation between allochems. A micrite cements the rocks together. This micrite also contains micro-peloids and fine accumulations of calcite. Dissolution seams and stylolites have developed between grains.</p> <p>Inclusion rich euhedral to anhedral dolomites are scattered around the sample and commonly occur in their finest form within the matrix. It appears that the more euhedral dolomites are associated with the cores of allochems particularly those with chalcedony nuclei. Dolomite had been calcified.</p> <p>The sample has some thick calcite filled fractures that cut across all allochems and features as well as more common finer fractures. The fractures are a regular thickness and occur singularly.</p>		
Pore types		None		
Reservoir quality		None		

OF C003 1190cm



C003	1190 cm			
Texture		Mud-wackestone		
Description		Well orientated accumulation of shell fragments, micropeloids and disarticulated bivalve fragments.		
Interpretation		A strong orientation suggests this was deposited in current swept environment. The fine grained nature suggests this was deposited distally from the source of deposition.		
Diagenesis		Stylolites and dissolution seams indicate chemical compaction followed deposition. There are several wide fractures (750 µm) that are infilled with a coarse calcite spar, these fractures have sharp edges and occur singularly. There are few thin fractures (30 µm) that branch off the larger fractures, and are filled by coarse calcite spar.		
Pore types		None		
Reservoir quality		None		

OF C003 1560 CM



1 cm

1560 cm	C003			
Texture		Dolomitised ooid pack-grainstone		
Description		<p>This shows a moderately well sorted assemblage of whole, broken and deformed ooids and aggregate grains. They have been compacted together creating sutured and point contacts between grains. Grains are commonly plastically deformed and more rarely broken.</p> <p>Bioclasts are rarely found outside coated grains and are found as rare fine coral fragments, coated echinoderm fragments, microgastropods and thin shelled bivalves that occur within mud-wackestone clasts. Other bioclasts are found within ooids at their nuclei. There are very rare poorly preserved biserial, uniserial and involute coil type foraminifera. Other common ooid cortices include grains of chalcedony, micrite spheres and euhedral-anhydral dolomite crystals, that have been calcified</p> <p>The ooids in this sample show a variety of ooid types from, coarse composite ooids, 500µm mean diameter superficial ooids with clear thin radial-fibrous outer coating with subtle micritic laminae to structureless centre to 820µm mean diameter micritic ooids that range from largely micrite spheres coated with a very thin fibrous coating amid a tangential crystal structure of micrite and organic material.</p>		
Interpretation		<p>The mixture of ooid type, sizes, and thicknesses of the cortices, associated grains and abrasion of laminae is suggestive that the ooids are allochthonous ooids. Some ooids that have a clear structure have a thick micrite outer core.</p>		
Diagenesis		<p>All allochems have been compacted leading to point contacts, sutured contacts and plastic deformation, and rarely breakages between allochems. A micrite cements the rock together. The micrite matrix also contains micro-peloids and fine needles of calcitic material.</p> <p>Inclusion rich euhedral to anhedral dolomites are scattered around the sample and commonly occur in their finest form within the matrix. It appears that the more euhedral dolomites are associated with the cores of allochems particularly those with chalcedony cores. Dolomites have been calcified as suggested by crystal morphology and catholuminescence.</p> <p>The sample has some thick calcite filled fractures that cut across all allochems and features as well as more common finer fractures. The fractures are a regular thickness and occur singularly.</p>		
Pore types		None		
Reservoir quality		None		

OF C003 1615 CM



C003	1615			
Texture		Bivalve Peloid Packstone		
Description		<p>This is a well orientated assortment of disarticulated thin shelled bivalves, echinoderm debris, rare biserial foraminifera, fine coral fragments, abraded brachiopod fragments, green algae and other shelly debris. Other allochems include rounded peloids.</p> <p>The thin shelled bivalves are typically 600µm in length.</p>		
Interpretation		The mixture of allochem types suggests this originated in probably photic moderate to high energy waters.		
Diagenesis		<p>Minor compaction is evident through broken bivalve shells and rare point contacts between grains. The sediment sits in a micrite mud. Common dissolution seams and stylolites anatomise through the muddy matrix and have formed around grains and span the thin section; this is evidence of chemical compaction.</p> <p>There are several wide fractures (750 µm) that are infilled with a coarse calcite spar, these fractures have sharp edges and occur singularly. There are few thin fractures (30 µm) that branch off the larger fractures, and are filled by coarse calcite spar.</p>		
Pore types		None		
Reservoir quality		None		

OF C003 2050 CM



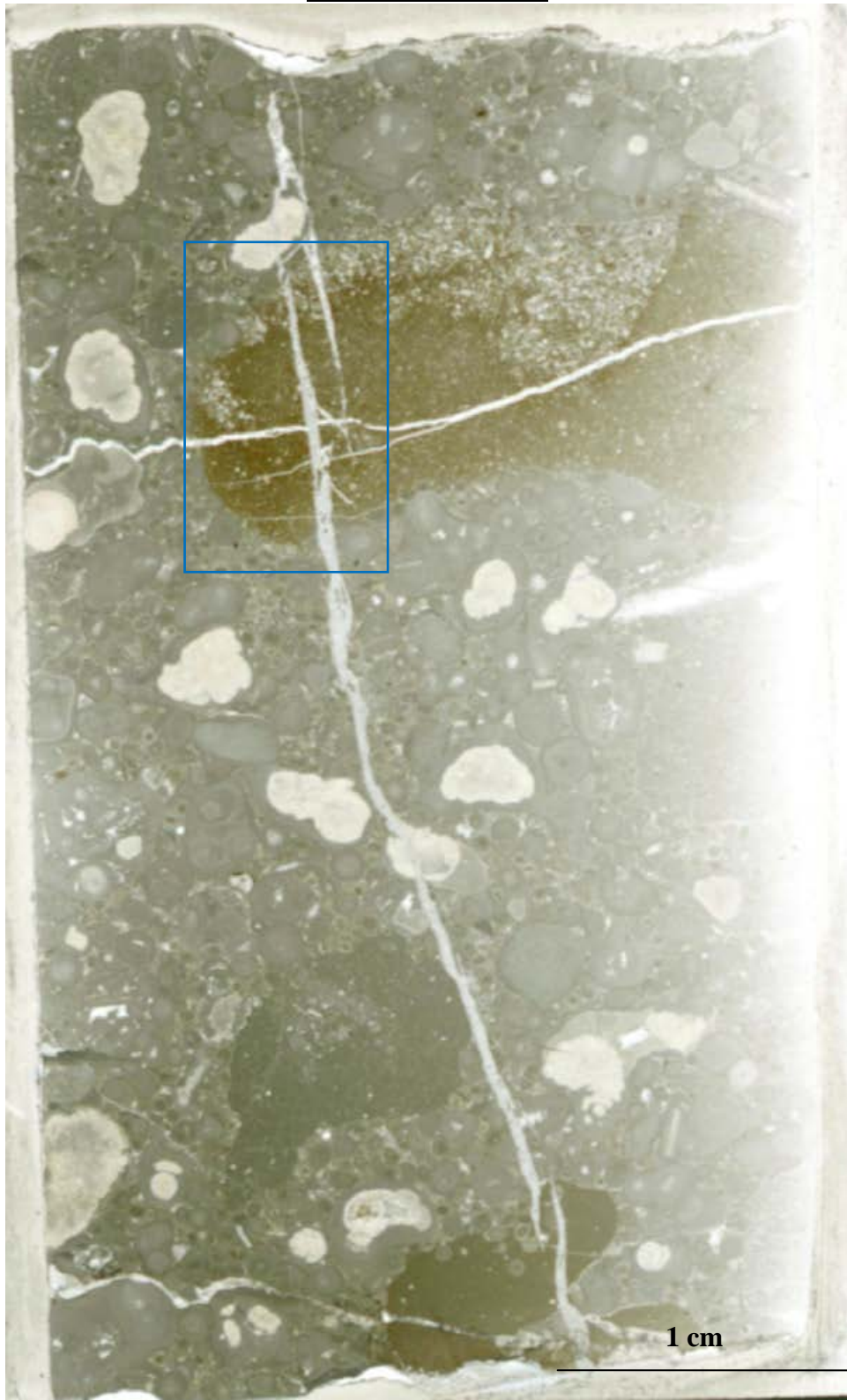
C003				
Texture	Bivalve mud-wackestone			
Description	<p>This is a poorly sorted bivalve dominated mud-wackestone. The section cuts through 2 facies types where the finer facies is a clast.</p> <p>The first facies, the finest facies consists of very fine grained accumulation of well oriented thin shelled bivalves and tiny shell fragments that are abraded. The second facies contains a much coarser assemblage that is strongly oriented containing thin shelled bivalves, and rare well rounded shelly debris. These allochems sometimes accumulate forming laminations, which can be seen in the thin section scan.</p>			
Interpretation	The strong orientation of allochems within both facies 1 and 2 suggest that these sediments may have been deposited in a current swept environment, that possibly, had the force to carry large clasts.			
Diagenesis	The strong orientation may in parts be due to compaction. Microfractures cut across all allochems and are filled with an equant calcite spar.			
Pore types	None			
Reservoir quality	None			

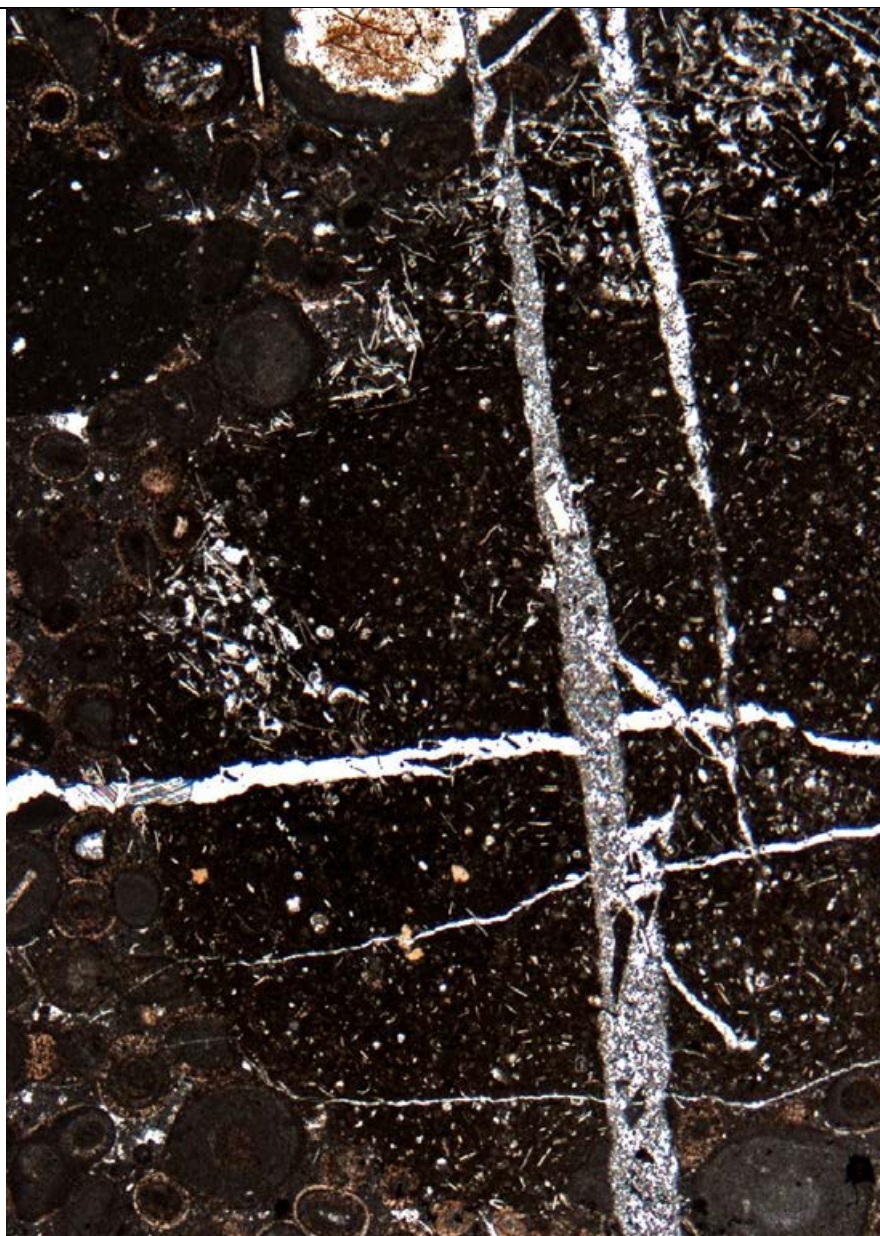
OF C003 2125CM



C003	2125			
Texture	A moderately well sorted assemblage of whole, broken and deformed ooids, rare compound ooids and bioclasts with micrite envelopes. Allochems have regularly have sutured contacts with an iron rich seam and common iron coatings. Allochems are commonly plastically deformed. Bioclasts most commonly form ooids nuclei and occur rarely as fine debris. Common bioclasts include poorly preserved microgastropods, multichambered foraminifera, abraded and disarticulated bivalves, brachiopods and echinoderm debris.			
Description	The mixture of ooid type, sizes, and thicknesses of the cortices, associated grains and abrasion of laminae is suggestive that the ooids are allochthonous ooids. Some ooids that have a clear structure have a thick micrite outer core; this may have been acquired during transport. The well defined ooid structures are characteristic of formation in quiet-water low turbulence environments (Flügel, 2004); this may possibly be due to ooids being transported from below the wave base or a lagoonal environment. In outcrop this is interpreted as part of a debris flow however there is much less mud in the assemblage compared to turbidite facies suggesting this may in fact have been part of a grain flow or other grain supported flow.			
Palaeoenvironment Interpretation	<p>All allochems have been compacted leading to point contacts, sutured contacts and plastic deformation between allochems. Dissolution seams and stylolites have developed between grains suggesting chemical compaction took place. Calcite microspar (probably originating from calcite rich pore waters due to compaction) cements the rocks together.</p> <p>Inclusion rich euhedral to anhedral dolomites are scattered around the sample and commonly occurring within the matrix. It appears that the more euhedral dolomites are associated with silica. Dolomite has been calcified.</p> <p>The sample has several thick, irregular sharp edged calcite filled fractures that cut across all allochems and features as well as more common finer fractures. The fractures are a regular thickness and occur singularly. Dissolution seams and selective regions of ooids and other allochems have been replaced by an iron oxide; this is possible due to neomorphism and exposure of the formation to air.</p>			
Diagenesis	<p>This shows a moderately well sorted assemblage of whole, broken and deformed ooids and rare compound ooids (no more than 1 mm in diameter). They have been compacted together creating sutured contacts. Allochems are commonly plastically deformed and more rarely broken.</p> <p>Bioclasts are only rarely found within ooids at their nuclei or rarely as fine debris. Bioclasts are commonly well rounded grains of calcite, which are probably from abraded and disarticulated bivalves and brachiopods; there are very rare poorly preserved biserial foraminifera. Other common ooid cortices include grains of chalcedony, micrite and euhedral-anhydral dolomite crystals (which have been calcified).</p> <p>The ooids in this sample show a variety of ooid types from 450µm mean diameter superficial ooids with clear thin radial-fibrous outer coating with a subtle micritic layered to structureless centre to 600µm mean diameter micritic ooids that range from largely coated micrite spheres with pervasive micritisation of the cortex to occurrences of subtle thinly laminated tangential cortices.</p>			
Pore types	None			
Reservoir quality	None			

C003 OOLITIC CHANNEL





Microphotograph 34 Mosaic of tabular clast that consist of fine abraded bivalve debris, echinoderm debris and occasional disarticulated bivalve fragments ?*Posidonia*.

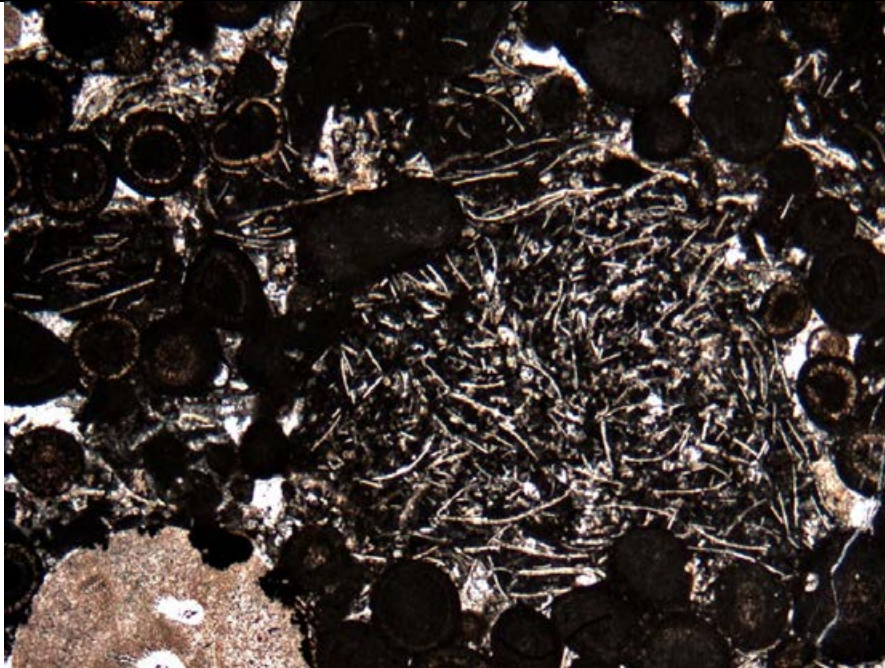
C003	Channel deposit			
Texture		Intraclastic ooid pack-grainstone		
Description		<p>Very poorly sorted assemblage of gravel to medium sand grade intraclasts, micritised ooids, micritic ooids, peloids, disarticulated bivalves.</p> <p>Two types of intraclast occur in this sample one is a mud-wackestone that consist of sparse micropeloids and tiny disarticulated thin shelled bivalves. The other intraclast type contains a much denser assemblage, the same as type one.</p>		
Interpretation		<p>The large variety in clast types and the coarse nature of this sample suggests this is probably a allochthonous limestone. Field relationships indicate that this sample come from a more proximal source when compared to other samples, where coarser material was deposited.</p>		

Diagenesis	Silica has preferentially replaced the internal parts of large micritic grains. Anhedra-euhedral dolomite rhombs are concentrated along microfractures and silica. Two microfractures set span the sample and are found running perpendicular to each other and are filled with an equant calcite spar.
Pore types	None
Reservoir quality	None

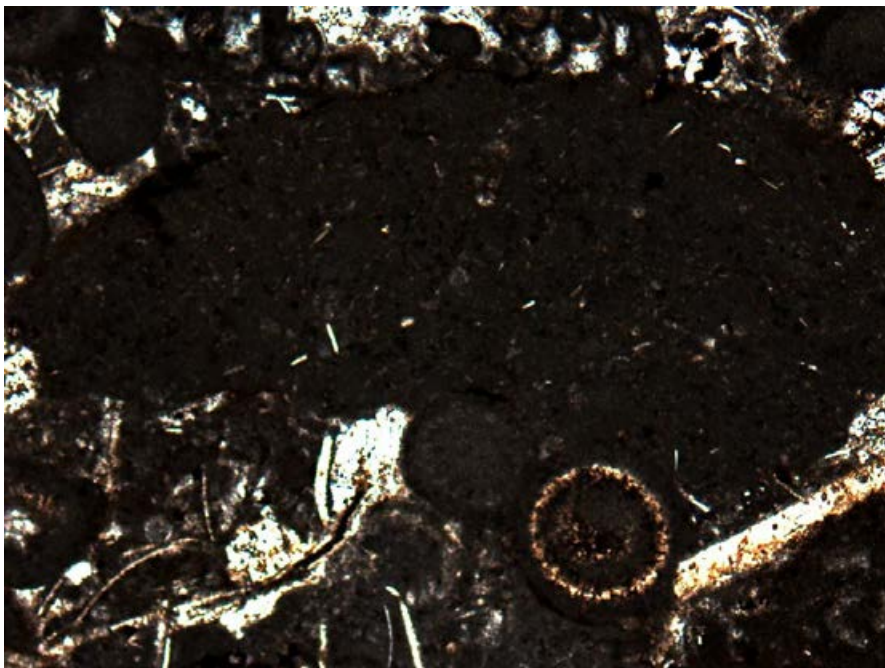
C003s 1150 cm



1 cm



Microphotograph 35 Wacke-packstone clasts dominated by disarticulated bivalves ?*Posidonia*. Note the echinoderm fragment in bottom left



Microphotograph 36 Mudstone clast, consists of tiny abraded fragments of thin shelled bivalves. Note the grainstone matrix.

C003				
Texture	Intraclastic ooid pack-grainstone			

Description	<p>Very poorly sorted assemblage of very coarse to medium sand grade micritised ooids, micritic ooids, peloids, intraclasts, coarse echinoderm fragments, disarticulated bivalves and much large oyster bivalves.</p> <p>Two types of intraclast occur in this sample on is a Mud-wackestone that consist of sparse micropeloids and tiny disarticulated thin shelled bivalves. The other intraclast type contains a much denser assemblage, the same as type one.</p>
Interpretation	<p>The large variety in clast types and the coarse nature of this sample suggests this is probably a allochthonous limestone. Field relationships indicate that this sample come from a more proximal source when compared to other samples, where coarser material was deposited.</p>
Diagenesis	<p>All echinoderm fragments have overgrowths of calcite spar. Patches of the sample, most notably within coarse allochems, silification has preferentially replaced parts. Dissolution seams and stylolites span the whole section and cut across all allochems. Anhedral-euhedral dolomite rhombs are scattered across the sample and mainly occur within the matrix of the rock. These dolomites have been calcified, where the outer cores are speckled. An iron oxide is common in association with dolomites.</p> <p>Microfractures span the sample and are found running parallel to each other and are filled with an equant calcite spar</p>
Pore types	None
Reservoir quality	None

Polished Slab Descriptions

Hand samples were gathered to see sedimentary structures on a larger scale as well allowing the author to analysis a larger area to improve understanding of the microfacies and diagenetic enhancements to the rock.

C002 525cm

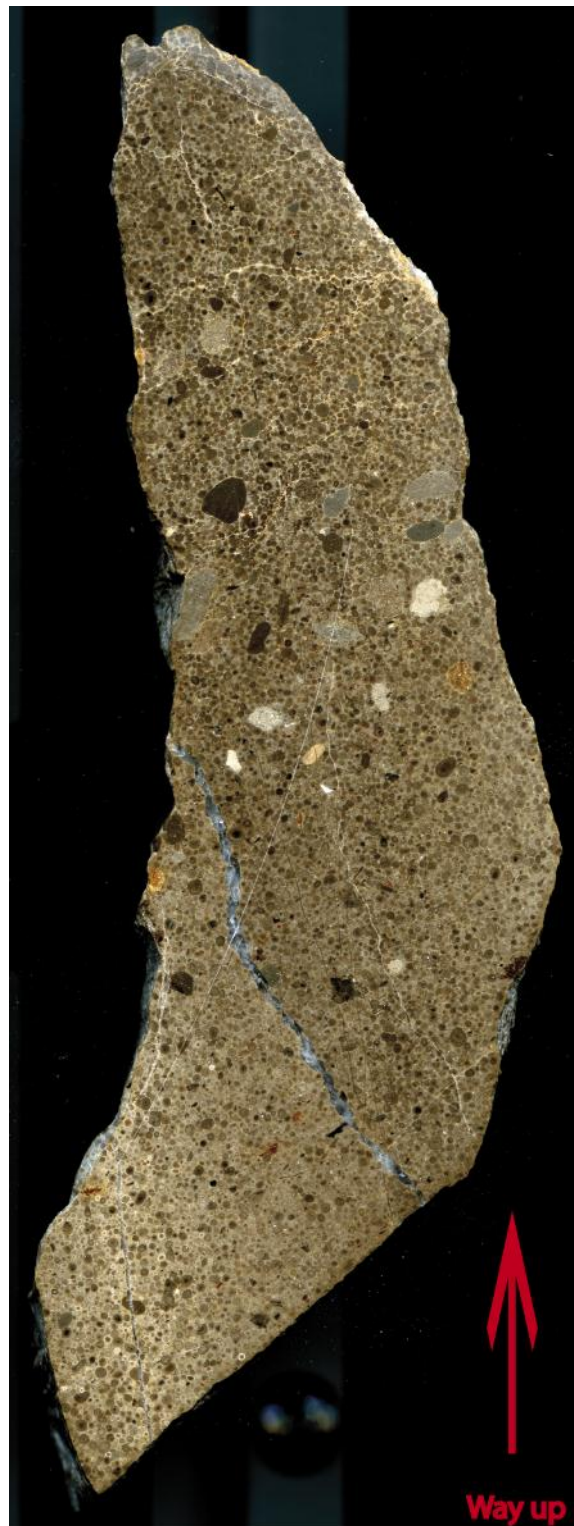


5 cm

Way up

C002	525 cm			
Texture		Peloid intraclastic pack-grainstone		
Description		Poorly sorted crudely oriented accumulation of granule sized rounded peloids and angular wackestone intraclasts. The matrix consists of very coarse sand grade ooids and peloid. Intraclasts range from yellow-brown to grey in colour and contain very little bioclastic material.		

C002 550cm



5 cm

C002	550 cm		
Texture	Ooid intraclastic pack-grainstone		
Description	<p>This is an oolitic peloidal grainstone that has an assortment of components that include subrounded to round radial-fibrous, superficial and micrite ooids, peloids, subangular intraclasts of mud-wackestone. The grainstone is poorly sorted with a wide range of grain sizes between different components. The ooids and peloids form the matrix of the rock that hosts much larger rip-up clasts of mud-wackestone intraclasts that commonly host disarticulated thin shelled bivalve fragments and other shelly material.</p> <p>Intraclasts range in composition with some appearing a grey-green whilst others have an almost pink appearance. Darker intraclasts are muddier than lighter intraclasts.</p> <p>Flakes of iron oxide are found amongst the sediment; iron oxide also lines some ooid laminae.</p> <p>The sample has two fracture sets. The finest fractures are filled with calcite and occur parallel to bedding, with branching vertical micro-fractures, these cut through both allochems and cement. The second fracture type runs vertical to bedding and can be considered a calcite vein; this cuts all allochems and cement.</p>		
Interpretation	This is interpreted as part of a turbidite that is hosting traction carpets that contain intraclasts.		

C002 645cm



5 cm

C002	645 cm			
Texture		Peloidal ooid pack-grainstone		
Description		Poorly sorted assortment of very coarse sand grade peloids and coarse sand grade ooids.		

C003 150cm



Way up

C003	150 cm			
Texture		<i>Posidonia</i> grainstone <i>Coquina</i>		
Description		This is a sample from the <i>coquina</i> bank that form a large part of location C003. The rock is a well oriented accumulation of <i>Posidonia</i> bivalve and peloids. The crinkly appearance is seen in outcrop and acts as a characteristic of this facies.		

C003 230cm



C003	230 cm		
Texture		Ooid intraclastic pack-grainstone	
Description		<p>Poorly sorted assortment of components that include subrounded to round radial-fibrous, micrite ooids and peloids. A grain rich matrix hosts much coarser well rounded peloids. The coarse peloids are evenly distributed across the sample.</p> <p>The sample has two fracture sets. The finest fractures are filled with microcrystalline calcite (appearing light brown) and occur oblique to bedding, with branching micro-fractures, follow allochems. The second fracture type runs horizontal to bedding and can be considered a calcite vein; these are only intermittent and appear as shear fractures.</p>	

C003 350cm



Way up

C003	350 cm			
Texture		Ooid intraclastic pack-grainstone		
Description		Poorly sorted accumulation of coarse sand grade micrite ooids, peloids and intraclasts that range from a light yellow to red orange colour. This sample has two fracture sets which both cut all allochems one is <1mm in diameter whilst the other, later fracture set is a very coarse calcite vein.		

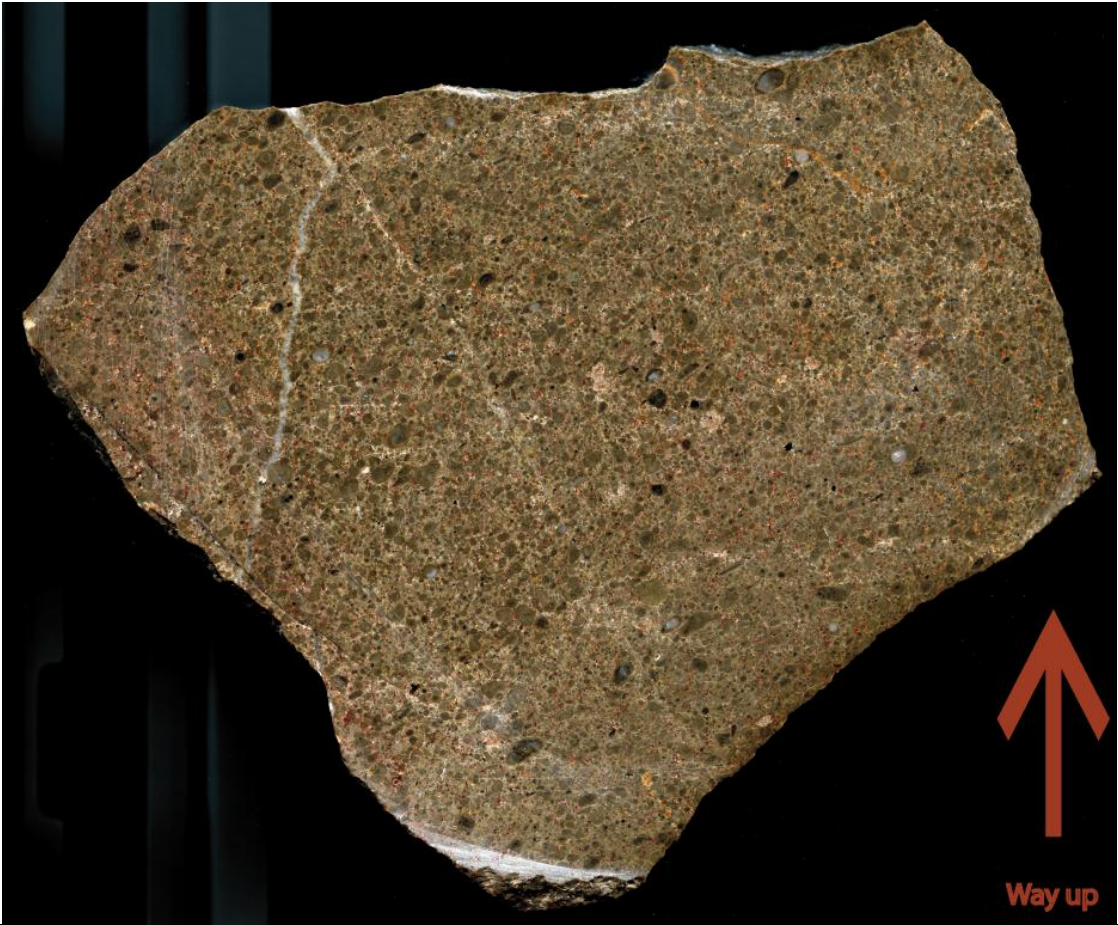
HAND SPECIMEN IMAGE C003 350CM



Way up

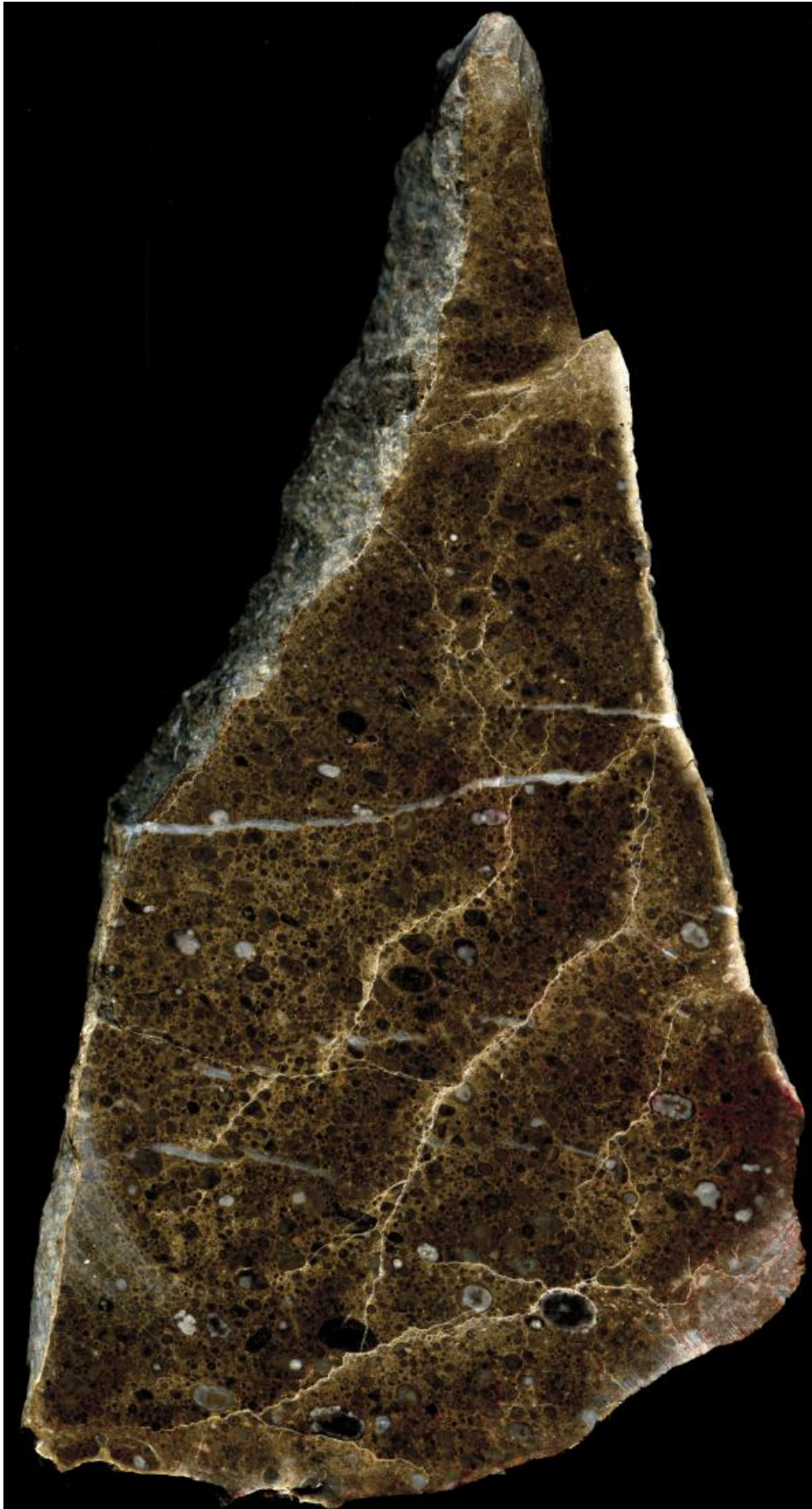
C003	350 cm			
Texture		Ooid intraclastic pack-grainstone		
Description		<p>Poorly sorted accumulation of very coarse sand grade micrite ooids, peloids and intraclasts (yellowish brown colour). This sample has three fracture sets the first appears brown in appearance is inconsistent following the path of dissolution seams. The other two fracture sets are calcite filled and both cut all allochems one is <1mm in diameter whilst the other, later fracture set is a >1.5mm thick tension fracture.</p>		

C003 1550cm



C003	1550 cm		
Texture		Ooid intraclastic pack-grainstone	
Description		Poorly sorted assemblage of very coarse grade peloids to coarse sand grade ooids. The majority of allochems are rounded to subrounded and indicate a crude orientation from left to right in this sample. The bottom of this sample appears to be more muddy containing coarser but sparsely distributed allochems in comparison to the rest of the rock.	

C003 1700



Way up

C003	1700 cm			
Texture		Peloidal ooid pack-grainstone		
Description		<p>Poorly sorted assortment of components that include subrounded to round radial-fibrous, micrite ooids, peloids. A ooids rich matrix hosts much coarser well rounded peloids that are often host a silica.</p> <p>The sample has two fracture sets. The finest fractures are filled with microcrystalline calcite (appearing light brown) and occur oblique to bedding, with branching micro-fractures, follow allochems. The second fracture type runs horizontal to bedding and can be considered a calcite vein; these are only intermittent and appear as shear fractures.</p>		

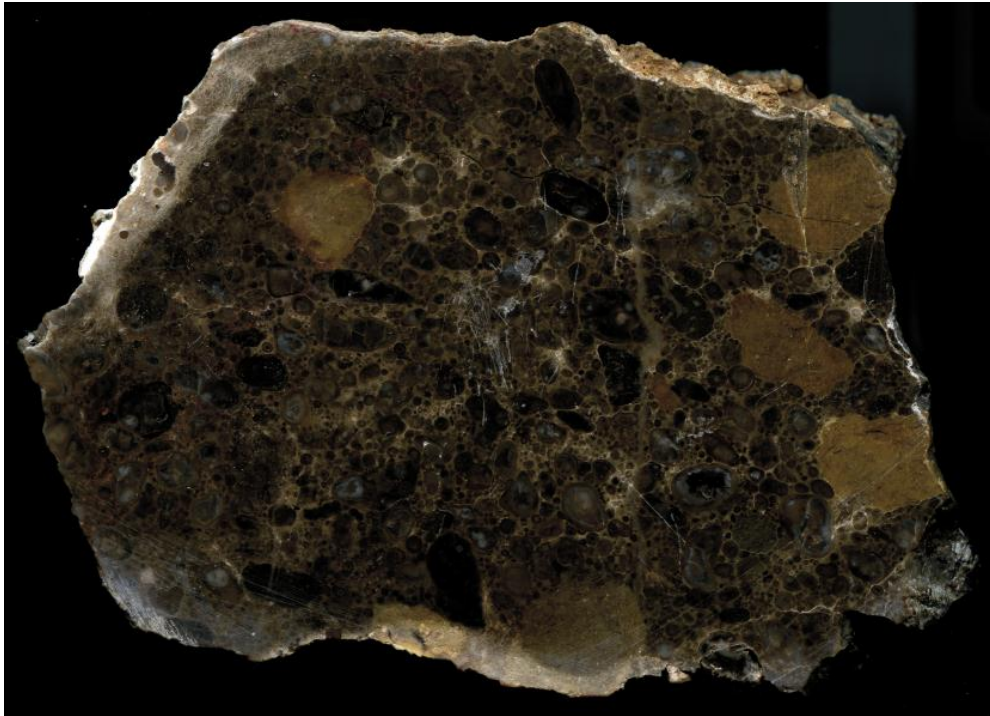
C003 1850cm



Way up

C003	1850 cm			
Texture		Ooid intraclastic pack-grainstone		
Description		Poorly sorted accumulation of coarse sand grade ooids, and very coarse sand grade peloids with rare very coarse rounded intraclasts, which range from black to orange in colour. This sample has a generally lighter colour compared to other samples this may be due to cements filling intergranular pore space.		

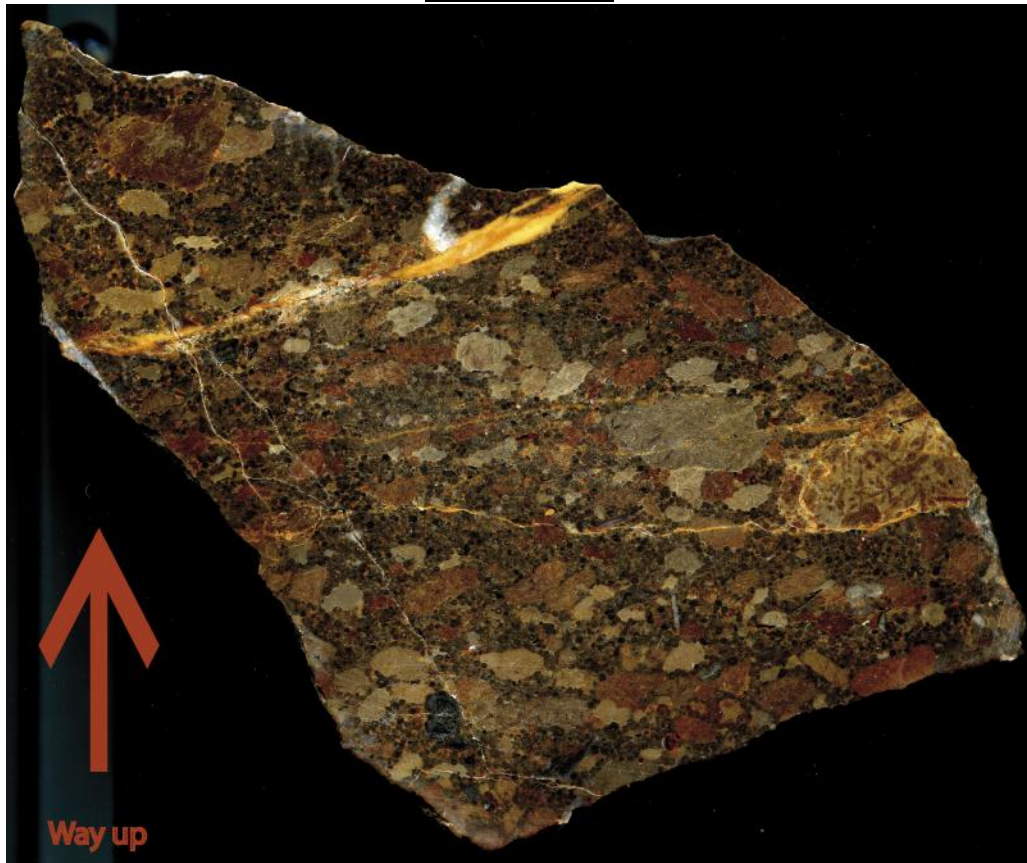
C003s 380cm



Way up

C003s	380 cm		
Texture	Intraclastic ooidal peloidal pack-grainstone		
Description	Very poorly sorted assemblage of a very coarse assortment of small pebble sized intraclasts, granule sized peloids and very coarse sand sized ooids. Intraclasts contain a light brown micrite and contain an abundance of thin shelled bivalves. Other allochems are micritised.		

C003s 1350cm



C003s	350 cm		
Texture		Intraclastic pack-grainstone	
Description		<p>Poorly sorted well oriented grainstone that has an assortment of components that include subrounded to round ooids, peloids, subangular intraclasts of mud-wackestone texture with a variety of components. Intraclasts commonly host disarticulated thin shelled bivalve fragments and other shelly material. The intraclasts range from bright red to light grey and yellow suggesting their overall composition ranges greatly. Flakes of iron oxide are found amongst the sediment iron oxide also lines some ooid laminae.</p> <p>The sample has two fracture sets. The finest fractures are filled with yellow-brown calcite and occur parallel to bedding, with branching vertical micro-fractures, these cut through both allochems and cement. The second fracture type runs vertical to bedding and cut all allochems and cement.</p>	

AMMONITICO ROSSO



C003	350 cm		
Texture		Ooid intraclastic pack-grainstone	
Description		Well weathered <i>Ammonitico Rosso</i> . Very little is preserved, only iron rich nodules are noted.	